2013-12-08

# Simulation-Based Optimization for Integrated Electric Utility Resource Planning and Deployment

Juan P. Saenz Corredor
*University of Miami,* juansaenz@gmail.com

UNIVERSITY OF MIAMI


SIMULATION-BASED OPTIMIZATION FOR INTEGRATED ELECTRIC UTILITY
RESOURCE PLANNING AND DEPLOYMENT


By

Juan P. Sáenz


A DISSERTATION


Submitted to the Faculty
of the University of Miami
in partial fulfillment of the requirements for
the degree of Doctor of Philosophy


Coral Gables, Florida

December 2013

UNIVERSITY OF MIAMI


A dissertation submitted in partial fulfillment of
the requirements for the degree of
Doctor of Philosophy


SIMULATION-BASED OPTIMIZATION FOR INTEGRATED ELECTRIC UTILITY
RESOURCE PLANNING AND DEPLOYMENT


Juan P. Sáenz


Approved:


_____
Nurcin Celik, Ph.D.
Assistant Professor of
Industrial Engineering

_____
Shihab Asfour, Ph.D.
Professor of
Industrial Engineering


_____
Joseph Sharit, Ph.D.
Research Professor of
Industrial Engineering

_____
Murat Erkoc, Ph.D.
Associate Professor of
Industrial Engineering


_____
Saman Zonouz, Ph.D.
Assistant Professor of
Electrical and Computer
Engineering

_____
M. Brian Blake, Ph.D.
Dean of the Graduate School

SÁENZ, JUAN PABLO                                 (Ph.D., Industrial Engineering)

Simulation-based Optimization for Integrated                      (December 2013)
Electric Utility Resource Planning and
Deployment.

Abstract of a dissertation at the University of Miami.

Dissertation supervised by Professor Nurcin Celik.
No. of pages in text. (204)

We have studied integrated electric utility networks in terms of long-term electric

utility resource planning, short-term environmental economic load dispatch, and the

optimal deployment of distributed generation sources within the electric network.   In

order to conduct these analyses, the development of a continuous-discrete modular

simulation and optimization framework and a particle filtering based multi-objective

optimization framework has been done.   The continuous-discrete modular simulation

includes the integration of discrete decisions and events with continuous processes within

the same simulation environment and the modular integration of different resources into

the simulation.   The multi-objective optimization framework includes the development of

a sequential importance sampling mechanism for multi-objective optimization,

leveraging the information contained within the non-dominated set of solutions to

increase the thoroughness of the generated solution and ensure that the algorithm does

not converge to local optimums. The evaluation of energy capacity plans include the use

of conventional energy generation sources, renewable energy generation sources, energy

storage alternatives and the evaluation of environmental policies (in terms of their effect

on energy capacity plans and their effectiveness in incentivizing environmentally friendly

energy generation sources). The optimization of the environmental load dispatch is achieved leveraging Bayesian particle filtering to evaluate the state of the load dispatch at each generation unit, and the Newton-Raphson method to ensure that power balance constraints are met. The optimization of different levels of penetration of distributed generation has been evaluated in terms of minimal cost, power loss and environmental impact.

To Jesus Christ, my Lord and Savior,

in whom I live, and move and have my being.

John 1: 1-5, 14

ACKNOWLEDGEMENTS

# TABLE OF CONTENTS

# LIST OF FIGURES

# LIST OF TABLES

# LIST OF ALGORITHMS

# Chapter 1: Introduction

Over the last 60 years, the consumption of energy in the U.S. has averaged an annual increase of 1.8% taking it from 34.62 Quadrillion Btu in 1950 to an estimated 98.00 Quadrillion Btu in 2010, as shown in Figure 1 (EIA, 2011). The energy used in electric power generation in the U.S. constitutes 40% of the total energy consumed, while 92% of the energy produced with coal is destined for energy power generation. Electric power generation is driven from coal (48%), nuclear energy (21%), natural gas (19%), renewable energy (10%) and oil (1%) (EIA, 2010). Furthermore, electricity production is the major source of most emissions of carbon dioxide ($CO_2$), sulfur oxides (SOx), and nitrogen oxides (NOx) (Intergovernmental Panel on Climate Change, 2010; Likens et al. 1996; Goddard Institute for Space Studies, 2010).
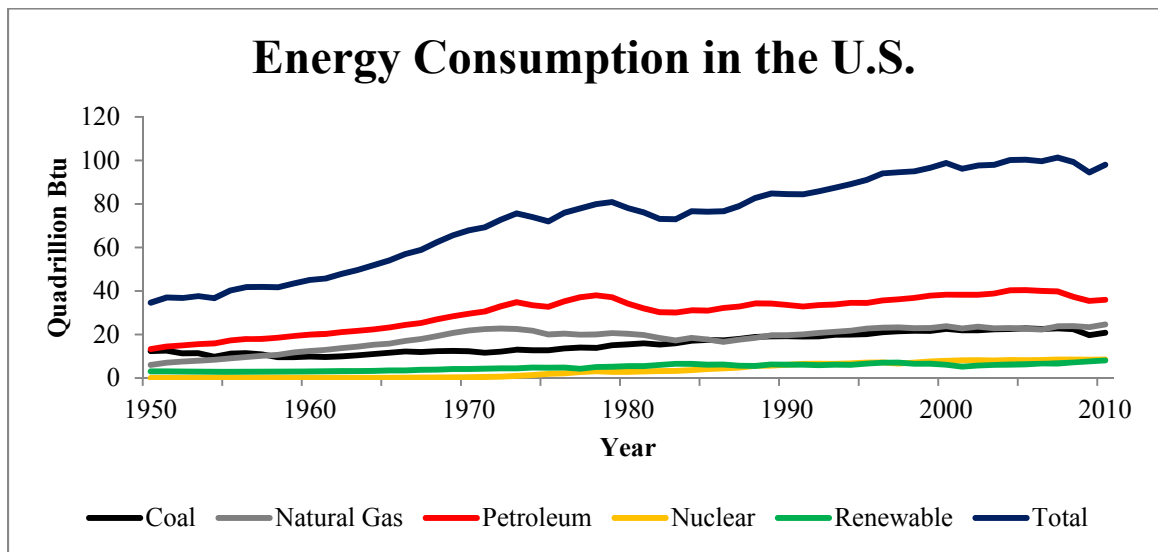


Figure 1: Total energy consumption in the U.S. by Source

This continued increase has occurred due to the fact that efficient and reliable electricity plays an essential role in a wide range of today's lives. It is essential to medical care, economic development, national security, education, communications, food and water supply, heating, cooling and lighting, among others. With this large span of electricity usage, expectations have risen for an uninterrupted electrical flow to be available whenever and wherever needed. Disruptions to the electric flow may occur due to short circuits in electrical lines caused by lightning storms or accidentally damaged wires, and may cause small electric outages. These small outages occur on a relatively common basis and last for short periods in locally restricted areas. On the other hand, the larger counterparts to these small outages might occur where large areas are affected due to a series of cascading events. An instance of such events happened in August 2003 where widespread outages occurred across the north eastern U.S. quite unexpectedly. A power line (the Eastlake 5) tripped because of some overgrown trees and automatically shut down. When this power line went offline, it went unnoticed due to a computer failure, and triggered a series of events that led to the worst electricity blackout in the history of U.S.; affecting an estimate of more than 50 million people (CBC, 2003). In order for the electricity network to respond to these types of disruptions promptly, it has to rely on a robust decision making mechanism that enables the system to respond quickly and effectively maintain a reliable electrical flow. Providing efficient and reliable electricity is an extremely complex technical challenge that involves real-time assessment, control and coordination of production at thousands of generators, transportation across an interconnected network of transmission lines, and delivery of

electricity to millions of customers by means of a distribution network (U.S.-Canada Power System Outage Task Force, 2004).

In this dissertation we propose to evaluate the integrated electric utility network in terms of three different aspects. The first aspect to analyze is the long-term electric utility resource planning, which is defined as the selection of power generation and conservation (i.e., storage systems) resources that will enable the network to meet customer demands for electricity over a multi-decade time horizon (Hobbs, 1995). The second aspect to evaluate is related to the short-term environmental economic load dispatch, which involves the short term implications of using a specific utility resource plan. The environmental economic load dispatch is defined as the operation of generation facilities to produce electricity at the lowest cost to reliably serve customers, recognizing any operational limits of generation and transmission lines (EPAct, 2005) taking into account the environmental effects of such endeavor. The third aspect to evaluate is associated with the optimal deployment of distributed generation sources within the electric network. Distributed generation is the term for energy cogeneration and small scale power production that is performed by some entities within the electric network independently from the central generating units. The optimal deployment of distributed generation aims to minimize the operational cost and power loss of the integrated electric network after deploying sources of distributed generation.

## 1.1. Long-term Electric Resource Planning

Conventionally, the long-term planning of electric power systems focuses on the determination of the operational capacities of only fossil fuel based energy generation systems. However, estimates are that conventional sources of energy can only meet our energy demands for another fifty to seventy years. Therefore, in an effort to find alternative forms of energy, the world has turned to hybrid conventional-renewable energy sources (e.g., solar, hydro, wind, geothermal, ocean and biomass) as a solution. Today, the majority of the citizens of the world are uniting to support the increasing role of renewable energy in our lives, and the stakeholders of electric utility planning seek optimum ways to actively involve the renewable energy (which was once viewed as an 'alternative' source of energy) in satisfying our energy needs in the upcoming decades.

Electricity production, primarily from burning coal, is the major source of most emissions of carbon dioxide ($CO_2$), which contributes to global warming by trapping heat in the earth's atmosphere; sulfur oxides (SOx), which are the main cause of acid rain that can make lakes and rivers too acidic for plant and animal life, and damage crops and buildings; and nitrogen oxides (NOx), which are combined with other chemicals to form ground-level ozone (smog) in the presence of the sunlight (Intergovernmental Panel on Climate Change, 2010; Likens et al. 1996; Goddard Institute for Space Studies, 2010). Renewable energy has a much lower environmental impact than conventional sources of energy and can significantly reduce the emission of greenhouse gases. Furthermore, renewable energy sources are free, (no associated operational or purchasing costs for the source), and are sustainable (hence these sources never run out). Other advantages of utilizing renewable sources of energy include a stimulated economy and an increased

number of job opportunities, improved national security and independence from foreign oil suppliers. In contrast, the use of fossil fuels makes the U.S. vulnerable to political instabilities, trade disputes, embargoes and a variety of other impacts, since more than 53% of U.S.'s oil has been imported as of 2003 (WORC, 2003). Due to these advantages and needs, the involvement of renewable sources in our electric power generation at the utility scale is inevitable and hence capacities of various kinds of renewable energy generation (e.g., wind and solar) as well as storage systems (e.g., compress air energy storage systems, batteries, and super-capacitors) should be considered in line with capacities of the conventional fossil fuel based means of energy generation for the long term survival of the utilities while incurring optimum multicriteria objectives (e.g. investment and operational costs, environmental impact) given increased market competition.

On the other hand, there are several challenges against the implementation of an effective capacity planning at the utility scale. First, power systems are very large scale and complex due to their uncertain, interactive and dynamic features. Second, the consequences (economic, reliability, or environmental) of alternative strategic resource planning scenarios should be evaluated at an integrated manner for various players (e.g., consumers, suppliers, government). Third, the planning process is further complicated by the growing uncertainty due to future load growth, resource availability (i.e., utilization, lifespan, and performances of power plants), construction (i.e., times, costs, and performances of newly introduced resources), regulatory and economic environment in which utilities operate, and raising environmental concerns such as global warming. Lastly, the long term planning of the power industry is considerably affected by the

competition in various sectors of the market including generation, transmission and distribution.

In this study, in terms long-term electric resource planning, we propose a continuous-discrete modular simulation and optimization framework (CoDiMoSO) in order to accurately estimate the capacity requirements of electric power generation and storage, involving conventional as well as renewable sources of energy generation. The framework developed in this work enables various stakeholders of electric utility resource planning to devise the best possible capacity plans, detailing the rated capacity for each energy generation and storage alternative included in the capacity plan, while saving from computational resources and costs. The goal of the optimization model is to minimize the financial investment of building, and operational cost of maintaining the combined renewable and fossil fuel based energy generation systems as well as minimizing the environmental impact (measured through the amount of greenhouse gases produced) while meeting the requested commercial, industrial, residential and transportation demand.

The CoDiMoSO decision making framework proposed in this research is composed of four modules for evaluation, and another one for optimization. The generation module (Module G) captures the functional details and characteristics of energy generation at the utility scale and includes renewable (solar and wind farms), and fossil fuel-based (coal, oil, and natural gas) energy sources. The storage module (Module S) encapsulates the attributes of various energy storage components that amass the excess production of energy such as NaS and Pb-Acid types of batteries, and compressed air energy storage systems (CAES). The transmission and distribution grid elements such as

the step-up and step-down substations and inverters are included in the transmission module (Module T), and variable demand arising from industrial, commercial, transportation, and residential customers as well as their seasonal and daily fluctuation is captured in the demand module (Module D). Finally, the optimization module (Module O) helps utilities determine the best possible combination of investment options that will result in minimized cost and environmental damage. Continuous-discrete modeling methodologies are used in the modeling of Module G, Module S, Module T, and Module D depending on the nature of the sub-system; and meta-heuristics are utilized for the solution mechanism of Module O. Because the literature on resource planning of electric utility systems that incorporates real data at this scale and scope is infrequent, the acquisition of realistic data has been an additional challenge. Here, the necessary data has been collected from various reliable sources such as the National Renewable Energy Laboratory (NREL) for solar irradiation profiles; the Energy Information Administration (EIA) and the Florida Public Service Commission (FPSC) for electricity consumption; EIA for fossil fuel energy production; EIA, Sharp, Mitsubishi and SunPower for cost and operational characteristics of PV panels; EIA, Siemens, GE, and Mitsubishi for cost and operational characteristics of Wind Turbines; and EIA for cost and operational characteristics of CAES. The constructed CoDiMoSO tool is used to 1) test impacts of several factors such as different conflicting objectives (e.g., minimum investment and operational cost, and minimum environmental hazard); future demand growth; efficiencies in PV panels, wind turbines, fossil fuel operating power plants, CAES, and batteries; and losses in transmission lines; on the total cost of the integrated generation and storage system and 2) to find an optimal investment policy of renewable and fuel-

based generation, as well as storage capacity. At this level, the proposed tool has been demonstrated for the sunshine state of Florida; however, the proposed CoDiMoSO framework is built with a generic approach so that it can be adopted for various other utilities in different states, or different countries.

## 1.2. Short-term Electric Load Dispatch

Short-term electric load dispatching involves the short term implications of using a specific utility resource plan. The economic load dispatch (ELD) is defined as the operation of generation facilities to produce electricity at the lowest cost to reliably serve customers, recognizing any operational limits of generation and transmission lines (EPAct, 2005). Factors that have an impact on achieving minimum dispatch costs include geographic factors such as the area, generation and transmission resources included in planning and economic load dispatch; and implementation factors including the frequency at which dispatch is performed, the quality of communication between the economic dispatch planners and the operators, the adequacy of the software tools for dispatch, and the coordination of dispatch across regions. In this study, we focus on the planning of the current, as well as future, load dispatch problem considering both geographic and implementation factors in a timely basis. Current dispatch involves load monitoring to ensure the balance of electric supply and electric load, while maintaining the system frequency, ensuring the appropriate reaction to changes in loads and maintaining the scheduled tie-line capacities; and monitoring flows on the transmission system to keep flows within admissible levels, keeping voltage levels within reliability

ranges. Planning for future dispatch involves scheduling generating units for each hour of the next day based on demand forecasts considering availability and ramp rates of generating units, minimum and maximum generating levels, the minimum time that a generator must run once it has been turned on, or stay idle once it has been turned off. It also involves the associated generation costs including efficiency, fuel and non-fuel operating costs, environmental compliance costs and start-up costs, and reliability assessments to ensure that the scheduled generation dispatch is also part of future dispatch planning (FERC, 2005).

Environmental economic load dispatching (EELD) problem is an extension of the ELD problem where environmental considerations are also taken into account. The objective of the EELD problem is not only to fulfill the demand reliably at the lowest possible cost, but also to minimize emissions and other environmentally adverse effects of electrical generation, transportation and distribution. Earlier literature on EELD considering the conflicting objectives of minimization of cost and pollution present simplified structures where constraints such as the power loss are not included in the analysis (Zahavi and Eisenberg, 1975; Nanda et al., 1988). The EELD problem also shares the inherent challenges of the ELD problem as in both cases the considered dynamic system is operating under uncertainty, is very large scale, and highly complex. The uncertainty in the system comes mainly from the variability in the load demand and the output from renewable energy sources which are mostly driven by changing weather conditions (e.g. temperature, humidity, wind speeds, and cloud cover). The scale of the problem is evidenced by facts such as the large amounts of generating capacity, emissions, the number of customers and revenues generated within the system. In

Florida alone there is a generating capacity of more than 55,000 MW, with emissions of more than 270 tons of sulfur dioxide, 170 tons of nitrogen oxide, and 121,000 tons of carbon dioxide; the state has more than 9.6 million customers with total electricity sales of more than $24 billion (EIA, 2010). The system has multiple characteristics that make it very complex: constraints to the system are quite intricate and include the ramp rates for the generators, thermal constraints on transmission lines, and bus voltage and angle constraints among many others; while most of the subsystems that interact are not linear, such as the energy output and the fuel inputs (Chakrabarti and Halder, 2010).

In order to address the challenges listed above, in this study, we propose a novel two-stage economic and environmental load dispatching framework. In the first stage, a demand forecasting algorithm is presented based on the wavelet transform adaptive method that forecasts the electricity demand for each demanding node within an interconnected bus system. In the second stage, a load dispatching algorithm is presented leveraging Bayesian particle filtering and Newton-Raphson methods for the economic and environmental load dispatching and power balancing, respectively. The framework performs the electricity dispatch by scheduling the generating capacity for each of the energy generation alternatives while ensuring that demand is always met and there is an adequate response to any abnormality; making the electricity generation, transmission and distribution network as robust and reliable as possible. In terms of short-term load dispatch, the proposed approach has been successfully demonstrated at a scale of western Virginia, where the performance of the proposed decision making framework has been demonstrated in a realistic setting using the IEEE 30 bus test system.

## 1.3. Distributed Generation Deployment

Distributed generation is the way in which energy requirements (heating, cooling, lighting, etc.) were met during the original stages of the electric power industry. Technological advances and economies of scale in energy production, transmission and distribution, as well as the increasing role of electricity in people's lives, have gradually enabled the development of the current electric network. In the current electric network most of the distributed generation has been replaced by gigawatt scale plants, located away from urban centers and connected through high-voltage transmission and low-voltage distribution lines linking virtually every building in the country. However, some entities (particularly industrial facilities) found it economically beneficial to have their own electric and heating generation systems independently from the central generation units. Furthermore, entities such as hospitals and telecommunication centers, which need highly reliable power, often installed their own generation units as a backup for emergencies. Even though these sources of distributed generation are usually are not controlled by the electric utilities, the overall electric network may also benefit from them as investments that would have been needed to supply these agents may be diverted to fulfill other needs of the network.

Nowadays, technological advances in microturbines, solar panels, reciprocating engines, digital controls and remote monitoring devices (among various others) have increased the opportunities and applications for "next generation" distributed generation, and given customers great flexibility to tailor energy systems to their specific needs. At the same time, electric utility companies are exploring the possibilities that distributed

generation may help address some of the requirements of the electric system, promoting greater energy security, economic competitiveness and environmental protection. However, increasing the penetration of distributed generation may increase security risks and cause crashes in the energy system, such that extreme conditions where there are maximum and minimum loads in the network determine the maximum amount of distributed generation that can be connected given the current network management and technical limitations of the system (Benitez-Rios et al. 2011) as well as issues with voltage violations, power losses, power quality, and reliability (Ackermann and Knyazkin, 2002). In terms of voltage violations, the presence of distributed generation may help to reduce variations. In terms of power losses, the deployment of distributed generation will generally decrease the amounts of power lost in the system. In terms of power quality, the presence of distributed generation may impact voltage flicker and harmonics. While in terms of reliability, the presence of distributed generation may enhance reliability if used to provide backup power or hinder the overall reliability of the grid if it is not properly interfaced with the network. Taking these factors into account, in this study, a novel multi-objective optimization framework based on particle filtering is proposed to evaluate the most beneficial penetration level of distributed generation, minimizing the total operational cost and the total power loss of the system, without posing security risks to the energy network.

In terms of distributed generation deployment, the main contribution in this work may be summarized as the introduction of a proposed particle filtering framework for multi-objective optimization, and the evaluation of the economic and power loss impacts of the deployment of distributed generation. Multi-objective optimization has been

classically addressed through combination or normalization methods that transform the problem to a single-objective optimization problem (Das and Dennis, 1998); or through the use of different versions of evolutionary algorithms (Fonseca and Fleming 1995, Zitzler and Thiele 1999, Deb, Patrap, Agrawal and Meyarivan 2002). The applications of the deployment of distributed generation have been addressed in various works from a single-objective perspective, that include maximizing the levels of distributed generation penetration after solving effects for voltage profiles (Koutroumpezis and Safigianni, 2009), the effect on the forecasted future base on different penetration scenarios (Foote et al., 2005) and the stability and control of the power networks (Benitez-Rios et al., 2011), among others. Building on these earlier works the proposed study aims at addressing the deployment of distributed generation from a multi-objective viewpoint.

In this work, a particle filtering framework has been presented for multi-objective optimization by adapting the state space model in two distinct ways. First, state vectors are expanded into matrices so that the different dimensions of each of the objectives that are to be optimized are taken into account. Second, in order to increase the accuracy of estimation, we use the non-dominated solution set generated in the sampling stages to update the resampling distributions. This way, as the iterations progress, the algorithm converges to the Pareto front of the sample space. Leveraging this framework, the optimization of distributed generation is evaluated in terms of the total power loss in the system and in terms of the operational costs of such deployment. In terms of deployment of distributed generation, the proposed framework has been demonstrated using the IEEE-30 bus test system. However, it has been constructed in a generic manner so that it can be employed by any networked bus system by inputting its characteristics into the

model, and specifying the number of sources of distributed generation that need to be deployed (or letting the framework suggest the optimal number of sources to use).

### 1.4. Summary of Proposed Contributions

The main contributions of this research may be categorized as theoretical and practical contributions to the integrated electric utility planning and deployment problem. The theoretical contributions mainly reside within the area of simulation based optimization and are directed towards the improvement of a continuous-discrete simulation framework and to the implementation of a particle filtering framework to multi-objective optimization. These contributions may be summarized by the following:

- *Contribution 1: A particle filtering based multi-objective optimization framework.* Here the development of a novel multi-objective optimization framework based on particle filtering that expands a single-objective optimization framework into a multi-objective environment is introduced. The framework includes the development of a sequential importance sampling mechanism for multi-objective optimization problems. These sampling mechanisms leverage the information contained within the non-dominated set of solutions generated by the framework to increase the thoroughness of the generated solution set, and use the non-dominated set's extreme points and the closest extreme points in the search space to ensure that the algorithm does not converge to local optimums.

- *Contribution 2: A continuous-discrete modular simulation and optimization framework*

  The continuous-discrete modular simulation includes the integration of discrete decisions and events with continuous processes within the same simulation environment, where the different spatiotemporal granularities from the discrete and continuous parts of the simulation have to be harmonized. It also includes the modular integration of different resources into the simulation, where different resources may be included or excluded from the simulation environment to accurately represent the available alternatives that are being considered within a specific simulation.

  The practical contributions of this study are related to the evaluation of electric utility capacity plans, the operation of electric utility resources to serve demand in an economic and environmentally friendly manner, and the location of distributed generation resources within an electric networked system. These contributions may be summarized as follows:

- *Contribution 3: The evaluation of energy capacity plans including environmental policies.*

  The evaluation of energy capacity plans includes the use of conventional energy generation sources, renewable energy generation sources and energy storage alternatives and the evaluation of environmental policies in terms of their effect on energy capacity plans, and their effectiveness in incentivizing environmentally friendly energy generation sources.

- *Contribution 4: The optimization of the environmental load dispatch.*

  The optimization of the environmental load dispatch is achieved leveraging Bayesian particle filtering to evaluate the state of the load dispatch at each generation unit, and the Newton-Raphson method to ensure that power balance constraints are met.

- *Contribution 5: The optimization of different distributed generation technologies in terms of minimal cost, power loss and environmental impact.*

  The optimization of different distributed generation technologies in terms of minimal cost, and power loss, has been achieved using the developed particle filtering based multi-objective optimization framework, so that specific different levels of penetration of distributed generation may be evaluated, or the framework may be used to suggest the optimal number of sources of distributed generation to deploy.

# Chapter 2: Literature Review

Previous works presented in the literature are summarized depending on their relationship to the study herein presented. A survey of methods addressing multi-objective optimization is summarized in Section 2.1, and a survey of the Bayesian particle filtering techniques is presented in Section 2.2. Section 2.3 presents a survey on long-term electric resource planning while Section 2.4 presents a survey on methods addressing the environmental economic dispatch problem.

## 2.1. Literature on Multi-objective Optimization

During the past few decades, many researchers have worked on algorithms to tackle multi-objective optimization problems. Some of the employed strategies include the use of evolutionary algorithms (Deb et al., 2002; Zhang and Li, 2007; Tang and Wang, 2012), multi-objective particle swarm optimization (Sun et al., 2008), multi-objective ant colony algorithms (López-Ibáñez and Stützle, 2012), and multiple trajectory search algorithms (Tseng and Chen, 2009), among others.

Evolutionary algorithms are well suited for multi-objective optimization due to their abilities to perform a global search and seek for Pareto optimal solutions simultaneously. The chronological development of some of the established evolutionary algorithms is depicted in Figure 2. Further developments to evolutionary algorithms include Zhang and Li (2007), who present the use of decomposition in multi-objective

17

optimization. Using decomposition, the authors develop a multi-objective optimization algorithm where a multi-objective optimization problem is decomposed into various scalar optimization sub-problems and optimized simultaneously. In order to reduce the computational load, the optimization of each sub-problem is performed only using information from the neighboring sub-problems. This algorithm has been benchmarked using a multi-objective 0-1 knapsack problem and has been found to perform at least as well as the NSGA-II algorithm (Deb et al., 2002). Further developments on evolutionary algorithms come from Tang and Wang (2012) who present a hybrid multi-objective evolutionary algorithm that incorporates the ideas of personal and global best from particle swarm optimization, and use multiple crossover operators to update the population. In their method, the population maintains a record of non-dominated personal best solutions, and uses this to perform an update that explores the region between one of the selected personal best solutions and one of the global best solutions. Chen et al. (2009) extend evolutionary algorithms in multi-objective optimization to include diversity in the solution set as an additional objective when solving the multi-objective optimization problems. Their algorithm is designed around the concept of individual diversity and presents satisfactory results in terms of overall convergence and diversity measures.

Particle swarm optimization tries to mimic the social behavior of animals such as birds, through the use of different interacting particles. These types of algorithms take advantage of both the global best solution and individual best solutions, to guide the particles. Improvements to multi-objective particle swarm optimization methods are presented by Mostaghim and Teich (2003) and Sun et al. (2008), in order to enhance the

searching abilities of particles and ensure an adequate coverage of the search space. Mostaghim and Teich develop the Sigma method as a way to find the best local guides for each particle of the population. This impacts the convergence and diversity of the solutions, especially in problems with a high number of objectives. Sun et al. (2008) present a particle swarm optimizer with cross-over operation in external repository using proportional distributions. This algorithm combines wide-ranged exploration with a cross-over operation, to maintain diversity of new found non-dominated solutions and enhance the solution searching abilities of particles. Furthermore, to prevent solutions from falling to local optimums cluster and disturbance is introduced to examine representative non-dominated solutions from an external repository.
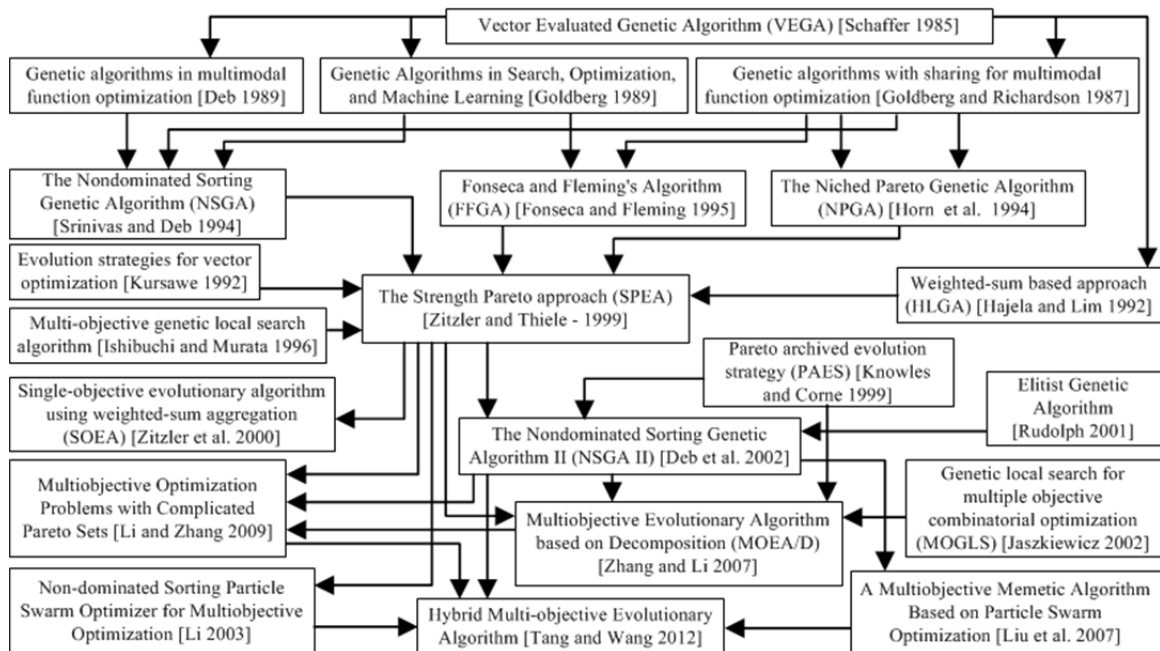


Figure 2: Development of evolutionary algorithms for multi-objective optimization

Ant colony optimization is inspired by the behavior of some ant species where a pheromone trail is laid and followed by the ants. In this technique, solutions are built

based on the components (pheromones) that other solutions have used previously, as well as a random component. Pheromones that are seldom used in the most successful solutions become less probable, while those pheromones that are used frequently have an increasing probability of being incorporated into new solutions. López-Ibáñez and Stützle (2012) present a formulation of algorithmic components that is able to describe most of the multi-objective ant colony optimization algorithms in the literature. Using this formulation the authors evaluate various multi-objective ant colony algorithms, and propose a new family of multi-objective ant colony algorithms where the framework is automatically configured. In order to defy the main drawbacks of the original binary ant colony algorithm on multi-objective optimization (which are the (1) ease of falling at local optimums, and (2) difficulty in finding Pareto optimal solutions) Qing et al. (2010) present a multi-population binary colony algorithm with concrete behaviors. This algorithm uses an environmental evaluation/reward model to reach the global optimum and improve searching efficiency.

Multiple trajectory search algorithms search the solution space by the use of multiple agents. Each entity performs a local search based on the appropriateness of multiple local search methods to the landscape of its neighborhood, in order to improve overall convergence. Tseng and Chen (2009) present a multiple trajectory search algorithm and apply it to various constrained and unconstrained multi-objective optimization problems. The presented algorithm generates a uniformly distributed set of solutions that are separated into foreground and background solutions. Subsequently, it chooses and applies one of the three local search methods on the solutions iteratively. These local search methods begin their search in a very large neighborhood, and contract

the neighborhood step by step until reaching a stopping size. An overall solution is obtained by repeating these local searches for different solutions.

Other techniques to solve multi-objective optimization problems include those presented by Wang et al. (2011) and Ünveren and Acan (2007). Wang et al. (2011) present an analysis of the advantages and disadvantages of Monte Carlo sampling, orthogonal Latin hypercube sampling and Hammerslet sequence sampling, and present a hybrid sampling technique that uses a 1-dimensional uniformity of orthogonal Latin hypercube sampling and multidimensional uniformity of Hammerslet sequence sampling. Based on the hybrid sampling technique, a multi-objective optimization method is developed. In this method, each objective is solved sequentially using the remaining objectives as inequities to form a single objective optimization problem. After the solutions of each individual problem are aggregated, a non-dominated set is generated. Ünveren and Acan (2007) propose a multi-objective optimization using the cross entropy method. The cross entropy method is a stochastic learning algorithm that has been proved to be successful in the solution of difficult single objective optimization problems. The authors extend the cross entropy method to multi-objective optimization by adapting the parameters of the cross entropy model using the information collected from non-dominated solutions on the Pareto front. In order to improve the performance of their method via stochastic learning, they introduce the use of clustering into the non-dominated solution set.

**2.2. Literature on Particle Filtering**

Particle filtering is a sequential Monte Carlo technique that approximates the probability density function of a posterior target state of a system of interest, by producing $N_P$ particles for each time $k$. One particular advantage of particle filtering is that non-Gaussian probability density functions can be modeled accurately. Furthermore, non-linear states and measurements may be modeled without using partial derivatives or linearization.

Since the work of Gordon et al. (1993), particle filtering methods have come across wide application areas such as fault detection (Azimi-Sadjadi and Krishnaprasad, 2004), chemical process estimation (Chen et al., 2004), image/signal processing and target recognition (Gordon et al., 1993; Doucet, et al., 2000; de Freitas, et al., 2000; Azimi-Sadjadi and Krishnaprasad, 2005), and state estimation of shop floors (Celik and Son, 2012).

To leverage some of the advantages that arise from the use of particle filtering Celik and Son (2012) incorporate the use of Bayesian particle filtering into a real-time simulation. Here, in order to determine the sources of abnormalities in the system, efficient inferences are made on the dynamic information from the system, as it becomes available. With this, the simulation may adapt to changing system conditions while incorporating prior information into the analysis and performing reduced sampling on the data. Moreover, significant savings in computational time are achieved by the use of prior information.

Del Moral (2004) discusses interacting particle systems in great detail, while presenting several of their applications including molecular analysis, finance, genetic

algorithms, hidden Markov chains and filtering problems. One of the applications addressed is rare event simulation, which can be used to obtain a solution for knapsack type and other optimization problems. This book by Del Moral (2004) opens a great door for investigating particle filtering methodologies over optimization problems, both in single-objective and multi-objective applications.

Lei (2002) introduces an adaptive random search for quasi-Monte Carlo optimization methods. The proposed approach implements ideas of population evolution from genetic algorithms, which enable the algorithm to adjust the search direction and steps according to the previous search result. The author proves that the algorithm has global convergence and proposes the design of hybrid quasi-Monte Carlo/genetic algorithms as a promising research endeavor.

Míguez (2007) proposes cost-reference particle filters (CRPF) as a method for the estimation of a discrete-time dynamic system. The state estimation is performed through the dynamic optimization of a cost function, which does not necessarily have to be tied to the measurements taken from the system. The proposed method is presented with generalizations that enable the derivation of SIR and Boot-strap filter algorithms, as well as convergence analysis. The CRPF has been used on the Hartmann 3 optimization problem, where it has provided competitive performance with an accelerated random search technique.

Particle filtering has been further used in optimization in the work of Hu et al. (2007) who introduce the model reference adaptive search for global optimization problems. Their method employs a parameterized probabilistic model on the solution space to generate a group of candidate solutions for each iteration. The candidate

solutions are then used to update the model's parameters so that the search in the following iterations will be biased toward the region that contains the best solutions. The authors prove the global convergence of the method in both continuous and combinatorial domains while adding numerical studies to illustrated the performance of the algorithm.

Ji et al. (2008) propose a generalized framework to use particle filtering for optimization incorporating the swarm move method from particle swarm optimization. In their work, the particle swarm optimization update equation is treated as the system dynamic in the particle filtering state space model and the optimization objective function is designed as the measurement of the state. Particle filtering is employed to track the movement of the particle swarm, which is presented as a novel stochastic optimization tool, where the ability of particle swarm optimization to search the optimal position is embedded into the particle filtering optimization method. Benchmark problems are used to show that the proposed method provides a noticeable improvement on both convergence speed and final fitness in comparison with the particle swarm optimization algorithm.

Zhou et al. (2008) present a particle filtering framework for optimization algorithms. Here, the authors consider the problem of global maximization, assuming that the problem can be represented by a real valued function that has a unique optimum. The authors assume that the state corresponds to the unobserved optimal solution of the problem that does not change as time goes by, and that the observations are the optimal function values with some noise. They present both a plain particle filter framework for optimization and a general particle filter for optimization, which is shown to be equivalent to the cross entropy method for optimization.

Míguez (2010) proposes Sequential Monte Carlo minimization procedures (SMCM) to recursively track the minima of a time evolving cost function. The presented SMCM procedures have a structure similar to particle filters, where paths for the state of the system are generated and the fittest paths are stochastically selected, and the surviving paths are ranked according to their cost. The paper presents an induction proof for the convergence of the SMCM algorithm to a sequence of minimizers of the cost function.

Figure 3 summarizes the interaction of particle filtering and multi-objective optimization and different contributions from the literature in each of these fields. Contributions in particle filtering include literature on target recognition, fault detection, shop floor estimation and optimization. Contributions in multi-objective optimization include evolutionary algorithms, multi-objective particle swarm optimization, and ant colony algorithms among others.
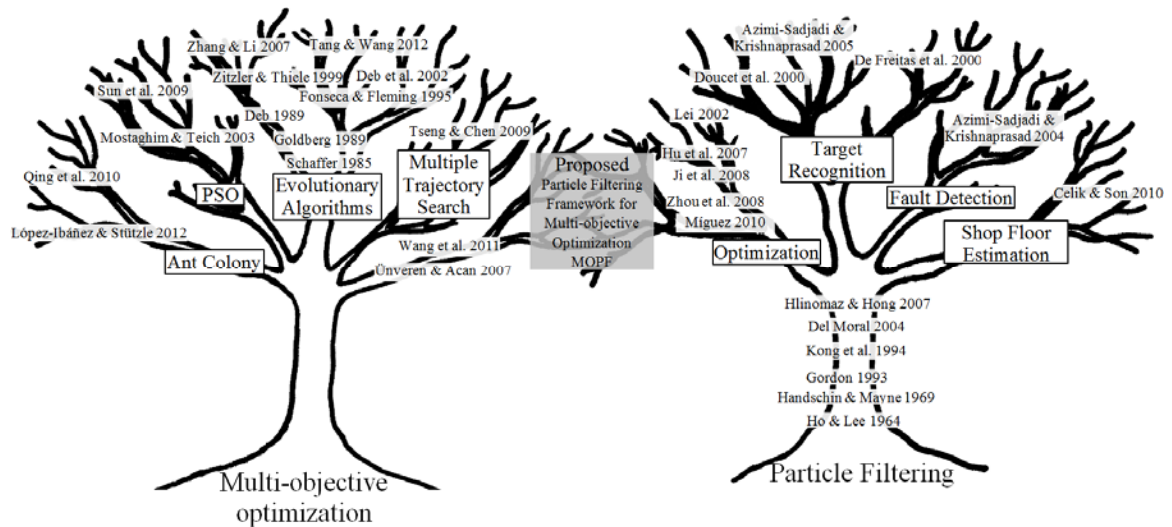


Figure 3: Overview of literature on multi-objective optimization and on particle filtering, including the proposed contribution

**2.3. Literature on Long-term Electric Resource Planning**

The goal of electric utility generation expansion planning is to seek an optimal generation capacity expansion system to meet demand in the most economical manner, subject to reliability and environmental constraints (Stoll, 1989; Wang and McDonald, 1994; and Maricar, 2004). The specific aim of electric utility integrated resource planning is to integrate supply-side and demand-side options in meeting customer energy-service needs and environmental improvements in a least-cost manner (Hobbs, 1995; and Maricar, 2004).

In the past three decades, the electric power system resource planning, including generation, demand, storage and distribution, has faced dramatic changes due to the development of more efficient resources, via the advances in technology and policy variations based on increased environmental awareness concerns. These changes have created a variety of options in resource components (i.e., generation, demand, storage, transmission, and distribution) that need to be addressed considering different criteria and constraints that these options bring about. To this end, researchers have attempted to address the aforementioned high-stakes problem of electric utility resource planning under uncertainty at different scales and scopes by proposing various techniques focusing on generation expansion planning and integrated resource planning of electric utilities. The solution attempts proposed in the literature can be classified into two major categories including economic-analytical approaches and simulation approaches.

From the perspectives of economic and analytical approaches, Malik (2001) presents a technique to model demand-side management (DSM) programs into production costing analyses within the framework of equivalent load duration curve, and

frequency and duration method. Also the importance of incorporating the cycling costs of power plants in the cost-effectiveness analysis of DSM programs is presented. Similarly, Hobbs and Nelson (1992) apply a bi-level nonlinear programming method to the electric utility industry. At the upper level, the model seeks to minimize costs or maximize benefits while controlling electric rates and subsidizing energy conservation programs. At the lower level customers puts their efforts to maximize their net benefit in electricity consumption and investing in conservation. The model's solutions shed light on utility issues including whether there can be a practical difference between various objectives, including minimizing cost and maximizing net social welfare. Regarding the analytical models, Gardner (2000) develops a modified z-substitutes method for the formulation of electric utility resource planning models so that they may be used in more general circumstances, expanding considerably its range of practical applications. Several other research works exploiting the multiattribute utility theory have also been proposed in the literature for particular problems of electric utility resource planning such as selecting portfolios for solar energy projects (Golabi et al., 1981), energy policy making (Jones et al., 1990), environmental impact assessment (McDaniels, 1996) and electric power system expansion planning (Voropai and Ivanova, 2002).

One major limitation shadowing the efforts around the analytical approaches is their inability to capture the great complexity residing in different components and their interlinkages. Therefore, the increased number of significant factors that need to be considered makes a theoretical model difficult to specify. The analytical approaches commonly focus on one single component of the electricity power generation systems. Second, the system input data that needs to be considered in the construction,

initialization as well as the tuning of the models, involves high levels of uncertainty enforcing increased number of freedoms to be considered (e.g., demand, hourly temperature, irradiation data for solar generation systems, wind speed data for wind farms, the price volatility data for fossil fuel-based power plants). As such, the variability of several different kinds of supply and demand for energy makes analytical modeling a prohibitive possibility, and the uncertainty of environmental factors, such as wind speed, makes a simulation incorporating uncertainty based on reliable past data more convenient than previous pure analytical concepts. An additional drawback of some particular techniques such as dynamic programming, and mixed integer programming models is that of high computational complexities as these methods involve exhaustive search to find the optimal sequence of decisions (investment plans in this case) from the initial state to the least-cost final state.

On the other extreme is the employment of simulations by means of physical emulators. In these cases an actual physical prototype is built, however building one of a system as large as the power grid for testing purposes and for observing the effects changes in any of its components is unrealistic, and not affordable; considering the time, and effort that it would take. Besides the enormous costs involved in adding actual additional capacity (e.g. solar panels, a different storage system), the underlying transmission network carrying the generated electricity from the supplier to the customer needs to be reliable and uninterrupted. Additionally, since the process changes over time and depends on past states of the system, a significant amount of interdependence exists among the power grid variables. All these factors make the power grid a complex and uncertain system. Therefore, computer simulation rises as an effective tool to address

this type of problem as it allows us to evaluate feasible investment plans in a realistic environment. As for the simulation models, Tekiner et al. (2010) uses Monte-Carlo simulation to generate numerous scenarios based on the component availabilities and anticipated demand for energy. The problem is then formulated as a mixed integer linear program, and optimal solutions are found based on the simulated scenarios considering the multiple problem objectives. More recently, Mazhari et al. (2011) develop a flexible tool to obtain an optimal capacity of an integrated photovoltaic system with storage units. Their proposed tool is based on hybrid (system dynamics model and agent-based model) simulation and meta-heuristic optimization with a goal of minimized investment and operational costs. Additional works in the literature following this line of research are compared in Table 1.

### 2.3.1. Prospects and Obstacles to the Development of Nuclear Energy Generation

Critical factors and concerns to the development of nuclear energy generation have been studied in the literature including the work of Marcus (2000), Trehan and Saran (2003), Rashad (2006), Ichihara (2010), and Gudowski (2005). The proposed framework relies on the feasibility of nuclear energy generation as a viable alternative within utility capacity planning. The works in this subsection present the factors that enable nuclear energy generation as a viable alternative within utility capacity planning, and also present those factors that have been regarded as barriers, and which may need to be addressed.

Table 1: Comparison of selected works on electric utility capacity planning

| Authors/ Year | Chowdhury et al., 2003 | Gurgur and Jones, 2010 | Papandreou and Shang, 2008 | Mazhari et al., 2011 |
|---|---|---|---|---|
| Specific problem addressed | to satisfy increasing customer demands of lower rates and higher service reliability in the competitive market | to calculate wind generation capacity values | to identify the sustainable design of utility systems that satisfies both economic and environmental goals | an optimal mixture of capacities from solar generation units as well as storage capacities |
| Approach | a probabilistic reliability based distribution system expansion and investment model | a Monte Carlo simulation based on Markov chains as a function of system penetration | a multiobjective optimization mixed integer linear programming model | hybrid (system dynamics model and agent-based model) simulation and meta-heuristics based optimization algorithm |
| Benefits | ▪ method identifies the best location for units in the local area and the minimum output requirements of the distributed generator(s) depending on the load | ▪ captures dominant factors of system uncertainty ▪ is mathematically tractable | ▪ minimization of costs are combined with minimization of environmental impacts ▪ most of the gaseous emissions are addressed | ▪ a top-down approach for capacity planning versus a bottom up approach for demand forecasting are coherently combined |
| Limitations/ Areas of improvement | ▪ right generator size for the cost-effectiveness of the additional generation should be analyzed using reliability techniques | ▪ estimation are sensitive to the choice of normal distributions | ▪ due limitations on available data availability only part of the sustainability indicators were investigated | ▪ validation with real consumption data of households is necessary ▪ smart-grid, and other renewables such as wind can be included |
| Scale of the system | small/medium | small | small/moderate | moderate |
| Computational burden | light | moderate | heavy | moderate |

Marcus (2000) studies the barriers and opportunities for the inclusion of nuclear energy generation into capacity planning. Here, the growth in energy demand and

increasing concerns related to climate change, are identified as key drivers to for the deployment of new nuclear power plants. On the other hand, the major barriers are related to cost, nuclear proliferation, safety and nuclear waste management. In addition to this, Marcus (2000) also studies the U.S. DOE Nuclear Energy Research Initiative program and the Accelerator Transmutation of Waste program; these programs are presented as critical initiatives focusing on the removal of barriers to the expansion of nuclear energy generation.

The work of Trehan and Saran (2003) proposes the resurgence for nuclear energy generation deployment based on advances in terms of reliability and cost, coupled with encouraging changes in the public and governmental opinion. This paper states that because of the accidents at Chernobyl and Three Mile Island no new nuclear power plants have been licensed since 1979, but recommends that the deployment of nuclear energy be revived. For this revival Trehan and Saran (2003) suggest the use of modular power plant construction, standardization, and one-step regulatory approval. Finally, the paper states that the development of nuclear energy generation is encouraged by the Kyoto protocol as an alternative, renewable technology, to reduce greenhouse gases product of fossil fuel combustion.

To create a common understanding on the direction that nuclear energy is taking, Ichihara (2010) addressed problems faced by both nuclear generation and the electric industry as a whole, including costs, energy supplies and environmental concerns. Further, Ichihara (2010) presents the state of the art of nuclear energy generation and future technologies, as well as strategies for their implementation.

Rashad (2006) states that innovation to reactor and fuel cycle technologies that ensure reduced nuclear waste, proliferation resistance and increased safety, is necessary for any major expansion in the deployment of nuclear energy generation. However, further innovation is also needed to nuclear fuel and facilities, addressing the risk of sabotage, theft and terrorist attacks. Rahsad (2006) also addresses other issues related to nuclear energy generation deployment, including economic competitiveness, safety waste management and environmental protection. This paper concludes that nuclear power may be considered as the only energy source that can provide electricity on a large scale with minimal environmental impact.

One of the largest challenges to the deployment of nuclear energy generation is posed by nuclear waste management poses. Gudowski (2005) presents the status of nuclear waste management and proposes waste partitioning and transmutation as an alternative to address this challenge. According to Gudowski (2005), the requirements for deep geological repositories of nuclear waste may be reduced through the use of a nuclear waste partitioning and transmutation system, however for this system to be economically viable there needs to be a commitment to the deployment of nuclear energy generation.

Another factor that presents both challenges and opportunities to nuclear energy generation is public policy. The enactment of legislation that hinders the development of other technologies such as taxes on emissions may incentivize nuclear energy generation; while, the enactment of legislation that restricts the management of nuclear waste, may disincentive the development of nuclear generation. Our proposed framework evaluates the effect of deploying nuclear energy generation within an integrated utility capacity plan in terms of cost and emissions. Based on this evaluation, the level for an emissions

tax that effectively incentivizes the deployment of nuclear energy generation may be established.

The incentives for the deployment of nuclear energy generation from the Energy Policy Act of 2005 (EPAct) are studied by George (2007). Here, George (2007) highlights the key features intended to incentivize the development, construction and operation of new nuclear power plants, within the EPAct. However, George (2007) cautions that because of the large financial barriers for new nuclear energy projects, the incentives from the EPAct may be insufficient to effectively lead to new nuclear energy projects. This paper concludes that if the risk factors concerning financing of new nuclear projects are not adequately addressed, it is possible that the EPAct may only spur the construction of a very few projects, before the subsidies available through the program are exhausted.

### 2.3.2. Utility Capacity Planning with Nuclear Energy Generation

There are various approaches in the literature for the integration of nuclear energy generation into a comprehensive utility capacity plan, including the work of Dapkus and Bowe (1984), Garrity and Wilkins (1993), Sheu (2008), and Kessides (2010). The work of Dapkus and Bowe (1984) uses stochastic dynamic programming to address the electric utility expansion planning problem. The proposed approach is tested on several case studies, where uncertainty in demand and technological availability is evaluated. Dapkus and Bowe (1984) consider that there is not a specific plan that is optimal under

uncertainty, and state that the amount of certainty for the adaptation of new technologies and the value of information regarding technological availability should be studied.

Garrity and Wilkins (1993) present a study of the potential of nuclear power generation, using boiling water reactors, to meet the energy generation needs of the U.S. over a 15 year planning horizon. In their analysis, Garrity and Wilkins (1993) determine the needs for additional energy generation for the regions of the North American Electric Reliability Council. These needs are forecasted based on a the national energy consumption, regional energy generation, peak energy consumption and the commission and decommission of energy generation plants, among others. Garrity and Wilkins (1993) perform the economic analysis based on an expansion planning model that calculates the optimal expansion for each region, and includes sensitivity analyses regarding both capital costs and fuel prices.

Sheu (2008) addresses nuclear energy generation capacity through the use of a multi-objective optimization programming approach. Building on the concepts of green supply chain management, Sheu (2008) formulates a linear multi-objective model to optimize the operations of both the nuclear power generation, and the corresponding induced-waste reverse logistics. Sheu (2008) states that using the proposed approach, the induced environmental impact, including the corresponding costs and risks, may be improved by up to 37.8%.

Kessides (2010) uses a cost-benefit analysis to evaluate the risks and uncertainties of nuclear energy generation, as well as other load base generating technologies. Furthermore, Kessides (2010) proposes the standardization of variables and parameters for nuclear power plant costing. Finally, Kessides (2010) proposes Monte Carlo

simulation to capture the different risks of nuclear power, and states that the evaluation of small scale reactors should be assessed through the use of real options.

## 2.4. Literature on Short-term Electric Load Dispatch

The goal of environmental economic load dispatch is to determine how to allocate the electric load demand across the different energy generating alternatives so that the cost and emissions are minimized, while ensuring that the operational restrictions and other system limitations are met. Among the main challenges regarding EELD are those regarding the relationship between power output and amount of each pollutant generated at each power plant, and those regarding the way to assign costs to the emitted pollution (Talaq et al., 1994).

A summary of the techniques addressing the EELD has been presented by Talaq et al. (1994). In their article, they classify the models into six categories depending on the strategy used. The first strategy addresses the minimization of emissions problem while disregarding costs as leveraged by Gent and Lamont (1971) and by Cadogan and Eisenberg (1975). The second strategy includes a maximum allowable cost on top of the first strategy. The third strategy proposed by Finnigan and Foaud (1974) minimizes the costs while constraining the total emissions of the system. Variations of these strategies lead to strategies four and five. In strategy four, Sullivan (1972) and Sullivan and Hackett (1973) extend strategy one to include ground level emissions concentration. Strategy five is a variation of strategy three that seeks to minimize the fuel costs of generation. Strategy six starts combining economic and environmental objectives, where

Lamont and Gent (1973) describe a method to minimize a tax on sulfur emissions, while Delson (1974) presents a method that assigns a price to the emissions and Zahavi and Eisenberg (1975) present the trade-off curve between emissions and costs. Other approaches addressing the EELD problem include Particle Swarm optimization (PSO), Bacteria Foraging Algorithms (BFA), Simulated Annealing (SA), differential evolution (DE) and $\epsilon$-constraint techniques.

The $\epsilon$-constraint technique used by Vahidinasab and Jadid (2010) takes one of the two objectives of the EELD as a preferred objective, namely to minimize costs, and the other objective, to minimize emissions, is taken as a constraint. The constrained objective is limited by calculated maximum and minimum values. The minimum value depends on the individual optimization of the system taking that particular constraint into consideration, while the maximum value depends on the performance of that objective when it is not considered and the preferred objective is optimized. This range for the emissions objective is split into  intervals, and the cost is optimized while constraining emissions to by each of the intervals. This way, the feasible solutions of these optimizations are Pareto-optimal. This approach has been found to be more efficient than the Strength Pareto Evolutionary Algorithm presented by Abido (2003), and can be easily modified to include other objectives. However the inclusion of these objectives increases the complexity of the algorithm exponentially.

A simulated annealing technique for particle swarm optimization is used by Kuo (2005) to address the EELD with a large penetration of wind energy. Here PSO is altered so that new velocities for the particles are accepted using the temperature parameter  of SA, therefore the velocities are not completely random as in the regular PSO. This

feature makes the algorithm more efficient than the traditional PSO. Along with this SA-PSO technique, a method to choose between the different Pareto-optimal solutions generated (called interactive bi-objective programming with variable trade-off) is used. Here, an iterative method is developed for the decision makers to adjust the weights given to the different objectives, which in turn enables them to reach the desired levels for each objective within the Pareto-optimal set. This method is similar to the goal-attainment method, but the weights of each do not need to be evaluated along the entire Pareto-optimal front, which leads to better computational performance. This method has been found to be more efficient than PSO and GA.

Gong et al. (2010) present a hybrid optimization algorithm based on PSO and DE. The algorithm is designed so that a PSO with time variant acceleration coefficients is used to explore the entire search space, while DE is proposed to explore the sub-space with sparse solutions. The proposed algorithm integrates various techniques including time variant acceleration coefficients, an external archive of elite particles, and a crowing distance-based approach. Furthermore, the algorithm introduces a modification strategy for power balance constraints, to ensure that any generated solution may be modified until it meets the power balance constraints. The proposed algorithm provides a diverse and well-distributed non-dominated set and is a viable alternative for solving the EELD.

Wu et al. (2010) present a multi-objective DE algorithm to address the EELD. In this version of the EELD, system power loss is treated as an extra objective for minimization and is included as a third objective. The differential evolution algorithm is based on a crossover and a mutation operation to generate new solutions, and checks the proposed new vectors against those that generated them for dominance. In the case that the vectors

are non-dominated with respect to each other the one with the lees crowded vector, with respect to the crowding entropy diversity measure is kept to further generate solutions. The proposed algorithm uses an external archive to store the global non-dominated solution set that is built using all of the solutions that the algorithm has found so far, in order to ensure that no non-dominated solutions from a "more crowded" vector are lost. The proposed approach is found to be more effective than other multi-objective evolutionary algorithms.

# Chapter 3: Continuous-Discrete Modular Simulation and Optimization for Electric Utility Resource Planning

A continuous-discrete modular simulation and optimization (CoDiMoSO) framework is developed as the most reasonable method for assessing the different options for creating a real system with a magnitude and cost at the utility scale. Through the proposed framework, the best combinations (capacities and portfolios) of different energy generation systems can be foreseen. For instance, a solar farm can be quintupled quickly in the model and its impact can be observed instantly, while the same experiment would be costly, difficult, disruptive, and extremely time consuming when designed for real world prototypes. The rearrangement of the relative locations and size of the city and different load profiles (i.e., number of industrial, commercial, residential and transportation customers) can be updated dynamically as new and more relevant information is available over time. As such, modular simulation allows for a great deal of flexibility in modeling, costs significantly less than its emulator type counterparts. The proposed modular simulation was developed with a great emphasis on credibility, a credibility that resides in the applied analytical models and well-established literature. Via the visualization features (i.e., connection arcs between different modeling units), the simulation model exhibits clarity in the way the model works such as the flow of entities and the interdependency amongst variables.

Several challenges exist while modeling the power grid system using a continuous-discrete modular simulation optimization approach. First, the best fitted distributions of the real data as well as their associated variability adjustment factors need to be defined in order to model the variability in demand, solar radiation, and wind speed with accuracy. Research from credible data sources has to be conducted in order to obtain the correct parameters for greenhouse gas (GHG) emissions, energy generation efficiency, and cost. The parameterization in the design, interactions and mechanics of an energy system such as the one studied in this work, is particularly important in these systems in order to reflect the changes that occur on a discrete basis and their interaction with the energy levels and other components of the system that are simulated on a continuous basis with accuracy. In real energy systems, energy is produced continuously and instantly consumed, stored or grounded. In our CoDiMoSO framework, this continuous production is simulated by entities created with fixed inter-arrival times, where each entity contains an amount of energy relative to the power output of the source over the inter-arrival time. The entity is subsequently sent to the grid and either stored, consumed or grounded. Limits for decision points have been determined in order to enable proper distribution of the energy and prevent some entities with higher energy levels than others from causing abrupt changes in the system. By having significantly small inter-arrival times (as close to the continuity as possible) compared to the overall simulation run-time, the loss of precision in the approximation (and hence in the framework), is minimized while still gaining the advantages in computational performance from discretization (with less computational burden than that of circuit-level model). The stoichiometry associated with the fossil fuel plant inputs and the resulting

greenhouse gases (costs to the environment) is also demanding as it requires detailed knowledge gained from the combination of research and collaboration in various disciplines such as chemistry, and material sciences. Figure 4 shows the overview of our proposed CoDiMoSO framework for the capacity planning of nuclear power generation. The proposed framework includes four major simulation modules for generation, storage, transport and demand; and one multi-objective optimization module, based on particle filtering. These different modules include various sub-modules. The module for energy generation is composed of sub-modules for fossil fuel, renewable and nuclear energy generation. The module of energy storage has sub-modules for compressed air energy storage and for energy storage using batteries. The module for energy transmission simulates the energy distribution grid, and includes a step-up and a step-down substation. The module for energy demand includes demand from residential, commercial, industrial and transportation sectors. The multi-objective particle filtering optimization (PFO) module, samples the state of the system, using the operational level of the different subsystems as well as the amounts of grounded electricity and load shed, in order to elaborate a non-dominated set of capacity plans, in terms of cost and emissions.

The modularity with which the framework has been built enables the framework adaptability to include the modules that are of particular interest, and exclude those that are not. It allows to study a system or a subsystem on its own or together with its interconnected systems. For instance, we can study a system in particular that has all of the submodules for generation in Module G, storage in Module S and demand in Module D, or a system that only has renewable energy generation from Module G, CAES from Module S, and residential demand from Module D. This modular approach provides a

useful way to investigate the large scale effects of very specific details within each component of the considered systems and enables the incorporation of different scenarios within each component of the systems without compromising the complete framework. Modularity is achieved using standardized connection points throughout the model where the different submodules link into the framework. It is because of this that, when an entity reaches Module T, it is always handled similarly regardless of its origin; it is indifferent for Module T if an entity comes from Module G or from Module S, since its attributes are standardized. The standardized modular connection points are used to connect entities leaving each of the submodules in Module G to Module T, entities leaving each of the submodules in Module S to Module T, entities leaving submodule T to each of the submodules in Module S, and entities leaving submodule T entering each of the submodules of Module D.
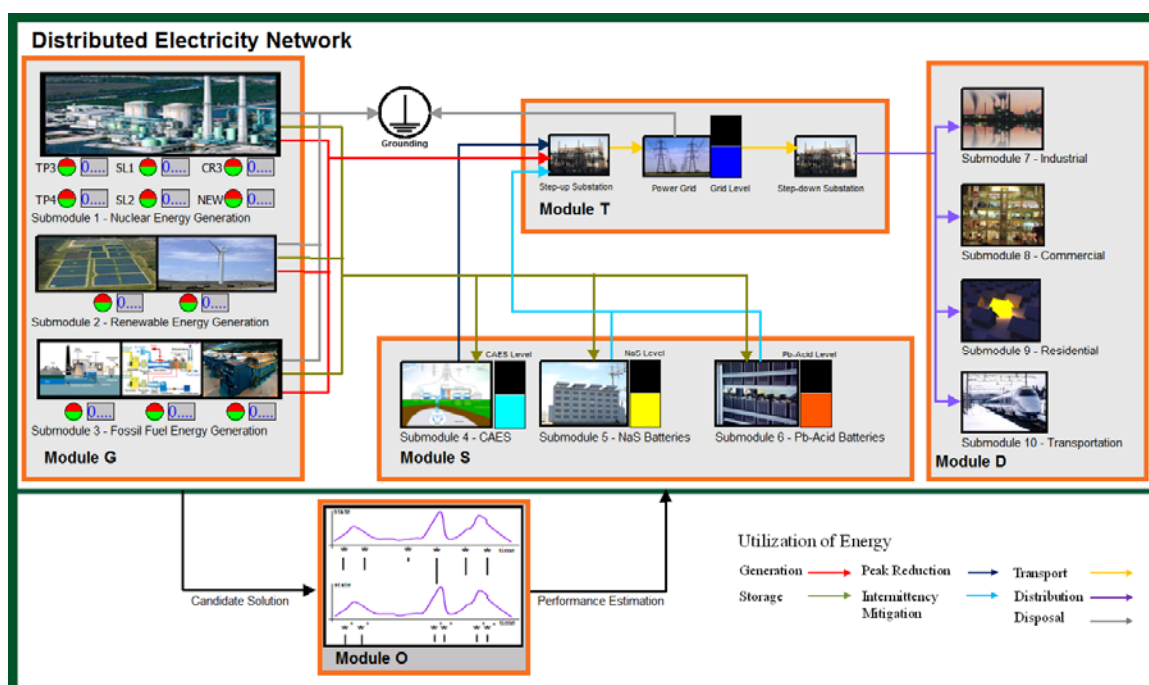


Figure 4: Overview of the major components of our proposed CoDiMoSO framework

The proposed CoDiMoSO framework operates by evaluating the cost and emissions of the different energy capacity plans that may be implemented, and is very useful to evaluate the implications of different public policy scenarios dictating regulations to the emissions resulting from energy generation. The non-dominated solution sets from the CoDiMoSO framework show what costs are incurred by achieving different levels of greenhouse gas emissions.

In order to obtain the non-dominated solution sets the CoDiMoSO framework loads the details and restrictions regarding each of the specific operational components of the different energy generating sources into a database. The database then sends the historical data to the CoDiMoSO. The database also sends these initial parameters to the PFO module as the initial state of the system, which are used to construct the prior probability density function for the system.

The PFO module updates the weights of the different energy sources and estimates the posterior state on the system. This is achieved by recording the state of the system, in terms of the energy demand and the net energy generation from each of the generation sources when the amount of energy produced by the integrated system is inadequate. The amount of energy produced by the system is considered inadequate in two cases. The first case includes moments when there is not enough energy to meet the demand and loads have to be shed, and the second case includes times when there is excess energy and it has to be grounded. As a result of this, the PFO module generates a new importance function in terms of the capacity of each energy generation alternative, whose goal is to minimize the number of times when the demand is unmet and when

excess energy has to be grounded. This function is then used to generate a new proposed capacity plan which is sent to the hybrid simulation module for evaluation.

The CoDiMoSO evaluates the performance of the proposed capacity plan. The PFO module tracks the state of the system throughout the length of the simulation. Based on the performance of the capacity plans and the updated state of the system, the particle filtering module recalculates the weights of the parameters in the simulation and iteratively elaborates new importance functions. This process continues until the expected mean performance newly proposed capacity plans is such that there are no benefits in terms of cost or emissions, compared to those achieved by the capacity plans in the current non-dominated set. At this stage the capacity plans that are part of the non-dominated solution set are considered the Pareto optimal for the predetermined scenario. After different scenarios have been evaluated a comprehensive plan with the optimal strategy to respond to each scenario is built. Figure 5 shows our proposed simulation optimization algorithm based on particle filtering.
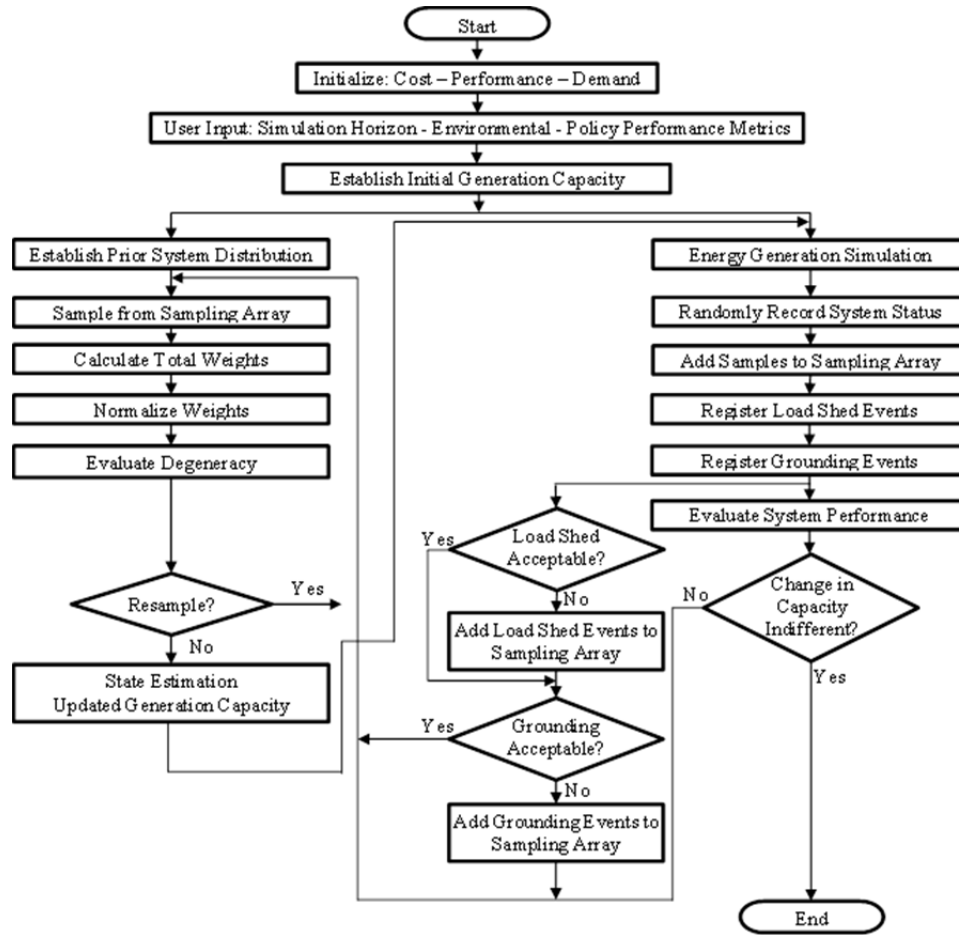
Figure 5: Overview of the particle filtering based optimization module

## 3.1. Energy Generation Module (G)

The module for energy generation, Module G, allows us to represent different types of energy generating system with precision, without impacting the rest of the systems in the model. Within Module G, Submodule 1 represents solar energy generation involving its capacity, efficiency, and the solar irradiance. Submodule 2 represents wind energy generation involving its capacity, efficiency, and the wind speed. Submodule 3 represents coal fired energy generation considering its capacity, GHG emissions, and specifics regarding its efficiency (e.g. effects of the furnace and the steam cycle).

Submodule 4 provides the details of natural gas fired energy generation involving a combined cycle; while submodule 5 represents oil fired energy generation. Finally, submodule 6 represents nuclear energy generation. Details of these submodules depicted in Figures 6 and 7 (using Arena 13.5 simulation package) are provided below.
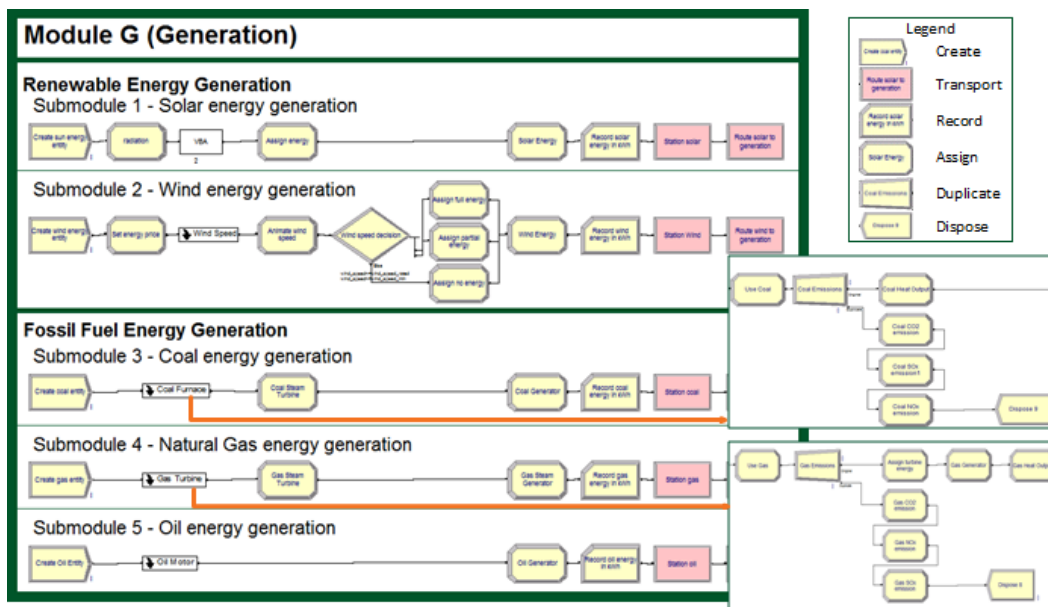


Figure 6: Energy generation from renewable and nonrenewable sources

### 3.1.1. Renewable Energy Generation

The renewable energy generation has been incorporated to Module G in order to represent the technologies that use renewable resources (e.g., sunshine, wind, hydro power) without a depletion concerns. While renewable energy generation has a low impact on the environment, it depend on resources that are very often location specific (e.g. wind energy generating plants can only be placed in locations where the wind meets certain requirements, and hydroelectric power plants can only be placed on bodies of water that meet some specific conditions). The energy generating systems included in

this study are presented below with the inclusion of other advantages and disadvantages specific to each system, and their applicability to the case of Florida.
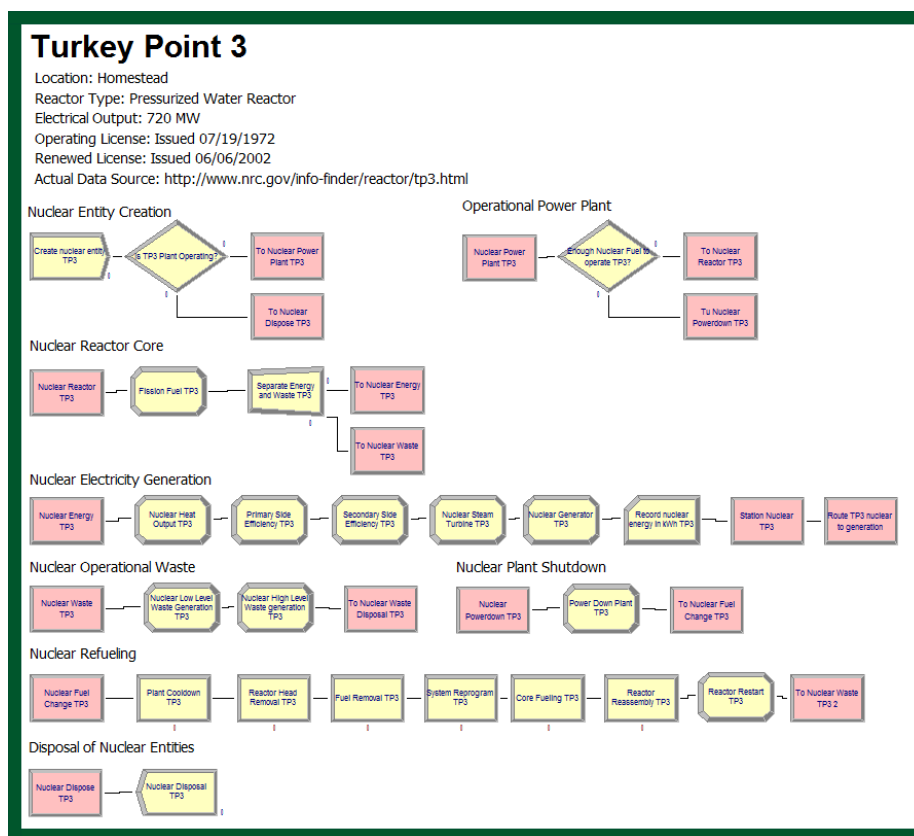


Figure 7: Nuclear energy generation sub-module (Turkey Point 3)

### 3.1.1.1.    Solar Energy Generation

The generation of electricity from solar energy is renewable, as it harnesses the power from the sun; clean, as its generation does not emit any air pollutants into the environment; and silent, as solar farms do not cause any audible contamination to their surroundings.   Furthermore, photovoltaic (PV) devices are based on a modular technology that can be expanded and applied to almost any landscape and at various

different scales (Kobayashi, 2003). Typical solar systems (PV cells that are grouped into panels and arrays of panels in a photovoltaic solar farm) are well-known for little maintenance required by them (Ho et al., 2009). The panels are made of tempered glass and are tested against extreme weather conditions. Most commercially available solar panels have a 25-year performance warranty with additional warranties up to 10-years for inverters and other system components. Solar energy also avoids the risks associated with disruptions in fuel supply and its associated price instability since there is no use of fossil fuels (Suna et al., 2008).

On the other hand, PV solar generation heavily depends on the solar irradiation that arrives at the Earth's surface. This solar irradiation is not constant and depends on the specific location, time of the day, season of the year, and weather conditions; affecting the amount of energy that can be produced regardless of the demand requested. Therefore, solar energy systems give rise to the need for energy storage systems and for alternate energy generation systems in order to ensure that the demand is met at all times (Dinçer, 2011). Another drawback of PV energy generation as of today is that its cost significantly exceeds that of traditional energy generating systems, even though this cost relationship is expected to become more favorable towards PV generation as technology continues to advance (Erdogu, 2009).

Known as the Sunshine State, Florida is the second largest solar energy generating state in the U.S. The 25MW, DeSoto Next Generation Solar Energy Center, located in DeSoto County, is the largest PV plant in the country. With more than 90,500 solar panels, its annual generation is enough to serve about 3,000 homes while preventing the emission of more than 575,000 tons of greenhouse gases over the project duration,

something equivalent to removing more than 4,500 cars from the road every year. The Space Coast Next Generation Solar Energy Center, located at Kennedy Space Center, has an estimated annual generation of 10MW (FPL, 2010). Furthermore, Florida has plans to construct additional PV farms such as the Babcock Ranch Solar Center in Charlotte County, the Florida Heartland Solar Center in Glades County and the Manatee Next Generation Solar Energy Center in Manatee County, as well as a farm in Hendry County. Extensive actions (including abundant proposals for new PV facilities) taken by the state of Florida to make a green state have led us to select it for our case study, and in order to preserve its validity, the continuous-discrete modular simulation and optimization framework described in this study is built considering the realistic environmental conditions. Furthermore, our decision making framework incorporates the characteristics of the PV panels that are currently being used and/or planned to be used in the future solar farms, especially in the ones in Florida.

Table 2 shows the electrical characteristics of selected PV panels that have been used in real-world industry size energy generating facilities with capacities of more than 1MW, including the SunPower modules used in the DeSoto Solar Energy Center and in the Space Coast Solar Energy Center, collected from various reliable sources including BP Solar, GoGreen Solar, Neco, Solar Home, SunPower and SunTech. Modules from Mitsubishi Electric have also been included into the comparison, even though these specific models are generally deployed in generating facilities of less than 1MW. Among the characteristics of these solar panels, the two most significant ones (namely cost and efficiency), are conflicting with each other such that a panel with a low cost commonly does not have a high efficiency.

Table 2: Comparison of characteristics of commercially used PV panels

| Manufacturer | Mitsubishi Electric | Kyocera | Sharp | Evergreen | Suntech | SunPower | BP Solar |
|---|---|---|---|---|---|---|---|
| Project Employing the PV Panel | Ballentine Vineyards | University of California, San Diego | Denver Intl. Airport | Neustrelitz Solar Park | Alamosa Solar Plant | Space Coast/ DeSoto Solar Energy Center | Long Island Solar Project |
| Generation Capacity | 87 kW | 1.2 MW | 2 MW | 8 MW | 8.2 MW | 10 MW/25MW | 32 MW |
| Date | Aug. 2007 | Sep. 2008 | Aug. 2008 | Jun. 2010 | Dec. 2007 | Apr./Oct. 2010 | Mid 2011 |
| Solar Modules | PV-UD175MF5 | KD205GX-LP | NU-U240F1 | ES-A-205 | STP280-24/Vd | E19 / 318 | BP 3220T |
| Peak Power ($P_{max}$ in watts) | 175 | 205 | 240 | 205 | 280 | 318 | 220 |
| Peak Power Voltage ($V_{mop}$ in volt) | 23.9 | 26.6 | 30.1 | 18.4 | 35.2 | 64.7 | 28.9 |
| Peak Power Current ($I_{mop}$ in amper) | 7.32 | 7.71 | 7.98 | 11.15 | 7.95 | 5.82 | 7.6 |
| Open Circuit Voltage ($V_{oc}$ in volt) | 30.2 | 33.2 | 37.4 | 22.8 | 44.8 | 64.7 | 36.6 |
| Short Circuit Current ($I_{sc}$ in amper) | 7.93 | 8.36 | 8.65 | 12.1 | 8.33 | 6.2 | 8.2 |
| Max. System Voltage (in volt) | 600 | 600 | 600 | 600 | 600 | 600 | 600 |
| Module Efficiency ($\eta$) | 12.70% | 16.00% | 14.70% | 13.10% | 14.40% | 19.50% | 13.20% |
| Dimensions | 65.3" x 32.8" | 59.1" x 38.0" | 64.6" x 39.1" | 65" x 37.5" | 77" x 39.1" | 61.4" x 41.2" | 65.6" x 39.4" |
| Price (in dollars) | ~731.03 | ~682.55 | ~741.34 | ~794.43 | ~638.40 | ~[1900-2089] | ~686.95 |

Legend:

The PV panel types considered in this study due to their efficiency and cost characteristics

(BP Solar, 2010; FPL, 2010; Solar Home 2010; Sunpower 2010; Suntech 2010)

In some solar farms, solar arrays may be connected to sun tracking devices in order to maximize the irradiance on the panels, and thus maximize their electric output. Table 3 shows the maximum number of solar modules that can be placed in a hectare, the maximum number of panels that can be connected into a single tracker block, and the maximum number of these tracker blocks that can be installed within a hectare focusing on the two PV panel types considered in this study.

Table 3: Characteristics of the PV panels selected for the case study of this research

| Manufacturer | Module | # of Cells | Width (mm) | Length (mm) | Panel Area ($m_2$) | Area ($m_2$) * | Max. Panel/ ha | Max. Panel Output ($W$) | Max. Panels/ Tracker Block ** | Tracker Blocks/$ha$ |
|---|---|---|---|---|---|---|---|---|---|---|
| Suntech (Lowest price) | STP280-24/Vd | 72 | 992 | 1956 | 1.941 | 3.881 | 2577 | 238 | 105 | 24.5 |
| SunPower (HighestEfficiency) | E19/318 | 96 | 1046 | 1559 | 1.631 | 3.261 | 3066 | 318 | 79 | 39 |
| * Using Ground Coverage Ratio of a Sun Power T0 Tracker of 0.5 | | | | | | | | | | |
| ** Using Sun Power T0 maximum tracker block power of 25kW, and rounded up | | | | | | | | | | |

(Suntech 2010; SunPower 2010)

PV devices are employed to convert solar energy into electricity. The photoelectric effect is the emission of electrons from the surface of a metal when exposed to sunlight, as shown in Figure 8. Once this physical process is applied to millions of electrons, sunlight is converted to electricity. The PV cells placed on solar arrays can be connected in series or parallel, and are used to obtain the required direct current (DC) output for an inverter that converts the current to alternating current (AC).

A solar cell's (or module's) maximum electrical power ($P_m$) is defined as a function of its electrical efficiency ($\eta$), its area ($A$) and the solar irradiance ($G_T$) as in Eq. (1) under standard test conditions (Skoplaki and Palyvos, 2009; and Dagdougui et al., 2010). Standard testing conditions are defined as 1000 W/m$_2$ solar flux conforming to

the standard reference AM 1.5G spectrum, and temperature of 25°C. The use of this flux value is quite convenient, as the efficiency in percent is numerically equal to the power output in mW/m$_2$ (Markvart, 2000).
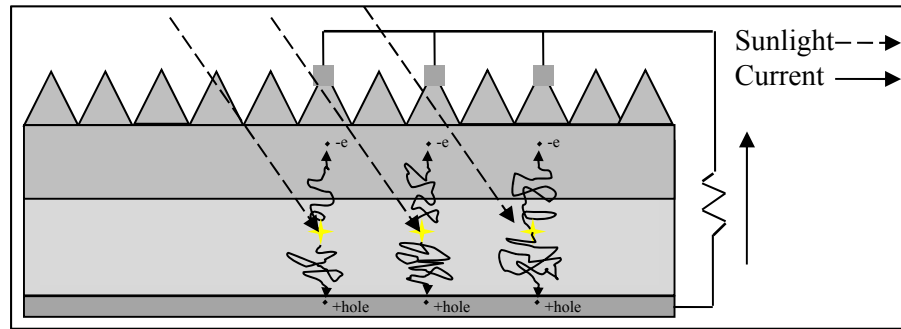


Figure 8: Generation of electricity from sunlight using a PV solar cell

The functionality of the PV devices explained above is incorporated into the proposed CoDiMoSO framework via Eq. (1). In this submodule (shown on Figure 6), entities are assigned with a value for solar irradiance using a schedule which assigns irradiation corresponding to the radiation of the particular hour of the year that is being simulated. The entities then enter a Visual Basic Application (VBA) element to assign a level to radiation, after which the energy as well as its cost are calculated using a variable that specifies the area of PV panels and the efficiency of these panels. The overnight costs of $6,171 per kW and annual fixed costs of $11.94 per kW, and a modular efficiency of 19.5% are employed in our framework based on the Energy Information Administration report (EIA, 2011), and SunPower PV panels, respectively. The solar radiation was calculated using the data collected from the pyranometer located at the University of Miami (UM) and the National Solar Radiation Database (NSRDB) of the National Renewable Energy Laboratory (NREL) as detailed in the next section.

$$P_m = \eta \times A \times G_T \hspace{2cm} \text{Eq. (1)}$$

### 3.1.1.2.    Data for Solar Irradiance

For accurate estimation of the solar energy generation via PV technology, accurate input of solar irradiation is critical.  However solar radiation data is rarely available in weather records, since its precise measurement requires steadily maintained fragile devices, such as pyranometers (Bois et al., 2008).  None the less, recent advances in remote sensing and image analysis make it possible to retrieve global daily solar radiation from satellite data (Solanki et al., 2005) leaving spatial variations of solar irradiation provided by terrain slope and aspect unaddressed.  In this study, in order to estimate the solar irradiation accurately, we combine satellite-sensed data with the data obtained from a locally positioned pyranometer, capturing spatial and temporal variability of solar radiation specific to the Miami area.  The satellite-sensed data is obtained from NREL's NSRDB. NREL collects solar irradiance data at both the Miami International Airport and at the Kendall-Tamiami Executive Airport, among many other sites.  These two sites are both approximately ten miles from the University of Miami; the Miami International Airport is positioned to the north of the university, while the Kendall-Tamiami Executive Airport is to the southwest.  The spatial and temporal variability data is obtained from UM-Industrial Assessment Center's Kipp and Zonen CMP-11 pyranometer which is located on the roof of engineering building at the University of Miami (see Figure 9).  The CMP-11 is a fast response pyranometer, with latency of less than five seconds, capable of collecting radiation data of up to 4000 $W/m^2$ designed for PV panel and thermal collector

testing. It has a sensitivity of $8.74 \ \mu V/W/m^2$ and it has been programmed to record solar irradiance data with intervals of one minute.


Figure 9: The University of Miami's Kipp and Zonen CMP-11 pyranometer

For this study, the irradiation with the spatial and temporal variability collected using the University of Miami's CMP-11 pyranometer, is used in conjunction with the built-in features of the Minitab software package, to determine the distribution that fits the best to the data (with the highest $R^2$ value); the best fitted distribution is shown in Eq. (2). Solar irradiation data obtained from NREL's NSRDB at the Miami International Airport and the Kendall-Tamiami Executive Airport, has also been fitted the best to the equation given by Eq. (3). In Eqs. (2) and (3), $WHr_{UM}$ is the solar irradiance in watt-hour per square meter, $Hour$ is the independent hour of the day, and $WHr_{NREL}$ is the solar irradiance.

$$WHr_{UM} = 681.846 \ e^{-0.0837294 \, * \, (Hour \, - \, 12.6742)^2} \qquad \text{Eq. (2)}$$

$$WHr_{NREL} = 557.157 \ e^{-0.0805276 \, * \, (Hour \, - \, 13.8046)^2} \qquad \text{Eq. (3)}$$

$$Diff_L = 130.634 e^{-0.110763 \, * \, (Hour \, - \, 12.1688)^2} \qquad \text{Eq. (4)}$$

$$WHr_{UM}{}^*(n) = \overline{WHr_{NREL}}(n) + Diff_L \qquad \text{Eq. (5)}$$

The data collected with the University of Miami's pyranometer has been compared to the data from NREL's NSRDB. We have found a latency in the data collected by NREL's NSRDB when comparing it to the data collected at the University of Miami. The comparison of the average radiation for the month of December shows that for the data collected at the UM, the maximum is at 12:00 PM, while for the data collected by NREL's NSRDB the maximum radiation is at 1:00 PM. This phenomenon can also be seen in the radiation when the sun rises such that in the data from the University of Miami, sunrise is evidenced at 6:00 AM while in the data from NREL's NSRDB it is at 7:00 AM. The same situation occurs with the sunset which is evidenced at 5:00 PM and 6:00 PM in the two different data sets, respectively. In order to mitigate the impact of this latency in our modeling framework, we have adjusted our comparison by one hour to match the data from these two data sources. After the adjustment is made, the comparison which is formulated by $Diff_L$ shows only a negligible amount of difference between the data sets obtained from NSRDB and the University of Miami's pyranometer, as shown in Figure 10. The distribution of the differences between the data collected at the University of Miami and the one obtained from NREL's NSRDB has found to be as in Eq. (4) where $Diff_L$ is the value predicted for $WHr_{UM} - WHr_{NREL}$ with a $R^2$ value of 98.0%.
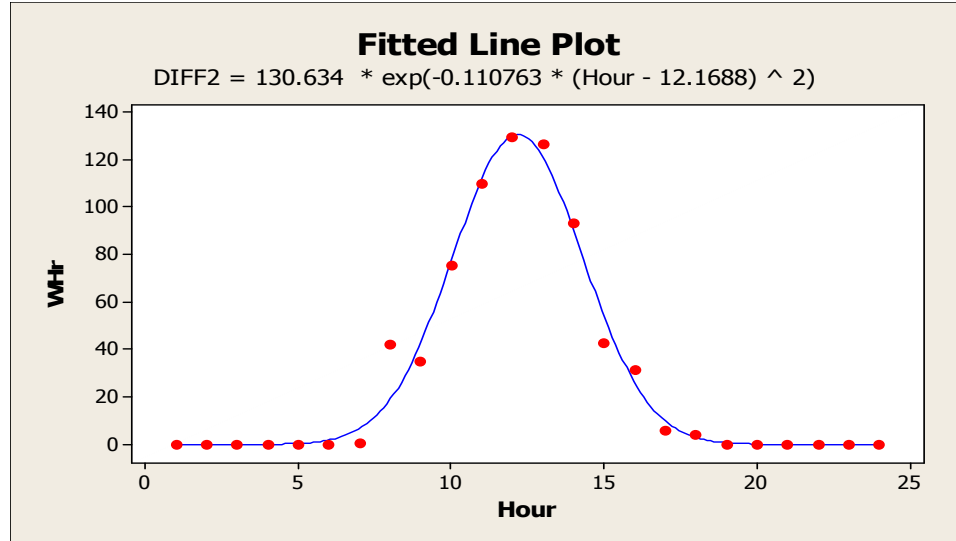
Figure 10: Data fit for the adjusted difference between $WHr_{\text{UM}}$ and $WHr_{\text{NREL}}$

Figure 11 shows exemplary monthly fits for $WHr_{\text{UM}}$ and $WHr_{\text{NREL}}$, as well as the fitted line of the best fit function used as a predictor of the actual data. The depicted data is comprised of the average solar irradiance values for each hour for the recorded periods of December 2010, and December 2000, 2001, 2002, 2003, 2004 and 2005 for $WHr_{\text{UM}}$ and $WHr_{\text{NREL}}$, respectively.

In the proposed continuous-discrete simulation modeling framework for the electric utility planning, the solar irradiation is represented using the satellite sensed data and the aforementioned fitted distributions for the adjusted difference. To this end, we first use the average of the satellite sensed data for each hour of the year using the data from 2000 through 2005, to generate the first phase of irradiation data; then, we combine this data with the distribution of the difference between the satellite sensed data and the pyranometer sensed data in order to include the spatial temporal variability using Eq. (5) where $WHr_{UM}{}^{*}(n)$ is the estimated solar irradiance for the n-th hour of the year and $\overline{WHr_{NREL}}(n)$ is the average of the satellite sensed irradiance for the $n^{\text{th}}$ hour of the year.

This latter distribution is used in the simulation model as irradiation input, where entities are assigned energy according to $P_m = \eta \times A \times G_T$.
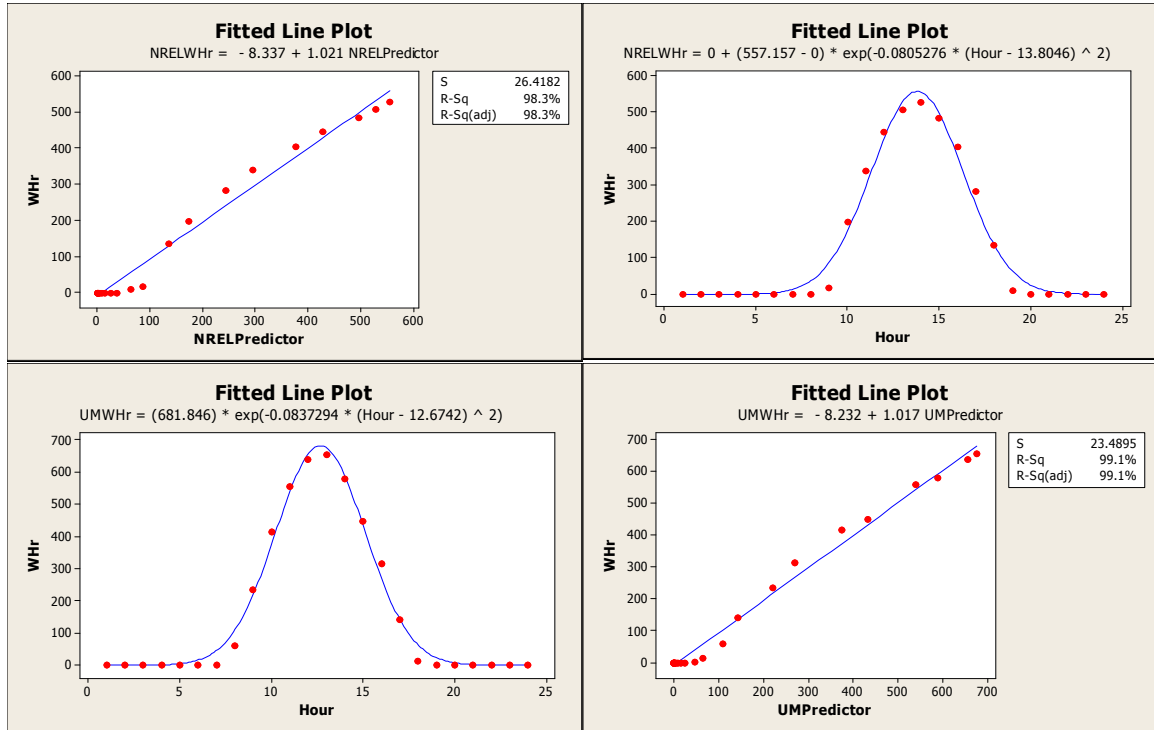


Figure 11: Fitted distributions for solar irradiance data collected at the UM and NREL's NSRDB

### 3.1.1.3. Wind Energy Generation

Wind energy is another widely recognized renewable source of energy. Lifecycle carbon dioxide ($CO_2$) emissions per unit of energy produced by a wind farm is estimated to be about 1% of that for coal plants and 2% of that for natural gas plants (Akpinar et al., 2007). Wind energy is also a sustainable source of energy that does not suffer from the risks associated to fuel shortages or price instability.

On the other hand, wind energy generation depends on wind availability, where the best locations often are remote to central places, and therefore transmission lines need to be built to connect wind farms to the grid. Furthermore, since wind power is proportional to the third power of the wind speed, the effects of intermittency in the wind speeds sharply influence the performance of the turbines (Zahedi, 2011). Due to this intermittent nature of wind power, its integration to a power grid poses threats to the grid's performance, which raises the need for energy storage systems (Erdogu, 2009). Also, the turbine blades are criticized to cause significant noise pollution and to have an aesthetic impact on the landscape.

Today, United States is the largest wind energy generating country in the world with a capacity to generate 40,180 MW (World Wind Energy Association, 2010). Even though there are no wind farms in Florida currently, FPL, Florida's largest utility company, is the parent of Next Era Energy Resources, the largest wind power generator of the United States. Next Era operates more than 75 wind projects in 17 states, with a total generating capacity of 7,800MW (NextEra, 2010). Within the state of Florida, FPL has proposed the St. Lucie wind energy project, which intends to build six wind turbines with a generating capacity of up to 13.8 MW, preventing the emission of more than 17,000 tons of carbon dioxide every year (FPL, 2008). Table 4 shows a comparison of characteristics of commercially used wind turbines that have been incorporated in the proposed CoDiMoSO framework including the turbine model manufactured by GE which is primarily considered for the St. Lucie wind energy project.

Table 4: Comparison of characteristics of commercially used wind turbines

| Manufacturer | GE | Vestas | Siemens | Mitsubishi | Suzlon |
|---|---|---|---|---|---|
| Model | TC2 2.5-100 | V90-3.0 | SWT-3.0-101 | MWT 95/2.4 | S.88 – 2.1 MW |
| Rated Power (MW) | 2.5 | 3 | 3 | 2.4 | 2.1 |
| Cut-in Wind Speed (m/s) | 3 | 3.5 | 3 | 3 | 4 |
| Cut-out Wind Speed (m/s) | 25 | 25 | 25 | 25 | 25 |
| Rated Wind Speed (m/s) | 12 | 15 | 12-13 | 12.5 | 14 |
| 50 Years Gust Wind Speed (m/s) | 59.5 | 59.5 | 70 | 59.5 | 59.5 |
| Hub Height (m) | 85 / 100 | 65 - 105 | 79.5 | 80 | 79 |
| Rotational Speed (rpm) | 14.1 | 8.6 - 18.4 | 6-16 | 9-16.9 | 15 - 17.6 |

(Mitsubishi Heavy Industries 2011; Next Era, 2010; Siemens, 2011; Suzlon 2011)

Wind turbine systems include blades connected to a driveshaft, which is in turn connected to a gearbox that drives an electric generator. The kinetic energy is converted into electricity by using this electric generator. The mechanical power extracted by a turbine system (including driveshaft, gearbox, and the electric generator) is given by Eq. (6), where $P_0$ is the power generated by the turbine, $\rho$ is the density of the air, $A$ is the area swept by the blades, $V$ is the upstream wind velocity at the entrance of the turbine, and $V_0$ is the downstream wind velocity at the exit of the blades.

$$P_o = \frac{1}{2}\rho A V^3 \frac{\left(1+\frac{V_0}{V}\right)\left[1-\left(\frac{V_0}{V}\right)^2\right]}{2} \qquad \text{Eq. (6)}$$

The power coefficient $C_P$, which is defined as $C_P = (1 + V_0/V)[1 - (V_0/V)^2]/2$ is the fraction of upstream wind power that is fed to the generator. The theoretical maximum for $C_P$ is achieved as 0.59 when $V_0/V = 1/3$. A practical maximum for $C_P$ can be assumed as one half so that the maximum power that a wind turbine can output is $P_{max} = \frac{1}{4}\rho A V^3$ (Patel, 2006). The rated power output from the generator of modern turbines is achieved when the upstream wind velocity is higher than their rated wind speed. For speeds lower to these, each model of turbine has its own power curve, and it is part of its specifications. In submodule 2 of the proposed

CoDiMoSO decision making framework (see Figure 6), entities are assigned with a wind speed in accordance to the distribution of the wind speed for the particular simulation month, where the wind speeds are calculated using data collected by NREL as detailed in the next section. Once an entity has been assigned a wind speed, the entity checks if its associated wind speed is sufficient to run the wind turbine at full capacity, at partial capacity or not at all. In case the sufficient wind speed is acquired, the corresponding amount of energy is generated. In the proposed initial setup, a rated and minimum operating wind speeds are assumed to be twelve meters per second and four meters per second, respectively. Also, the corresponding practical maximum value for $C_P$ of $1/2$ is adopted in this study.
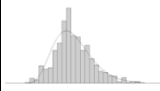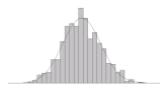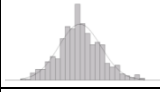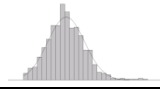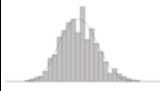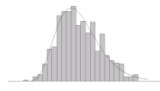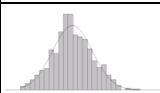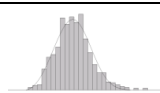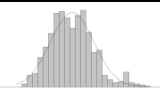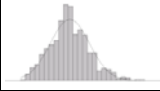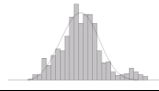
### 3.1.1.4.    Data for Wind Speed

In this study, in order to accurately estimate the wind speed, we used the wind speed data collected by NREL for the years 2004 to 2006. In this dataset, the wind speed is recorded at ten-minute intervals (six readings per an hour) at NREL's 5131 site in North Carolina (NREL, 2009). This data is a part of a larger project for the development of a collection of wind integration datasets that provide a consistent set of wind profiles for both the eastern and the western United States, help increase the performance of wind integration studies, and estimate the power production from possible wind plants at these locations. NREL's 5131 station has been chosen in our study since the monthly average wind speed at this location is very close to that reported by FPL at the St. Lucie Wind Project, with

only 14% difference on average; and it is the geographically closest location to the state of Florida.

In this research, in order to estimate the typical wind speed, average wind speeds are obtained for each hour of each day of the year using six wind speed readings (with ten-minute intervals). The data is then disaggregated into the different months of the year in order to capture seasonal effects such as the occurrences of higher wind speeds during the late winter (around February) and early spring (around March) than during the summer. The disaggregated monthly data is fitted to the probability distributions shown in Table 5, which have been incorporated into the CoDiMoSO framework.

Table 5: Fitted distributions for monthly wind speed data

| Month | Fitted Distribution | Sq. Error | Plot | Month | Fitted Distribution | Sq. Error | Plot |
|---|---|---|---|---|---|---|---|
| January | 2 + Gamm (0.8, 7.45)<br>Mean: 7.96<br>Var: 4.38 | 0.004606 | | July | Norm (6.16, 1.68)<br>Mean: 6.16<br>Var: 2.81 | 0.001278 | |
| February | Norm (7.74, 2.03)<br>Mean: 7.74<br>Var: 4.12 | 0.002476 | | August | Norm (5.79, 1.64)<br>Mean: 5.79<br>Var: 2.68 | 0.001109 | |
| March | 1 + 14 Beta (5.58, 6.32)<br>Mean: 7.58<br>Var: 4.39 | 0.001959 | | September | 2 + Gamm (0.735, 6.76)<br>Mean: 6.97<br>Var: 3.37 | 0.001688 | |
| April | Norm (8.44, 2.08)<br>Mean: 8.44<br>Var: 4.34 | 0.001701 | | October | 2 + Weib (4.9, 3.22)<br>Mean: 6.47<br>Var: 2.51 | 0.001375 | |
| May | 2 + 10 Beta (3.27, 3.09)<br>Mean: 7.10<br>Var: 3.56 | 0.000801 | | November | Norm (6.81, 1.87)<br>Mean: 6.81<br>Var: 3.51 | 0.002399 | |
| June | Norm (6.38, 1.73)<br>Mean: 6.38<br>Var: 3.01 | 0.002372 | | December | 1 + Weib (6.58, 3.52)<br>Mean: 7.08<br>Var: 4.94 | 0.002871 | |

### 3.1.2. Fossil Fuel Energy Generation

Fossil fuels are considered non-renewable sources of energy due to the large amount of time required for their formation (millions of years), and their current rate of depletion.

Approximately 70% of the electricity generated in the United States comes from fossil fuels as of 2010 (EIA, 2010) in spite of the fact that the achieved efficiencies are quite low.  Energy can be harvested from three major forms of fossil fuels including coal, oil, and natural gas.

Coal is the most commonly used fossil fuel in the U.S., and can be categorized as lignite, sub-bituminous, bituminous, and anthracite depending on the amount of carbon it contains.  Coal with the lower contents of carbon is almost exclusively used in electric generation, while coal with higher carbon contents is commonly used in space heating.  Oil is a liquid composed of decayed organic matter that occurs naturally in underground reservoirs.  It is extracted as petroleum and sent to a refinery for separation into its various components.  The United States is the world's largest oil consumer, as oil accounts for 97 percent of the fuel used by the United States' transportation sector (Black and Veatch, 2009).  Natural gas is a mixture of hydrocarbons: methane (primarily), ethane, propane, nitrogen, water vapor, and carbon dioxide.  Natural gas may be extracted from reservoirs or gas streams, or it can be separated from other petroleum products such as crude oil during the refining process.  After being separated from its liquid components, the gas is refined to remove hydrogen sulfide and other sulfur compounds.  Natural gas can be compressed into liquefied natural gas or compressed natural gas for transportation over long distances, even though it is used as fuel in the form of a gas.

The models presented in the literature (Smrekar et al., 2009; Wu et al., 2006; Yang et al., 2010; Williams et al., 1994; and Borg 1982) as well as the generation Module G presented in this study rely on understanding the processes that drive fossil fuel energy generation. Fossil fuels in general and coal in particular are used to produce electricity

and heat through combustion. Coal is usually pulverized and burned in a furnace with a boiler. The water in the boiler is converted into steam. The steam drives the turbines of a generator to produce electricity. Energy from oil is produced using reciprocating engines that drive power generators. Because of its ease of transportation, oil is typically used to run power stations that cannot or are very difficult to connect to a power grid, such as the ones on islands. Natural gas is used in combustion turbines that use the gas instead of steam to turn the turbines that produce electricity. There are also combined cycle power plants (e.g., those in Turkey Point and West County in Florida) that use the excess heat from the combustion of natural gas to heat water in a boiler and drive a steam-powered generator.

The basic reaction that drives fossil fuel combustion converts fuel and oxygen into heat, carbon dioxide and water. When the oxygen used in the reaction is obtained from the air, the reaction can be formulated as in Eq. (7), where the stoichiometric coefficients x and y depend on the fuel type. If the temperature of the reaction is high enough, the nitrogen may stop being inert, with the bond between the nitrogen molecules breaking and nitrous oxides are produced according to Eq. (8). Sulfur impurities in the fuel (mainly in coal) such as hydrogen sulfide $H_2S$ or hydrosulfide ions part of carbon chains $HS^-$ lead to the formation of sulfur dioxide, as shown in Eq. (9).

$$C_x H_y + \left(x + \frac{y}{4}\right)O_2 + 3.76\left(x + \frac{y}{4}\right)N_2 = xCO_2 + \left(\frac{y}{2}\right)H_2O + 3.76\left(x + \frac{y}{4}\right)N_2 \quad \text{Eq. (7)}$$

$$N_2 + O = NO + N \qquad\qquad \text{Eq. (8)}$$

$$2\,H_2S + O_2 = S_2 + 2H_2O \qquad\qquad \text{Eq. (9)}$$
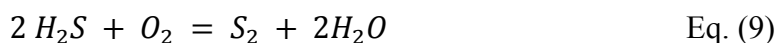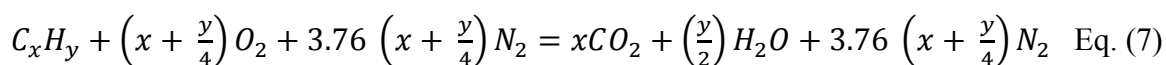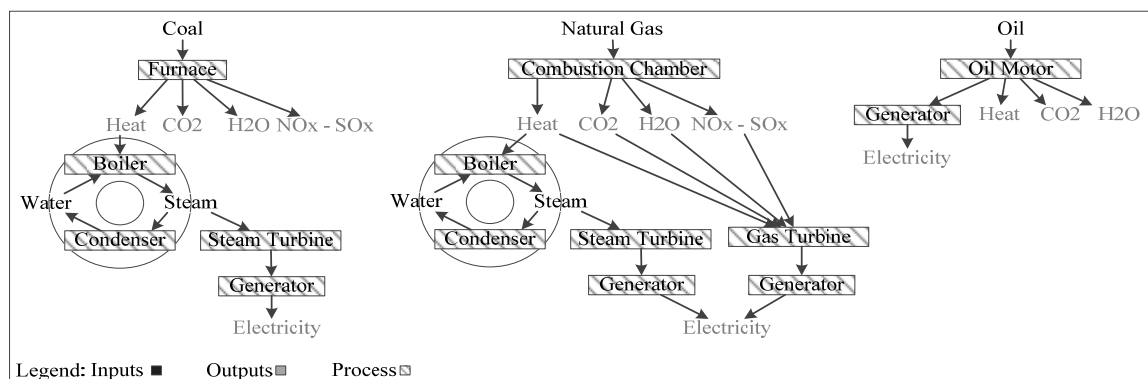
Figure 12: Process differences of energy generation from various types of fossil fuels

Figure 12 shows the different processes used in fossil fuel generation. The CoDiMoSO framework proposed in this study incorporates these processes as part of its energy generation Module G, in submodules 3, 4 and 5 as shown in Figure 6. In submodule 3, entities enter the furnace where the amount of coal used as well as the products of combustion, $CO_2$, $NO_x$, $SO_x$ and heat are recorded. The heat is then input to the steam turbine, which then is used in the electric generator to calculate the amount of energy generated. In submodule 4 entities enter the turbine, where as a product of combustion $CO_2$, $NO_x$, $SO_x$ and heat are generated as well as the energy that turns the turbine. The turbine's output is used to calculate the energy produced by this process and the heat is used as input of a steam turbine. The total energy of submodule 4 is calculated using the energy from both the electric generator from the gas turbine and the electric generator from the steam turbine. Submodule 5 uses a process similar to the previous two plants, but the fuel is used in an oil motor that outputs the energy to move the electric generator, as well as the known products of combustion $CO_2$, $NO_x$, $SO_x$ and heat. In addition to the input and output parameters of aforementioned processes, the proposed CoDiMoSO framework incorporates the parameters of efficiency and emissions related to these same processes in order to enhance its modeling validity and represent the system

as accurately as possible. Here, because much of the fleet of coal-fired power plants operating in North America was built during the 1960s, efficiency performance has been largely unchanged over the last forty years. Also, the need to retrofit pollution control equipment has not favored efficiency improvements (IEA, 2010). Therefore the average efficiency of coal power plants is assumed to be 35.1% based on the report by IEA (2007). The average coal used is assumed to have a heat value of 9,902 Btu per pound (6.398 KWh per Kg) and a sulfur content of 1.01% by weight (EIA, 2010). A newly commissioned combined cycle power plant is assumed to have an efficiency of 59% (Siemens, 2010), and the average heat value for the natural gas used in Florida is accepted as 1025 Btu per cubic foot (8.506 KWh per cubic meter) (EIA, 2010).

### 3.1.3. Nuclear Fuel Energy Generation

The main difference between a nuclear energy generation and fossil fuel energy generation is the method used to produce the heat required to run electric generators. Nuclear energy comes from the heat generated by the splitting of uranium atoms in nuclear fission. This process occurs as the nucleus of an atom splits into smaller, lighter nuclei. In nuclear reactors U-235 and U-238 are used, U-238 is the fuel while U-235, which is an unstable isotope, is used to start the nuclear reaction. One fission reaction triggers others, which in turn trigger more, until there is a chain reaction and fission becomes self-sustaining. Rods made from materials that absorb neutrons are inserted among the uranium fuel and control the nuclear reaction. The control rods slow or accelerate the reaction as they are inserted or withdrawn to varying degrees. In addition

to the control rods boron is dissolved in the core's coolant to absorb neutrons and control the process.

The nuclear energy released by the fission heats the coolant in the reactor's core; this refrigerates the reactor and transports the heat from the reactor to the steam generator. In pressurized water reactors, there are two sets of piping. The first set, the primary side, contains the core's coolant; the second set, the secondary side, contains water that drives the steam generator. In this type of reactors the fluids from these piping systems do not mix. A pressurizer prevents the coolant from the primary side from boiling, while allowing it to reach temperatures of up to 600° Fahrenheit. The heat is transferred to the secondary side in the steam generator, since the water from the secondary side is at a lower pressure it boils and becomes the steam that drives the generator. The process is shown in Figure 13.
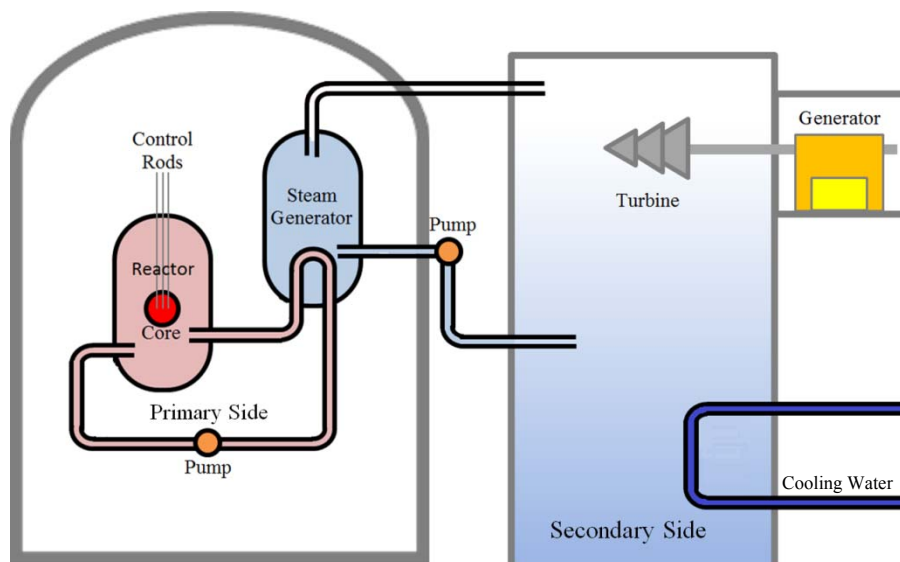


Figure 13: Overview of a pressurized water nuclear reactor

The United States is the largest nuclear energy producer in the world with an installed capacity of more than 100,000 Million Kilowatts distributed among 104 operable units across 31 states (EIA, 2011).  In the state of Florida there are 3 nuclear power plants, the Cristal River nuclear plant in Citrus County, the St Lucie nuclear plant in St Lucie County and the Turkey Point nuclear plant in Miami-Dade County.  The Cristal River nuclear power plant operates an 860 MW pressurized light water reactor that began operating on March 13, 1977 and is in the process of renewing its operational license, which is set to expire on December 2016.  The St Lucie nuclear plant operates two 839 MW pressurized light water reactors.  The first reactor began operating on December 21, 1976 and has a license to operate until March 2036; and the second reactor began operating on August 8, 1983 and has a license until April 2043.  The Turkey Point nuclear plant operates two 693 MW pressurized light water reactors.  The first reactor began operating on December 14, 1972 and has a license to operate until July 2032; while the second reactor began operating on September 7, 1973 and has a license to operate until April 2033.  As of 2009, the total nuclear capacity of 3,924 MW represented 6.64% of the state's energy generation capacity; however with a generation of 29,117 GWHr nuclear energy generated 13.36% of Florida's electricity (EIA, 2011).

Florida Power and Light, and Progress Energy, have submitted a combined license application to the Federal Energy Regulatory Commission for the construction and operation of two 2200MW nuclear power generation plants each, Turkey Point 6 and Turkey Point 7, and Levy County 1 and Levy County 2, respectively.  These units are based on a Westinghouse AP1000 light water reactor design.  Florida Power and Light's plants will be located at Turkey Point, where there are five power plants already, two

natural gas/oil steam electric generating units (Turkey Point 1 and Turkey Point 2), two pressurized water reactor nuclear units (Turkey Point 3 and Turkey Point 4), and one natural gas combined cycle steam electric generating unit (Turkey Point 5). Construction of Unit 6 is to be completed during 2021, and construction of Unit 7 is to be completed in 2022.

The main characteristics of this type of plants include a net electrical power of 1117 MW with a thermal power of 3415 MWt. These plants are designed to accept step load changes (increases or decreases) of 10 percent, and ramp load changes of 5 percent per minute, when operating between 15 and 100 percent of capacity without insertion of the control rods or operation of the steam generator safety valves. During load follow the plant is designed to make load changes of less than 10 percent at 2 percent per minute, when operating between 50 and 100 percent, in order to respond to grid frequency changes.

This type of plants is designed to achieve availability greater than 93 percent considering all outages, including a rate of reactor trips when the control rods are inserted to stop the nuclear reaction, of less than one per year. The plants' core is designed for an 18 month fuel cycle, with a refueling process that may be conducted in less than 17 days. This type of plant is designed to operate for 60 years without replacement of the reactor vessel, under conservative assumptions. The design of the plant's major components (steam generators, reactor coolant pumps, reactor fuel, reactor turbines and reactor generator) is based on equipment that has already been deployed in existing power plants, so that these components may be replaced during the plant's lifetime without shortening it.

These plants are designed to be constructed and operated in such a way that the release of reactive materials to the environment meets all environmental regulations, while it alerts operators if limit levels are approached. Redundancy and independence are implemented so that the failure of a single active safety system cannot prevent the required safety actions from taking place. Adequate control is given so that containment is provided to completely enclose the reactor system, and so that any piping that may serve as a path for an uncontrolled release of radioactive materials is automatically isolated in the event of a threat of such a release.

The reactor core is made of 157, 14 foot, 17x17 fuel assemblies, and consists of three radial regions which have different fuel enrichments that range from 2.35 to 4.8 percent. Daily load follow is achieved through the use of reduced-worth control rods, which eliminate the need for changes in the boron concentration, and the equipment needed to process these changes. Refueling operations in these plants is done in what has become the standard for these operations, the head of the reactor vessel is removed and the core is configured using a refueling machine that handles the fuel from above. New fuel is stored in high density racks that can store up to 72 assemblies, while spent fuel is stored in racks with space for 619 fuel assemblies.

The reactor vessel is cylindrical with hemispherical bottom head and removable top head, it is the high pressure containment boundary used to support and surround the reactor core. The vessel is approximately 40 feet high and has an inner diameter of approximately 13 feet, it is clad in stainless steel and designed to withstand pressures of up to 17.1 MPa and temperatures of up to 650 °F. The reactor core is located as low as possible within the vessel to reduce the reflood time in case of accidents.

The design of the steam generators is based on currently deployed equipment that is designed for direct attachment to the reactors coolant pumps. The design of the nuclear reactor includes two steam generators that employ a steam separator area sludge trap with clean out provisions and thermally treated nickel-chromium-iron *Alloy 690* tubes. Each generator's channel head attaches to two reactor coolant pumps, and is designed for manual and robotic access for inspection, sleeving, plugging and nozzle dam placement operations. The reactor coolant pumps are designed with no seals to prevent seal failure loss of coolant accidents. The pumps' motor is located below the steam generator's head to simplify the loop piping and to eliminate the possibility of fuel uncover during potential small loss of coolant accidents. The pumps are designed so that they are not damaged due to the loss of all cooling water until a safety related pump trip occurs; this system provides the pump protection in the case of extended loss of coolant water. The reactor coolant system has it piping configured in two main coolant loops that use a 31 inch diameter hot leg pipe to transport reactor coolant to the steam generator. Two 22 inch cold leg pipes complete the circuit by transporting the reactor coolant back into the reactor vessel.

Figure 6 shows how the different processes for nuclear electricity generation are included in the proposed HMS framework. As entities arrive to the different nuclear plants they check if the plant is currently operational. If the plant is not operating they are routed to a disposal block, if the plant is operating entities are routed to the nuclear core. In the reactor core the amount of nuclear fuel is checked, if there is enough fuel for nuclear fission the entities enter the nuclear reactor and go through the nuclear fission process. If there is not enough fuel for nuclear fission a nuclear refuel process is

triggered. After entities go through nuclear fission they are duplicated so that one entity goes to the electricity generation and the other goes to the nuclear waste generation. In the electricity generation based on the nuclear fission, the heat produced is calculated, after this the efficiency of both the primary and secondary sides is factored in, after which entities enter the nuclear steam turbine system. The output from the nuclear turbine is used by the nuclear electric generator to assign each entity with the corresponding amount of energy that it is to deliver to the grid. Entities that go to the nuclear waste generation go through two processes, a process for low level waste generation and a process for high level waste generation, after which they are sent to the nuclear disposal. In the case that a refueling process is activated the plant is shut down and processes for the replacement of the fuel rods within the nuclear core begin. In the refueling process, entities enter a plant cool down stage; after cool down entities are sent to a reactor head removal process. The reactor head removal process is followed by the fuel removal process. Once this fuel removal process is completed there is a system reprogramming stage, followed by the actual reactor fueling process. Finally the reactor is reassembled and a signal is sent that the plant may ramp up to operational status. Entities that go through the refueling process are sent to the nuclear disposal once all of the processes are completed.

### 3.2. Energy Storage Module (S)

Energy storage systems are necessary to deal with 1) fluctuations in demand (e.g., grid system applications), 2) intermittency in generation from renewable sources, and 3)

reliability concerns in electricity distribution (Eyer et al., 2004). Grid system applications of storage include arbitrage (buying electricity to charge the storage plant when price is low, so that it can be sold at a later time when the price is high), central generation capacity (the use of energy storage systems as an alternative to adding central generation capacity), ancillary services (support services required in energy transmission that ensure the integrity and reliability of the network, network stability, and voltage control), the reduction of transmission capacity requirements, transmission congestion relief (by discharging stored energy during peak demand periods) and the deferral of transmission and distribution upgrades. Utility customer applications of storage include time-of-use energy cost management, demand charge management, service reliability and service power quality. The electric service reliability application entails use of energy storage to provide highly reliable electric service. In the event of a complete power outage, the storage system provides energy to ride through outages of extended duration or to complete an orderly shutdown of processes or to transfer to on-site generation resources.

These advantages may be achieved through the use of different energy storage systems such as pumped hydro storage (PSH), compressed air energy storage (CAES), batteries, hydrogen storage and supercapacitors, whose details are provided below and in Tables 6 and 7. Table 6 shows the key characteristics of the main types of energy storage systems, while Table 7 summarizes their main advantages and disadvantages.

Table 6: Properties of energy storage systems

| Energy Storage System | PHS | CAES | Lead-acid battery | Sodium-sulfur battery | Hydrogen fuel cell | Supercapacitor |
|---|---|---|---|---|---|---|
| Rated Capacity ($MW$) | 100 - 5000 | 5 - 300 | 0 - 20 | 0.05 - 8 | 0 - 50 | 0 - 0.3 |
| Discharge at Rated Capacity ($h$) | 1 - 24 + | 1 - 24 + | 0.0027 - 2 + | 0.0027 - 2 + | 0.0027 - 24 + | $2.7 \times 10^{-7} - 1$ |
| Power Capacity Cost ($/$kW$) | 5 – 100 | 2 – 50 | 50 – 400 | 300 – 500 | 425 – 725 | 300 – 2000 |
| Response Time | Minutes | Minutes | < 1/4 cycle | < 1/4 cycle | < 1/4 cycle | < 1/4 cycle |
| Cycle Efficiency (%) | 71 - 85 | 70 - 89 | 70 - 90 | 75 - 90 | 20 - 66 | 84 - 95 |
| Cycle Life | 10,000 - 30,000 | 8,000 - 12,000 | 500 - 1,000 | 2,500 - 4,500 | 1000 + | 100,000 + |
| Space Requirements ($m^2/kWh$) | 0.02 | 0.01 | 0.058 | 0.019 | 0.003 - 0.006 | 0.04 |
| Life ($years$) | 40 - 60 | 20 - 40 | 5 - 15 | 10 - 15 | 5 - 20 | 8 - 20 |

(DOE, 2011)

Table 7: Main advantages and disadvantages of energy storage systems

| Energy Storage System | Main Advantages | Main Disadvantages |
|---|---|---|
| PHS | High Capacity, Low Cost | Special Site For Reservoir Required |
| CAES | High Capacity, Low Cost, Underground | Special Site Required, Needs Natural Gas |
| Lead-acid battery | Low Capital Cost | Limited Life Cycle When Deeply Discharged |
| Sodium-sulfur battery | High Power Density, High Efficiency, 99% Recyclable | Production Costs, Safety Concerns |
| Hydrogen fuel cell | Very Low Self Discharge | High Capital Costs |
| Supercapacitor | Long Cycle Life, High Efficiency | Low Energy Density |

Among various types of energy storage systems, PSH systems store potential energy from height differences in water levels by pumping water from a lower water level reservoir to an upper level reservoir. It can provide relatively high efficiency, large power capacity, large storage capacity, and a long life, at a low cycle cost ($0.1- 1.4/ kWh/cycle$) (Chen et al., 2009). Hydrogen storage is composed of three separate processes: a hydrogen production process, a process for its storage, and a combustion process for its use. For production, an electrolyzer produces hydrogen and oxygen from water by introducing an electric current; while for use, a hydrogen fuel cell converts

hydrogen and oxygen back into water, releasing the stored energy. Hydrogen storage has a more expensive capital cost than other systems and has a low storage conversion efficiency. This type of storage may be an option for certain applications, such as when grid reinforcement is expensive, or when there are limiting environmental policies or concerns for other options. Supercapacitors store energy by means of an electrolyte solution between two solid conductors. They have a durability of 8 to 10 years with a very high efficiency. They are capable of deep discharge/overcharge and have an extremely high power density (Hadjipaschalis et al., 2009). However, supercapacitors have a high energy dissipation rate of between five and forty percent per day and their cost is quite high.

CAES systems typically use an existing underground site (a salt dome, a rock cavern or an abandoned mine), and store gas at approximately 4–8MPa. There are currently two operating CAES plants in the world, a 290 MW facility in Huntorf, Germany built in 1978, and a 110 MW plant in McIntosh, Alabama commissioned 1991. Along with PHS, CAES systems are the only technologies suitable for large scale power and high energy storage applications. They share many of the same attractive qualities of PHS, such as high power capacity, large energy storage capacity, a quick start-up, a long storage period, and a relatively high efficiency (Beaudin et al., 2010). Succar and Williams (2008) show that the electrical output of a turbine in a CAES system is given by the equation in Eq. (10), where $E$ is the electrical output of the turbine, the integral is the work generated by the expansion of air and fuel in the turbine, $w_{TOT}$ is the total mechanical work generated in the process, $m_T$ is the air mass flow rate, $t$ is the time requires to deplete a full reservoir at full power, $\eta_M$ is the mechanical efficiency of the

turbine and $\eta_G$ is the efficiency of the electric generator. The work generated by the process is limited by the law of ideal gases $PV = nRT$, where $w_{TOT} \leq nRT \ \ln V_2/V_1$, where $V_1$ is the initial volume and $V_2$ is the final volume (Ter-Gazarian, 1994). A CAES system can use up to 67% less natural gas than a regular gas turbine generator (Gardner and Haynes, 2007).

$$E = \eta_M \eta_G \int_0^t m_T w_{TOT} dt \qquad \text{Eq. (10)}$$

Batteries store energy through a reversible chemical reaction. There are various types of batteries including Lead-Acid, Nickel-Cadmium, Sodium-Sulfur, Zinc-Bromine and Vanadium redox batteries. Lead Acid batteries have been used for more than 130 years, and still are the most common rechargeable electrochemical device for small to medium scale applications, and are most commonly found in vehicles. Lead-acid batteries have a low-cost, high reliability, strong surge capabilities, high efficiency, and are usually good for uninterruptible power supply and power quality (Chen et al. 2009). Lead-acid batteries are rechargeable and have the reversible reaction given by Eq. (11). Sodium-Sulfur batteries are a very attractive emerging technology because they can be cycled 2500 times, have high power density ($150-240W/kg$), are efficient, and have a 600% rated pulse power capability that can last $30s$ (Dufo-Lopez et al., 2009). Sodium-Sulfur batteries are rechargeable and environmentally friendly since the batteries are sealed and allow no emissions during operation, and more than 99% of the overall materials of the battery, by weight, can be recycled. Sulfur batteries have the reaction equation given by Eq. (12).

$$Pb + PbO_2 + 2H_2SO_4 = 2PbSO_4 + 2H_2O \qquad \text{Eq. (11)}$$

$$2Na + 3S = Na_2S_3 \hspace{4cm} \text{Eq. (12)}$$
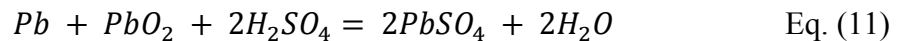
From the energy systems described above the proposed continuous-discrete modular simulation optimization framework models a CAES system which offers a large energy storage capacity and high power capability (submodule 7), and a combination of Lead-Acid and Sodium-Sulfur battery systems (submodules 8 and 9); where Lead-Acid batteries provide a low-cost energy storage system with high reliability, and Sodium-Sulfur batteries offer a relatively longer operating life than Lead-Acid batteries and are more environmentally friendly. In submodule 7 the amount of energy stored is determined via the level of air in the CAES cavern as well as the efficiency of the compressor that is used to store the air. When demand is requested from the CAES system such that the system needs to switch to the gas expansion stage, natural gas and the pressurized air are used in order to run a high pressure and a low pressure turbine. The turbines turn an electric generator that delivers the energy, and the energy level in the CAES system is adjusted after taking into account the operational efficiencies of these mechanisms.

### 3.3. Energy Transmission Module (T)

In our proposed CoDiMoSO framework, generated energy usage and its distribution is carried out by both a step-up and a step-down substation sub-module. The step-up substation records the total amount of energy generated and then decides the use of the energy from each entity between the different types of storage, the electrical grid or, if there is no capacity in these systems, grounding. The energy from the entities may be

used to feed the grid directly, if the level in the grid falls below a certain threshold. If the energy in the grid is above this threshold and there is available storage capacity, then the energy from the entities is stored. In the event that there is no capacity for storage available, then the energy is grounded. When energy is stored in the Sodium-Sulfur or the Lead-acid battery system, the storage system with the lowest amount of energy is used; consequently, when energy is being used from the battery systems, it is taken from the system with the highest energy amount. The CAES system is used for storage only when the energy level in both the Sodium-Sulfur and the Lead-acid battery systems is above preset thresholds. In the step-down substation sub-module, the entities use the energy from either the grid, the storage systems, or if the demand cannot be met they are disposed as load shed.

When energy is stored in the CAES system, the framework attempts to reduce the utilization of the fossil fuel plants by reducing the current operational capacity by 10%. However, a minimum runtime value for each of the plants limits the scale down mechanism. The minimum runtime value specifies the minimum frequency with which scale down operations may occur at each facility. In the case that energy is grounded, the scale down mechanism is activated not only for the fossil fuel plants, but also for the nuclear power plants, subject to the same type of minimum runtime restriction.

The load shed of an entity points out that the current operational capacity of the energy generation systems is not adequate. When this happens the framework triggers a mechanism that increases the operating level of the power plants to full capacity. This mechanism starts by increasing the capacities of the nuclear power plants, followed by that of the natural gas, oil and coal plants. The scale up mechanism is limited by a

minimum downtime value, similar to the one that constraints the step up mechanism, that limits the frequency with which these step up operations may occur. The minimum downtime and minimum runtime values are used to incorporate the fact that energy generating plants take time to adjust their operational levels and thus changes to the operational levels cannot be completed immediately.

### 3.4. Energy Demand Module (D)

The generated energy is demanded by four major sectors which are namely residential, commercial, industrial, and transportation. The residential sector encompasses single or multifamily houses and mobile homes; the commercial sector includes firms not engaged in farming, manufacturing or transportation as well as public-street and highway lighting, interdepartmental electricity sales and electricity sales to public authorities; the industrial sector includes the goods-producing sector of the economy, including manufacturing, agriculture, construction, fisheries and forestry; and finally, the transportation sector demand includes electricity used for transportation as well as for railroads and railways (EIA, 2010). In 2009, U.S. was the largest electricity consumer in the world with 3.741 trillion kilowatt-hours energy consumed (EIA, 2010). Here, the residential sector accounts for 36.43% of the energy consumed in the United States in 2009, the commercial sector for 35.36%, the industrial sector for 23.58% and the transportation sector for 0.21%. Within U.S., Florida is the third largest electricity consuming state where its total consumption is equal to 6.2% of the national total (EIA, 2009). Table 8 shows the monthly average energy demand in Florida by sector and Table 9 shows the

energy consumption in Florida by sector; where residential, commercial, industrial and transportation demand respectively represent 51.59%, 34.05%, 10.77% and 3.59% of the total consumption on average. The proposed CoDiMoSO framework as well as the demand forecasting algorithm developed as part of its demand Module D is based on this data collected from EIA. The details of this demand estimation algorithm and the modeling of the Module D are provided in the next section.

Table 8: Average Monthly Energy Consumption in Florida in MWHr

| Month | Residential | Commercial | Industrial | Transportation | Total |
|-------|-------------|------------|------------|----------------|-------|
| January | 8,803,173 | 5,985,862 | 2,195,723 | 599,765 | 17,584,523 |
| February | 8,058,046 | 5,453,321 | 1,836,417 | 586,655 | 15,934,439 |
| March | 7,568,938 | 5,549,920 | 1,890,909 | 613,185 | 15,622,954 |
| April | 7,709,337 | 5,765,914 | 1,924,423 | 617,393 | 16,017,067 |
| May | 8,757,720 | 6,172,947 | 2,012,225 | 640,456 | 17,583,348 |
| June | 10,732,322 | 6,745,917 | 2,075,317 | 690,803 | 20,244,358 |
| July | 11,797,190 | 7,002,154 | 2,051,942 | 714,208 | 21,565,494 |
| August | 12,176,168 | 6,974,548 | 2,103,445 | 711,388 | 21,965,549 |
| September | 12,064,284 | 7,196,393 | 2,048,301 | 781,462 | 22,090,440 |
| October | 10,453,153 | 6,706,603 | 2,007,966 | 699,078 | 19,866,799 |
| November | 8,329,819 | 6,085,163 | 1,934,046 | 687,660 | 17,036,687 |
| December | 8,177,016 | 6,017,060 | 1,850,992 | 631,230 | 16,676,299 |
| Total | 114,627,166 | 75,655,802 | 23,931,706 | 7,973,283 | 222,187,955 |

Table 9: Energy Consumption in Florida 2005 – 2009 in MWHr

| Year | Residential | Commercial | Industrial | Transportation | Total |
|------|-------------|------------|------------|----------------|-------|
| 2005 | 115,413,716 | 73,688,692 | 24,969,487 | 8,139,922 | 222,211,817 |
| 2006 | 118,245,990 | 75,231,267 | 26,627,845 | 8,356,444 | 228,461,546 |
| 2007 | 118,609,290 | 77,101,935 | 25,634,560 | 8,519,587 | 229,865,372 |
| 2008 | 108,724,268 | 76,472,457 | 21,227,378 | 7,408,353 | 213,832,456 |
| 2009 | 112,142,565 | 75,784,660 | 21,199,255 | 7,442,106 | 216,568,586 |
| Average | 114,627,166 | 75,655,802 | 23,931,705 | 7,973,282 | 222,187,955 |

### 3.4.1. Algorithm for Estimating Electricity Demand by Various Sectors

The algorithm is developed to enable accurate estimation of electricity demand by various sectors in a timely manner, and is embedded into the Module D of the CoDiMoSO framework. Here, the algorithm estimates the hourly energy consumption rate by various sectors by considering the monthly energy consumption reported by seven largest utility companies in the state of Florida (FPSC, 2009), the average daily temperature recorded at the Miami International Airport, and the daily peak energy demand information from FPL. In addition to the temperature in each hour of the day, the algorithm also differentiates whether this day is a weekday, weekend, or a holiday, and whether or not the particular hour is flagged as a consumption peak or not while predicting the total hourly as well as monthly consumption. It should be noted here that the hourly temperature values also encompass the weather as well as the climate affect. Exemplary plots representing the weekly energy demand by different sectors are provided in Figure 14 for reference.
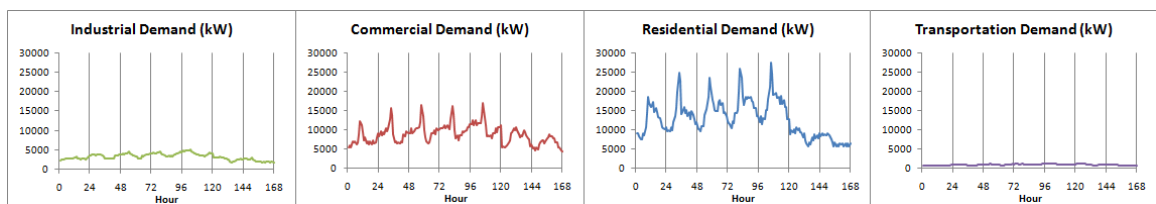


Figure 14: Exemplary plots representing the hourly energy demand by different sectors

Algorithm 1 shows the operation of the algorithm where $m$ is the index for the months of the year, $t$ is the index for hours of the month, $y$ is the index for the consumption sectors (residential, commercial, industrial, transportation), $z$ is the index for weekdays and weekends, $w$ is the index for holidays and non-holidays, $CH(t)$ is the

energy consumption at a given hour $t$, $CM(t)$ is the total energy consumption of the month to which hour t belongs, $CF(t)$ is the consumption factor of hour $t$, $T(t)$ is the temperature at a given hour t, $T_l$ is the temperature at which electric heating begins operating, $T_h$ is the temperature at which electric cooling begins operating, $T_{HS}$ is the temperature at which electric heating is set, $T_{CS}$ is the temperature at which electric cooling is set, $F_{EH}$ is the electric heating factor, $F_{EC}$ is the electric cooling factor, $F_o$ is the occupancy factor, $F_{Hd}(w)$ is the holiday factor for holiday $w$, $F_M(m)$ is the month factor, and $F_{MN}(m)$ is the month normalization factor.

Load Monthly Consumption Data, Daily Temperature Data, Holidays, Weekdays – Weekends;
CF(t) = 1
If (T(t) < T$_l$) CF(t) = CF(t) + F$_{EH}$ * (T$_{HS}$ − T(t))
If (T(t) > T$_h$) CF(t) = CF(t) + F$_{EC}$ * (T(t) - T$_{CS}$)
A = Max (5000 Sin(t * π / 12 + 1.15) -4400 , 0 )
If (y = Residential) {If (z = Weekday) {
                              If (A > 0){F$_O$ = 200 + (800 + 250 Sin(0.1 +  5t * π)  + 160 Cos (t * π / 12 + 2.4) +
A)}
                              Else {F$_O$ = 200 + (800 + 250 Sin(0.1 +  5t * π)  + 350 Cos (t * π / 12 + 2.4))}}
                    If (z  = Weekend) {
                              F$_O$ = 140 + (560 + 200 Sin(0.1 +  5t * π)  + 300 Cos (t * π / 12 + 2.4 ))}
                              CF(t) = CF(t) * F$_O$}
If (y = Commercial){If (Day = Weekday) {
                              If(A > 0){F$_O$ = 200 + (600 + 80 Sin(1 +  5t * π)  + 60 Cos (t * π  + 2.3 ) + A)}
                              Else {F$_O$ = 200 + (800 + 80 Sin(1 +  5t * π)  + 60 Cos (t * π  + 2.3))}
                    If (z = Weekend) {
                              F$_O$ = 140 + (420 + 80 Sin(1 +  5t * π)  + 60 Cos (t * π + 2.3))}
                              CF(t) = CF(t) * F$_O$}
If (y = Industrial){If (z = Weekday) {
                              F$_O$ = 200 + (2400 + 20 Sin(5t * π)  + 10 Cos (t * π + 2.5))}
                    If (z = Weekend) {
                              F$_O$ = 140 + (1680 + 25 Sin(5t * π)  + 5 Cos (t * π + 2))}
                              CF(t) = CF(t) * F$_O$}}
If (w = Holiday) CF(t) = CF(t) * F$_{Hd}$(w)
F$_M$(m) = Sum (CF(t))
F$_{MN}$(m)= CM(t)/ F$_M$(m)
CH(t) = CF(t) * F$_{MN}$(m)

Algorithm 1: Hourly energy demand allocation for the different sectors

The algorithm is used to distribute a month's total energy consumption for each residential, commercial, industrial and transportation sector into each of the month's hours based on the aforementioned factors. The algorithm begins by assigning each hour of the month with an initial consumption factor ($CF(t)$) of 1. For hours whose temperature is lower than $T_l$ the consumption factor is adjusted to $1 + F_{EH}(T_{HS} - T(t))$, for hours whose temperature is higher than $T_h$ the consumption factor is adjusted to $1 + F_{EC}(T(t) - T_{CS})$. Then, the parameters that take into account whether the hour is during a consumption peak ($A$), and/or, whether it is part of a weekend ($z$), are factored in, and each hour's consumption factor is adjusted to $CF(t) = CF(t)F_o$. Next, the impact of holidays is factored in and $CF(t) = CF(t)F_{Hd}(w)$ for hours during holidays. Once all of the consumption factors have been calculated for all of the hours of the year, each month's consumption and normalization factors are calculated as in $\sum_{t \in m} CF(t) = F_M(m)$ and $F_{MN}(m) = \frac{CM(t)}{F_M(t)}$. The consumption of each individual hour within each sector is then calculated by distributing the month's total consumption based on the consumption factors $CH(t) = CF(t) F_{MN}(m)$.

Figure 15 shows the differences in the estimated energy consumption for a randomly selected winter day (January 31$^{st}$) versus a randomly selected day in the middle of the summer (August 31$^{st}$). As depicted, the overall consumption for the summer day is larger than that of the winter day while the hours at which the peak demand occur varies by the different sectors.
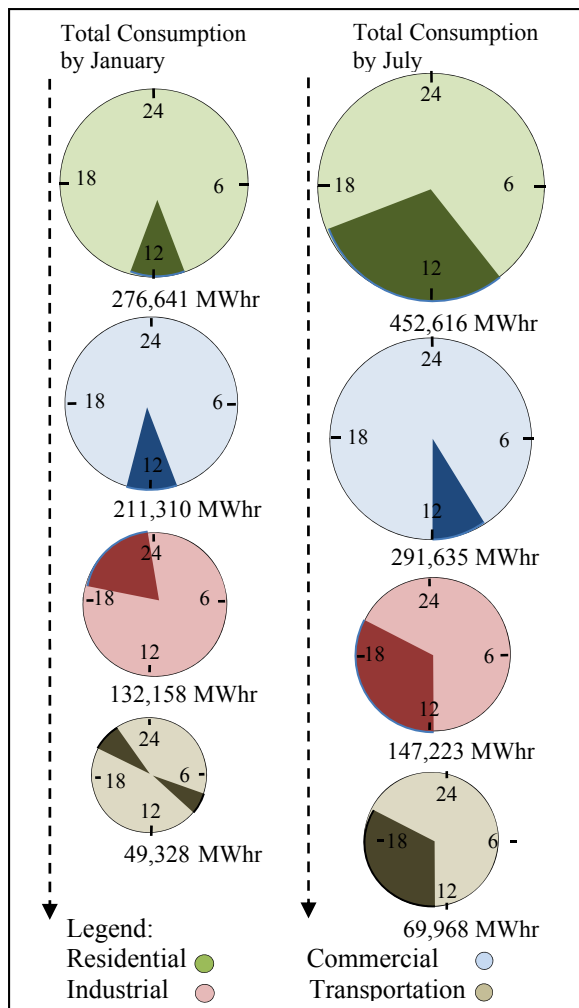
Figure 15: Estimated energy consumption in Florida for a winter and a summer day by sector

The algorithm has been implemented using Visual Basic and embedded into the simulation model via a VBA block to conduct estimation of the energy consumption for 35,040 consecutive hours. Implementation wise, using solely a VBA block for the CoDiMoSO framework involves running the algorithm every time an entity necessitating energy demand is created, and would require a considerable amount of computational resources. On the other hand, using solely an Excel file to store the results from the algorithm and retrieving the information from that file via another VBA block means that the Excel file must be accessed every time an entity necessitating energy demand is

created. In this case, even though it may not essentially require computational resources to run the algorithm, it does require them to link the CoDiMoSO framework with the Excel file. Alternatively, we have created Arena schedule components to store the results obtained by the algorithm. These schedule components enable us to export the model to an Access database. Within the Access database the schedules are located and modified using the algorithm; once this modification was completed the updated CoDiMoSO framework was imported back into Arena from the Access database. This way, considerable savings have been realized in the utilization of computational resources.

The energy demand Module D incorporating the algorithm has been implemented in Arena as shown in Figure 16. Here as entities arrive, they are assigned with an amount of energy to be consumed according to the results of the algorithm, and are routed to a step-down substation submodule. In the step-down substation submodule, the energy demanding entities either use the energy from the grid (instantaneous utilization), from the storage systems, or they get disposed if the demand cannot be met. Disposal of an entity for the last case indicates that the current usage level of the energy generating systems is not adequate and attempts to trigger a mechanism for increasing the operating level of the natural gas, oil and coal plants to full capacity. The scale up mechanism is constrained with a minimum downtime value (similar to the one that constraints the step up mechanism in Module S) which restricts the frequency with which these operations may occur. These minimum runtime and minimum downtime values are imposed to Module D and Module S in order to consider the fact that fossil fuel energy generating plants take time to adjust their operational levels and to be realized, hence cannot be made instantaneously.
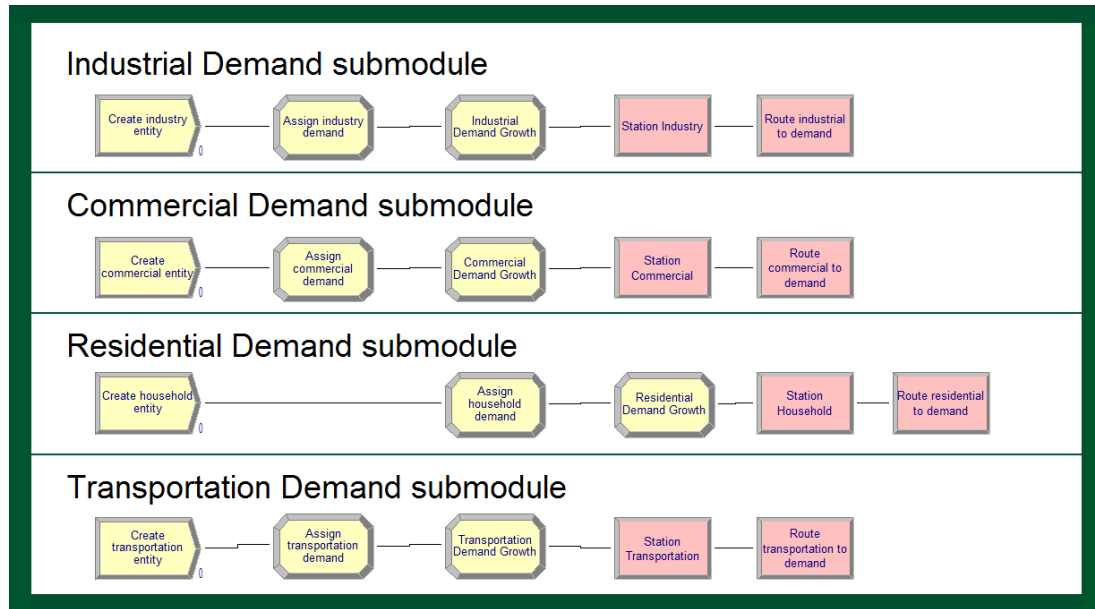
Figure 16: Energy Demand Module D

## 3.5. Optimization Module (O)

In order to determine the optimal parameters for the integrated system in terms of minimized total cost and greenhouse gas emissions of the energy generation and storage systems, subject to the demand of the state of Florida we have developed a particle filtering optimization module. The optimization module takes samples from the state of the system within the simulation and based on these samples proposes a new generation capacity for each of the different generation and storage systems that attempts to minimize cost and greenhouse gas emissions, while meeting operational restrictions regarding demand, and load shedding. The simulation is then run again with the updated generation and storage capacities in an iterative process that stops once an indifference zone is reached and there is no significant improvement in terms of greenhouse gas emissions or cost.

The formulation of the optimization problem is given in Eqs. (13) - (25). The objective is to determine the rated capacity for energy generation and storage ($C_i$) which minimizes the overall costs of meeting energy demand, as well as minimizes the emission of greenhouse gases generated as a consequence. These objectives are optimized while keeping the rated capacity of energy generating storage facilities within predetermined ranges, as well as satisfying the electricity demand and keeping the energy balanced for all components of the system.

$$\min \sum_i C_i(B_i + F_i) + \sum_i \sum_j G_{it} U_{it} \qquad \text{Eq. (13)}$$

$$\min \sum_i \sum_l \sum_t E_{it} P_{il} \qquad \text{Eq. (14)}$$

Subject to

$$Df \sum_j D_{jt} \leq \sum_i E_{it} \qquad \forall t \qquad \text{Eq. (15)}$$

$$A_{it} = A_{it-1} F_i + \sum_{i=1}^{6} E_{it} - Df \sum_j D_{jt} - sum_{i=7}^{9} \sum_{j=1}^{J} E_{it} - O_t \qquad \forall t \qquad \text{Eq. (16)}$$

$$G_{5t} = \eta a_p g_t \qquad \forall t \qquad \text{Eq. (17)}$$

$$C_5 = 1000 \eta a_p \qquad \text{Eq. (18)}$$

$$E_{6t} \leq \frac{1}{4} \rho a_w v_t^3 \qquad \forall t \qquad \text{Eq. (19)}$$

$$E_6 = 432 \rho a_w \qquad \text{Eq. (20)}$$

$$C_i \geq Cl \qquad \forall i \qquad \text{Eq. (21)}$$

$$C_i \leq Cu \qquad \forall i \qquad \text{Eq. (22)}$$

$$E_{it} \leq C_i \qquad \forall i, t \qquad \text{Eq. (23)}$$

$$A_{it} \leq C_i \qquad i \in [7,9] \qquad \text{Eq. (24)}$$

$$E_{it} \leq A_{it-1} \qquad i \in [7,9], \forall t \qquad \text{Eq. (25)}$$

The proposed formulation uses index $i$ for the different energy generation and storage alternatives (nuclear, coal, natural gas, oil, solar, wind, CAES, lead-acid batteries and Sodium-Sulfur batteries), $j$ for electricity demanding sectors (residential, industrial, commercial and transportation), $l$ for the different greenhouse gases ($CO_2$, NOx, SOx), and $t$ for the time. The total costs of meeting the electricity demand depend on the costs associated to energy generation and energy storage. These costs have separate components that are time invariant and time variant respectively.

The time variant component is based on the electricity generated by each facility at every point in time ($G_{it}$) and by the fuel costs associated with the operation of these facilities ($U_{it}$). The time invariant component depends on the rated capacity of each facility ($C_i$), the base cost of each of these facilities ($B_i$) and the fixed costs of operating facilities ($F_i$). The energy in each storage system at any time is given by $A_{it}$, while the efficiency of these storage systems is given by $F_i$. The amount of energy grounded is given by $G_t$. The amount of solar energy generated is given by $G_{5t}$, the amount of wind energy generated is given by $G_{6t}$, the solar irradiance is given by $I_t$, the electrical efficiency of the solar panels is given by $\eta$ and the total area of the solar panels is given by $a_p$. The density of the air is $\rho$, the area swept by the blades is $a_w$ and the upstream wind velocity at the entrance of the turbine is $v_t$.

Greenhouse gas emission is a result of the use of fossil fuels. In energy generation and storage facilities, the emission of pollutants depends on the amount of electricity generated at every point in time, and the amount of each pollutant that using this type of facility entails ($P_{il}$). In addition, the energy demanded by each sector during every time unit ($D_{jt}$) must be fulfilled by the energy generation and storage facilities, up

to a specified fulfillment factor ($Df$), so that the fraction of the total demand specified by this factor is fulfilled at all times. The rated capacity of energy generation and storage facilities has lower and upper limits ($Cl$ and $Cu$). Finally, the operational capacity of these energy generation and storage facilities is bounded by their respective rated capacities.

Algorithm 2 shows the operation of the PFO algorithm. The algorithm begins by setting initial values for the capacity of all power generation and storage resources, ensuring that there is a large amount of excess capacity for each. After this the simulation duration, maximum load shed and grounding frequencies are determined. Once these frequencies are established the algorithm enters into a loop, while the indifference region has not been reached and the capacity of each resource is updated. Inside this loop, the simulation begins and resets the clock, while the abnormality duration and sampling frequency and the system's status are established. After these parameters have been set, an initial temporal array is stored for the abnormality duration, the temporal array is then updated as time passes to include only the latest states of the system. A permanent storage array then samples randomly from the system once for every window of the size given by the sampling frequency. In the event that an abnormality (load shed or grounding) occurs the temporal storage array is saved into the corresponding abnormality array such that the time when the abnormality occurred is in the middle of the array. Final abnormality arrays are then created by including the random sampling array to them. If there has been an excess of either type of abnormality the particle filtering algorithm will sample from the corresponding abnormality array and propose a new capacity for each resource correspondingly. If neither of the abnormality

metrics have been violated the particle filtering algorithm will sample from the random sampling array and propose decreased capacities based on the filters results. The iterative process continues until a significantly better generation capacity plan cannot be generated.

---

Set initial capacity for all power generation and storage resources
Set: Simulation Duration TMAX, Maximum Load Shed Frequency LSMAX, Maximum Grounding Frequency GMAX
Set Final Capacity = Initial Capacity        Set Capacity = 0
While |Capacity – Final Capacity| > Indifference Threshold
Capacity = Final Capacity
While T < TMAX
Determine abnormality duration, D = .5      // 30 Minutes
Determine sampling frequency, F = 4      // 4 Hours
Define the System_Status = (Nuclear_running_cap, Coal_running_cap, Gas_running_cap, Oil_running_cap, SolarCap, WindCap, Nuclear_KwH, Coal_KwH, Gas_KwH, Oil_KwH, Solar_KwH, Wind_KwH, CAES_Level, NaS_Battery_Level, PbA_Battery_Level, Grid_Level, Industrial_KwH, Commercial_KwH, Residential_KwH, Transportation_KwH, t%28800, Grounding, Load Shed)
Record system status into temporal storage array on line T  // Save initial temporal array
If T>D      // Update temporal array
Randomly sample once every F time units
Record abnormalities
T = T+1        // Advance simulation time
Create final load shed event array
Create final grounding event array
If Loadshed > LSMAX            //Update plant capacity based on load shed        Go To Filter (load shed array)
If Grounding > GMAX            //Update plant capacity based on grounding        Go To Filter (grounding array)
Filter (Array){            //Particle Filter
    Sample from Array
    Calculate total weights
    Normalize weights
    Estimate Generation Capacity // NuclearCap, CoalCap, GasCap, OilCap, SolarCap, WindCap            }
If Loadshed > LSMAX                                Increase current generation capacity based on Estimated Capacity
If Grounding > GMAX                                Decrease current generation capacity based on Estimated Capacity
If Loadshed < LSMAX & Grounding < GMAX        Decrease current generation capacity based on Estimated Capacity
Set Final Capacity based on current generation

---

Algorithm 2: Generation of the optimal capacity of electric resources based on Particle Filtering

**3.6. Evaluation of the Continuous-Discrete Modular Simulation and**

**Optimization for Electric Utility Resource Planning**

A Visual basic Application (VBA) control form has been created to enable the users to select which modules to include into the simulation and the capacity of each of the energy generating resources (in the fossil fuel and renewable energy generation modules), and energy storage resources (in the energy storage module) that are to be included. Furthermore, the user control form is used to select which of the nuclear power reactors in the state of Florida (from the five that are operating, and the four proposed reactors) to include in the simulation, as well as the planning horizon for which the simulation is set to run. The form is shown in Figure 17.



Figure 17: Simulation parameter selection control form

In order to illustrate the effectiveness of the proposed framework, we have designed a set of experiments with two main scenarios addressing the specifics of the

state of Florida. The first scenario includes a capacity plan that uses the currently installed nuclear energy generation capacity, while the second scenario includes the proposed four new nuclear reactors, as part of the nuclear energy generation capacity. In both of these scenarios annual demand increases according to the average for the next 20 years from the Energy Outlook (EIA, 2011) are considered. These increases in demand are estimated as 0.08% for residential demand, 1.08% for commercial demand, 0.82% for industrial demand, and 4.18% for transportation demand. Both scenarios have been run over planning horizons starting from 3 years through 30 years.

Tables 10 and 11 show the costs for commissioning and operating each of the proposed energy generation systems. Here the base cost is incurred only once as the facility is built, these base costs are multiplied by an eventuality factor that includes provisions for unanticipated events that will drive up the projects costs that (even though they are unanticipated) typically happen in these types of projects. The operation and maintenance costs have been split into fixed and variable costs; fixed costs are incurred occur annually and depend on the facility's size, while variable costs are incurred as the facility operates and are mainly related to fuel consumption.

Table 10: Costs of building and operating a power generating facility

| Energy Generation Technology | Base Cost ($/kW) | Eventuality Factor | Total Base Cost ($/kW) | Operation and Maintenance Variable Cost ($mills/kWh) | Operations and Maintenance Fixed Cost ($/kW) |
|---|---|---|---|---|---|
| Coal | 2,625 | 1.07 | 2,809 | 4.20 | 29.31 |
| Gas/Oil Combined Cycle | 917 | 1.08 | 991 | 3.07 | 14.44 |
| Combustion Turbine | 626 | 1.05 | 658 | 6.90 | 10.77 |
| Nuclear | 4,567 | 1.15 | 5,275 | 2.00 | 87.69 |
| Wind | 2,251 | 1.07 | 2,409 | 0 | 27.73 |
| Photovoltaic | 4,474 | 1.05 | 4,697 | 0 | 25.73 |

(EIA 2011)

Table 11: Costs of building and operating an energy storage system

| Energy Storage Technology | Base Cost ($/kW) | Eventuality Factor | Total Base Cost ($/kW) | Operations and Maintenance Variable Cost ($mills/kWh) | Operations and Maintenance Fixed Cost ($/kW) |
|---|---|---|---|---|---|
| CAES | 890 | 1.05 | 935 | 4.92 | 19 |
| NaS Battery | 389 | 1.07 | 416 | 0 | 35 |
| Pb Acid Battery | 540 | 1.05 | 567 | 0 | 28 |

(EIA 2011)

Figure 18 shows the overall mapping of the interaction of the different modules in the simulation and the required parameters that are involved in the calculation of the total costs, emissions and nuclear waste generated by the system.

### 3.6.1. Minimizing Total Cost with Installed Nuclear Capacity

In the first case, we evaluate the total cost of fulfilling the electricity demand of Florida up to a fulfillment factor of 95%, planning for nuclear energy generation up to the current installed capacity in the state. This is used as a baseline in order to understand the benefits or drawbacks of planning a nuclear expansion that includes four 1,100 MW AP1000 Nuclear plants.
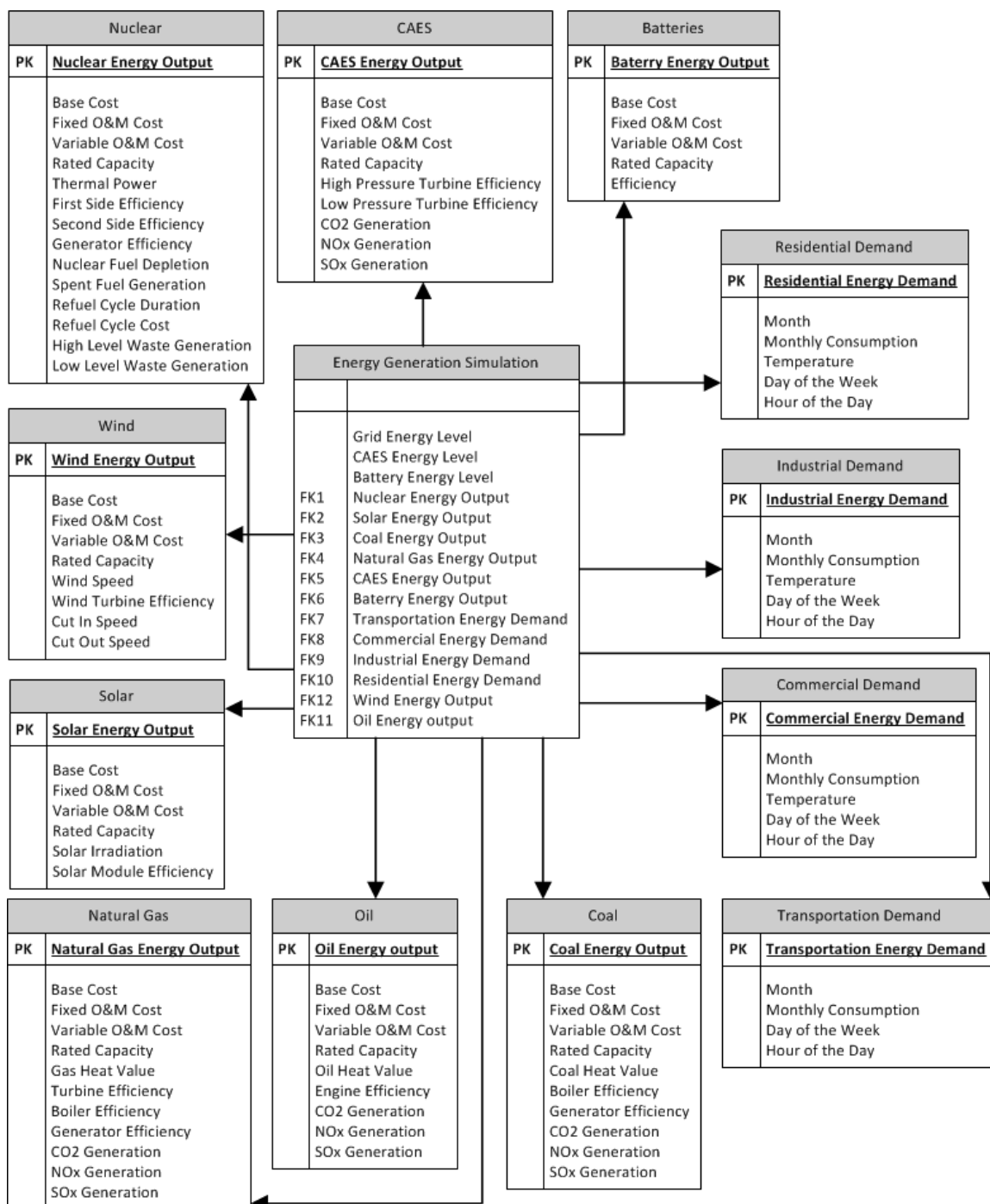
Figure 18: Data mapping for the interaction between the different modules of the generation simulation

Figure 19 shows the different non-dominated solution sets generated for each of the 10 proposed time horizons, in terms of total costs and emissions, per year. The figure shows how the non-dominated solution sets improve as the time horizon grows. The

non-dominated solution set for a time horizon of 3 year has a solution of minimum cost of $16,372 million and emissions of 36.213 million tons of greenhouse gases, per year; while the minimum cost solution for a 30 year planning horizon has a cost of $ 4,628 million, with emissions of 31.226 million tons of greenhouse gases, per year. This implies an overall cost decrease of 71.73% with respect to the costs of a 3 year planning horizon. In terms of minimum emissions the best solution from the non-dominated set for a planning horizon of 3 years has emissions of 10.346 million tons of greenhouse gases per year at an annual cost of $ 69,637 million, while the best solution from the non-dominated set for a planning horizon of 30 years has emissions of 9.112 million tons of greenhouse gases with a cost of $ 11,936 million per year, which entails a decrease of 11.92% annually with respect to the 3 year planning horizon. It is important to highlight that the non-dominated solution set for any given planning horizon dominates those generated for all shorter planning horizons, thus showing the benefits of performing long term planning.
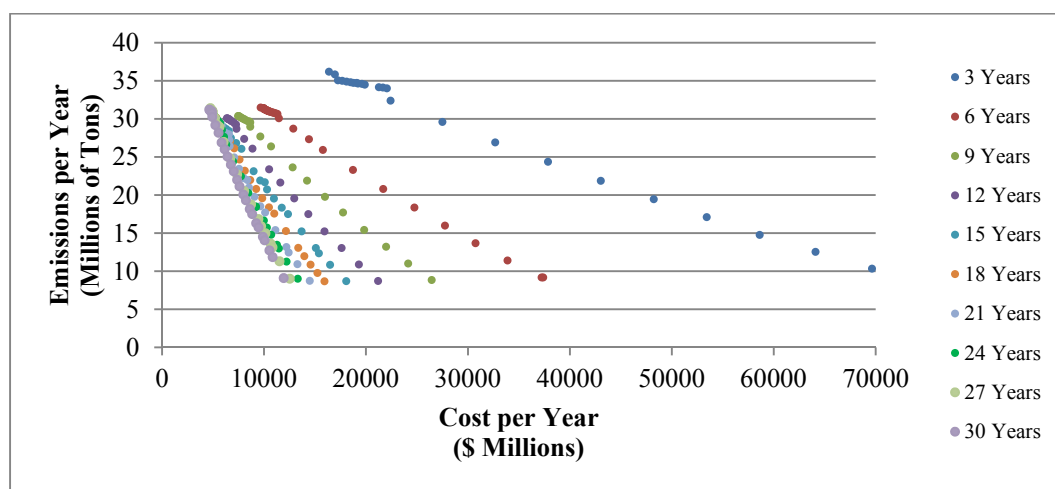


Figure 19: Non-dominated solution sets generated for different planning horizons

The evolution of the capacity plan with the minimum cost is shown in Figure 20. The figure shows how as the planning horizon expands the total yearly cost decreases. This displays how the base construction costs become a less significant factor to the overall yearly cost and how the decrease in the total costs is smaller, as the planning horizon expands. This effect can be confirmed when comparing the decrease in total cost from expanding the planning horizon from 18 years to 21 years, to that of expanding the planning horizon from 24 to 27 years, in the first case the reduction in cost is of 5.12% (from $ 5,328 million per year to $5,055 million per year) while in the latter case the reduction is of 2.31% (from $ 4,861 million per year to $4,749 million per year).
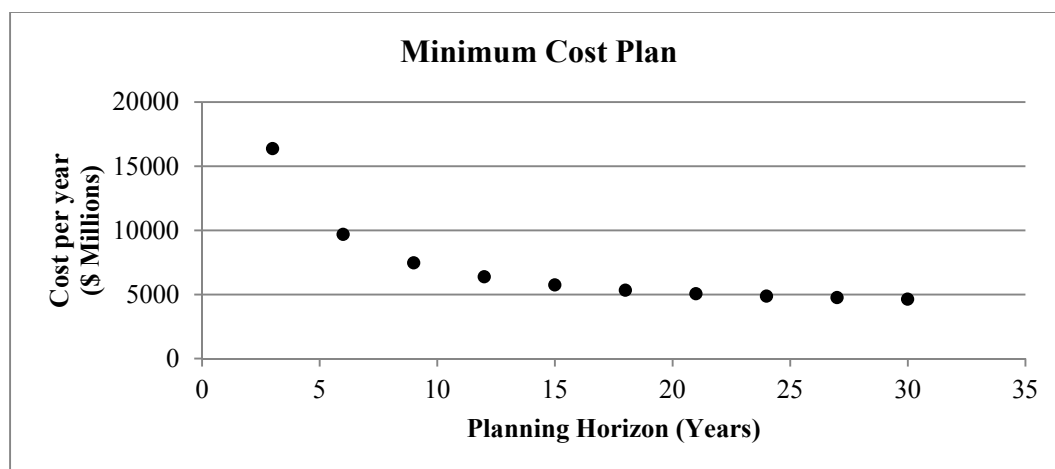


Figure 20: Minimum cost capacity plan for different planning horizons

Figure 21 shows the evolution of the minimum emissions capacity plan. In this case, the figure shows that as the planning horizon with the minimum yearly emissions is the planning horizon of 18 years, with emissions of 8.699 million tons of greenhouse gases per year. The figure shows that the yearly emissions decrease up to this point, starting with emissions of 10.346 million tons of greenhouse gases per year for a

planning horizon of 3 years. Starting at this point the yearly emissions increase until they reach a level of 9.112 million tons of greenhouse gases per year with a planning horizon of 30 years.
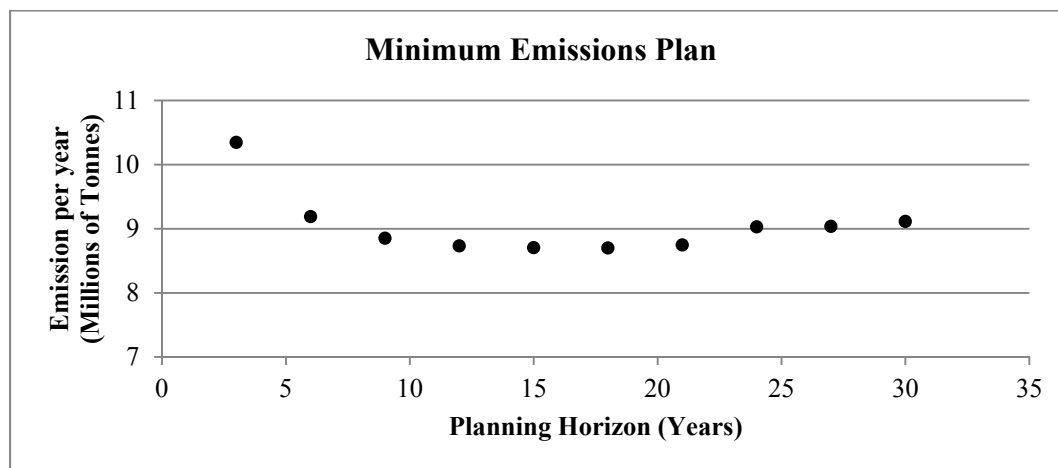


Figure 21: Minimum emissions capacity plan for different planning horizons

Table 12 shows the total generation capacity for the minimum cost capacity plan for each of the different planning horizons. The table shows how as the planning horizon expands the total energy generation and storage capacity expands, the annual costs decrease and the annual emissions reach a level that averages 30.620 million tons per year. In this case, with the solutions of minimum cost, the need for extra energy that arises from an expanded planning horizon is usually met with an expanded fossil fuel generation capacity. However there were two instances, when the planning horizon is of 15 years and of 30 years, where the need for extra energy from expanding the planning horizon was met with an expansion in the storage capacity and a reduction in fossil fuel energy generation.

Table 12: Costs and capacity of the minimum cost solution

| Planning Horizon | Annual Costs $ Millions | Annual Emissions Millions of Tons | Nuclear Generation Capacity MW | Fossil Fuel Generation Capacity MW | Renewable Generation Capacity MW | Storage Capacity MW | Total Generation Capacity |
|---|---|---|---|---|---|---|---|
| 3 | 16,371.67 | 36.213 | 3,924 | 20,048 | 0 | 765 | 23,972 |
| 6 | 9,674.33 | 31.518 | 3,924 | 20,524 | 0 | 668 | 24,448 |
| 9 | 7,455.00 | 30.399 | 3,924 | 20,694 | 0 | 882 | 24,618 |
| 12 | 6,368.92 | 30.093 | 3,924 | 21,005 | 0 | 895 | 24,929 |
| 15 | 5,733.93 | 29.377 | 3,924 | 20,497 | 0 | 2,802 | 24,421 |
| 18 | 5,327.89 | 30.193 | 3,924 | 21,619 | 0 | 1,056 | 25,543 |
| 21 | 5,055.24 | 30.499 | 3,924 | 21,999 | 0 | 1,056 | 25,923 |
| 24 | 4,860.83 | 30.843 | 3,924 | 22,467 | 0 | 958 | 26,391 |
| 27 | 4,748.52 | 31.431 | 3,924 | 23,077 | 0 | 984 | 27,001 |
| 30 | 4,628.00 | 31.226 | 3,924 | 22,752 | 0 | 2,301 | 26,676 |

Table 13 shows the total generation capacity for the minimum emissions capacity plan for each of the different planning horizons. The table shows that renewable energy generation dominates these solutions, as it represents 88.45% of the total energy generation capacity, on average. However, in these solutions fossil fuel energy generation represents 7.75% of the total generation capacity, on average. The total energy generation capacity expands by 576 MW for each extra year added to the planning horizon, while the effect on the energy storage capacity is not very large and energy storage averages 3,295 MW. It is important to note that comparing the minimum emissions capacity plan to the minimum cost capacity plan, the minimum emissions capacity plan has 78,819 MW more energy generation and storage capacity, as the total capacity is 310% larger on average, than that of the minimum cost capacity plan.

Figure 22 shows the capacity breakdown for the different solutions on the non-dominated solution set a planning horizon of 30 years, ranking them by their annual cost. The figure shows that in the solution with the lowest total cost nuclear energy generation represents 13.64% of the total generation and storage capacity, while in the solutions with the lowest emissions it represents 3.41% of the total generation and storage capacity. As

the solutions on the non-dominated set increase in cost and decrease in emissions the share of fossil fuel energy generation decreases from 78.43% in the minimum cost solution to 7.63% in the minimum emissions solution, and the share of renewable energy generation increases from 0% to 85.93%, in the minimum cost and minimum emissions solutions respectively.  In these solutions the energy storage capacity ranges from 2.98% to 8.86% of the total energy generation and storage capacity.

Table 13: Costs and capacity of the minimum emissions solution

| Planning Horizon | Annual Costs $ Millions | Annual Emissions Millions of Tons | Nuclear Generation Capacity MW | Fossil Fuel Generation Capacity MW | Renewable Generation Capacity MW | Storage Capacity MW | Total Generation Capacity |
|---|---|---|---|---|---|---|---|
| 3 | 69,636.67 | 10.346 | 3,924 | 7,429 | 85,445 | 3,074 | 96,797 |
| 6 | 37,386.67 | 9.187 | 3,924 | 7,578 | 87,162 | 3,136 | 98,664 |
| 9 | 26,456.67 | 8.851 | 3,924 | 7,654 | 88,034 | 3,167 | 99,611 |
| 12 | 21,194.17 | 8.733 | 3,924 | 7,808 | 89,805 | 3,231 | 101,537 |
| 15 | 18,069.33 | 8.704 | 3,924 | 7,965 | 91,608 | 3,296 | 103,497 |
| 18 | 15,930.56 | 8.699 | 3,924 | 8,076 | 92,891 | 3,342 | 104,891 |
| 21 | 14,495.24 | 8.747 | 3,924 | 8,238 | 94,756 | 3,409 | 106,918 |
| 24 | 13,309.58 | 9.028 | 3,924 | 8,532 | 95,341 | 3,357 | 107,797 |
| 27 | 12,532.59 | 9.036 | 3,924 | 8,651 | 97,457 | 3,431 | 110,033 |
| 30 | 11,936.33 | 9.112 | 3,924 | 8,842 | 99,601 | 3,507 | 112,367 |
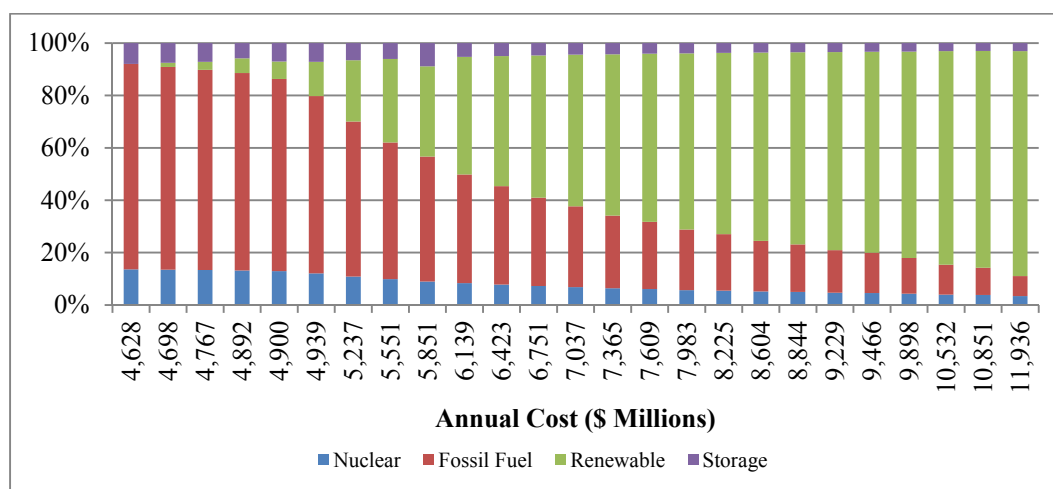


Figure 22: Composition of the non-dominated capacity plans for a planning horizon of 30 years

### 3.6.2.   Minimizing Total Cost with Expanded Nuclear Capacity

In the second case we evaluate the total cost of fulfilling the electricity demand of Florida up to a fulfillment factor of 95%, planning for an expansion in the nuclear energy generation from the current installed capacity to include four new 1,100 MW AP1000 Nuclear reactors.  This expansion implies an increase in the nuclear generation capacity of 112%, taking the total nuclear energy generation capacity from 3,924 MW to 8,324 MW.

Figure 23 shows the different non-dominated solution sets generated for each of the 10 proposed time horizons, in terms of total costs and emissions, per year.  The figure shows the same trends than in the first case, where the non-dominated solutions sets provide better annual costs and emissions, as the time horizon increases.  Here the solution of minimum cost for the 30 year planning horizon represents a 77.36% reduction in the overall cost compared to the 3 year planning horizon; $5,111 million per year, compared to $22,577 million per year.  The same phenomenon occurs with respect to the minimum emission solutions where the decrease from the 30 year planning horizon, compared to the 3 year planning horizon, is of 31.37% (a decrease from 0.102 million tons of greenhouse gases per year to 0.070 million tons of greenhouse gases per year).  In this case, as in the first, the non-dominated solution set for any given planning horizon dominates those generated for all shorter planning horizons.
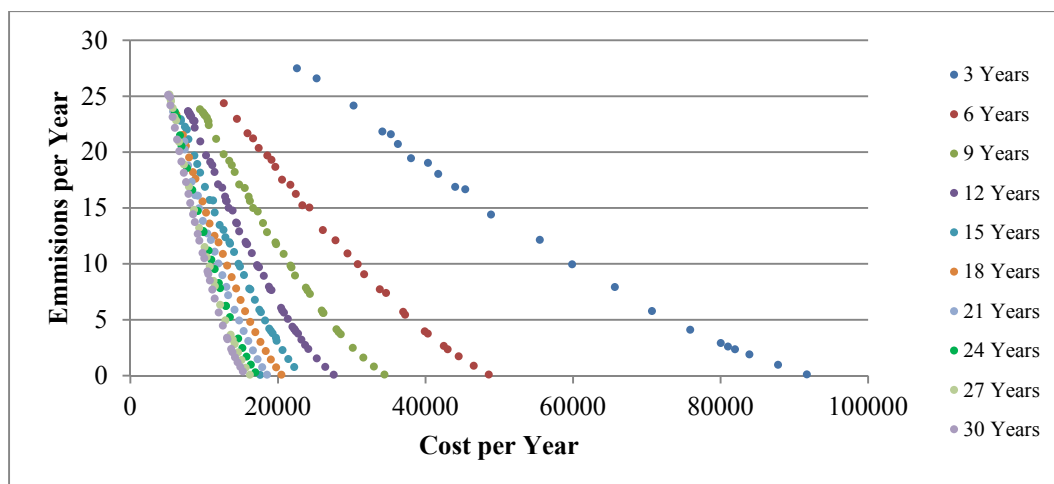
Figure 23: Non-dominated solution sets generated for different planning horizons

Figure 24 shows the capacity plan of minimum cost for the different planning horizons. The figure further evidences how as the capacity plan increases the total yearly costs decrease, with smaller decreases with each further increase in the planning horizon. This shows how the operational costs, which are independent of the planning horizon, become a more important component of the total cost, and cost reductions that are of 7.29% when expanding the planning horizon from 18 to 21 years (from $6,239 million per year to $5,784 million per year), become of 3.36% when expanding the planning horizon from 27 to 30 years (from $5,289 million per year to $5,111 million per year).
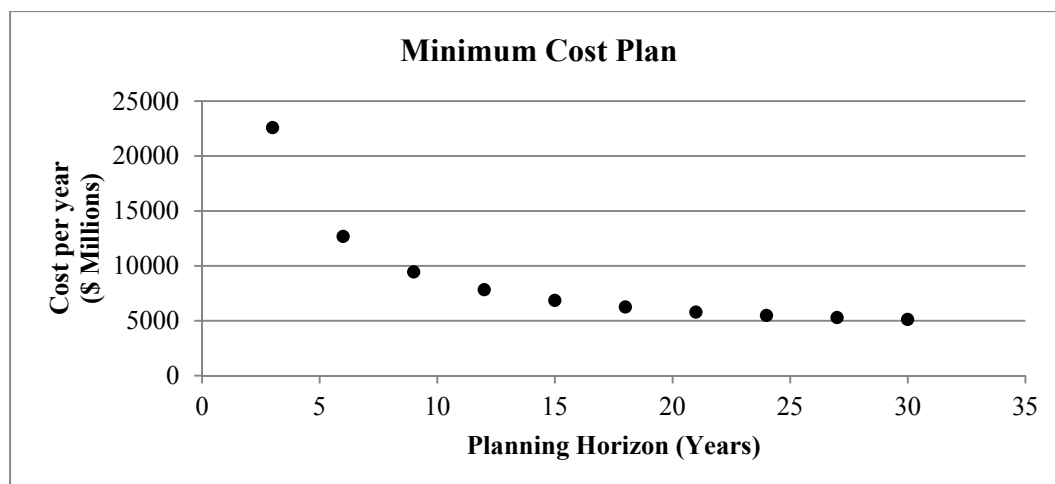
Figure 24: Minimum cost capacity plan for different planning horizons

Figure 25 shows the capacity plan of minimum emissions for the different planning horizons. The figure shows that as the planning horizon increases the total yearly emissions tend to decrease, although this does not happen in every case. The maximum yearly emissions, for the 3 year planning horizon, are of 0.102 million tons of greenhouse gases per year, while the minimum emissions, for the 30 year planning horizon, are of 0.070 million tons of greenhouse gases per year. However, in the non-dominated solution sets going from a planning horizon of 12 years to one of 15years implies an increase in the minimum emissions per year from 0.083 million tons to 0.086 million tons of greenhouse gases per year. Similarly, going from a planning horizon of 18 years tone of 21 years implies an increase in the minimum emissions per year from 0.074 million tons to 0.076 million tons of greenhouse gases per year. This suggests that in these solutions the randomness from the simulation may have an important impact in the output of renewable energy generation systems, which in turn impacts output needed from the fossil fuel energy generation systems. Since fossil fuel energy generation systems drive most of the greenhouse gas emissions, changes due to randomness become

very important since these systems, in these minimum emissions solutions, average just 0.0692% of the total energy generation capacity.
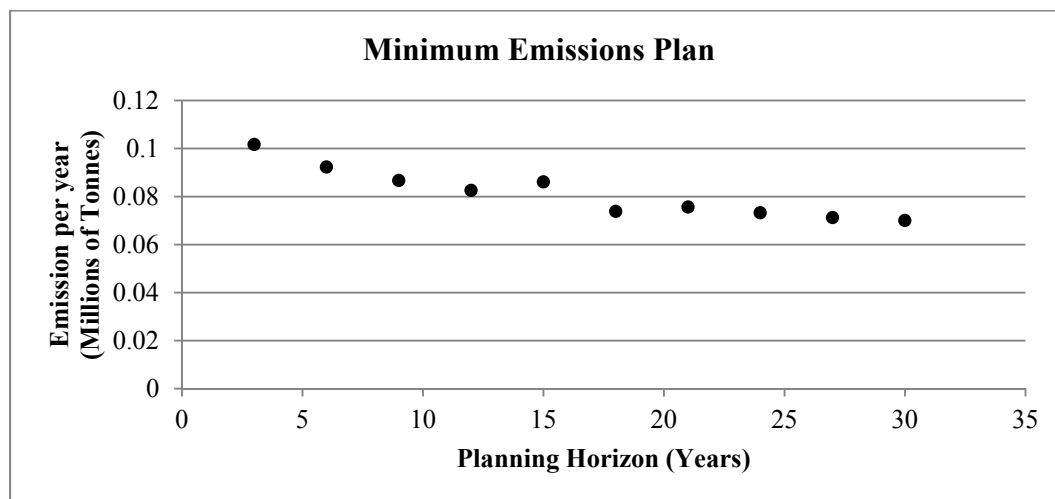


Figure 25: Minimum emissions capacity plan for different planning horizons

The total generation capacity, for the capacity plans with minimum cost for the different planning horizons, is shown in Table 14. This table shows the same general trends from the first case where, as the planning horizon increases, the total energy generation capacity increases or there is an increase in energy storage capacity to meet increasing energy demand. In this case, with the inclusion of the extra nuclear generation capacity, the annual greenhouse gas emissions reach an average of 24.006 million tons per year. This emissions level represents a 21.6% reduction in annual greenhouse gas emissions compared to the first case, with no nuclear capacity expansion.

Table 15 shows the total generation capacity for the capacity plans with minimum emissions, for the different planning horizons. In this case, like in the case with no expanded nuclear capacity, renewable energy generation dominates the total energy generation capacity, and represents 93.48% of the total capacity on average, while fossil

fuel energy generation represents only 0.0692% of the total generation capacity, on average. In this case, there is an average of 951 MW of energy generation capacity, and 29 MW of energy storage capacity, added for each year that the planning horizon increases. Comparing the minimum emissions capacity plan to the minimum cost capacity plan there is an increase in the total generation and storage capacity of 104,200 MW, as the generation of the minimum emissions capacity plan is 410% larger than that of the minimum cost capacity plan, on average.

Table 14: Costs and capacity of the minimum cost solution

| Planning Horizon | Annual Costs $ Millions | Annual Emissions Millions of Tons | Nuclear Generation Capacity MW | Fossil Fuel Generation Capacity MW | Renewable Generation Capacity MW | Storage Capacity MW | Total Generation Capacity |
|---|---|---|---|---|---|---|---|
| 3 | 22,577.33 | 27.491 | 8,324 | 15,824 | 0 | 794 | 24,148 |
| 6 | 12,670.33 | 24.370 | 8,324 | 16,149 | 0 | 668 | 24,473 |
| 9 | 9,431.00 | 23.833 | 8,324 | 16,474 | 0 | 861 | 24,798 |
| 12 | 7,811.17 | 23.663 | 8,324 | 16,758 | 0 | 895 | 25,082 |
| 15 | 6,838.67 | 22.945 | 8,324 | 16,097 | 0 | 2,802 | 24,421 |
| 18 | 6,238.89 | 23.366 | 8,324 | 16,625 | 0 | 2,661 | 24,949 |
| 21 | 5,783.81 | 23.622 | 8,324 | 17,559 | 0 | 1,592 | 25,883 |
| 24 | 5,474.58 | 23.987 | 8,324 | 17,993 | 0 | 1,543 | 26,317 |
| 27 | 5,288.52 | 25.143 | 8,324 | 18,677 | 0 | 984 | 27,001 |
| 30 | 5,111.00 | 25.122 | 8,324 | 18,352 | 0 | 2,301 | 26,676 |

Table 15: Costs and capacity of the minimum emissions solution

| Planning Horizon | Annual Costs $ Millions | Annual Emissions Millions of Tons | Nuclear Generation Capacity MW | Fossil Fuel Generation Capacity MW | Renewable Generation Capacity MW | Storage Capacity MW | Total Generation Capacity |
|---|---|---|---|---|---|---|---|
| 3 | 91,706.67 | 0.102 | 8,324 | 89 | 110,070 | 3,813 | 118,483 |
| 6 | 48,595.00 | 0.092 | 8,324 | 92 | 111,727 | 3,870 | 120,142 |
| 9 | 34,452.22 | 0.087 | 8,324 | 91 | 114,141 | 3,988 | 122,556 |
| 12 | 27,565.00 | 0.083 | 8,324 | 90 | 117,281 | 4,143 | 125,695 |
| 15 | 23,180.00 | 0.086 | 8,324 | 96 | 118,651 | 4,178 | 127,071 |
| 18 | 20,478.33 | 0.074 | 8,324 | 84 | 121,515 | 4,205 | 129,924 |
| 21 | 18,525.71 | 0.076 | 8,324 | 88 | 123,955 | 4,290 | 132,368 |
| 24 | 17,201.25 | 0.073 | 8,324 | 87 | 127,491 | 4,329 | 135,903 |
| 27 | 16,196.30 | 0.071 | 8,324 | 87 | 131,028 | 4,367 | 139,438 |
| 30 | 15,539 | 0.070 | 8,324 | 88 | 135,758 | 4,588 | 144,170 |

Figure 26 shows the composition of the generation and storage capacity for the different solutions on the non-dominated solution set for the 30 year planning horizon. The figure shows that the solutions of lower costs are composed primarily of fossil fuel energy generation, which represents 68.8% of the total generation capacity of the minimum cost solution, while the solutions of minimum emissions are composed primarily of renewable energy generation, which represents 94.17% of the total generation capacity of the minimum emissions solution. Nuclear energy generation represents 31.2% of the total energy generation capacity of the minimum cost solution and its share of the total generation capacity drops to 5.77% in the minimum emissions solution. The total energy generation capacity increases from 26,676 MW in the minimum cost solution to 144,170 MW in the minimum emissions solution.
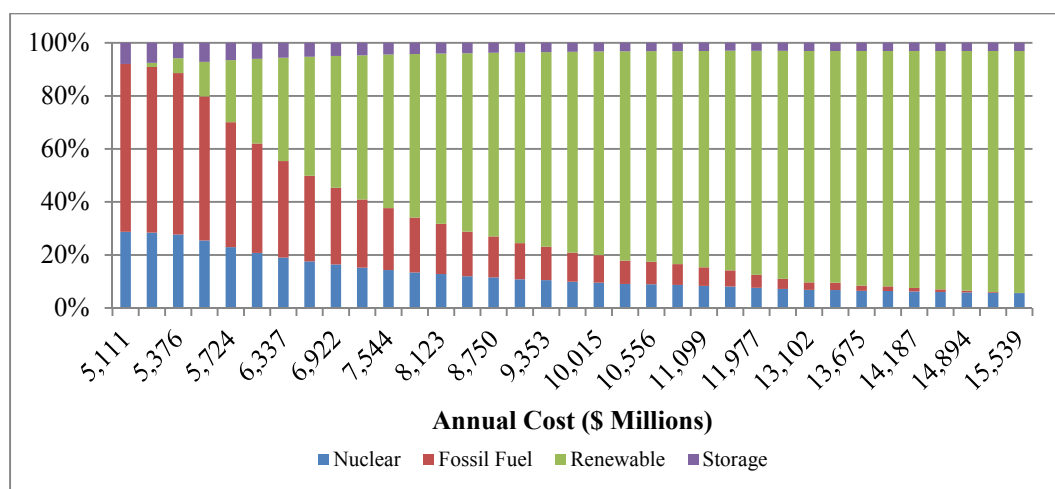


Figure 26: Composition of the non-dominated capacity plans for a planning horizon of 30 years

A comparison of the composition of the minimum cost solution for the 30 year planning horizon for the cases with the current nuclear generation capacity and the expanded generation capacity is shown in Figure 27. The figure shows how the

expansion of the nuclear energy generation capacity represents an increase in its participation of the total energy generation and storage capacity of 15.09% that is taken from the fossil fuel energy generation capacity, while the energy storage capacity is almost unaltered, as it changes from 7.93% to 7.94% of the total generation and storage capacity. In this case there are no sources of renewable energy generation, for the cost of generating energy with these sources is higher than that of fossil fuel energy generation. Implementing the nuclear capacity expansion under a minimum cost scenario takes the annual costs from $4,628 million to $5,111 million which represents an increase in total costs of 10.44%, however this increase in total cost is compensated by a decrease in total emissions of 19.55%, as total yearly emissions decrease from 31.23 million tons of greenhouse gases to 25.12 million tons of greenhouse gases. We can determine that in order to encourage shifting from a capacity plan that includes the current installed nuclear capacity to one that includes the expanded nuclear capacity, under a scenario of minimum total cost, a greenhouse gas emissions tax of at least $79.13 per ton is needed.
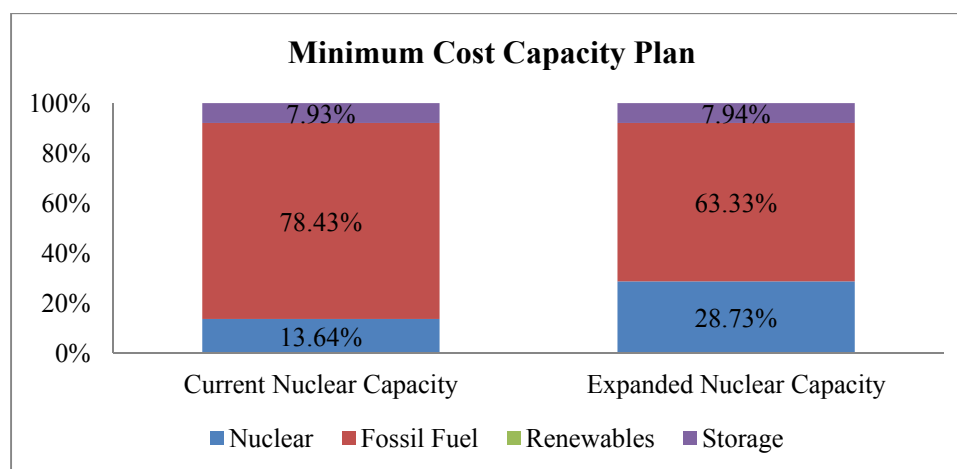


Figure 27: Composition of the minimum cost capacity plans for a planning horizon of 30 years

Figure 28 shows the comparison of the composition of the minimum emissions solution for the 30 year planning horizon for the cases with the current nuclear generation capacity and the expanded generation capacity. The figure shows that with the expanded nuclear generation capacity there is an expansion in the share of renewable energy generation sources of 5.33%, from 85.93% to 91.26%, and a reduction of fossil fuel energy generation sources from 7.63% to 0.06%. The composition of energy storage sources has little change, from 3.03% to 3.08%, while nuclear energy generation represents 3.41% of the total energy generation and storage capacity in the first case and 5.60% in the second case. It is important to mention that in terms of total capacity there is an increase in renewable energy generation from 99,601MW to 135,758 MW. It is believed that this increase is permitted by the fast response times of the nuclear energy generation systems which enable the mitigation of the high intermittency of the renewable energy generation systems, without compromising the system's security and ensuring that all the constraints are met. The inclusion of the expanded nuclear capacity, enables the minimum emissions solution to reach a yearly emissions level of 0.07 million tons of greenhouse gases, compared to a level of 9.11 million tons of greenhouse gases, however the cost of reaching these levels is of $15,246.67 million per year and $11,936.33 million per year. Nevertheless, in the case of minimizing total emissions, deploying a capacity plan with expanded nuclear capacity is favorable, since yearly emissions levels of 9.08 million tons per year, which are less than those achieved by the minimum emissions solution with no expanded nuclear capacity, can be obtained at a cost of $10,556 million tons per year. Under a scenario of minimum emissions it is better to deploy a capacity plan with the expanded nuclear capacity, than to use one that has the

current nuclear capacity. It is important to highlight that issues concerning the security and cyber-security of nuclear energy generation as well as potential hazards that may arise when considering the management of nuclear waste have not been included in the present study and should be addressed in future research.
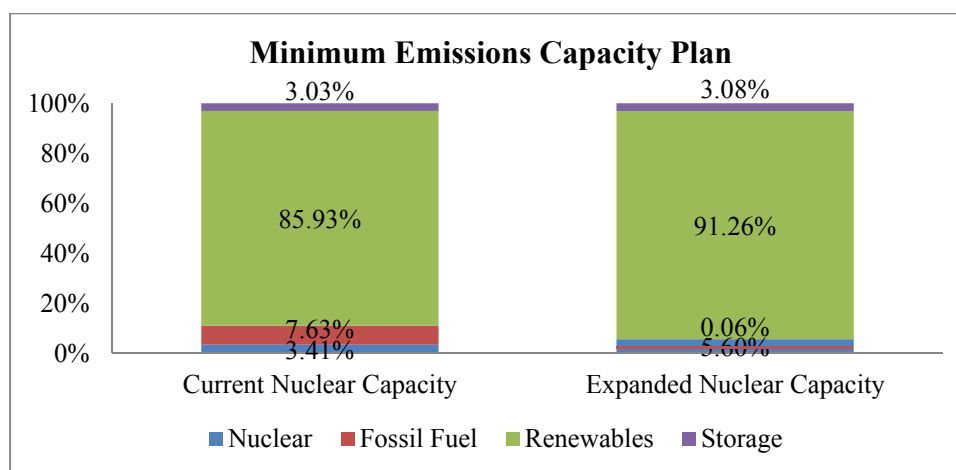


Figure 28: Composition of the minimum emissions capacity plans for a planning horizon of 30 years

### 3.6.3. Computational Performance of the Continuous-Discrete Modular Simulation and Optimization

Figure 29 shows the different feasible solutions proposed by the optimization algorithm across 500 iterations for a planning horizon of 3 years with no expansion in the nuclear energy generation capacity. The figure shows how solutions are generated, by populating solutions within local non-dominated solution sets. As the algorithm finds better solutions (solutions in darker areas), these are used to generate new non-dominated solution sets and a "layering" effect may be seen, as new local non-dominated solution sets are generated. Furthermore, in the circled area, it may be seen that as better solutions are found, the algorithm will continue creating solutions in that direction, before trying to

populate the non-dominated solution set, using information from the rest of the solutions

that, at that point, are on the non-dominated solution set.
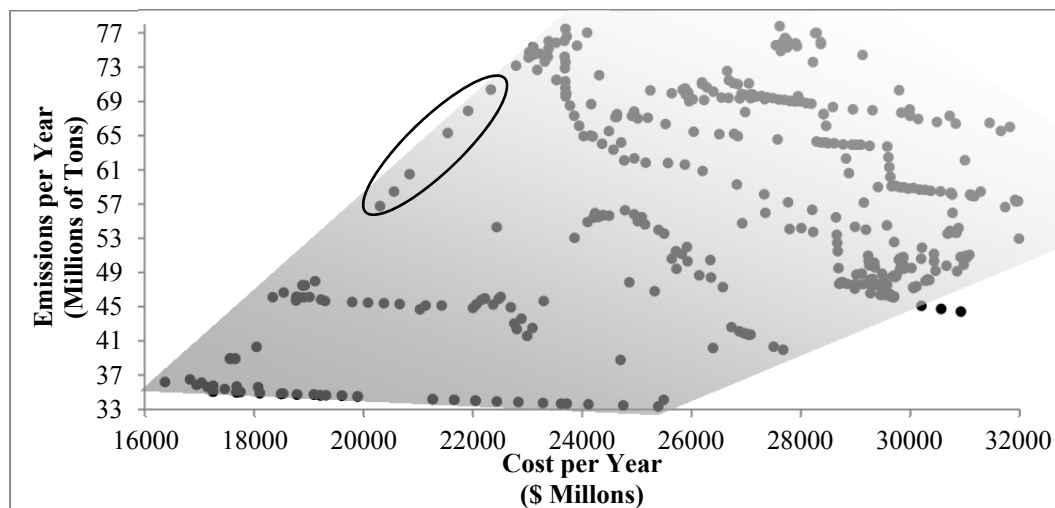


Figure 29: Solutions generated by the multi-objective optimization algorithm based on particle filtering for a planning horizon of 3 years using the current nuclear generation capacity

We have developed a simulation based decision making framework that has enabled us to establish the best possible combination of resource investments for electric power generation and storage capacities and evaluate the effectiveness of including an expansion to the nuclear energy generation capacity as part of the comprehensive energy capacity plan. The developed tool involves a modular modeling approach for the processes of different nature that exist within this complex system focusing on the details regarding nuclear energy generation, and will help the utility companies conduct resource planning using the developed particle filtering based optimization for multi-objective optimization in a realistic simulation environment.

# Chapter 4: Multi-objective Optimization based on Particle Filtering

In order to extend the employment of particle filtering to multi-objective optimization, we present a novel framework for multi-objective optimization using particle filtering. The proposed framework employs the information from the non-dominated solution set generated during each iteration in both the sequential importance sampling and the resampling stages. The use of these two sampling stages deals with potential problems that may arise from the use of a singular transition in the parameter vector, which commonly arise in simple sequential Monte Carlo algorithms. In the sequential importance sampling stage the update of the posterior distribution is based only on the particles from the non-dominated solution set that has been constructed so far, in a fashion similar to the kernel smoothing of parameters proposed by Liu et al. (2007). The use of the sequential importance sampling stage lets the algorithm sample from an approximation to the problems optimal Pareto front, while the resampling stage is intended to help the algorithm to converge to the global optimal solutions efficiently.

## 4.1. Overview of Particle Filtering

A system may be described by the state-space model shown in Eqs. (26) and (27), where $\theta_k$ is the state of the system at time $k$, $\psi_k$ is the observation taken from the system, $v_k$ is the system noise, and $v_k$ is the measurement noise.

$$\theta_k = g(\theta_{k-1}, v_k), \qquad k = 1,2,\dots \qquad \text{Eq. (26)}$$

$$\psi_k = h(\theta_k, v_k), \qquad k = 0,1,\dots \qquad \text{Eq. (27)}$$

Using $p(\theta_k|\theta_{k-1})$ as the transition density function and $p(\psi_k|\theta_k)$ as the likelihood density function, the particle filtering problem consists of estimating the posterior probability density function of the state given all of the observations, $b_k(\theta_k) = p(\theta_k|\psi_{0:k})$, where $\psi_{0:k} = (\psi_0, \dots, \psi_k)$. A prediction and an update step are involved in attaining the estimated posterior probability density function. In the prediction step, the conditional probability $p(\theta_k|\psi_{0:k-1})$ is estimated using the previous step's updated conditional probability $p(\theta_{k-1}|\psi_{0:k-1})$ and the Chapman-Kolmogorov equation (Doucet et al. 2000). The relationship between these probabilities can be summarized such that the importance weights function is equal to the multiplication of the likelihood function and prior probability density function divided by the incremental likelihood. Here, the prior probability density function is given by the prediction equation, the likelihood function is given by observation model, and the incremental likelihood is given by the denominator, as shown in Eq. (28).

$$b_k(\theta_k) = \frac{p(\psi_k|\theta_k)\, p(\theta_k|\psi_{0:k-1})}{p(\psi_k|\psi_{0:k-1})} \qquad \text{Eq. (28)}$$

Since the integrals from the update and prediction steps given by the Chapman-Kolmogorov equation are usually intractable, particle filtering represents the probabilities via a set of randomly selected weighted samples (Doucet et al. 2000). The posterior density function is approximated as $\sum_{i=1}^{N} \omega_k^i \delta(\theta_{0:k} - \theta_{0:k}^i)$, by letting $\{\theta_{0:k}^i\}$ be a set of

particles for $i = 1, \dots, N$ with associated normalized weights $\sum_i \omega_k^i = 1$, where $\delta$ denotes the Dirac delta function. Furthermore, since taking samples directly from the posterior probability function is usually unfeasible, these samples are drawn from a different importance function $q(\theta_k | \psi_{0:k})$. An advantage to sampling from the importance function is that it can be chosen freely so long as the approximation from Eq. (29) holds. Additionally, if the importance function is chosen to factorize such as in Eq. (30), then particles from the $k - 1$ step ($\theta_{0:k-1}^i$) may be augmented by $\theta_k \sim q(\theta_k | \theta_{0:k-1}, \psi_{1:k})$ to get the new particles $\theta_{0:k}^i$. Weights are updated according to Eq. (31), and because of the way that the importance function is factorized, the posterior density may be approximated by $\sum_{i=1}^{N_s} \omega_k^i \delta(\theta_k - \theta_k^i)$, and there is no need to preserve the history of observations $\psi_{1:k-1}$, nor the trajectories of the samples $\theta_{0:k-1}^i$.

$$\omega_k^i \propto \frac{p(\theta_{0:k}^i | \psi_{0:k})}{q(\theta_{0:k}^i | \psi_{0:k})} \qquad \text{Eq. (29)}$$

$$q(\theta_{0:k} | \psi_{0:k}) = q(\theta_k | \theta_{0:k-1}, \psi_{0:k}) q(\theta_{0:k-1} | \psi_{0:k-1}) \qquad \text{Eq. (30)}$$

$$\omega_k^j = \omega_{k-1}^j \frac{p(\psi_k | \theta_k^i) p(\theta_k^i | \theta_{k-1}^i)}{q(\theta_k^i | \theta_{0:k-1}^i, \psi_{0:k})} \qquad \text{Eq. (31)}$$

## 4.2. Particle Filtering-based Optimization

An optimization problem with $m$ decision variables may be described as in Eqs. (32) and (33), where $x$ is the decision vector, and it is assumed that there exists a unique optimal solution $x^*$.

$$x^* = \arg\min f(x) \qquad \text{Eq. (32)}$$

$$x = (x_1, x_2, \ldots, x_m) \in R^m \qquad \text{Eq. (33)}$$

Zhou et al. (2008) have shown that the optimization problem in Eqs. (32) and (33) may be formulated as a particle filtering problem by representing it with an appropriate state space model. The appropriate state space model for this is defined in Eqs. (34) and (35), where $\theta_k$ is the unobserved state, $\psi_k$ is the observation, $v_k$ is the observation noise (which is an independent identically distributed sequence with a probability density function $\varphi(\cdot)$ and assumed to be non-negative), and the unobserved initial state $\theta_0$ is equal to $x^*$.

$$\theta_k = \theta_{k-1}, \qquad k = 1, 2, \ldots \qquad \text{Eq. (34)}$$

$$\psi_k = f(\theta_k) - v_k, \qquad k = 0, 1, \ldots \qquad \text{Eq. (35)}$$

For this state-space model the transition density function is given in Eq. (36), where $\delta$ is the Dirac delta function, and the likelihood function is given by Eq. (37).

$$p(\theta_k|\theta_{k-1}) = \delta(\theta_k - \theta_{k-1}) \qquad \text{Eq. (36)}$$

$$p(\psi_k|\theta_k) = \varphi(f(\theta_k) - \psi_k) \qquad \text{Eq. (37)}$$

The reasoning behind the model is that the optimal solution is generated by an unobserved stationary state, while it is only possible to observe the optimal function values with some noise ($\psi^* = f(\theta^*)$). Furthermore, it is only possible to observe function values at least as large as the optimal ($\psi_k \geq \psi^*$), since $\psi_k = f(\theta_k)$. In this

case, the posterior probability function is given by Eq. (38). It can be seen that with each iteration, the posterior probability density function is adjusted by the performance of the previous solution and generates a new posterior probability distribution.

$$b_k(\theta_k) = \frac{\varphi(f(\theta_k) - \psi_k) b_{k-1}(\theta_k)}{\int \varphi(f(\theta_k) - \psi_k) b_{k-1}(\theta_k) d\theta_k} \qquad \text{Eq. (38)}$$

It is expected that if $\psi_k$ decreases in relation to $k$, the posterior density $b_k$ will be getting closer to the density function of $\theta_k$, as the Dirac delta function concentrates around $x^*$. From an optimization point of view, this means that as $k$ increases, the density defined on the solution space ($b_k$) becomes more concentrated on the optimal solution. Finally, it should be noted that in order to solve the optimization problem from Eqs. (32) and (33), $b_k$ has to be recursively estimated for the model in Eqs. (34) and (35), while constructing a decreasing sequence of observations $\psi_k$.

The presented formulation may be extended to multi-objective optimization problems by including $n$ different objective functions and redefining $f(x)$ to $f(x) = (f1(x), f2(x), \dots, fn(x))$. In this case now there is rarely a single solution $x^*$ that minimizes $f_i(x), \forall i$, there is a set of solutions that may be considered non-dominated and part of the optimal solution set.

Here, a solution vector $\alpha$ is said to dominate a solution vector $\beta$ if and only if the conditions in Eqs. (38) and (40) are met. Furthermore, $\alpha$ is said to cover $\beta$ if and only if $\alpha$ dominates $\beta$ or $f(\alpha) = f(\beta)$ (Zitzler et al., 2000). A solution vector $x^*$ is considered Pareto optimal if it is a non-dominated solution vector.

$$\forall i \in \{1,2,\dots,n\}: f_i(\alpha) \le f_i(\beta) \qquad \text{Eq. (39)}$$

$$\exists j \in \{1,2,\dots,n\}: f_j(\alpha) < f_j(\beta) \qquad \text{Eq. (40)}$$

Based on the extension of the formulation of the optimization problem presented in Eqs. (32) and (33) to a multi-objective setting, we propose a novel framework for multi-objective optimization based on particle filtering.

## 4.3. Description of the Proposed Framework

The proposed framework uses four stages, an initialization stage, a sequential importance sampling stage, a resampling stage and a stopping stage. In the initialization stage, the initial non-dominated set $\psi_0$ is defined as an empty set, and the initial sampling distribution $b_0$ is defined as a uniform distribution between the sampling space's maxima and minima, however, if the search space is unbounded, prior knowledge regarding the problem is to be used to establish appropriate bounds $(\theta_{min}, \theta_{max})$. Furthermore, in problems where prior information indicates that a uniform distribution is not the most adequate, the prior sampling distribution may be adjusted to another distribution function that is more suitable to the specific application. Furthermore, in this initialization stage the number of particles for the sequential importance sampling stage ($N$) and minimum number of sequential sampling iterations ($P$) are defined, as well as the number of extreme points ($L$) used and number of particles ($M$) to sample for the resampling stage.

Once the initialization stage has been completed, the sequential importance sampling stage is performed. In this stage samples are taken from the sampling

distribution, and are evaluated for performance and feasibility, based on the problem's objectives and constraints. At this point, a strategy to deal with the problem's constraints and the samples that do not meet them must be implemented. Some possible strategies include, using only the particles which meet the problem's constraints and removing those that do not meet these constraints, while another possible strategy involves the use of numerical methods to adjust the particles so that they meet the constraints. Because of the different constraints that different problems may impose on the optimization, it is not possible to propose one single strategy with which to address this potential feasibility problem that will satisfy every case. Once a set of feasible samples is obtained it is used to construct the non-dominated solution set, which is constructed through the evaluation of the objective functions for each of the samples, and the comparison of their performance.

Based on the samples, the non-dominated solution set and the sampling distribution may be updated. In order to update the sampling distribution, the samples from the non-dominated solution set are sorted based on their performance on one of the problem's objectives, which is selected arbitrarily. With the ordered sample set, weights may be updated so that they are proportional to the smallest component of the Minkowski distance of order 1 between each sample on the non-dominated solution set and it subsequent sample in the set. We propose to use the smallest component of the Minkowski distance of order 1, so that more samples are drawn between consequent samples that are further away from each other, and less samples are drawn from sections of the non-dominated solution set that are more densely populated, however other orders of the Minkowski distance may be used if it is more suitable in the specific application of

the framework to have weights that are distributed differently. The particles from subsequent samplings are shown in Figure 30, where it may be seen how the non-dominated solution set is populated with more members as the algorithm progresses, as more particles are drawn from what, so far, is our best approximation of the Pareto front. Sequential sampling is performed iteratively for a minimum of $P$ iterations or until there is no change in the non-dominated set from one iteration to the next.
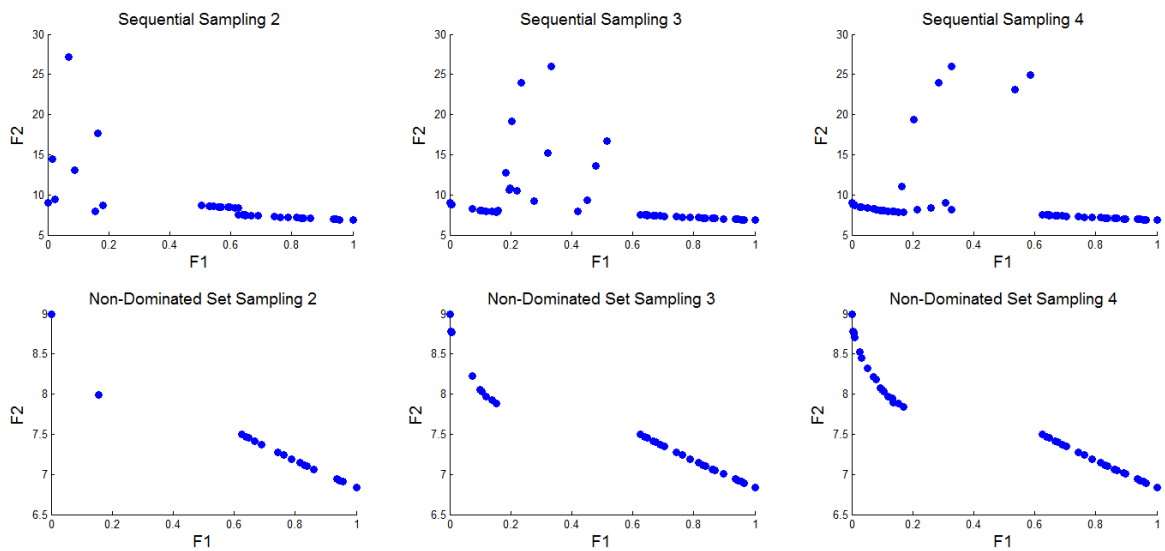


Figure 30: Particles drawn from the sequential importance sampling stage

In the resampling stage, a set $A$ is constructed using all of the samples that have the best performance on each of the problem's objectives. A resampling distribution is created for each member of this set and their $L$ closest extreme points in the sampling space, such that there is resampling from $AL$ distributions. However, if there is no information regarding the closest extreme points to the members of set $A$, $L$ random points within the sampling space are used to create the resampling distributions. Once the resampling distributions have been built $M$ random samples are evaluated so that the non-

dominated solution set may be updated. The use of this resampling stage tries to avoid that the algorithm converges to local optimum Pareto fronts.

Once the resampling stage is completed, the sequential importance sampling resumes. These iterative processes continue until a predetermined stopping criteria is reached, this may be when a preset number of iterations are performed, or when there are no changes in the non-dominated solution set for a predetermined number of iterations. Once this happens the final non-dominated solution set is presented as the solution to the multi-objective optimization problem. Algorithm 3 outlines the proposed framework for particle filtering based multi-objective optimization (MOPF).

In Algorithm 3, the initialization stage is done in steps 1 through 4; the sequential importance sampling stage is performed in steps 5 through 10; and the resmpling stage is performed in steps 11 through 15. The stopping stage is evaluated in step 16. It is important to point out that in steps 8 and 14 an approximate method, like Parzen estimation is used to construct continuous approximations to the sampling functions so that the new samples are not drawn from the previous non-dominated solution set and its empirical weighted distribution, but include parts of the sampling space that were not previously considered.

1. Initialize the algorithm's parameters:
   Prior sampling distribution $b_0 = unif(\theta_{min}, \theta_{max})$
   Initial non-dominated set $\psi_0 = \emptyset$
   Number of particles to sample in the first sampling stage $N$
   Minimum number of iterations of the sequential importance sampling stage $P$
   Number of extreme points used to construct the resampling distributions $L$
   Number of particles to sample in the resampling stage $M$
   Iteration counter $k = 1$
2. Sample $\{\theta_k^i\}_1^N$ from $b_0$.
3. Evaluate the problem's constraints, choose and apply a strategy to adjust $\{\theta_k^i\}$ to meet the constraints of the problem, if these are not met.
4. Let $\psi_k$ be the samples on the non-dominated set built comparing the performance of the samples from $\theta_k$ and $\psi_{k-1}$, according to Eqs. (39) and (40).
5. Reset the sequential iterations counter $p = 0$.
6. Order the samples according to their performance in one of the optimization's objectives.
7. Let $\hat{b}_k(\theta_k) = \sum_{i=2}^{N-1} w_k^i \delta(\theta_k - \theta_k^i)$, where weights $w_k^i \propto \min_{j=1}^n \frac{\left|\psi_k^{i,j} - \psi_k^{i+1,j}\right|}{\left|\psi_k^{1,j} - \psi_k^{N,j}\right|}, i = 1,2, \dots, N-1$.
8. Construct a continuous approximation $\tilde{b}_k(\theta_k)$ from $\hat{b}_k(\theta_k)$ and Sample $\{\theta_{k+1}^i\}_{i=1}^N$ independently from $\tilde{b}_k(\theta_k)$.
9. Evaluate the problem's constraints, and apply a strategy to adjust $\{\theta_k^i\}$ to meet the constraints of the problem, and let $\psi_k$ be the samples on the non-dominated set.
10. If $p < P$ or $\psi_k \neq \psi_{k-1}$, let $k = k + 1$, $p = p + 1$ and go to step 5; else go to step 11.
11. Generate a subset $A$ from $\psi_k$ which includes all of the samples that have the best performance for each of the individual objective functions.
12. Find the $L$ closest extreme points to each of the members of the set $A$, in the absence of such information choose $L$ random points within the sampling space.
13. For each of the $al$ points selected in step 11 let $\hat{b}_k^l(\theta_k) = \sum_{i=1}^L \sum_{j=1}^A w_k^{i,j} \delta(\theta_k^i - \theta_k^j)$, where weights $w_i^{j,k} \propto 1/M$.
14. Construct a continuous approximation $\tilde{b}_k^l(\theta_k)$ from $\hat{b}_k^l(\theta_k)$ and Sample $\{\theta_{k+1}^i\}_{i=1}^M$ independently from $\tilde{b}_k^l(\theta_k)$.
15. Evaluate the problem's constraints, and apply a strategy to adjust $\{\theta_k^i\}$ to meet the constraints of the problem, and let $\psi_k$ be the samples on the non-dominated set.
16. If a stopping criterion is satisfied, then stop; else, $k = k + 1$ and go to step 5.

Algorithm 3: Proposed particle filtering-based multi-objective optimization

## 4.4. Evaluation of the Proposed Framework for Multi-objective Optimization based on Particle Filtering

In order to illustrate the validity of the proposed framework, we have used five well-known benchmark functions from Zitzler, Deb and Thiele (ZDT) (Zitzler et al., 2000) as listed in Table 16, and have compared the results obtained by the proposed MOPF framework with the methods listed in Table 17. The comparison of the different algorithms has been performed based on the convergence metric (Khare et al., 2003), generational distance (Van Veldhuizen, 1999) and diversity metric (Deb et al., 2002).

Table 16: Benchmark problems used in experiments

| ZDT1 | |
|---|---|
| $m = 30$; $x_i \in [0,1]$; $i = 1, \ldots, m$ | $f_1(x) = x_1$ $f_2(x) = g(x)\left(1 - \sqrt{\frac{f_1(x)}{g(x)}}\right)$ $g(x) = 1 + 9\sum_{i=2}^{m} \frac{x_i}{m-1}$ |
| ZDT2 | |
| $m = 30$; $x_i \in [0,1]$; $i = 1, \ldots, m$ | $f_1(x) = x_1$; $f_2(x) = g(x)\left(1 - \left(\frac{f_1(x)}{g(x)}\right)^2\right)$; $g(x) = 1 + 9\sum_{i=2}^{m} \frac{x_i}{m-1}$ |
| ZDT3 | |
| $m = 30$; $x_i \in [0,1]$; $i = 1, \ldots, m$ | $f_1(x) = x_1$; $f_2(x) = g(x)\left(1 - \sqrt{\frac{f_1(x)}{g(x)}} - \frac{f_1(x)}{g(x)}\sin\left(10\pi f_1(x)\right)\right)$; $g(x) = 1 + 9\sum_{i=2}^{m} \frac{x_i}{m-1}$ |
| ZDT4 | |
| $m = 10$; $x_1 \in [0,1], x_i \in [-5,5]$; $i = 2, \ldots, m$ | $f_1(x) = x_1$; $f_2(x) = g(x)\left(1 - \sqrt{\frac{f_1(x)}{g(x)}}\right)$; $g(x) = 1 + 10(m-1) + \sum_{i=2}^{m}\left(x_i^2 - 10\cos(4 - \pi x_i)\right)$ |
| ZDT6 | |
| $m = 10$; $x_i \in [0,1]$; $i = 1, \ldots, m$ | $f_1(x) = x_1$; $f_2(x) = g(x)\left(1 - \left(\frac{f_1(x)}{g(x)}\right)^2\right)$; $g(x) = 1 + 9\left(\frac{\sum_{i=2}^{m} x_i}{m-1}\right)^{\frac{1}{4}}$ |

Table 17: Algorithms used for comparison purposes

| Algorithm | Acronym |
|---|---|
| Fonseca and Fleming's Algorithm (Fonseca and Fleming, 1995) | FFGA |
| Hajela and Lin's weighted-sum based approach (Hajela and Lin, 1992) | HLGA |
| The Niched Pareto Genetic Algorithm (Horn et al., 1994) | NPGA |
| The Non-dominated Sorting Genetic Algorithm (Srinivas and Deb, 1994) | NSGA |
| The Non-dominated Sorting Genetic Algorithm II (Deb et al., 2002) | NSGA2 |
| A single-objective evolutionary algorithm using weighted-sum aggregation (Zitzler et al., 2000) | SOEA |
| The Strength Pareto Evolutionary Algorithm (Zitzler and Thiele, 1999) | SPEA |

The convergence metric (Khare et al., 2003) is designed to evaluate the distance between the non-dominated solution set that an algorithm has reached and the problem's global Pareto front. The convergence metric (CM) is defined as in Eq. (41) where $|\theta|$ is the number of non-dominated solutions in the set $\theta$, and $d_i$ is the Euclidean distance between the solution $i \in \theta$ and its nearest member of the Pareto front. In terms of the convergence metric, smaller values are preferable since a small value for the metric implies that there is a small distance between the non-dominated solution set and the Pareto front. The generational distance (GD) (Van Veldhuizen, 1999) is another metric designed to assess the distance between the non-dominated solution set that an algorithm has reached and the global Pareto front, and is defined as in Eq. (42). Similar to the case of the convergence metric, smaller values in the generational distance imply that there are smaller distances between the non-dominated solution set and the Pareto front, and hence are preferred. The diversity metric (DM) (Deb et al., 2002) is designed to evaluate the spread within the non-dominated solution set that an algorithm has reached. The diversity metric is defined as in Eq. (43), where $d_i$ is the Euclidean distance between points $i$ and $i + 1$ in the non-dominated solution set $\theta$, $\bar{d}$ is the average of these distances; and $d_f$ and

$d_l$ represent the distance between the extreme points on the Pareto front and boundary solutions of $\theta$. In this case, smaller values of the diversity metric imply a more even distribution of the members of the non-dominated solution set.

$$CM = \frac{\sum_{i=1}^{|\theta|} d_i}{|\theta|} \qquad \text{Eq. (41)}$$

$$GD = \frac{\sqrt{\sum_{i=1}^{|\theta|} d_i^2}}{|\theta|} \qquad \text{Eq. (42)}$$

$$DM = \frac{d_f + d_l + \sum_{i=1}^{|\theta|-1} |d_i - \bar{d}|}{d_f + d_l + (|\theta|-1)\bar{d}} \qquad \text{Eq. (43)}$$

The methods compared to the MOPF framework have been evaluated using 250 generations, a population size of 100, a crossover rate of 0.8, a mutation rate of 0.01, a niching parameter of 0.48862 and a domination pressure of 10. The selection of the parameters for the MOPF framework has been done based on the computational time and the performance, using particle set sizes ($N$) ranging from 50 to 150 particles, and using the number of times resampling was performed as a stopping criterion, and varying this process between 10 to 50 times.

The framework has been evaluated using problems ZDT3 and ZDT4. ZDT3 has been selected since we have noticed that, because of the discontinuous nature of the Pareto front of this problem, the MOPF framework struggles to reach the optimal non-dominated solution set. The problem ZDT4 has been selected since it is a problem in which the algorithms that are being compared have not been able to reach the Pareto front under the proposed parameters (Zitzler et al., 2000). The performance has been evaluated in terms of CM; however there is a very strong relationship between the CM and the GD, in which we have found an $R^2$ greater than 83% when preforming linear regression on the

CM predicted by the GD, and believe we could use either metric indistinctively for the analysis.

When performing linear regression on the CM using the number of particles and the number of iterations as predictors, we have found that the number of iterations is a significant predictor and that the CM improves as the number of iterations increases. Furthermore, we have encountered that the same relationship occurs when preforming the linear regression on the GD; however we have found that the DM is independent from both the number of particles and iterations with p-values greater than 0.25. In terms of computational time, both the number of particles and iterations have a direct impact on performance. Table 18 shows the time used by the MOPF with the different particle set sizes and iteration numbers used for problem ZDT4, while Table 19 shows the CM under the same setting.

Table 18: Computational time for problem ZDT4

| | | Particles | | | | |
|---|---|---|---|---|---|---|
| | | 50 | 75 | 100 | 125 | 150 |
| | 10 | **10.864** | 10.987 | 11.735 | 13.019 | 15.765 |
| | 15 | 14.571 | 17.055 | 18.500 | 18.847 | 20.172 |
| | 20 | 19.276 | 20.437 | 24.203 | 25.272 | 27.054 |
| | 25 | 25.221 | 26.173 | 28.501 | 31.518 | 32.614 |
| **Resampling Stages** | 30 | 27.650 | 31.714 | 36.167 | 37.250 | 39.498 |
| | 35 | 32.933 | 38.703 | 38.597 | 43.182 | 46.510 |
| | 40 | 37.012 | 41.221 | 46.497 | 47.881 | 49.553 |
| | 45 | 42.591 | 45.986 | 48.347 | 55.812 | 54.840 |
| | 50 | 50.023 | 56.882 | 55.041 | 60.237 | **61.068** |

Table 19: Convergence Metric for problem ZDT4

| | | Particles | | | | |
|---|---|---|---|---|---|---|
| | | **50** | **75** | **100** | **125** | **150** |
| **Resampling Stages** | 10 | **8.146** | 6.972 | 5.696 | 5.508 | 6.659 |
| | 15 | 4.458 | 3.025 | 3.677 | 5.292 | 5.827 |
| | 20 | 1.921 | 1.130 | 2.521 | 3.995 | 1.614 |
| | 25 | 0.961 | 1.183 | 3.154 | 1.950 | 4.434 |
| | 30 | **0.000** | 0.001 | 0.001 | 1.659 | 1.939 |
| | 35 | 0.508 | 0.529 | 0.515 | 0.520 | 2.718 |
| | 40 | 0.535 | 0.001 | 0.506 | 0.502 | 0.001 |
| | 45 | 0.491 | 0.489 | 0.517 | 0.001 | 0.001 |
| | 50 | 0.001 | 0.001 | 0.001 | 0.001 | 0.001 |

Using these metrics, non-dominated solution sets have been developed for both the ZDT3 and ZDT4 problems; Figure 31 shows the non-dominated solution set for problem ZDT4, as an example. Using the a fuzzy logic mechanism to select the best compromise solution (Abido, 2006), with linear membership functions the best compromise solution for problem ZDT3 is achieved with 100 particles for the sequential importance sampling stage and letting the algorithm use the resampling stage 15 times, while the best compromise solution for problem ZDT4 is achieved with 75 particles for the sequential importance sampling stage and letting the algorithm use the resampling stage 20 times. When using a quadratic membership function for the CM objective, the best compromise solution for problem ZDT3 is achieved with 50 particles for the sequential importance sampling stage and using the resampling stage 35 times, while the same parameters, 75 particles for the sequential importance sampling stage and using the resampling stage 20 times, lead to the best compromise solution for problem ZDT4. Based on these results we have selected to evaluate the MOPF algorithm using 100 particles in the sequential importance sampling stage, since this is the largest number of particles from the best compromise solutions, and since increasing the number of

particles does not increase computational time as significantly as increasing the number of iterations does (as can be seen in Table 18); and allowing the algorithm to use the resampling stage 25 times, which is between the parameters that lead to the best solutions. Furthermore, we have used 3 extreme points ($L$) to generate the resampling distributions and 30 particles ($M$) in the each of the sampling distributions of the resampling stages.
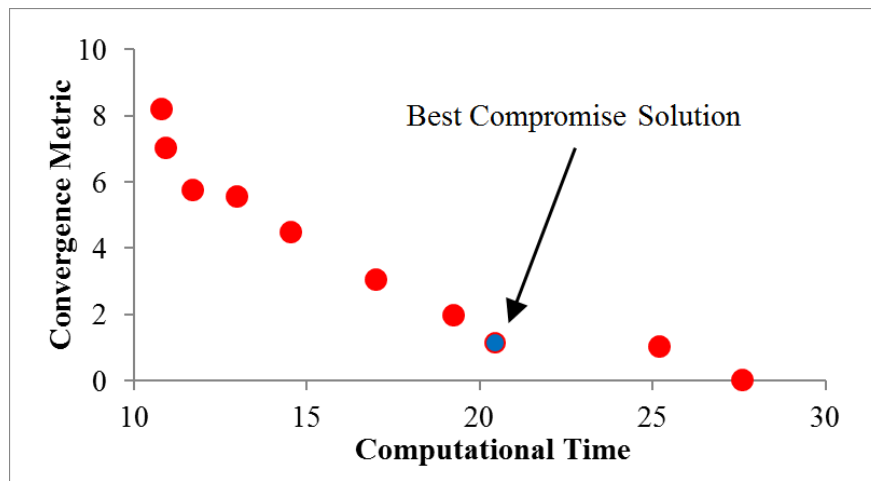


Figure 31: Non-dominated solution set for performance based on particle set size and iteration number

We have performed 20 consecutive executions of each of the comparison methods in Table 17, as well as of the MOPF framework, for each of the benchmark problems. The presented results come from the best non-dominated front generated with each method. Figure 32 shows an example of the evolution of the MOPF framework as the iterations progress, using problem ZDT4. In the figure, we can see the effect of both sequential importance sampling and resampling, as most of the solutions from the oval labeled S1 come from the sequential importance sampling stage, while most of the

solutions from the rectangles S2-1 and S2-2 come from the sampling distributions of the resampling stage.
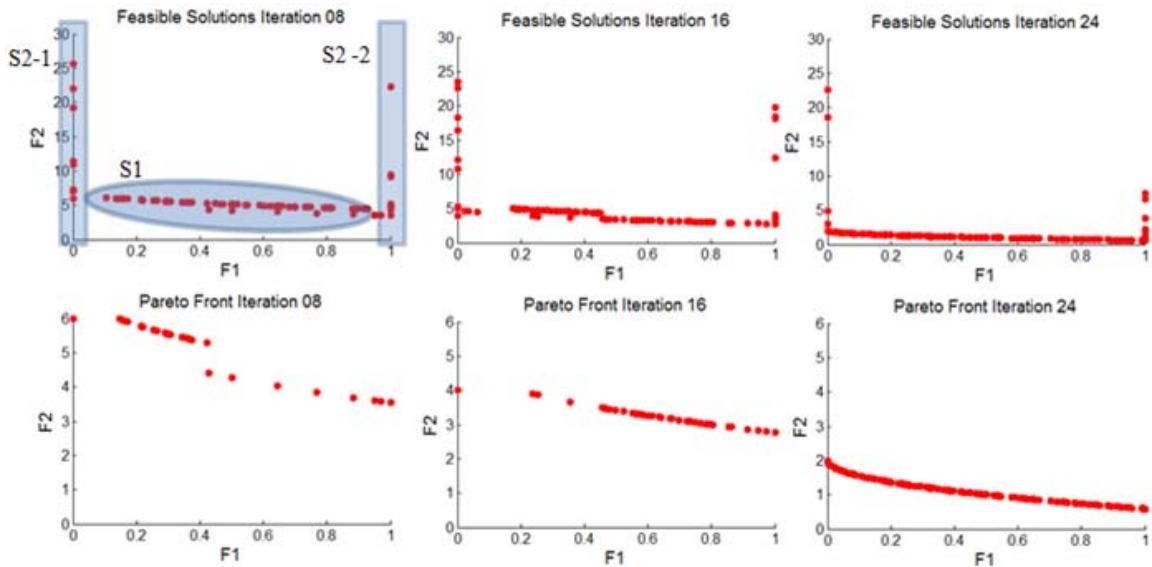


Figure 32: Screenshot representation of the evolution of the MOPF framework

Figure 33 shows the non-dominated solution sets provided by the different algorithms for the problem ZDT1 (see Table 16). Problem ZDT1 has a convex Pareto front that poses challenges to achieving a diverse non-dominated front, and leverages the fact that some implementations of multi-objective optimization algorithms give a higher importance to solutions that cover a larger number of solutions and "individual champion" solutions (solutions that are optimal for an individual objective function (Deb, 1999)) are given less importance. In the results, we can see that the non-dominated set from the MOPF framework clearly dominates those from the FFGA, HLGA, NPGA, NSGA, NSGA II and SOEA algorithms. The non-dominated solution set from the MOPF framework dominates most of the solutions from the non-dominated set of the SPEA algorithm, while it is not dominated by any of them. The figure also shows that

there is adequate diversity within the non-dominated set from the MOPF framework and although the solution set is not evenly distributed, it has solutions that are very close to Pareto solution generated with each of the "individual champion" solutions for each function. In order to achieve this diversity, the MOPF framework's resampling stage is critical for this problem. Since in the resampling stage the particles are taken from the extreme points of the non-dominated solution set and the closest extreme points in the sample space, the framework is able to improve diversity instead of extensively populating regions within the non-dominated solution's extreme points.
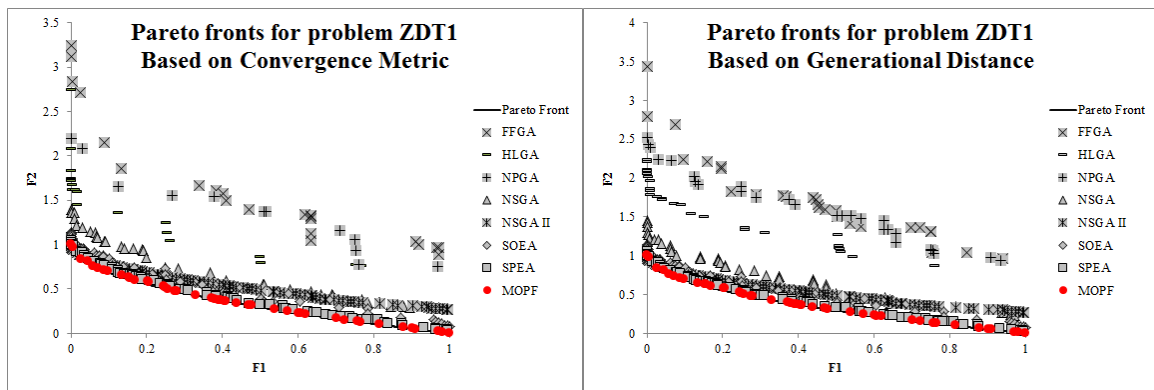


Figure 33: Pareto fronts for ZDT1 test problem

Figure 34 shows the non-dominated solution sets provided by the different algorithms for the problem ZDT2 (see Table 16). Problem ZDT2 is the nonconvex counterpart to problem ZDT1, and in this case diversity should not be a challenge as was the case in problem ZDT1. Here, we can see in the results that the non-dominated sets from the FFGA, HLGA, NPGA, NSGA, NSGA II, SOEA and SPEA algorithms are all dominated by the non-dominated set from the MOPF framework. Furthermore, the non-dominated set from the MOPF framework has acceptable diversity and there are solutions

generated close to the extreme points of the Pareto front. The sequential importance sampling stage of the MOPF framework becomes more important in achieving the diversity in this case. This is due to the fact that in the sequential importance sampling stage, samples are taken proportionally to the smallest component of the Minkowski distance of order 1 between the solutions in the non-dominated solution set, more samples are drawn from regions in the non-dominated front that are less densely populated than from regions where the solutions are closer to each other.
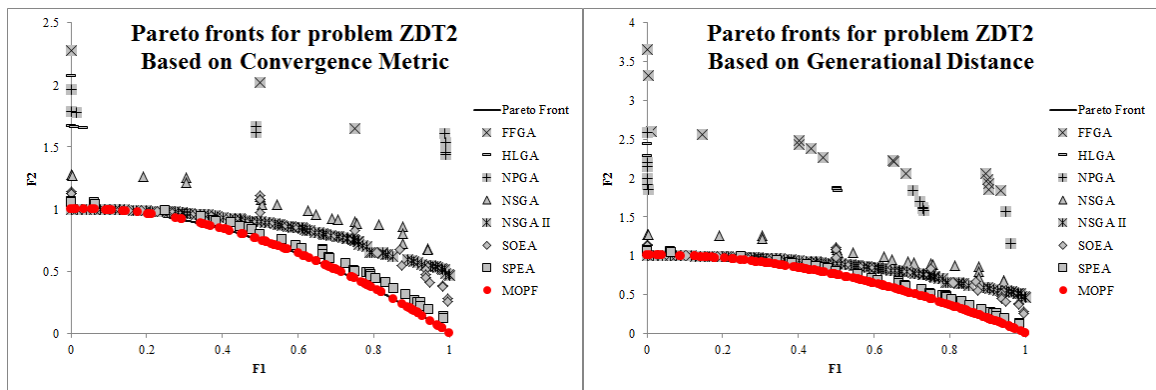


Figure 34: Pareto fronts for ZDT2 test problem

Figure 35 shows the non-dominated solution sets provided by the different algorithms for the problem ZDT3 (see Table 16). ZDT3 has a discontinuous Pareto front which leads to problems to many multi-objective optimization algorithms since competition among solutions within each sub-region of the non-dominated solution set may lead to the disappearance of solutions corresponding to some sub-regions. Here, we can see in the results that the non-dominated set from the MOPF framework clearly dominates the non-dominated set from the FFGA, HLGA and NPGA algorithms. When doing individual comparisons between the non-dominated solution set from the MOPF

framework with those from the NSGA and NSGA II algorithms, we can see that the solution space is almost equally divided between the parts that are dominated by MOPF framework and the parts that are dominated by NSGA and NSGA II algorithms, respectively. Furthermore, we can see that the non-dominated solution sets from SOEA and SPEA algorithms dominate most of the solutions from the MOPF framework. We can see how the discontinuity in the Pareto front poses challenges to the MOPF framework where in the non-dominated solution set with the best convergence metric, one of the sub-regions of the Pareto front is not corresponded by solutions on the non-dominated front. Furthermore, even with the use of the resampling stage, in the non-dominated front with the best convergence metric, there is only one solution close to an "individual champion" solution and in the non-dominated solution set with the best generational distance there are no solutions close to the "individual champion" solutions. However, it should be noted that the algorithm's sequential importance sampling stage is able to populate the sub-regions where the algorithm has found at least two different solutions.
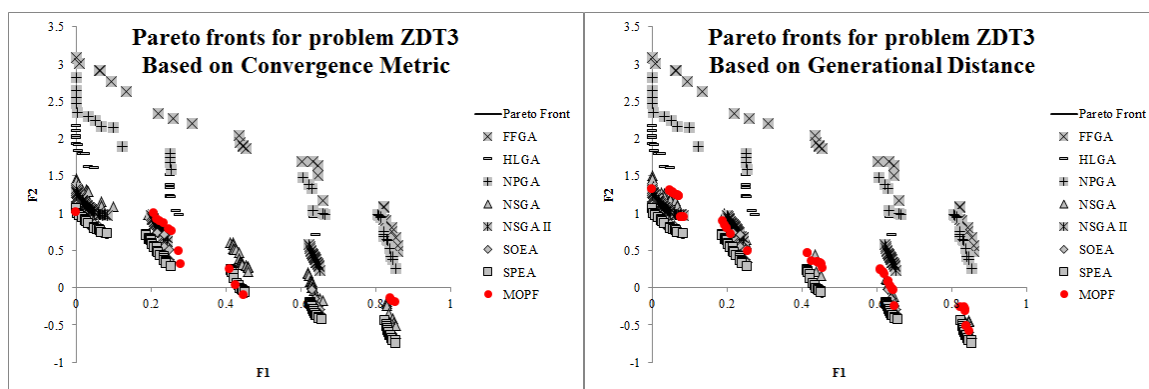


Figure 35: Pareto fronts for ZDT3 test problem

Figure 36 shows the non-dominated solution sets provided by the different algorithms for the problem ZDT4 (see Table 16). Zitzler et al. (2000) have designed ZDT4 to test an algorithm's ability to deal with multimodality since there are more than $7.9 \times 10^{11}$ local Pareto fronts. In this case, we can see in the results that the non-dominated set from the MOPF framework clearly dominate the non-dominated solution sets from the FFGA, HLGA, NPGA, NSGA, NSGA II, SOEA and SPEA algorithms. In order to address multimodality, the proposed MOPF framework relies on the resampling stage. Here, as samples are taken from the non-dominated solutions set's extreme points and the closest extreme points of the solution space, the algorithm has a better chance of improving from one local Pareto front to the global Pareto front. Contrasting this, the sequential importance sampling stage should be very good at populating the achieved local optimum, since it draws samples from within the non-dominated solution set. With multimodal functions such as this one, the number of iterations used in the algorithm has a substantial effect on the algorithm's ability to converge to the optimal solution, while increasing the number of samples does not have such a significant impact. This can be evidenced in Table 19, where the number of non-dominated solution sets produced with a convergence metric with a value lower than one increase as the number of times resampling is performed increases.

Figure 37 shows the non-dominated solution sets provided by the different algorithms for the problem ZDT6 (see Table 16). ZDT6 is designed to pose two distinct challenges to multi-objective optimization algorithms. The first challenge comes from the fact that the Pareto front is biased for solutions where $f_1$ is close to one, and the solutions are not uniformly distributed across the Pareto front. The second challenge

arises from the fact that the feasible solutions are concentrated away from the Pareto front and few of the solutions are near the optimal. Here, like in the cases of problem ZDT2 and ZDT4, we can see that the non-dominated set from the MOPF framework clearly dominates the non-dominated solution sets from the FFGA, HLGA, NPGA, NSGA, NSGA II, SOEA and SPEA algorithms. Out of the two challenges posed by the problem, the MOPF framework is weaker at dealing with the solution density problem. This problem is addressed by the resampling stage, where directions different than those within the non-dominated solution set are explored.
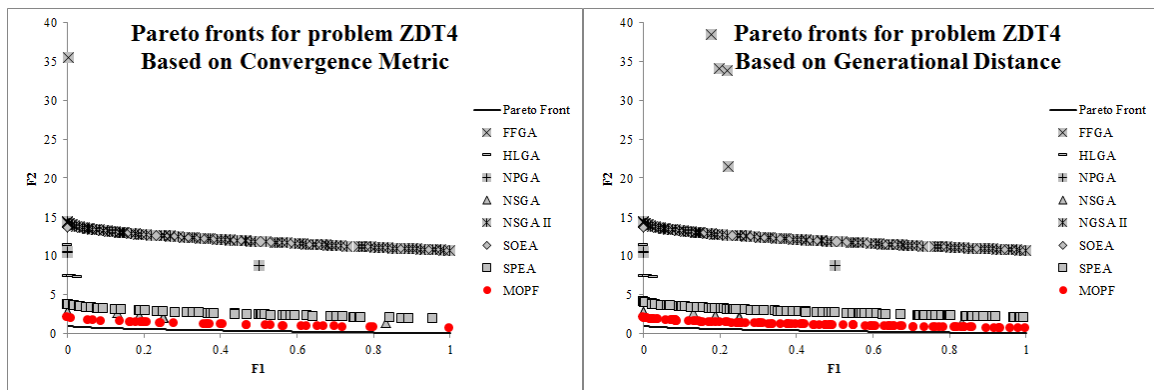


Figure 36: Pareto fronts for ZDT4 test problem

Table 20 shows the performance of the non-dominated solution sets, and compares the convergence metric, generational distance and diversity metric from each of the different algorithms for problems ZDT1, ZDT2, ZDT3, ZDT4, and ZDT6. In terms of ZDT1, we can see that the convergence metric of the MOPF framework is almost one order of magnitude better than that from the SPEA algorithm, which in turn outperforms the rest of the compared algorithms. In terms of the generational distance, the MOPF is still the best algorithm even though it does not outperform the rest of the algorithms by

such a wide margin. In terms of diversity metric, NSGA II is the best rated algorithm while the MOPF framework is rated as the one with the lowest diversity. We can see that for problem ZDT1, the MOPF framework can produce the non-dominated fronts closest to the Pareto front although they are the least evenly spread out.
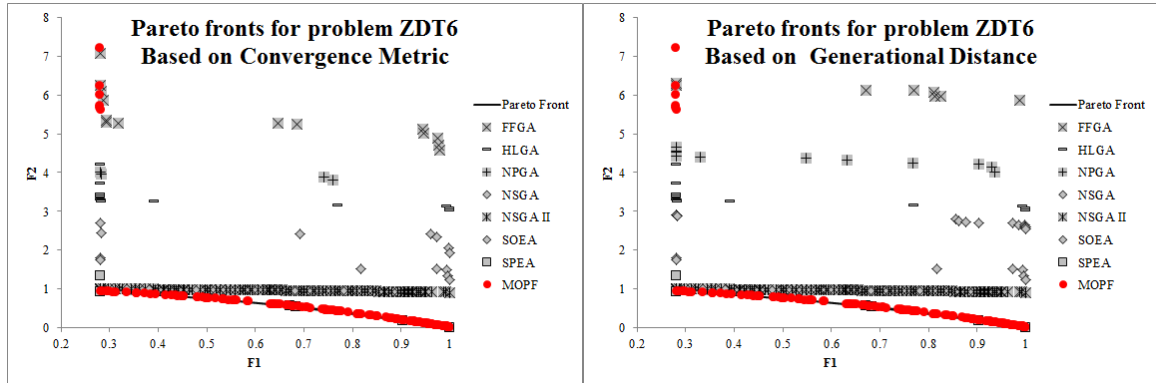


Figure 37: Pareto fronts for ZDT6 test problem

Table 20: Performance Metrics

|  |  | Algorithm | | | | | | | |
|---|---|---|---|---|---|---|---|---|---|
|  |  | FFGA | HLGA | NPGA | NSGA | NSGA II | SOEA | SPEA | MOPF |
| **ZDT1** | CM | 0.9775 | 0.6706 | 0.7683 | 0.2062 | 0.1263 | 0.0734 | 0.0290 | **0.0034** |
| | GD | 0.2036 | 0.1500 | 0.1707 | 0.0324 | 0.0150 | 0.0112 | 0.0034 | **0.0009** |
| | DM | 0.7405 | 0.7761 | 0.7438 | 0.6050 | **0.5115** | 0.7406 | 0.5195 | 0.7779 |
| **ZDT2** | CM | 1.0811 | 0.8044 | 0.8406 | 0.2777 | 0.1251 | 0.1786 | 0.0463 | **0.0008** |
| | GD | 0.3841 | 0.3151 | 0.2756 | 0.0609 | 0.0145 | 0.0436 | 0.0071 | **0.0001** |
| | DM | 0.7729 | 0.8702 | 0.7587 | 0.6332 | **0.5897** | 0.9383 | 0.7504 | 0.6966 |
| **ZDT3** | CM | 1.1156 | 0.6525 | 0.8324 | 0.1540 | 0.1779 | 0.0436 | **0.0130** | 0.1310 |
| | GD | 0.2299 | 0.1569 | 0.1540 | 0.0235 | 0.0201 | 0.0095 | **0.0017** | 0.0246 |
| | DM | 0.7880 | 0.7034 | 0.7663 | 0.7450 | 0.7973 | 0.9864 | **0.6796** | 0.8054 |
| **ZDT4** | CM | 43.0715 | 7.9685 | 8.5976 | 1.3908 | 11.1547 | 12.6337 | 1.8007 | **0.5042** |
| | GD | 14.5792 | 3.6630 | 4.3206 | 0.5062 | 1.1248 | 12.6337 | 0.1901 | **0.0507** |
| | DM | **0.7563** | 0.8455 | 0.8273 | 0.8599 | 0.9373 | 1.0000 | 0.8827 | 0.8628 |
| **ZDT6** | CM | 4.5347 | 2.4790 | 3.0166 | 1.5214 | 0.2561 | 0.8148 | **0.1365** | 0.2204 |
| | GD | 1.1805 | 0.6918 | 1.0414 | **0.5273** | 0.0285 | 0.3089 | 0.0681 | 0.0893 |
| | DM | 0.8828 | 0.8301 | 0.9018 | 0.8274 | 0.7590 | 0.9165 | **0.7372** | 0.9937 |

With respect to problem ZDT2, we can see in Table 20 that, similar to the results obtained for problem ZDT1, the convergence metric of the MOPF framework is significantly (almost sixty times) smaller than those obtained from the SPEA algorithm while outperforming the rest of the compared algorithms. In terms of the generational distance, the MOPF algorithm reveals the best results with a metric that is almost two orders of magnitude better than the next algorithm, SPEA. In terms of diversity metric, NSGA II is noted to perform the best, while the MOPF framework ranks third behind NSGA. Here, we can see that for problem ZDT2, the MOPF framework can produce the non-dominated fronts closest to the Pareto front with a better than average diversity.

In relation to problem ZDT3 we can see that, in terms of the convergence metric, the best rated algorithm is the SPEA algorithm, while the worst rated algorithm is the FFGA algorithm. The MOPF framework ranks third, after the SOEA algorithm with a result that is ten times larger than that of the SPEA algorithm. In terms of the generational distance, the MOPF framework ranks fifth after SPEA, SOEA, NSGA II and NSGA algorithms, with a metric that is more than fourteen times larger than that of SPEA. In terms of diversity, SPEA is also the best ranked algorithm while the MOPF framework is next to last. However, it should be noted in this case that the metric of the MOPF framework is just nineteen percent worse than that of SPEA. Overall, it can be concluded that because of the discontinuous nature of its Pareto front, problem ZDT3 poses serious challenges to the MOPF framework and that its performance is inferior to that of some of the compared algorithms.

When analyzing the results from problem ZDT4 it is evidenced that the convergence metric of the MOPF framework is noticeably better than that of the

compared algorithms, and only the SPEA and NSGA algorithms are within one order of magnitude of the MOPF framework. In terms of generational distance, the MOPF framework is also the best ranked while only the metrics from the SPEA and NSGA algorithms are within one order of magnitude. In terms of the diversity metric, FFGA is the best rated algorithm while the MOPF framework is rated fifth, with a diversity that is still better than average. For problem ZDT4, the MOPF framework produces the non-dominated fronts that are closest to the Pareto front with a diversity that is slightly better than average.

When looking at problem ZDT6 the convergence metric of the MOPF framework is ranked second after that of the SPEA algorithm with a metric that is more than sixty percent larger than that of that from the SPEA algorithm which is also eighty five percent smaller than the average. In terms of generational distance, the MOPF framework is ranked third behind the NSGA II and SPEA algorithms. In terms of the diversity metric, the best ranked algorithm is the SPEA algorithm while the MOPF framework is ranked last with a metric that is almost thirty five percent larger than that of the SPEA algorithm. For problem ZDT6, the MOPF framework can produce the non-dominated fronts that are closest to the Pareto front even though these are the least diverse. Here, it is important to highlight the large effect that a few very distant solutions have on the generational distance metric. In the case that these few solutions, with the highest values for $f_1$ were removed from the non-dominated solution set, the generational distance that could be achieved with the MOPF framework is as low as 0.0149, which is almost half of the 0.0285 from the NSGA II algorithm.

The presented approach promises suitability for both combinatorial and numerical optimization problems as it is able to sample from within a non-dominated solution set in sequential importance stage, and from the extreme points of the non-dominated solution set and the nearest extreme points of the sample space in the resampling stage.

The performance of the proposed approach has been evaluated against that of well established algorithms in the literature. Results have shown that the MOPF framework is able to perform better than its competitors in problem instances of convexity, non-convexity, multimodality and non-uniformity; especially in terms of distance from the non-dominated solution set and the Pareto front. In problems involving discrete Pareto fronts, the MOPF framework does not perform as well as its competitors and has room for improvement.

# Chapter 5: Economic and Environmental Load Dispatching Framework using Particle Filtering

The economic and environmental load dispatching framework developed in this study is comprised of two main stages (see Figure 19). In the first stage, the demand forecasting algorithm incorporating linear regression estimates demand for every load bus (PQ) in the system and evaluates the state of energy generation for each energy generating bus (PV). This algorithm utilizes external as well as internal inputs from the system such as the temperature and weather conditions and the actual energy consumption. Then, in the second stage, the forecasts obtained from stage one, as well as the raw consumption data, are fed into the load dispatching algorithm incorporating particle filtering and the Newton-Raphson method. Next, this algorithm estimates the behavior of the energy load at all of the buses and across each of the lines between them. The load dispatching algorithm then decides the energy that has to be fed into the grid so that the system remains balanced, demand is met, and none of the lines are overloaded while meeting the operational restrictions of each of the energy generating plants. This estimation of the system is optimized using a simulation mechanism that takes advantage of the hidden Markov chain in the particle filter algorithm and is able to quickly evaluate the performance in terms of cost and environmental impact of the different dispatch alternatives. Using these performance measures, the load dispatching algorithm using particle filtering can update the sampling distribution and establish a new dispatch policy.

This iterative process also enables us to introduce an optimization procedure to select the number of particles needed by the system in order to prevent the occurrences of degeneracy and loss of diversity while improving computational performance. Another advantage given by this iterative process is that resampling rules can also be tuned to the problem in order to ensure that the thresholds controlling the permissible particle weights are adjusted in each iteration.
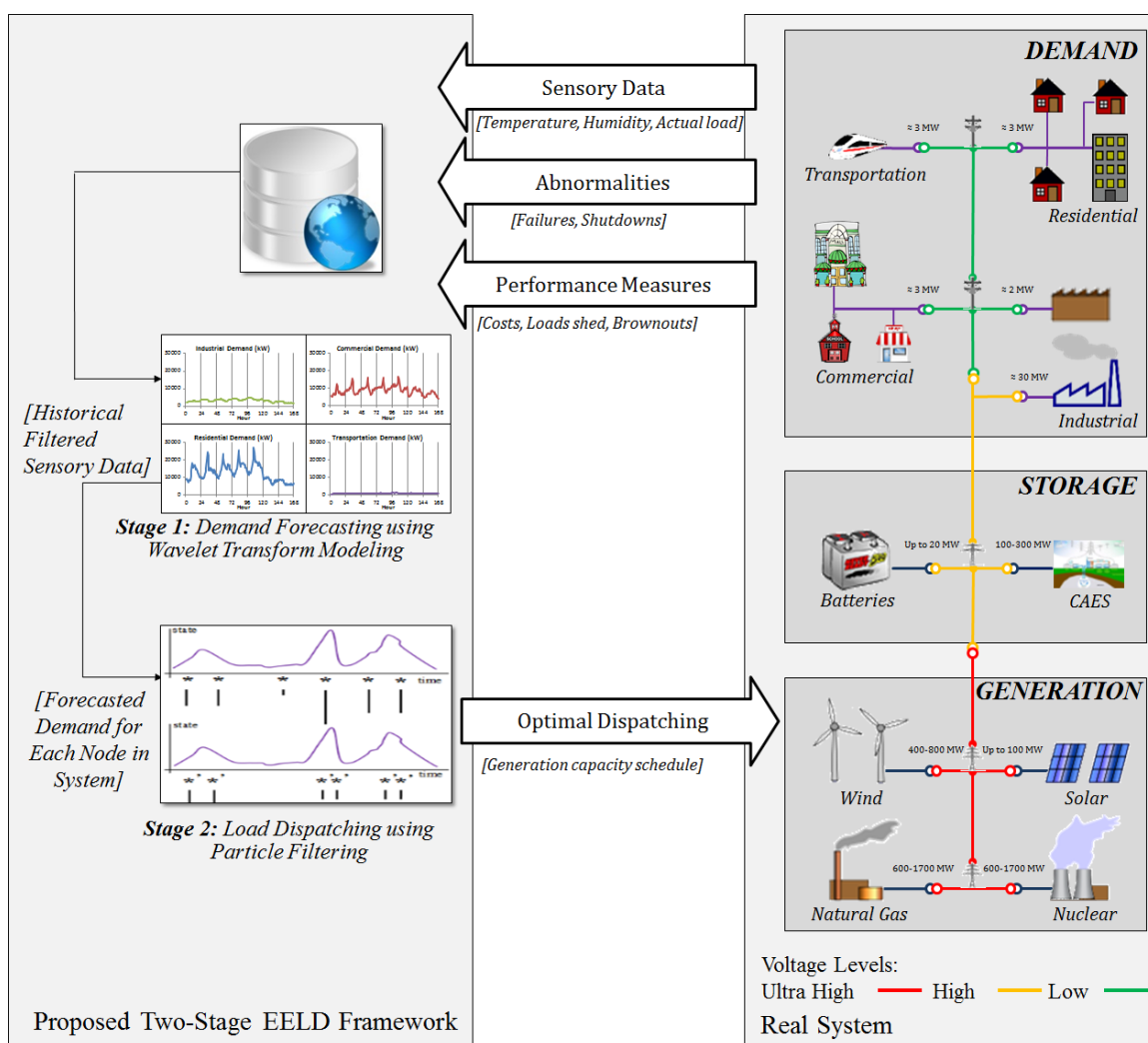


Figure 38: Overview of the proposed economic and environmental load dispatching framework

### 5.1. Formulation of the EELD Problem

The EELD problem has two distinct objectives; to minimize fuel costs and to minimize emissions while satisfying system constraints. The formulation of the problem is presented in Eq. (44) through Eq. (53), where the decision variables are the real $(P_G)$ and reactive $(Q_G)$ power generated at each generation bus. Eq. (44) and Eq. (45) are the total cost of the electricity generated per hour and the total amount of emissions per hour, respectively. The generation capacity constraint that warrants all energy generating plants operate within their operational limits is represented by Eq. (46). The power balance constraints are represented by Eq. (47) through Eq. (50), and ensure that the load provided to the system meets the demand at all times while considering the energy losses during transmission. The line flow constraints are represented by Eq. (51) through Eq. (53), and guarantee the secure operation of the power grid system.

$$Minimize\ F(P_G) = \sum_{i=1}^{N_G} a_i + b_i P_{G_i} + c_i P_{G_i}^2 \qquad \text{Eq. (44)}$$

$$Minimize\ E(P_G) = \sum_{i=1}^{N_G} [10^{-2}(\alpha_i + \beta_i P_{G_i} + \gamma_i P_{G_i}^2) + \zeta_i e^{\lambda_i P_{G_i}}] \qquad \text{Eq. (45)}$$

$$\text{s.t.} \qquad P_{G_i}^{min} \le P_{G_i} \le P_{G_i}^{max} \qquad \text{Eq. (46)}$$

$$\sum_{i=1}^{N_G} P_{G_i} - P_D - P_{loss} = 0 \qquad \text{Eq. (47)}$$

$$P_{G_i} - P_{D_i} - V_i \sum_{j=1}^{N_B} V_j [G_{ij} cos(\delta_i - \delta_j) + B_{ij} sin(\delta_i - \delta_j)] = 0 \qquad \text{Eq. (48)}$$

$$Q_{G_i} - Q_{D_i} - V_i \sum_{j=1}^{N_B} V_j [G_{ij} sin(\delta_i - \delta_j) + B_{ij} cos(\delta_i - \delta_j)] = 0 \qquad \text{Eq. (49)}$$

$$P_{loss} = \sum_{j=1}^{N_B} g_k [V_i^2 + V_j^2 - cos(\delta_i - \delta_j)] \qquad \text{Eq. (50)}$$

$$S_{l_k} \le S_{l_k}^{max} \qquad \text{Eq. (51)}$$

$$S_{l_k} = (V_i \angle \delta_i) I_{ij}^* \qquad \text{Eq. (52)}$$

$$I_{ij} = (V_i \angle \delta_i) \times [(V_i \angle \delta_i - V_j \angle \delta_j) \times y_{ij} + (V_j \angle \delta_i) \times j \tfrac{y}{2}] \qquad \text{Eq. (53)}$$

Here $a_i$, $+b_i$ and $c_i$ are the cost coefficients; $N_G$ represents the number of generating units; $P_{G_i}$ is the real power generated at the $i^{th}$ bus; $Q_{G_i}$ is the reactive power generated at the $i^{th}$ bus, $\alpha_i$, $\beta_i$, $\gamma_i$, $\zeta_i$, and $\lambda_i$ are the coefficients of the $i^{th}$ generator's emissions characteristics; $P_{G_i}^{min}$ is the minimum operating output of unit $i$; $P_{G_i}^{max}$ is the maximum operating output of unit $i$; $N_B$ is the number of buses; $P_{D_i}$ is the real load at bus $i$; $Q_{D_i}$ is the reactive load at the bus $i$; $V_i$ is the voltage magnitude at bus $i$; $G_{ij}$ is the transfer conductance between buses $i$ and $j$; $\delta_i$ is the voltage angle at bus $i$; $B_{ij}$ is the transfer conductance and susceptance between bus $i$ and bus $j$; $g_k$ is the conductance of the $k^{th}$ line which connects buses $i$ and $j$; $S_{l_k}$ is the apparent power flow through transmission line $k$; $S_{l_k}^{max}$ is the upper limit for transmission line $k$; $I_{ij}$ is the current flow from bus $i$ to bus $j$; $y_{ij}$ is the line admittance between buses $i$ and $j$; and $y$ is the shunt susceptance of the line.

### 5.2. Dynamic Load Dispatching Algorithm

In the electricity power networks considered in this study, the observations of the generating (PV) buses are derived from the estimations of the real and reactive power at all buses except one using the Newton-Raphson method. The observation of the last bus,

also called the slack bus, is calculated after the observations of the rest of the buses are estimated in order to assure that the system is balanced and the power loss of the energy dispatch plan is taken into consideration.

The procedure to conduct the particle filter is shown in Figure 39. The first step involves the initialization of the algorithm where the clock is set to 0, the sample set sizes are established, a parameter $l$ is defined, a prior conditional density function is set and samples are taken from the conditional density function. In the second step, the historical data for the loads at each of the buses, as well as the results of the demand forecasting algorithm, are obtained and used to update the forecasted loads. During the same step, the information for the impedance of the distribution lines is obtained and the admittance of these lines is calculated. Next, a confirmation check for sudden changes in the system is performed, this is done in intervals between five and fifteen minutes, since the output of renewable energy generation is not very reliable and makes the load changes occur with such frequencies. If there are no changes, the dispatch from the previous state is sent to the system. If changes have been detected in the system, the estimate for the state has to be updated and a new dispatch decision needs to be made. In order to update the state of the system, a new set of particles is sampled from $q(\cdot)$. Once the sample has been taken, the total weight for each sample is assigned and these weights are normalized. Once the normalized set of samples and weights has been established, evaluation of the measure of degeneracy is performed for this set. If the level of degeneracy is inadmissible, the importance function $q(\cdot)$ is resampled and the process returns to earlier stage. If there is no need to resample, the state estimation is performed for real and reactive power generation. The estimates for the state as well as the data for

admittance are then inputted into the simulation, where the simulation evaluates the feasibility of the state and its measure of performance. If the performance is unacceptable or the solution is infeasible, a new sample from the importance function $q(\cdot)$ is resampled and the process returns to that stage. Once the desired performance level is reached, the dispatch decision is sent to the real system and the time is updated for the next state.
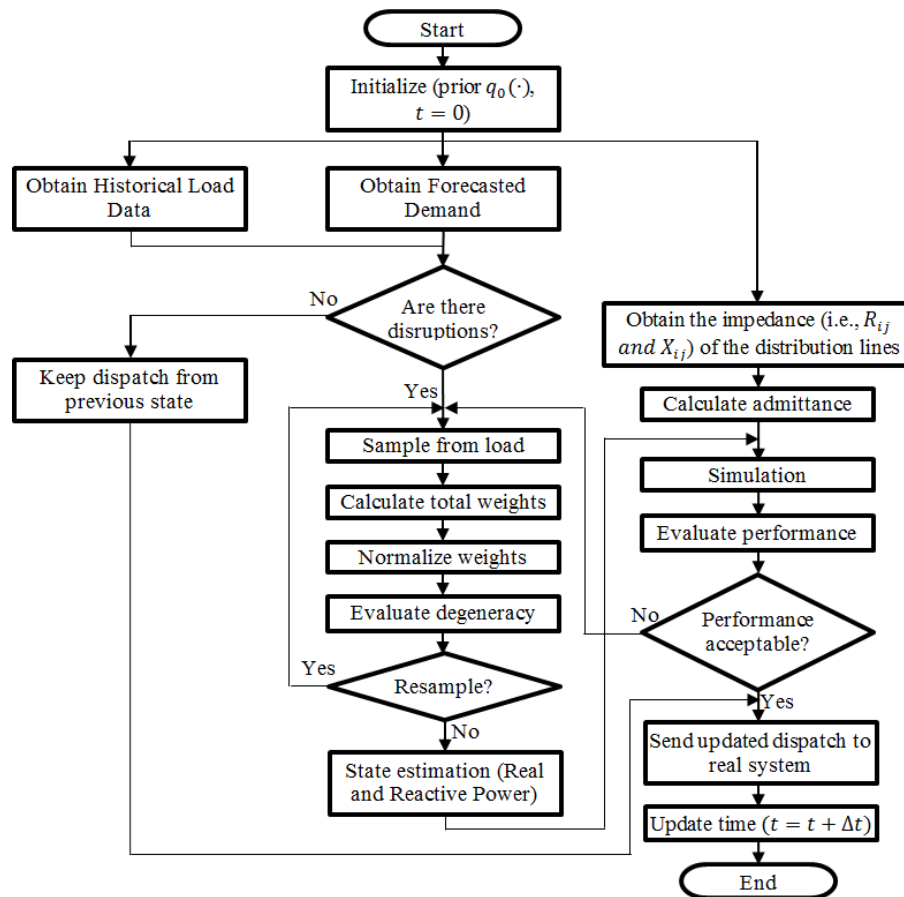


Figure 39: Flowchart of operations performed at dynamic load dispatching algorithm

### 5.2.1. Power Balancing using Newton-Raphson Method

In order to ensure that the constraints from the EELD problem are met when the load dispatching algorithm is employed, the Newton-Raphson method is used (Weber, 1997;

Grainger and Stevenson, 1994). The Newton-Raphson method is a numerical analysis technique that approximates the roots of a function. Based on the calculation of a function and its derivative at a given point; the method iterates by using estimates for the roots that are equal to the previous estimate minus the quotient of the function over its derivative, evaluated at that precious estimate. The extension to $n$ dimensions of this method uses the Jacobian matrix of partial derivatives. In this case, the inverse of the Jacobian evaluated at the previous estimate is pre-multiplied to the negation of the function evaluated at the previous estimate. This operation yields the difference between the new estimate for the root of the function and the prior estimate.

For power balancing, this method is helpful in evaluating the values of the voltages and phase angles at each of the system's buses, given a predefined amount of power generated at each, but one, of the energy generating buses. The Newton-Raphson method is used to find the roots of the power balance equations (see Eqs. (48) and (49)) by solving Eqs. (54), (55) and (56) where the method usually uses voltages of 1 p.u. and angles of 0° at every bus as a starting point.

$$\begin{bmatrix} \Delta\theta \\ \Delta|V| \end{bmatrix} = -J^{-1}\begin{bmatrix} \Delta P \\ \Delta Q \end{bmatrix} \qquad \text{Eq. (54)}$$

$$\Delta P_{G_i} = -P_{G_i} + \sum_{j=1}^{N_B} |V_i||V_j|[G_{ij}cos(\delta_i - \delta_j) + B_{ij}sin(\delta_i - \delta_j)] \qquad \text{Eq. (55)}$$

$$\Delta Q_{G_i} = -Q_{G_i} + \sum_{j=1}^{N_B}|V_i||V_j|[G_{ij}sin(\delta_i - \delta_j) + B_{ij}cos(\delta_i - \delta_j)] \qquad \text{Eq. (56)}$$

The Jacobian is composed of four separate parts: the partial derivative for the real power in terms of the angles, the partial derivative of the real power in terms of the voltages, the partial derivative for the reactive power in terms of the angles, and the partial derivative of the reactive power in terms of the voltages. Using this method, the

voltages and angles for each bus are updated until a tolerance has been met and the precision in the estimates for the roots of the power balance equations is adequate. The use of this method ensures that the values for the generation, proposed by the particle filtering algorithm, meet the power balance constraints in terms of real and reactive power, and are suitable as a candidate solution to the optimization of the EELD problem, as shown in Figure 40.

| Particle Filtering | →Generation for the PV buses→ | Newton-Raphson Method | →Generation for the Slack bus, angles and voltages for every bus→ | Real System Dispatching |
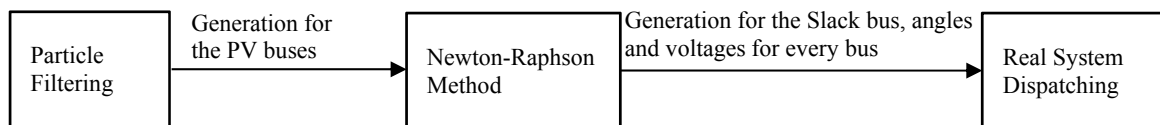
Figure 40: Relationship of the particle filtering and the Newton-Raphson method in determination of the dispatch decision

## 5.3. IEEE-30 Bus Test System

In order to demonstrate the validity of the environmental and economic load dispatching framework proposed in this study, we used the IEEE-30 bus test system where the data regarding the characteristic of this system is obtained from the Power Systems Test Case Archive of the Department of Electrical Engineering at the University of Washington (University of Washington, 2011). The IEEE-30 bus test system represents a portion of the American Electric Power System in the Midwestern US. It is used in the literature (Hota et al., 2010; Panigrahi et al., 2011; Liao 2011; Bhagwan and Patvardhan, 1999) as a standard test case for power systems. The system is shown in Figure 41 and consists of a total of 30 buses and 41 lines. Out of these 30 buses, there are 6 buses that generate electricity, 22 buses that demand electricity and 5 buses that neither generate nor request electricity. The load data for the 30 buses is shown in Table 21.

In this work, the load and reactance for each particular bus at any given time is assumed to be normally distributed with a mean equal to the value reported in the IEEE-30 data set and a variance such that the data is within 10% of the mean with a probability of 0.9. Figure 42 shows the load and reactance information of each of the buses.
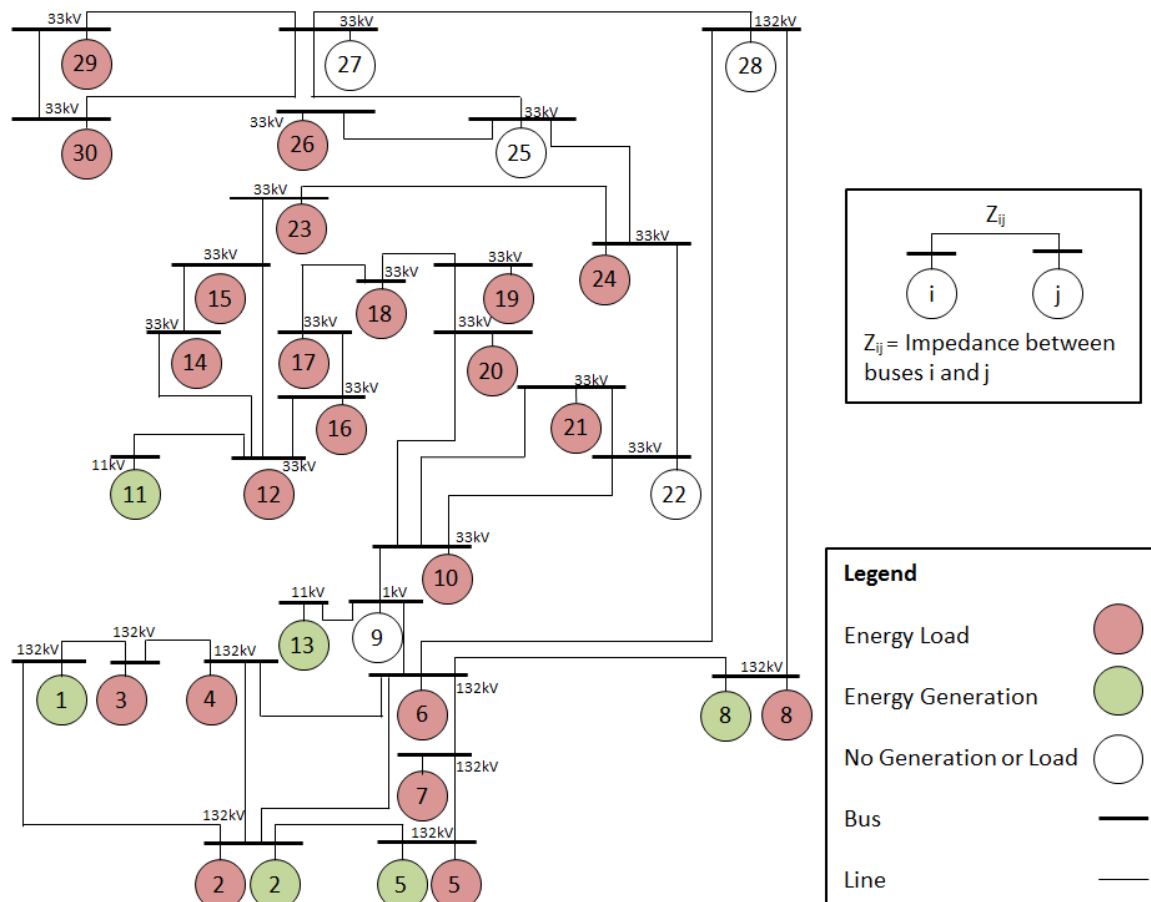


Figure 41: IEEE-30 Bus Test System

Table 21: IEEE-30 Load Data

| Bus | Load MW | MVAR | Bus | Load MW | MVAR |
|---|---|---|---|---|---|
| 1 | 0 | 0 | 16 | 3.5 | 1.8 |
| 2 | 21.7 | 12.7 | 17 | 9 | 5.8 |
| 3 | 2.4 | 1.2 | 18 | 3.2 | 0.9 |
| 4 | 7.6 | 1.6 | 19 | 9.5 | 3.4 |
| 5 | 94.2 | 19 | 20 | 2.2 | 0.7 |
| 6 | 0 | 0 | 21 | 17.5 | 11.2 |
| 7 | 22.8 | 10.9 | 22 | 0 | 0 |
| 8 | 30 | 30 | 23 | 3.2 | 1.6 |
| 9 | 0 | 0 | 24 | 8.7 | 6.7 |
| 10 | 5.8 | 2 | 25 | 0 | 0 |
| 11 | 0 | 0 | 26 | 3.5 | 2.3 |
| 12 | 11.2 | 7.5 | 27 | 0 | 0 |
| 13 | 0 | 0 | 28 | 0 | 0 |
| 14 | 6.2 | 1.6 | 29 | 2.4 | 0.9 |
| 15 | 8.2 | 2.5 | 30 | 10.6 | 1.9 |
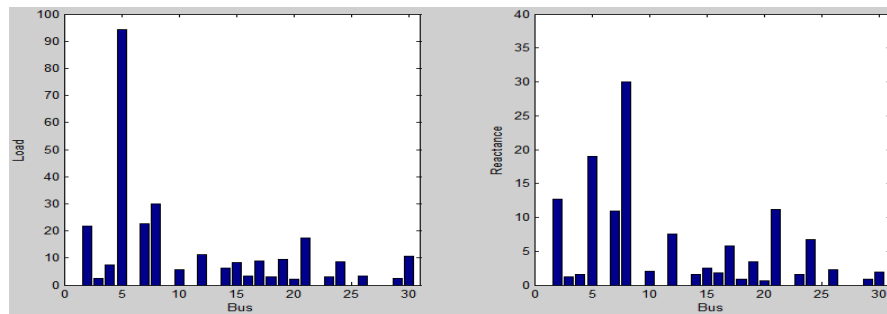


Figure 42: Load and reactance of the IEEE-30 buses

During the initialization of the environmental and economic load dispatching framework developed in this work, the bus and the line data is downloaded from separate files so that the model is as generic as possible and can be easily modified and extended beyond the IEEE-30 bus test system. Once the system data is loaded, the model identifies the number of PV and of PQ buses in the system, as well as the slack bus that will be used to balance the constraints. This identification is vital for handling the different scenarios that each of these types of buses may be involved in. For PV buses,

the generated power and voltage are given as an input to balance the power equations. However for PQ buses, the voltage magnitude has to be solved additionally while the power balance restrictions are met. This implies that for the PV buses, the unknown for solving power balance equations is the voltage phase angle; while for the PQ buses, both the voltage magnitude and voltage phase angles are unknown. Once the system identifies the different types of buses and the values for the operative level constraints, a maximum and minimum power generation is established for every PV bus. Next, the state of the particle filtering algorithm is initialized, where the voltages and angles are originally assumed to be 1 p.u. and 0°. Using this initial state, the data for the historical load of each bus, and the forecasted load for each bus, the particle filter model produces an estimate for the next states. This estimation is fed into the Newton-Raphson method which takes the estimated state and uses it to determine if this state meets the power balance restrictions. If the restrictions are fully met, the estimate may be evaluated to determine its performance in terms of both cost and emissions. On the other hand, if the estimate does not meet the restrictions, the Newton-Raphson method is used to generate the real and reactive power of the slack bus so that the state converges to an adjusted state that complies with the restrictions and can be evaluated.

## 5.4. Evaluation of the Economic and Environmental Load Dispatching Framework

In order to illustrate and demonstrate the validity of the proposed environmental and economic load dispatching framework, we first conduct experimentation on the load dispatching algorithm using particle filtering via synthetic functions. Once the performance of this main decision making algorithm is established via the use of

synthetic experimentation, the complete framework is tested using IEEE-30 bus test system incorporating actual data. All of the algorithms presented in this section have been implemented using Matlab R2010b, with the use of object oriented programming technique which enables the framework to be generic and modular (i.e., modules can be shared with other applications for different problems).

### 5.4.1. Experiments with Synthetic Functions

The particle filtering algorithm is used to calculate the load dispatching for the IEEE-30 bus system using the load data provided in the Power Systems Test Case Archive of the Department of Electrical Engineering at the University of Washington. Here, we use two separate complex synthetic functions to update the states for the particle filter: $x_t = \cos(a^2\pi x_{t-1}) + \frac{7b^3}{1+a^2} + \frac{x_{t-1}}{2}e^{(\log(\Gamma(3))+\log(\Gamma(2))-\log(\Gamma(2+3)))}$ and $x_t = 2b^2 x_{t-1} + \cos(a\pi x_{t-1})$, where $a$ and $b$ are parameters which are arbitrarily selected as $a = 0.6$ and $b = 0.8$, $u_t$ is the forecast for the state at time $t$ and $\Gamma(\cdot)$ is the gamma function. The measurement functions are selected as $z_t = bx_{t-1}$ and $z_t = abx_{t-1}$, respectively. Figure 43 shows the results for the object oriented implementation of the first synthetic function used in the particle filtering algorithm for the IEEE-30 bus system.
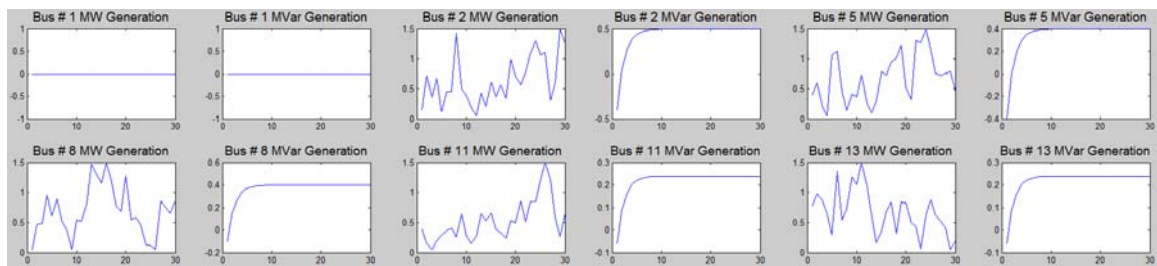


Figure 43: Overview of the results obtained using synthetic functions for particle filtering

Synthetic functions are used to update the state in order to ensure that the particle filtering algorithm tracks the state closely before it is embedded into the actual environmental and economic load dispatching system. The use of smaller particle set sizes enables the algorithm to improve computational efficiency, while the use of larger particle set sizes tries to ensure that no degeneracy problems arise. The use of smaller number of replications improves the computational efficiency of the algorithm, while the use of larger number of replications enables the algorithm more time steps to approximate the state function. Table 22 shows the electricity dispatch decisions obtained using 30, 60, 90 and 120 replications, as well as using particle set sizes ranging from 50 to 300 particles, respectively for the first synthetic function. It should be noted here that the dispatch with the lowest cost is achieved using a particle set size of 50 and 120 replications while the dispatch with the lowest emissions is achieved using a particle set size of 300 with 60 replications or when using a particle set size of 250 with 90 replications. The average cost for the minimum cost dispatch is of $630.9592 per hour while the average emissions for the minimum emissions dispatch are of 0.1956 tons per hour.

Table 23 shows the energy dispatch decisions obtained for the second synthetic function using 30, 60, 90 and 120 replications, as well as using particle set sizes ranging from 50 to 300 particles. The dispatch with the lowest cost is achieved using a particle set size of 100 with 60 replications, while the dispatch with the lowest emissions is achieved using a particle set size of 50 with 60 replication. The average cost for the minimum cost dispatch is of $649.4688 per hour while the average emissions for the minimum emissions dispatch are of 0.2011 tons per hour.

Table 22: Power generated using the first synthetic function

| Particle Set Size | Average Dispatch (MW) | | | | | | Min Cost ($/h) | Min Emissions (ton/h) | Average Cost ($/h) | Average Emissions (ton/h) |
|---|---|---|---|---|---|---|---|---|---|---|
| | Bus 1 | Bus 2 | Bus 5 | Bus 8 | Bus 11 | Bus 13 | | | | |
| **30 Replications** | | | | | | | | | | |
| 50 | 79.4967 | 47.8236 | 44.1987 | 34.3384 | 40.3180 | 42.6417 | 635.9950 | 0.1963 | 766.5149 | 0.3114 |
| 100 | 132.6257 | 29.2912 | 31.3735 | 33.9944 | 30.8025 | 31.8871 | 637.7783 | 0.1956 | 815.4137 | 0.2998 |
| 150 | 111.4556 | 36.0541 | 35.2001 | 36.9207 | 34.2888 | 36.7829 | 630.7288 | 0.2006 | 860.4027 | 0.4396 |
| 200 | 86.2904 | 42.0866 | 39.3278 | 38.4009 | 41.6373 | 40.9996 | 633.4816 | 0.1949 | 752.4709 | 0.2808 |
| 250 | 71.3424 | 42.8289 | 42.5831 | 43.4909 | 44.1109 | 43.4819 | 630.2862 | 0.1949 | 701.9784 | 0.2435 |
| 300 | 137.9166 | 30.4923 | 30.4160 | 30.4307 | 30.3125 | 30.6517 | 642.0610 | 0.1952 | 828.7271 | 0.3050 |
| **60 Replications** | | | | | | | | | | |
| 50 | 61.8401 | 43.5275 | 45.3209 | 45.3586 | 46.2474 | 45.0339 | 627.9248 | 0.1948 | 681.8861 | 0.2261 |
| 100 | 143.7564 | 22.3620 | 23.5086 | 33.6551 | 37.1821 | 30.1329 | 643.1946 | 0.1982 | 845.9040 | 0.3151 |
| 150 | 131.5222 | 34.4291 | 30.6506 | 32.7782 | 29.8676 | 30.7503 | 636.8753 | 0.1956 | 812.6716 | 0.2886 |
| 200 | 85.1087 | 40.6978 | 40.5167 | 40.0830 | 41.0316 | 40.8136 | 630.0669 | 0.1949 | 724.2452 | 0.2459 |
| 250 | 79.7918 | 41.0291 | 41.0947 | 44.7877 | 41.4662 | 40.8867 | 627.2984 | 0.1951 | 771.1373 | 0.3361 |
| 300 | 125.0701 | 29.1349 | 35.6924 | 32.2408 | 35.6467 | 32.6630 | 628.6959 | 0.1947 | 853.4169 | 0.3576 |
| **90 Replications** | | | | | | | | | | |
| 50 | 71.2167 | 37.9090 | 38.7133 | 48.7023 | 46.6128 | 46.4432 | 626.1545 | 0.1961 | 790.7710 | 0.3873 |
| 100 | 95.9582 | 39.1116 | 39.4447 | 36.3731 | 42.4015 | 35.8578 | 632.1887 | 0.1951 | 780.8389 | 0.2928 |
| 150 | 116.8590 | 35.2005 | 36.6071 | 32.3642 | 33.4354 | 35.7527 | 630.7927 | 0.1951 | 837.4086 | 0.3505 |
| 200 | 63.5817 | 42.4036 | 45.7798 | 48.2000 | 45.8401 | 42.1915 | 627.5485 | 0.1951 | 715.8214 | 0.2719 |
| 250 | 98.1939 | 39.4238 | 37.3405 | 35.7742 | 40.1471 | 38.6564 | 632.2607 | 0.1947 | 797.5019 | 0.3149 |
| 300 | 85.5663 | 37.3839 | 36.1194 | 48.7479 | 38.0523 | 43.0988 | 624.6552 | 0.1968 | 750.2018 | 0.2881 |
| **120 Replications** | | | | | | | | | | |
| 50 | 61.1379 | 44.6466 | 46.2672 | 48.1079 | 42.3058 | 45.0753 | 623.6993 | 0.1954 | 686.1910 | 0.2301 |
| 100 | 89.0592 | 38.6921 | 42.4764 | 45.1311 | 34.7842 | 38.3924 | 626.1876 | 0.1960 | 740.3991 | 0.2687 |
| 150 | 55.7863 | 46.4897 | 46.5282 | 46.0758 | 45.1692 | 47.2951 | 629.6504 | 0.1949 | 676.6032 | 0.2213 |
| 200 | 73.9178 | 42.0971 | 47.3027 | 44.8739 | 41.0765 | 38.6632 | 627.9751 | 0.1953 | 715.4426 | 0.2516 |
| 250 | 98.8432 | 37.8181 | 37.7336 | 38.4936 | 37.7317 | 38.1251 | 630.2799 | 0.1951 | 749.9315 | 0.2569 |
| 300 | 73.0859 | 40.3364 | 42.8355 | 43.8253 | 42.6326 | 45.3431 | 627.2417 | 0.1949 | 713.8045 | 0.2490 |

Table 23: Power generated using the second synthetic function

| Particle Set Size | Average Dispatch (MW) | | | | | | Min Cost ($/h) | Min Emissions (ton/h) | Average Cost ($/h) | Average Emissions (ton/h) |
|---|---|---|---|---|---|---|---|---|---|---|
| | Bus 1 | Bus 2 | Bus 5 | Bus 8 | Bus 11 | Bus 13 | | | | |
| **30 Replications** | | | | | | | | | | |
| 50 | 159.4439 | 26.5291 | 25.8886 | 26.2762 | 25.5302 | 27.7551 | 646.1840 | 0.1959 | 893.3113 | 0.3458 |
| 100 | 145.3275 | 31.9843 | 28.5951 | 58.6040 | 32.0765 | 26.2794 | 638.3310 | 0.2084 | 984.0069 | 0.5513 |
| 150 | 50.0004 | 47.4236 | 46.9896 | 46.6724 | 48.5329 | 47.9026 | 631.6021 | 0.1950 | 689.0434 | 0.2505 |
| 200 | 110.0394 | 33.4511 | 38.4951 | 34.4810 | 36.2308 | 37.1197 | 629.3091 | 0.1950 | 816.1592 | 0.3386 |
| 250 | 175.4047 | 22.2987 | 23.9575 | 24.3404 | 22.3052 | 24.1375 | 648.9307 | 0.1976 | 953.9672 | 0.3941 |
| 300 | 164.1329 | 26.0403 | 25.9088 | 24.4574 | 26.6712 | 24.5585 | 649.6498 | 0.1960 | 916.4108 | 0.3636 |
| **60 Replications** | | | | | | | | | | |
| 50 | 88.8126 | 38.6193 | 46.5182 | 33.5253 | 41.8541 | 39.1559 | 636.9771 | 0.1945 | 753.3595 | 0.2755 |
| 100 | 87.2681 | 40.2766 | 40.3416 | 40.2605 | 39.1560 | 41.1356 | 629.2274 | 0.1950 | 751.1309 | 0.2744 |
| 150 | 107.9415 | 35.1572 | 38.0637 | 36.0946 | 36.5304 | 35.9411 | 629.3216 | 0.1947 | 810.3746 | 0.3289 |
| 200 | 101.6782 | 37.6143 | 37.9195 | 37.1715 | 36.6404 | 37.4049 | 643.4113 | 0.1973 | 731.8832 | 0.2410 |
| 250 | 130.1668 | 48.0060 | 29.9490 | 34.7537 | 25.4812 | 23.5876 | 646.4778 | 0.2043 | 929.9791 | 0.5180 |
| 300 | 185.4759 | 21.1280 | 21.6748 | 22.5100 | 21.9366 | 20.1712 | 829.8526 | 0.2856 | 978.4687 | 0.4005 |
| **90 Replications** | | | | | | | | | | |
| 50 | 164.3216 | 28.8402 | 25.0570 | 24.6770 | 23.2134 | 25.5468 | 685.8877 | 0.2079 | 902.8238 | 0.3397 |
| 100 | 178.9773 | 22.0451 | 22.4618 | 25.2444 | 21.2055 | 22.5868 | 653.6028 | 0.1983 | 955.5247 | 0.3832 |
| 150 | 85.4937 | 40.0715 | 40.0926 | 40.6061 | 41.0346 | 41.0380 | 629.9737 | 0.1950 | 728.4668 | 0.2483 |
| 200 | 79.4143 | 40.4767 | 44.6362 | 40.0019 | 43.3598 | 40.5218 | 633.4279 | 0.1947 | 737.0350 | 0.2799 |
| 250 | 45.3538 | 48.4590 | 48.4515 | 48.0555 | 47.8887 | 48.9198 | 630.7127 | 0.1949 | 666.6917 | 0.2222 |
| 300 | 105.8039 | 38.0881 | 36.6707 | 36.5690 | 36.1099 | 36.3703 | 630.8331 | 0.1948 | 800.0645 | 0.3120 |
| **120 Replications** | | | | | | | | | | |
| 50 | 45.8828 | 46.4950 | 47.6084 | 46.7910 | 49.8499 | 50.3250 | 630.8966 | 0.1947 | 655.5919 | 0.2077 |
| 100 | 156.6774 | 29.2009 | 26.1635 | 25.4668 | 27.0119 | 26.6232 | 659.6336 | 0.1981 | 876.3563 | 0.3195 |
| 150 | 42.2600 | 50.1094 | 49.4594 | 49.8153 | 47.0118 | 49.1234 | 629.7296 | 0.1951 | 705.1828 | 0.2846 |
| 200 | 103.9317 | 37.7144 | 35.0474 | 39.9386 | 37.4757 | 35.1237 | 627.5269 | 0.1955 | 773.3833 | 0.2826 |
| 250 | 148.3708 | 30.2545 | 28.8187 | 27.2367 | 28.0781 | 27.8587 | 650.7094 | 0.1961 | 849.7375 | 0.3025 |
| 300 | 183.6528 | 21.7099 | 22.4634 | 19.8058 | 24.7564 | 20.3992 | 665.0419 | 0.2011 | 974.8041 | 0.3940 |

### 5.4.2. Validation using the IEEE-30 Bus Test System

After validating the performance of the particle filtering algorithm using synthetic

experiments, we have used the realistic data from the IEEE-30 bus test system as shown

in Table 21 as the constant load at each one of the buses. The initial state of the particle

filtering algorithm is determined via sampling from a normal distribution that is centered

around the load for each bus and has a standard deviation equal to 10% of that load. The

state is updated using equal parts from the previous state and from a new sample. The

measurement function is updated for each bus by using an arbitrary parameter multiplied

by the previous state $z_t = a_i x_{t-1}$, where $a_i$ varies for each one of the buses. Table 24

shows the minimum cost results obtained using the algorithm where the dispatch of the

minimum cost is obtained using a particle set size of 100 particles with 60 replications.

Table 24: Minimum cost power generation in IEEE-30 bust test system with constant load

| | Particle Set Size | Minimum Emissions Dispatch (MW) | | | | | | Cost ($/h) | Emissions (ton/h) | Power Loss (MW) |
| | | Bus 1 | Bus 2 | Bus 5 | Bus 8 | Bus 11 | Bus 13 | | | |
|---|---|---|---|---|---|---|---|---|---|---|
| 30 Replications | 50 | 12.1930 | 46.1852 | 63.5223 | 63.1993 | 53.5018 | 47.3744 | 621.5204 | 0.2030 | 2.5760 |
| | 100 | 20.6470 | 34.6702 | 49.3785 | 68.3288 | 53.1593 | 60.1693 | 617.7467 | 0.2020 | 2.9530 |
| | 150 | 13.4270 | 46.8705 | 76.1749 | 55.8134 | 42.8540 | 50.6411 | 624.2119 | 0.2034 | 2.3810 |
| | 200 | 5.6850 | 36.1626 | 81.4110 | 63.3676 | 34.8883 | 64.4769 | 619.3329 | 0.2117 | 2.5920 |
| | 250 | 23.0040 | 25.6284 | 83.8177 | 64.4493 | 48.1351 | 40.6082 | 621.0327 | 0.2076 | 2.2430 |
| | 300 | 28.8690 | 34.8956 | 62.7295 | 65.9996 | 37.4090 | 56.2965 | 617.9351 | 0.2008 | 2.7990 |
| 60 Replications | 50 | 46.7880 | 28.7661 | 53.8430 | 68.5877 | 25.5930 | 63.1703 | 628.4812 | 0.2045 | 3.3480 |
| | 100 | 12.2400 | 45.8097 | 54.9720 | 69.3135 | 49.5956 | 54.1792 | 617.3068 | 0.2039 | 2.7100 |
| | 150 | 15.3290 | 62.8538 | 77.5912 | 48.9692 | 47.3441 | 33.5988 | 640.2227 | 0.2059 | 2.2870 |
| | 200 | 32.8860 | 27.5144 | 68.9873 | 68.5057 | 54.0593 | 33.9100 | 622.7716 | 0.2040 | 2.4620 |
| | 250 | 32.1480 | 33.7435 | 81.9195 | 64.8144 | 22.6733 | 50.6288 | 623.7635 | 0.2073 | 2.5270 |
| | 300 | 5.9150 | 53.4929 | 63.5690 | 63.9460 | 38.7584 | 60.5169 | 622.5653 | 0.2071 | 2.7980 |
| 90 Replications | 50 | 4.7350 | 34.7585 | 95.7642 | 57.5226 | 52.8276 | 39.9262 | 628.1567 | 0.2160 | 2.1340 |
| | 100 | 12.6050 | 47.9046 | 75.1850 | 68.9628 | 30.5961 | 50.6820 | 618.3937 | 0.2083 | 2.5360 |
| | 150 | 33.0260 | 32.4097 | 46.5837 | 61.8439 | 52.6887 | 60.0842 | 624.8872 | 0.1987 | 3.2370 |
| | 200 | 28.5270 | 41.2627 | 48.4913 | 69.8561 | 42.5282 | 55.7078 | 617.9088 | 0.2003 | 2.9730 |
| | 250 | 15.6230 | 32.2774 | 46.4358 | 68.6134 | 58.9469 | 64.6300 | 619.8845 | 0.2049 | 3.1270 |
| | 300 | 10.6380 | 27.8288 | 64.9902 | 69.1031 | 62.2446 | 51.0645 | 619.5332 | 0.2080 | 2.4700 |
| 120 Replications | 50 | 22.1290 | 31.4047 | 72.8362 | 59.4395 | 39.7014 | 60.4777 | 619.8647 | 0.2026 | 2.5890 |
| | 100 | 24.3690 | 49.1982 | 68.8513 | 63.4836 | 44.6781 | 35.2603 | 623.4985 | 0.2018 | 2.4410 |
| | 150 | 17.5360 | 65.3784 | 45.3685 | 68.9945 | 37.0571 | 52.3141 | 629.3896 | 0.2061 | 3.2480 |
| | 200 | 9.2770 | 33.0019 | 80.6950 | 62.1776 | 42.8298 | 57.8683 | 618.8052 | 0.2086 | 2.4500 |
| | 250 | 3.0920 | 48.9620 | 85.6296 | 68.3384 | 42.4744 | 37.1750 | 622.5074 | 0.2147 | 2.2720 |
| | 300 | 4.7970 | 35.4122 | 65.5475 | 68.3172 | 61.6989 | 50.0632 | 620.2377 | 0.2089 | 2.4360 |

Table 25 shows the minimum emissions results obtained using the load dispatching algorithm where the dispatch of the minimum emissions is obtained using a particle set size of 100 particles with 30 replications. The solutions generated by the algorithm reveal that the best cost dispatching decisions are achieved keeping the output from the first generator relatively low compared to the other five, with generation at 27.5% of the output of the second generator (which is also the second one with the smallest output). In the best emissions output, the generation from the first generator increases to 79.7% of that of the second generator which is still the second one with the smallest output, but whose output varies very little between the best cost and best emissions solutions.

Table 25: Minimum emissions power generation in IEEE-30 bust test system with constant load

| | Particle Set Size | Minimum Emissions Dispatch (MW) | | | | | | Cost ($/h) | Emissions (ton/h) | Power Loss (MW) |
|---|---|---|---|---|---|---|---|---|---|---|
| | | Bus 1 | Bus 2 | Bus 5 | Bus 8 | Bus 11 | Bus 13 | | | |
| 30 Replications | 50 | 32.8830 | 42.2031 | 49.5917 | 54.0130 | 52.8888 | 56.8586 | 634.4592 | 0.1959 | 3.0380 |
| | 100 | 38.7760 | 47.2165 | 59.6570 | 34.6463 | 54.0439 | 51.8138 | 647.9090 | 0.1945 | 2.7540 |
| | 150 | 37.4400 | 51.9040 | 44.9132 | 42.4098 | 51.4194 | 58.5579 | 643.8847 | 0.1951 | 3.2450 |
| | 200 | 34.8700 | 52.2135 | 60.5084 | 36.5876 | 54.4651 | 47.4301 | 646.8489 | 0.1952 | 2.6750 |
| | 250 | 37.6380 | 55.0651 | 39.8619 | 45.3441 | 53.9327 | 54.9320 | 645.1479 | 0.1960 | 3.3730 |
| | 300 | 35.8880 | 45.5236 | 66.9632 | 43.0154 | 46.7961 | 47.7761 | 637.6172 | 0.1956 | 2.5620 |
| 60 Replications | 50 | 40.9500 | 35.9067 | 64.1400 | 48.2954 | 51.8370 | 44.8545 | 635.6105 | 0.1962 | 2.5830 |
| | 100 | 38.0840 | 57.1874 | 51.0916 | 51.8433 | 36.0175 | 52.3002 | 638.1542 | 0.1972 | 3.1240 |
| | 150 | 45.9030 | 47.9177 | 60.2762 | 31.1882 | 48.6460 | 52.3514 | 654.1897 | 0.1949 | 2.8820 |
| | 200 | 36.5380 | 48.6090 | 59.6859 | 35.8394 | 56.7741 | 48.6444 | 647.3434 | 0.1949 | 2.6910 |
| | 250 | 33.7320 | 40.7389 | 44.4777 | 62.9778 | 49.9668 | 54.7522 | 625.0769 | 0.1978 | 3.2450 |
| | 300 | 54.2900 | 44.7734 | 63.3561 | 22.1007 | 41.9312 | 60.0798 | 667.4594 | 0.1976 | 3.1310 |
| 90 Replications | 50 | 35.0210 | 56.6595 | 47.4034 | 50.0924 | 33.7240 | 63.8703 | 638.5252 | 0.1982 | 3.3710 |
| | 100 | 31.9200 | 56.8938 | 47.0236 | 30.7297 | 60.9524 | 58.9981 | 656.7956 | 0.1967 | 3.1180 |
| | 150 | 37.3420 | 47.6140 | 58.3466 | 46.9396 | 36.8522 | 59.2669 | 635.6449 | 0.1960 | 2.9610 |
| | 200 | 36.3890 | 45.9066 | 54.2839 | 46.1366 | 51.0066 | 52.5509 | 636.7392 | 0.1946 | 2.8730 |
| | 250 | 44.3140 | 35.5081 | 55.0544 | 22.6142 | 64.4530 | 64.4751 | 664.4666 | 0.1977 | 3.0190 |
| | 300 | 37.2960 | 40.4325 | 54.5185 | 43.4973 | 51.1821 | 59.4132 | 637.6726 | 0.1947 | 2.9400 |
| 120 Replications | 50 | 28.4180 | 44.4741 | 67.6899 | 37.4908 | 44.3083 | 63.7127 | 638.4668 | 0.1969 | 2.6940 |
| | 100 | 36.8840 | 53.0848 | 59.4462 | 52.1535 | 35.8630 | 48.8134 | 634.4786 | 0.1970 | 2.8450 |
| | 150 | 42.3690 | 53.8522 | 69.2422 | 30.5306 | 26.9450 | 63.5303 | 656.3823 | 0.1998 | 3.0690 |
| | 200 | 32.7710 | 52.8974 | 62.4178 | 37.6004 | 43.7098 | 56.7834 | 643.0019 | 0.1956 | 2.7800 |
| | 250 | 32.0960 | 39.3083 | 68.6554 | 37.9584 | 49.3653 | 58.5992 | 638.6664 | 0.1962 | 2.5820 |
| | 300 | 41.7710 | 38.0273 | 59.6132 | 28.8151 | 58.9456 | 59.0466 | 654.0938 | 0.1957 | 2.8190 |

Figure 44 shows the Pareto optimal front for the solutions obtained using 300 particles and 750 replications. Within this Pareto optimal front the best compromise

solution is that which satisfies the different goals to the furthest extent simultaneously. In this case, the best compromise solution has a cost of \$621.38/h with emissions of 0.1983 ton/h and generation of 27.537, 41.031, 58.569, 60.439, 41.809, and 56.858 for the six generators, respectively.

Table 26 shows the comparison of the proposed environmental and economic load dispatching framework (PF-EELD) with other methods presented to solve the EELD problem. The use of NSGA algorithm for the EELD problem is introduced by Abido (2003B), while the use of the NPGA for this same problem is introduced by Abido (2003C). In our comparison, the performance of the SPEA algorithm is taken from Abido (2003A), while the performances for the NSGA, NPGA and MOBF algorithms, under the considered setting are taken from Panigrahi et al. (2011). It should be noted that the results produced by the proposed PF-EELD framework are comparable in terms of emissions while significantly promising in terms of cost.
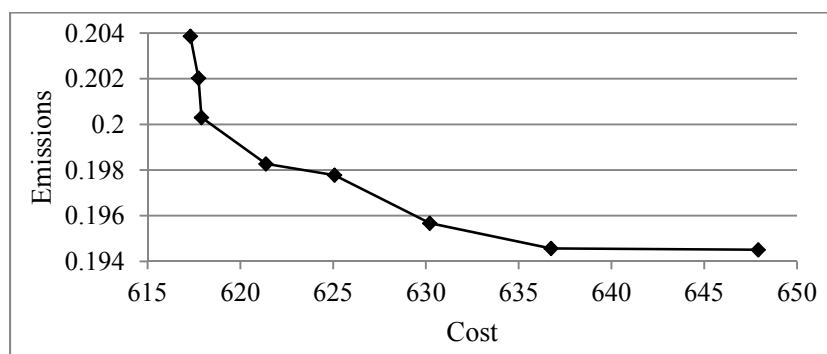


Figure 44: Pareto optimal front

Table 26: Comparison of PF-EELD with other methods

| | | PF-EELD | SPEA | NSGA | NPGA | MOBF |
|---|---|---|---|---|---|---|
| Minimum Emissions | P1 | 0.3878 | 0.4798 | 0.4403 | 0.4753 | 0.3980 |
| | P2 | 0.4722 | 0.5287 | 0.4940 | 0.5162 | 0.4521 |
| | P3 | 0.5966 | 0.6711 | 0.7509 | 0.6513 | 0.5516 |
| | P4 | 0.3465 | 0.5317 | 0.5060 | 0.4363 | 0.4190 |
| | P5 | 0.5404 | 0.5301 | 0.5364 | 0.5988 | 0.5091 |
| | P6 | 0.5181 | 0.1257 | 0.1375 | 0.1896 | 0.5338 |
| | Cost ($/h) | 647.91 | 651.63 | 649.24 | 657.59 | 641.43 |
| | Emissions (ton/h) | 0.1945 | 0.2047 | 0.2048 | 0.2017 | 0.1942 |
| | | PF-EELD | SPEA | NSGA | NPGA | MOBF |
| Minimum Cost | P1 | 0.1224 | 0.1598 | 0.1358 | 0.1127 | 0.1763 |
| | P2 | 0.4581 | 0.3534 | 0.3151 | 0.3747 | 0.3581 |
| | P3 | 0.5497 | 0.7960 | 0.8418 | 0.8057 | 0.7429 |
| | P4 | 0.6931 | 0.9718 | 1.0431 | 0.9031 | 0.5970 |
| | P5 | 0.4960 | 0.4971 | 0.4664 | 0.1347 | 0.3861 |
| | P6 | 0.5418 | 0.0868 | 0.0631 | 0.5331 | 0.5977 |
| | Cost ($/h) | 617.31 | 620.17 | 620.87 | 620.46 | 619.03 |
| | Emissions (ton/h) | 0.2039 | 0.2283 | 0.2368 | 0.2243 | 0.2177 |

### 5.4.3. Validation using a Dynamic Version of the IEEE-30 Bus Test System

In this section, in order to further extend the results obtained from this study and demonstrate the performance of the proposed framework under instantly changing environment, we have used a dynamic version of IEEE-30 bus test system with a dynamically updating load at each one of the buses. The load data presented in the original IEEE-30 bus was assumed to be an average load. Using temperature and humidity data for June 20 and June 21, 2011 for the city of Roanoke, Virginia; hourly real and reactive loads were simulated for each one of the 21 load demanding buses in the IEEE-30 system. Table 27 shows the weather data collected each hour of June 21, while the tables with the real and reactive loads for each bus for each hour are provided in the Appendix. The forecasting algorithm is updated after each hour's load is captured and the system calculates the new dispatch for each of the buses.

In Table 27, the average temperature is 77.83 degrees with an average humidity of 56.5% for June 20, and the average temperature is 73.5 degrees with an average humidity of 81.75% for June 21. As a consequence of these conditions the simulated average consumption for the buses drops by 3.06% for June 21 compared to June 20. Table 28 shows the minimum cost results obtained using the load dispatching algorithm for the demand of June 21 using a particle set size of 50. The dispatch of the minimum cost is obtained using 90 replications on 6 of the 24 different instances; while in 9 instances it is achieved using 60 replications, and in the other 9 instances the best cost is achieved using 30 replications. In the minimum cost results obtained using the load dispatching algorithm for the demand of June 21 using a particle set size of 150, the dispatch of the minimum cost is obtained using 90 replications on 12 of the 24 different instances, while in 7 instances it is achieved using 60 replications, and in the other 5 instances the best cost is achieved using 30 replications. Table 29 shows the minimum cost results obtained using the load dispatching algorithm for the demand of June 21 using a particle set size of 250. Here, the dispatch of the minimum cost is obtained using 90 replications on 16 of the 24 different instances, while in 7 instances it is achieved using 60 replications, and in 1 instance it is achieved with 30 replications. Comparing the results obtained with the different particle set sizes we can see that out of the 24 dispatching decisions obtained with each set size, in 9 cases the lowest cost results are obtained with a set of 50 particles, in 6 cases the lowest cost results are obtained with a set of 150 particles, and in the other 9 cases the lowest cost results are obtained with a set of 250 particles.

Table 27: Weather data for the city of Roanoke

| June 20 | Temperature (F) | Humidity (%) | June 21 | Temperature (F) | Humidity (%) |
|---------|-----------------|--------------|---------|-----------------|--------------|
| 0:00 | 73.9 | 73 | 0:00 | 72 | 87 |
| 1:00 | 73 | 68 | 1:00 | 69.1 | 87 |
| 2:00 | 73.9 | 64 | 2:00 | 70 | 90 |
| 3:00 | 73.9 | 62 | 3:00 | 69.1 | 90 |
| 4:00 | 73 | 64 | 4:00 | 68 | 90 |
| 5:00 | 73 | 61 | 5:00 | 66.9 | 93 |
| 6:00 | 73 | 64 | 6:00 | 66.2 | 94 |
| 7:00 | 75 | 60 | 7:00 | 66.9 | 90 |
| 8:00 | 75.9 | 60 | 8:00 | 68 | 90 |
| 9:00 | 78.1 | 56 | 9:00 | 72 | 84 |
| 10:00 | 80.6 | 51 | 10:00 | 75.9 | 71 |
| 11:00 | 82.9 | 47 | 11:00 | 81 | 62 |
| 12:00 | 87.1 | 44 | 12:00 | 84.2 | 62 |
| 13:00 | 86 | 44 | 13:00 | 88 | 53 |
| 14:00 | 86 | 44 | 14:00 | 88 | 55 |
| 15:00 | 82.4 | 42 | 15:00 | 89.1 | 55 |
| 16:00 | 82.9 | 41 | 16:00 | 73.9 | 79 |
| 17:00 | 81 | 45 | 17:00 | 75.9 | 76 |
| 18:00 | 80.1 | 48 | 18:00 | 71.6 | 88 |
| 19:00 | 78.1 | 52 | 19:00 | 70 | 90 |
| 20:00 | 75.9 | 58 | 20:00 | 71.1 | 90 |
| 21:00 | 75 | 60 | 21:00 | 70 | 97 |
| 22:00 | 75.2 | 61 | 22:00 | 69.1 | 93 |
| 23:00 | 72 | 87 | 23:00 | 68 | 96 |

Table 28: Minimum cost dispatch using a particle set size of 50

| Hour | 30 Replications | | | | | | | | | 60 Replications | | | | | | | | | 90 Replications | | | | | | | | |
|---|---|---|---|---|---|---|---|---|---|---|---|---|---|---|---|---|---|---|---|---|---|---|---|---|---|---|---|
| | Bus 1 | Bus 2 | Bus 5 | Bus 8 | Bus 11 | Bus 13 | Cost ($/h) | Emissions (ton/h) | Power Loss (MW) | Bus 1 | Bus 2 | Bus 5 | Bus 8 | Bus 11 | Bus 13 | Cost ($/h) | Emissions (ton/h) | Power Loss (MW) | Bus 1 | Bus 2 | Bus 5 | Bus 8 | Bus 11 | Bus 13 | Cost ($/h) | Emissions (ton/h) | Power Loss (MW) |
| 0:00 | 14.042 | 94.761 | 36.427 | 56.153 | 26.619 | 41.496 | 634.496 | 0.225 | 3.432 | 33.622 | 89.575 | 63.310 | 40.035 | 5.000 | 37.775 | 650.290 | 0.223 | 3.251 | 33.624 | 89.573 | 63.302 | 40.033 | 5.000 | 37.785 | 650.288 | 0.223 | 3.251 |
| 1:00 | 43.215 | 48.193 | 42.973 | 19.455 | 56.711 | 56.591 | 623.632 | 0.197 | 3.063 | 43.213 | 48.188 | 42.973 | 19.457 | 56.716 | 56.591 | 623.628 | 0.197 | 3.063 | 70.193 | 73.155 | 60.241 | 38.337 | 12.845 | 12.947 | 658.607 | 0.222 | 3.643 |
| 2:00 | 46.328 | 64.236 | 38.926 | 37.923 | 48.114 | 35.479 | 626.885 | 0.200 | 3.197 | 46.324 | 64.237 | 38.933 | 37.887 | 48.098 | 35.527 | 626.900 | 0.200 | 3.198 | 10.463 | 77.764 | 52.578 | 35.787 | 59.904 | 33.900 | 631.761 | 0.210 | 2.587 |
| 3:00 | 72.454 | 15.527 | 28.416 | 50.994 | 61.467 | 36.103 | 624.744 | 0.213 | 3.711 | 72.437 | 15.545 | 28.416 | 50.994 | 61.466 | 36.103 | 624.716 | 0.213 | 3.711 | 33.111 | 23.209 | 52.687 | 50.448 | 49.929 | 45.446 | 579.496 | 0.197 | 2.581 |
| 4:00 | 90.239 | 78.457 | 5.000 | 32.369 | 29.233 | 27.396 | 685.926 | 0.237 | 5.794 | 52.804 | 19.378 | 23.620 | 66.280 | 61.211 | 57.295 | 572.874 | 0.208 | 3.688 | 14.516 | 70.488 | 37.686 | 44.543 | 35.943 | 56.900 | 588.661 | 0.206 | 3.176 |
| 5:00 | 55.807 | 37.905 | 37.188 | 61.589 | 38.482 | 27.729 | 579.195 | 0.204 | 3.030 | 55.798 | 37.903 | 37.187 | 61.589 | 38.483 | 27.740 | 579.185 | 0.204 | 3.030 | 55.809 | 37.904 | 37.186 | 61.588 | 38.483 | 27.730 | 579.197 | 0.204 | 3.030 |
| 6:00 | 42.550 | 70.245 | 49.688 | 15.071 | 44.829 | 39.135 | 627.442 | 0.202 | 2.822 | 42.545 | 70.243 | 49.687 | 15.071 | 44.829 | 39.143 | 627.436 | 0.202 | 2.822 | 42.555 | 70.243 | 49.687 | 15.070 | 44.828 | 39.135 | 627.444 | 0.202 | 2.822 |
| 7:00 | 40.605 | 96.031 | 44.426 | 50.531 | 9.344 | 21.696 | 641.945 | 0.230 | 3.553 | 15.515 | 65.596 | 71.508 | 21.368 | 27.917 | 59.916 | 608.618 | 0.207 | 2.739 | 15.556 | 65.593 | 71.509 | 21.370 | 27.876 | 59.916 | 608.624 | 0.207 | 2.739 |
| 8:00 | 37.712 | 73.836 | 50.410 | 38.926 | 19.432 | 47.563 | 622.327 | 0.206 | 3.259 | 37.707 | 73.853 | 50.410 | 38.914 | 19.432 | 47.563 | 622.352 | 0.206 | 3.260 | 40.652 | 50.875 | 52.341 | 30.349 | 47.533 | 73.737 | 593.775 | 0.196 | 2.872 |
| 9:00 | 17.781 | 86.470 | 59.537 | 54.058 | 60.534 | 5.000 | 667.635 | 0.223 | 2.920 | 90.421 | 38.680 | 45.715 | 5.000 | 54.976 | 50.047 | 727.165 | 0.217 | 4.379 | 90.446 | 38.656 | 45.715 | 5.000 | 54.976 | 50.047 | 727.200 | 0.217 | 4.379 |
| 10:00 | 41.907 | 68.834 | 55.715 | 31.665 | 45.858 | 45.936 | 672.811 | 0.199 | 3.042 | 8.870 | 112.565 | 44.394 | 20.674 | 49.105 | 54.862 | 739.017 | 0.242 | 3.597 | 8.689 | 112.570 | 44.402 | 20.839 | 49.104 | 54.863 | 738.868 | 0.242 | 3.594 |
| 11:00 | 58.777 | 68.689 | 55.714 | 31.665 | 45.824 | 45.936 | 722.995 | 0.201 | 3.860 | 58.628 | 68.770 | 55.714 | 31.665 | 45.890 | 45.936 | 722.937 | 0.201 | 3.858 | 26.480 | 112.570 | 44.180 | 19.929 | 49.088 | 54.862 | 779.049 | 0.236 | 4.362 |
| 12:00 | 49.364 | 71.687 | 35.279 | 64.537 | 50.967 | 38.296 | 707.529 | 0.205 | 4.314 | 49.387 | 71.665 | 35.280 | 64.537 | 50.967 | 38.294 | 707.524 | 0.205 | 4.314 | 49.514 | 71.539 | 35.279 | 64.538 | 50.967 | 38.294 | 707.498 | 0.205 | 4.315 |
| 13:00 | 101.354 | 81.477 | 16.459 | 58.430 | 12.107 | 44.995 | 805.652 | 0.246 | 7.277 | 62.941 | 44.695 | 71.444 | 51.111 | 45.535 | 30.570 | 709.690 | 0.201 | 3.406 | 62.494 | 44.697 | 71.444 | 51.111 | 45.535 | 30.570 | 709.699 | 0.201 | 3.407 |
| 14:00 | 16.326 | 52.864 | 70.202 | 68.212 | 59.396 | 45.141 | 684.132 | 0.204 | 3.078 | 41.104 | 46.062 | 76.722 | 62.351 | 39.923 | 45.830 | 688.012 | 0.200 | 3.109 | 41.091 | 46.062 | 76.726 | 62.543 | 39.923 | 45.831 | 687.998 | 0.200 | 3.109 |
| 15:00 | 61.153 | 77.066 | 29.480 | 42.245 | 41.875 | 26.731 | 667.387 | 0.211 | 4.133 | 61.175 | 77.045 | 29.482 | 42.245 | 41.873 | 26.730 | 667.385 | 0.211 | 4.133 | 22.506 | 57.526 | 37.610 | 62.447 | 53.997 | 53.358 | 631.832 | 0.201 | 3.360 |
| 16:00 | 4.059 | 80.468 | 55.507 | 42.989 | 43.631 | 57.540 | 654.299 | 0.213 | 3.175 | 4.032 | 80.469 | 55.532 | 42.989 | 43.625 | 57.540 | 654.304 | 0.213 | 3.174 | 35.762 | 57.297 | 88.841 | 16.251 | 28.408 | 57.645 | 666.709 | 0.207 | 3.184 |
| 17:00 | 6.331 | 62.105 | 89.632 | 34.079 | 30.418 | 50.182 | 612.305 | 0.213 | 2.572 | 6.391 | 62.105 | 89.572 | 33.973 | 30.417 | 50.290 | 612.368 | 0.213 | 2.573 | 3.589 | 45.426 | 81.061 | 36.074 | 42.336 | 64.267 | 609.912 | 0.208 | 2.578 |
| 18:00 | 12.923 | 51.187 | 48.841 | 47.124 | 47.936 | 64.387 | 601.003 | 0.201 | 2.980 | 10.537 | 77.241 | 34.608 | 47.335 | 43.204 | 59.904 | 623.185 | 0.210 | 3.429 | 66.030 | 50.045 | 38.984 | 32.941 | 51.660 | 33.223 | 644.898 | 0.202 | 3.475 |
| 19:00 | 7.978 | 29.105 | 120.000 | 61.984 | 46.860 | 5.000 | 610.400 | 0.251 | 2.480 | 8.021 | 29.061 | 120.000 | 61.985 | 46.860 | 5.000 | 610.398 | 0.251 | 2.480 | 39.564 | 37.381 | 69.362 | 57.719 | 8.861 | 58.515 | 602.524 | 0.207 | 2.954 |
| 20:00 | 16.900 | 45.442 | 89.243 | 48.994 | 20.414 | 53.077 | 606.990 | 0.210 | 2.665 | 16.921 | 45.446 | 89.243 | 48.894 | 20.414 | 53.093 | 607.022 | 0.210 | 2.666 | 78.809 | 58.895 | 54.902 | 5.000 | 49.355 | 28.382 | 698.424 | 0.213 | 3.998 |
| 21:00 | 46.447 | 22.647 | 61.622 | 39.670 | 49.387 | 41.704 | 590.309 | 0.199 | 2.462 | 46.453 | 22.647 | 61.622 | 39.669 | 49.386 | 41.700 | 590.314 | 0.199 | 2.462 | 25.481 | 63.117 | 54.288 | 6.379 | 59.334 | 48.190 | 631.677 | 0.204 | 2.774 |
| 22:00 | 76.382 | 31.642 | 31.232 | 44.582 | 23.266 | 58.924 | 627.474 | 0.212 | 4.015 | 76.358 | 31.642 | 31.255 | 44.582 | 23.266 | 58.924 | 627.436 | 0.211 | 4.014 | 18.149 | 76.462 | 79.455 | 12.991 | 43.718 | 33.753 | 636.719 | 0.213 | 2.516 |
| 23:00 | 42.550 | 70.245 | 49.688 | 15.071 | 44.829 | 39.135 | 627.442 | 0.202 | 2.822 | 42.545 | 70.243 | 49.687 | 15.071 | 44.829 | 39.143 | 627.436 | 0.202 | 2.822 | 42.555 | 70.243 | 49.687 | 15.070 | 44.828 | 39.135 | 627.444 | 0.202 | 2.822 |

Table 29: Minimum cost dispatch using a particle set size of 250

| Hour | 30 Replications | | | | | | | | | 60 Replications | | | | | | | | | 90 Replications | | | | | | | | |
|---|---|---|---|---|---|---|---|---|---|---|---|---|---|---|---|---|---|---|---|---|---|---|---|---|---|---|---|
| | Bus 1 | Bus 2 | Bus 5 | Bus 8 | Bus 11 | Bus 13 | Cost ($/h) | Emissions (ton/h) | Power Loss (MW) | Bus 1 | Bus 2 | Bus 5 | Bus 8 | Bus 11 | Bus 13 | Cost ($/h) | Emissions (ton/h) | Power Loss (MW) | Bus 1 | Bus 2 | Bus 5 | Bus 8 | Bus 11 | Bus 13 | Cost ($/h) | Emissions (ton/h) | Power Loss (MW) |
| 0:00 | 92.171 | 49.728 | 32.636 | 54.695 | 20.528 | 20.760 | 663.311 | 0.226 | 4.452 | 53.149 | 50.014 | 42.089 | 65.787 | 29.334 | 28.960 | 602.273 | 0.205 | 3.267 | 43.766 | 49.654 | 32.072 | 61.999 | 39.437 | 42.651 | 596.417 | 0.201 | 3.513 |
| 1:00 | 87.405 | 49.711 | 36.471 | 54.441 | 19.996 | 20.158 | 650.521 | 0.223 | 4.106 | 69.707 | 51.401 | 36.255 | 50.429 | 30.515 | 29.387 | 624.450 | 0.208 | 3.619 | 48.027 | 50.067 | 45.762 | 65.656 | 28.878 | 28.689 | 593.158 | 0.204 | 3.004 |
| 2:00 | 92.405 | 52.117 | 34.439 | 52.135 | 20.498 | 20.598 | 669.866 | 0.226 | 4.383 | 54.269 | 51.887 | 43.479 | 63.866 | 28.834 | 28.673 | 608.755 | 0.205 | 3.199 | 44.076 | 53.478 | 33.684 | 59.873 | 38.465 | 41.615 | 602.989 | 0.200 | 3.380 |
| 3:00 | 92.076 | 51.258 | 28.506 | 52.591 | 20.665 | 20.688 | 655.313 | 0.227 | 4.534 | 53.330 | 51.476 | 37.791 | 64.282 | 28.917 | 28.763 | 593.744 | 0.206 | 3.308 | 43.961 | 51.472 | 27.759 | 60.348 | 39.044 | 42.223 | 588.449 | 0.201 | 3.562 |
| 4:00 | 93.345 | 51.041 | 29.096 | 15.604 | 35.187 | 37.276 | 672.287 | 0.222 | 4.649 | 44.229 | 51.181 | 39.821 | 65.990 | 29.447 | 29.315 | 575.410 | 0.204 | 3.083 | 36.596 | 50.030 | 30.080 | 62.311 | 38.997 | 42.262 | 571.955 | 0.201 | 3.376 |
| 5:00 | 86.740 | 42.887 | 32.652 | 58.568 | 19.882 | 18.891 | 626.474 | 0.224 | 3.929 | 90.194 | 49.220 | 30.943 | 17.022 | 35.203 | 37.357 | 660.948 | 0.219 | 4.269 | 43.041 | 49.737 | 41.422 | 66.749 | 28.896 | 28.707 | 570.465 | 0.205 | 2.882 |
| 6:00 | 97.892 | 49.187 | 21.770 | 54.081 | 20.205 | 20.572 | 660.249 | 0.234 | 4.794 | 57.668 | 49.774 | 31.888 | 65.400 | 28.941 | 28.693 | 592.239 | 0.208 | 3.450 | 35.866 | 60.880 | 44.812 | 14.688 | 49.463 | 56.169 | 617.453 | 0.199 | 2.964 |
| 7:00 | 93.654 | 51.884 | 11.586 | 47.500 | 30.042 | 28.967 | 657.165 | 0.228 | 4.938 | 60.728 | 50.375 | 10.823 | 59.308 | 39.156 | 42.343 | 602.167 | 0.209 | 4.037 | 47.084 | 61.959 | 37.413 | 10.360 | 49.149 | 55.977 | 630.401 | 0.201 | 3.227 |
| 8:00 | 95.930 | 51.265 | 12.585 | 45.739 | 30.008 | 28.794 | 663.061 | 0.230 | 5.240 | 61.965 | 49.947 | 11.908 | 57.827 | 38.917 | 42.036 | 606.579 | 0.209 | 4.519 | 48.904 | 62.064 | 38.359 | 7.528 | 49.520 | 56.330 | 636.732 | 0.202 | 3.624 |
| 9:00 | 98.665 | 51.824 | 14.790 | 45.675 | 30.157 | 28.868 | 679.958 | 0.231 | 5.350 | 60.105 | 53.700 | 31.229 | 65.851 | 29.186 | 28.320 | 609.954 | 0.209 | 3.772 | 52.700 | 62.485 | 40.108 | 7.476 | 49.363 | 56.158 | 652.304 | 0.202 | 3.671 |
| 10:00 | 78.365 | 52.604 | 34.107 | 62.854 | 28.442 | 28.425 | 668.006 | 0.215 | 4.336 | 58.944 | 63.613 | 46.796 | 9.259 | 49.466 | 56.270 | 691.996 | 0.202 | 3.887 | 19.501 | 62.511 | 43.335 | 63.910 | 46.683 | 47.801 | 624.394 | 0.203 | 3.281 |
| 11:00 | 140.990 | 09.918 | 41.646 | 34.158 | 22.328 | 23.942 | 823.302 | 0.280 | 6.108 | 54.389 | 51.464 | 43.875 | 59.888 | 38.723 | 41.985 | 651.124 | 0.200 | 3.452 | 46.733 | 63.047 | 62.280 | 11.405 | 49.838 | 56.699 | 691.893 | 0.200 | 3.129 |
| 12:00 | 140.243 | 32.298 | 68.108 | 32.242 | 17.964 | 17.338 | 861.909 | 0.281 | 6.134 | 71.103 | 55.036 | 69.836 | 51.471 | 30.014 | 28.931 | 713.697 | 0.208 | 3.646 | 54.742 | 54.208 | 74.926 | 66.159 | 28.053 | 27.882 | 689.015 | 0.208 | 3.225 |
| 13:00 | 147.297 | 21.015 | 91.269 | 20.011 | 16.274 | 16.184 | 905.636 | 0.305 | 6.234 | 128.049 | 19.275 | 91.114 | 22.383 | 26.918 | 23.165 | 847.502 | 0.270 | 5.087 | 65.571 | 52.717 | 91.284 | 60.660 | 19.970 | 18.915 | 716.365 | 0.219 | 3.301 |
| 14:00 | 151.193 | 21.862 | 106.670 | 21.960 | 6.636 | 6.250 | 933.682 | 0.329 | 7.027 | 147.616 | 22.504 | 107.058 | 24.388 | 6.269 | 6.520 | 921.179 | 0.323 | 6.811 | 143.891 | 24.600 | 107.796 | 25.145 | 6.399 | 6.370 | 910.078 | 0.316 | 6.657 |
| 15:00 | 111.528 | 25.271 | 115.800 | 27.713 | 16.815 | 16.800 | 826.829 | 0.273 | 4.863 | 93.307 | 22.741 | 115.598 | 30.088 | 27.484 | 23.843 | 785.012 | 0.252 | 3.998 | 62.568 | 20.767 | 115.480 | 24.935 | 42.724 | 45.757 | 743.558 | 0.230 | 3.167 |
| 16:00 | 72.003 | 20.842 | 120.000 | 30.740 | 17.067 | 17.101 | 682.801 | 0.252 | 3.336 | 52.584 | 20.138 | 119.577 | 33.152 | 27.728 | 24.027 | 654.910 | 0.241 | 2.789 | 23.394 | 17.136 | 120.000 | 27.435 | 42.939 | 45.986 | 641.119 | 0.237 | 2.473 |
| 17:00 | 108.037 | 17.887 | 98.828 | 25.243 | 21.007 | 14.341 | 752.048 | 0.256 | 4.324 | 87.719 | 19.329 | 98.120 | 28.186 | 27.437 | 23.781 | 707.691 | 0.233 | 3.552 | 56.891 | 16.678 | 98.174 | 23.415 | 42.882 | 45.794 | 670.002 | 0.215 | 2.815 |
| 18:00 | 125.320 | 15.932 | 99.785 | 20.757 | 5.186 | 8.349 | 780.772 | 0.286 | 5.154 | 123.619 | 15.474 | 100.078 | 22.345 | 5.215 | 8.494 | 775.334 | 0.284 | 5.050 | 122.297 | 34.605 | 92.921 | 15.183 | 4.383 | 6.233 | 776.940 | 0.276 | 5.447 |
| 19:00 | 151.543 | 32.944 | 44.552 | 30.947 | 17.776 | 17.218 | 765.378 | 0.268 | 5.558 | 133.420 | 31.373 | 44.357 | 30.969 | 17.741 | 17.179 | 770.015 | 0.271 | 5.620 | 62.775 | 54.276 | 46.698 | 50.294 | 29.861 | 28.848 | 628.935 | 0.204 | 3.334 |
| 20:00 | 98.045 | 52.371 | 30.113 | 52.454 | 20.068 | 20.205 | 682.612 | 0.232 | 4.808 | 58.237 | 52.469 | 39.586 | 64.204 | 28.797 | 28.604 | 614.837 | 0.206 | 3.450 | 50.066 | 51.791 | 29.340 | 60.246 | 58.768 | 41.908 | 608.992 | 0.202 | 3.671 |
| 21:00 | 105.635 | 51.303 | 24.890 | 54.218 | 20.384 | 20.393 | 703.443 | 0.240 | 5.378 | 58.039 | 50.735 | 24.024 | 61.564 | 38.979 | 42.164 | 623.279 | 0.205 | 4.160 | 44.417 | 62.923 | 47.510 | 14.400 | 49.400 | 56.185 | 652.913 | 0.199 | 3.490 |
| 22:00 | 92.388 | 50.497 | 25.459 | 55.013 | 19.944 | 20.119 | 650.564 | 0.229 | 4.606 | 74.243 | 52.341 | 25.345 | 51.110 | 30.573 | 29.486 | 621.726 | 0.212 | 4.084 | 43.699 | 50.648 | 24.541 | 62.200 | 39.120 | 42.471 | 582.891 | 0.203 | 3.664 |
| 23:00 | 99.492 | 28.495 | 26.298 | 38.060 | 16.832 | 16.713 | 586.592 | 0.237 | 4.438 | 57.875 | 51.029 | 34.257 | 65.144 | 28.663 | 28.426 | 599.609 | 0.207 | 3.382 | 48.724 | 51.007 | 23.542 | 61.323 | 38.919 | 42.119 | 593.842 | 0.203 | 3.626 |

In terms of emissions, Table 30 shows the minimum emissions results obtained using the load dispatching algorithm for the demand of June 21 using a particle set size of 50. We can see that the dispatch of the minimum cost is obtained using 90 replications on 11 of the 24 different instances; while in 6 instances it is achieved using 60 replications, and in the other 7 instances the best cost is achieved using 30 replications. In the minimum emissions results obtained using the load dispatching algorithm for the demand of June 21 using a particle set size of 150, we can see that the dispatch of the minimum cost is obtained using 90 replications on 12 of the 24 different instances, while in 4 instances it is achieved using 60 replications, and in the other 8 instances the best cost is achieved using 30 replications. Table 31 shows the minimum emissions results obtained using the load dispatching algorithm for the demand of June 21 using a particle set size of 250. We can see that the dispatch of the minimum cost is obtained using 90 replications on 21 of the 24 different instances, while in 3 instances it is achieved using 60 replications, and in 1 instance it is achieved with 30 replications. Comparing the results obtained with the different particle set sizes we can see that out of the 24 dispatching decisions obtained with each set size, in 11 cases the lowest cost results are obtained with a set of 50 particles, in 7 cases the lowest cost results were obtained with a set of 150 particles, and in the other 6 cases the lowest cost results are obtained with a set of 250 particles.

Table 30: Minimum emissions dispatch using a particle set size of 50

| Hour | 30 Replications | | | | | | | | | 60 Replications | | | | | | | | | 90 Replications | | | | | | | | |
|---|---|---|---|---|---|---|---|---|---|---|---|---|---|---|---|---|---|---|---|---|---|---|---|---|---|---|---|
| | Bus 1 | Bus 2 | Bus 5 | Bus 8 | Bus 11 | Bus 13 | Cost ($/h) | Emissions (ton/h) | Power Loss (MW) | Bus 1 | Bus 2 | Bus 5 | Bus 8 | Bus 11 | Bus 13 | Cost ($/h) | Emissions (ton/h) | Power Loss (MW) | Bus 1 | Bus 2 | Bus 5 | Bus 8 | Bus 11 | Bus 13 | Cost ($/h) | Emissions (ton/h) | Power Loss (MW) |
| 0:00 | 14.042 | 94.761 | 36.427 | 56.153 | 26.619 | 41.496 | 634.496 | 0.225 | 3.432 | 13.919 | 94.800 | 36.427 | 56.152 | 26.703 | 41.496 | 634.552 | 0.225 | 3.431 | 33.624 | 89.574 | 63.385 | 40.073 | 5.000 | 37.825 | 650.626 | 0.223 | 3.251 |
| 1:00 | 43.021 | 48.215 | 42.973 | 19.436 | 56.880 | 56.590 | 623.579 | 0.197 | 3.060 | 43.052 | 48.223 | 42.973 | 19.455 | 56.861 | 56.591 | 623.583 | 0.197 | 3.060 | 70.193 | 73.155 | 60.241 | 38.337 | 12.845 | 12.947 | 658.607 | 0.222 | 3.643 |
| 2:00 | 46.262 | 64.237 | 38.997 | 37.920 | 48.099 | 35.488 | 626.823 | 0.200 | 3.194 | 46.328 | 64.236 | 38.926 | 37.922 | 48.114 | 35.479 | 626.885 | 0.200 | 3.197 | 10.303 | 77.763 | 52.580 | 35.946 | 59.903 | 33.900 | 631.633 | 0.210 | 2.586 |
| 3:00 | 72.042 | 15.931 | 28.417 | 50.994 | 61.466 | 36.104 | 624.084 | 0.213 | 3.704 | 72.437 | 15.545 | 28.416 | 50.994 | 61.466 | 36.103 | 624.716 | 0.213 | 3.711 | 32.796 | 32.210 | 52.783 | 50.449 | 49.928 | 45.665 | 579.340 | 0.197 | 2.579 |
| 4:00 | 90.239 | 78.457 | 5.000 | 32.369 | 29.233 | 27.396 | 685.926 | 0.237 | 5.794 | 32.763 | 19.378 | 23.620 | 66.342 | 61.211 | 57.294 | 572.874 | 0.208 | 3.688 | 32.763 | 19.378 | 23.620 | 66.321 | 61.211 | 57.295 | 572.839 | 0.208 | 3.668 |
| 5:00 | 55.807 | 37.905 | 37.188 | 61.589 | 38.482 | 27.729 | 579.195 | 0.204 | 3.030 | 55.798 | 37.903 | 37.187 | 61.589 | 38.483 | 27.740 | 579.185 | 0.204 | 3.030 | 55.808 | 37.905 | 37.181 | 61.589 | 38.483 | 27.728 | 579.196 | 0.204 | 3.030 |
| 6:00 | 42.910 | 70.245 | 49.688 | 15.071 | 44.829 | 39.135 | 628.469 | 0.202 | 2.964 | 42.905 | 70.243 | 49.687 | 15.071 | 44.829 | 39.143 | 628.463 | 0.202 | 2.964 | 42.915 | 70.243 | 49.687 | 15.070 | 44.828 | 39.135 | 628.472 | 0.202 | 2.964 |
| 7:00 | 42.623 | 70.245 | 49.688 | 15.071 | 44.829 | 39.135 | 627.650 | 0.202 | 2.896 | 42.628 | 70.243 | 49.687 | 15.071 | 44.829 | 39.143 | 627.673 | 0.202 | 2.896 | 42.628 | 70.243 | 49.687 | 15.070 | 44.828 | 39.135 | 627.652 | 0.202 | 2.896 |
| 8:00 | 46.295 | 96.031 | 44.426 | 50.607 | 9.343 | 21.697 | 658.392 | 0.230 | 3.780 | 21.015 | 65.388 | 71.508 | 21.369 | 28.032 | 59.916 | 621.841 | 0.206 | 2.808 | 20.634 | 65.395 | 71.509 | 21.370 | 28.396 | 59.916 | 621.697 | 0.206 | 2.801 |
| 9:00 | 37.565 | 73.859 | 50.410 | 38.961 | 19.433 | 47.563 | 622.051 | 0.206 | 3.172 | 37.570 | 73.858 | 50.411 | 38.956 | 19.433 | 47.563 | 622.057 | 0.206 | 3.172 | 39.565 | 50.875 | 52.341 | 30.349 | 47.557 | 37.737 | 616.661 | 0.197 | 2.734 |
| 10:00 | 17.781 | 86.470 | 59.537 | 54.058 | 60.534 | 5.000 | 667.635 | 0.223 | 2.920 | 17.779 | 86.471 | 59.537 | 54.059 | 60.534 | 5.000 | 667.635 | 0.223 | 2.920 | 65.043 | 18.691 | 26.919 | 48.624 | 34.514 | 46.572 | 554.972 | 0.209 | 3.421 |
| 11:00 | 42.054 | 68.796 | 55.713 | 31.665 | 45.753 | 45.936 | 672.850 | 0.199 | 3.045 | 41.873 | 68.804 | 55.714 | 31.666 | 45.920 | 45.936 | 672.769 | 0.199 | 3.041 | 8.699 | 112.560 | 44.402 | 20.839 | 49.104 | 54.865 | 738.847 | 0.242 | 3.594 |
| 12:00 | 58.579 | 68.776 | 55.714 | 31.667 | 45.929 | 45.936 | 722.897 | 0.201 | 3.856 | 58.561 | 68.804 | 55.714 | 31.666 | 45.920 | 45.936 | 722.905 | 0.201 | 3.856 | 25.305 | 112.560 | 44.402 | 20.839 | 49.104 | 54.865 | 777.706 | 0.236 | 4.328 |
| 13:00 | 49.364 | 71.687 | 35.279 | 64.537 | 50.096 | 38.296 | 707.529 | 0.205 | 4.314 | 49.387 | 71.665 | 35.280 | 64.537 | 50.096 | 38.294 | 707.524 | 0.205 | 4.314 | 49.514 | 71.539 | 35.296 | 45.358 | 50.967 | 38.294 | 707.498 | 0.205 | 4.315 |
| 14:00 | 101.354 | 81.477 | 16.459 | 58.430 | 12.107 | 44.995 | 805.652 | 0.246 | 7.277 | 62.941 | 44.695 | 71.444 | 51.111 | 45.455 | 35.304 | 709.690 | 0.201 | 3.406 | 61.225 | 43.103 | 53.357 | 68.503 | 30.444 | 55.023 | 697.059 | 0.203 | 4.111 |
| 15:00 | 16.326 | 52.864 | 70.202 | 68.212 | 59.396 | 45.141 | 684.132 | 0.204 | 3.078 | 16.287 | 52.849 | 70.201 | 68.212 | 59.451 | 45.141 | 684.146 | 0.204 | 3.077 | 41.058 | 46.063 | 76.722 | 62.576 | 59.923 | 45.830 | 687.965 | 0.200 | 3.109 |
| 16:00 | 61.153 | 77.066 | 29.480 | 42.245 | 41.875 | 26.731 | 666.387 | 0.211 | 4.133 | 61.175 | 77.045 | 29.482 | 42.245 | 41.873 | 26.730 | 667.385 | 0.211 | 4.133 | 22.506 | 57.526 | 37.610 | 62.447 | 53.597 | 53.358 | 631.832 | 0.201 | 3.360 |
| 17:00 | 4.059 | 80.468 | 55.507 | 42.999 | 43.631 | 57.540 | 654.299 | 0.213 | 3.175 | 7.387 | 78.414 | 72.082 | 54.416 | 37.463 | 34.010 | 645.513 | 0.215 | 3.175 | 12.011 | 71.985 | 51.087 | 63.467 | 42.823 | 42.789 | 632.584 | 0.208 | 3.148 |
| 18:00 | 6.243 | 62.104 | 89.635 | 34.111 | 30.421 | 50.231 | 622.285 | 0.213 | 2.572 | 6.223 | 62.105 | 89.659 | 34.105 | 30.428 | 50.247 | 622.294 | 0.214 | 2.572 | 3.550 | 45.425 | 81.066 | 36.111 | 42.335 | 64.266 | 609.890 | 0.208 | 2.578 |
| 19:00 | 12.923 | 51.181 | 48.841 | 47.124 | 47.936 | 64.387 | 601.003 | 0.201 | 2.980 | 7.049 | 84.833 | 35.866 | 66.831 | 34.087 | 44.120 | 621.490 | 0.221 | 3.368 | 47.580 | 42.302 | 47.248 | 64.745 | 18.299 | 52.572 | 603.068 | 0.204 | 3.322 |
| 20:00 | 7.978 | 29.105 | 120.000 | 61.986 | 46.860 | 5.000 | 610.403 | 0.251 | 2.480 | 8.021 | 29.061 | 120.000 | 61.985 | 46.860 | 5.000 | 610.398 | 0.251 | 2.480 | 39.460 | 37.380 | 69.363 | 57.719 | 8.861 | 58.619 | 602.470 | 0.207 | 2.955 |
| 21:00 | 16.658 | 45.604 | 59.242 | 49.098 | 20.356 | 53.073 | 606.937 | 0.211 | 2.666 | 16.573 | 45.598 | 89.243 | 49.097 | 20.408 | 53.091 | 606.910 | 0.211 | 2.665 | 95.638 | 42.582 | 51.000 | 27.026 | 27.515 | 31.905 | 692.326 | 0.221 | 4.319 |
| 22:00 | 46.448 | 22.648 | 61.622 | 39.676 | 49.383 | 41.700 | 590.304 | 0.199 | 2.462 | 5.334 | 56.392 | 56.089 | 46.715 | 60.973 | 35.910 | 585.487 | 0.206 | 2.399 | 5.302 | 56.394 | 56.089 | 46.714 | 61.004 | 35.910 | 585.508 | 0.206 | 2.399 |
| 23:00 | 76.382 | 31.642 | 31.232 | 44.582 | 23.266 | 58.924 | 627.474 | 0.212 | 4.015 | 76.358 | 31.642 | 31.255 | 44.582 | 23.266 | 58.924 | 627.436 | 0.211 | 4.014 | 18.037 | 76.455 | 79.456 | 12.991 | 43.834 | 33.755 | 636.709 | 0.213 | 2.513 |

Table 31: Minimum emissions dispatch using a particle set size of 250

| Hour | 30 Replications | | | | | | | | | 60 Replications | | | | | | | | | 90 Replications | | | | | | | | |
|---|---|---|---|---|---|---|---|---|---|---|---|---|---|---|---|---|---|---|---|---|---|---|---|---|---|---|---|
| | Bus 1 | Bus 2 | Bus 5 | Bus 8 | Bus 11 | Bus 13 | Cost ($/h) | Emissions (ton/h) | Power Loss (MW) | Bus 1 | Bus 2 | Bus 5 | Bus 8 | Bus 11 | Bus 13 | Cost ($/h) | Emissions (ton/h) | Power Loss (MW) | Bus 1 | Bus 2 | Bus 5 | Bus 8 | Bus 11 | Bus 13 | Cost ($/h) | Emissions (ton/h) | Power Loss (MW) |
| 0:00 | 74.050 | 34.704 | 99.406 | 49.261 | 5.831 | 5.945 | 651.649 | 0.237 | 3.131 | 53.149 | 50.014 | 42.089 | 65.787 | 29.334 | 18.960 | 602.273 | 0.205 | 3.267 | 43.766 | 49.654 | 32.072 | 61.999 | 39.437 | 42.651 | 596.417 | 0.201 | 3.513 |
| 1:00 | 72.366 | 35.113 | 100.382 | 48.942 | 5.227 | 5.191 | 646.438 | 0.238 | 3.146 | 69.707 | 51.401 | 36.255 | 50.429 | 30.515 | 29.387 | 624.450 | 0.208 | 3.619 | 48.027 | 50.067 | 45.762 | 65.656 | 28.878 | 28.689 | 593.158 | 0.204 | 3.004 |
| 2:00 | 75.428 | 37.632 | 99.754 | 46.953 | 5.627 | 5.711 | 659.900 | 0.238 | 3.296 | 54.269 | 51.884 | 43.479 | 63.866 | 28.834 | 28.673 | 608.755 | 0.205 | 3.199 | 44.076 | 53.478 | 33.684 | 59.873 | 38.465 | 41.615 | 602.989 | 0.200 | 3.380 |
| 3:00 | 69.347 | 37.094 | 98.343 | 47.443 | 5.911 | 6.146 | 656.017 | 0.234 | 3.034 | 53.330 | 51.476 | 37.791 | 64.282 | 28.917 | 28.763 | 593.744 | 0.206 | 3.308 | 43.961 | 51.472 | 27.759 | 60.348 | 39.044 | 42.228 | 588.449 | 0.201 | 3.562 |
| 4:00 | 83.379 | 7.238 | 30.646 | 64.182 | 35.294 | 40.133 | 619.661 | 0.225 | 3.972 | 44.229 | 51.181 | 39.821 | 65.990 | 29.447 | 29.315 | 575.410 | 0.204 | 3.083 | 36.596 | 50.030 | 30.080 | 62.311 | 38.997 | 42.263 | 571.955 | 0.201 | 3.376 |
| 5:00 | 64.360 | 33.544 | 99.218 | 50.435 | 5.513 | 5.518 | 616.255 | 0.234 | 2.918 | 80.895 | 5.000 | 32.445 | 65.109 | 35.380 | 40.298 | 612.805 | 0.224 | 3.457 | 43.041 | 49.737 | 41.422 | 66.749 | 28.890 | 28.707 | 570.465 | 0.205 | 2.882 |
| 6:00 | 71.938 | 33.676 | 96.643 | 48.779 | 5.505 | 5.487 | 632.679 | 0.235 | 3.114 | 57.668 | 49.774 | 31.888 | 65.400 | 38.941 | 38.693 | 592.239 | 0.208 | 3.450 | 50.083 | 49.107 | 20.716 | 61.527 | 39.022 | 42.213 | 587.965 | 0.204 | 3.755 |
| 7:00 | 73.501 | 35.803 | 94.320 | 46.365 | 5.813 | 5.904 | 634.561 | 0.234 | 3.011 | 60.728 | 50.375 | 10.825 | 59.308 | 39.156 | 42.343 | 602.167 | 0.209 | 4.037 | 47.084 | 61.133 | 33.328 | 64.412 | 46.864 | 47.708 | 673.859 | 0.201 | 3.227 |
| 8:00 | 76.072 | 35.356 | 94.572 | 44.736 | 5.656 | 5.936 | 640.427 | 0.235 | 3.247 | 62.881 | 49.947 | 11.908 | 57.827 | 38.917 | 42.036 | 606.305 | 0.209 | 4.435 | 8.721 | 61.047 | 34.500 | 63.200 | 46.906 | 47.897 | 576.272 | 0.208 | 3.190 |
| 9:00 | 81.677 | 35.449 | 95.243 | 44.753 | 5.335 | 5.573 | 661.255 | 0.239 | 3.411 | 60.105 | 53.700 | 31.229 | 65.851 | 29.186 | 28.320 | 609.954 | 0.209 | 3.772 | 12.002 | 61.260 | 36.342 | 63.193 | 46.971 | 48.107 | 588.589 | 0.206 | 3.256 |
| 10:00 | 78.365 | 52.604 | 34.107 | 62.834 | 28.442 | 28.425 | 668.006 | 0.215 | 4.336 | 66.248 | 55.192 | 38.598 | 66.723 | 29.196 | 28.438 | 651.338 | 0.210 | 3.935 | 19.501 | 62.511 | 43.335 | 63.910 | 46.683 | 47.801 | 624.394 | 0.203 | 3.281 |
| 11:00 | 118.180 | 39.313 | 50.489 | 39.004 | 22.923 | 21.929 | 765.781 | 0.246 | 4.964 | 14.010 | 68.885 | 58.994 | 69.824 | 39.933 | 37.987 | 659.433 | 0.209 | 2.760 | 53.022 | 54.518 | 55.913 | 67.707 | 29.801 | 29.016 | 649.141 | 0.205 | 3.015 |
| 12:00 | 140.242 | 32.981 | 68.108 | 32.242 | 17.964 | 17.338 | 861.909 | 0.281 | 6.134 | 71.103 | 55.036 | 69.836 | 51.471 | 30.014 | 28.931 | 713.697 | 0.208 | 3.646 | 54.742 | 54.208 | 74.926 | 66.115 | 28.053 | 27.882 | 689.015 | 0.208 | 3.225 |
| 13:00 | 147.297 | 21.015 | 91.269 | 20.011 | 16.274 | 16.184 | 905.636 | 0.305 | 6.234 | 128.049 | 19.275 | 91.114 | 22.383 | 26.918 | 23.165 | 847.502 | 0.270 | 5.087 | 65.571 | 52.717 | 91.284 | 60.660 | 19.970 | 18.915 | 716.363 | 0.219 | 3.301 |
| 14:00 | 151.193 | 21.862 | 106.674 | 21.960 | 6.636 | 6.250 | 933.692 | 0.329 | 7.027 | 147.616 | 22.504 | 107.058 | 24.388 | 6.269 | 6.520 | 921.179 | 0.323 | 6.811 | 151.407 | 23.476 | 107.041 | 19.840 | 6.515 | 6.392 | 936.455 | 0.330 | 7.127 |
| 15:00 | 111.528 | 25.271 | 115.802 | 27.713 | 16.815 | 16.800 | 826.835 | 0.273 | 4.863 | 93.307 | 22.741 | 115.598 | 30.088 | 27.484 | 23.843 | 785.012 | 0.252 | 3.998 | 36.792 | 54.774 | 115.633 | 64.661 | 20.637 | 19.586 | 708.672 | 0.236 | 3.025 |
| 16:00 | 72.003 | 20.842 | 120.000 | 30.740 | 17.067 | 17.101 | 682.801 | 0.252 | 3.336 | 52.584 | 20.138 | 119.577 | 33.152 | 27.728 | 24.027 | 654.910 | 0.241 | 2.789 | 23.394 | 17.136 | 120.000 | 27.435 | 42.939 | 45.986 | 641.119 | 0.237 | 2.473 |
| 17:00 | 108.037 | 17.887 | 98.828 | 25.243 | 21.007 | 14.341 | 752.048 | 0.256 | 4.324 | 87.719 | 19.329 | 98.120 | 28.186 | 27.437 | 23.781 | 707.691 | 0.233 | 3.552 | 31.876 | 49.611 | 98.560 | 63.616 | 20.559 | 19.510 | 633.732 | 0.220 | 2.712 |
| 18:00 | 125.320 | 15.932 | 99.785 | 20.757 | 5.186 | 8.349 | 780.772 | 0.286 | 5.154 | 123.619 | 15.474 | 100.078 | 22.345 | 5.215 | 8.494 | 775.354 | 0.284 | 5.050 | 71.665 | 7.461 | 178.880 | 6.840 | 5.292 | 6.224 | 763.221 | 1.948 | 6.187 |
| 19:00 | 131.543 | 32.944 | 44.552 | 30.947 | 17.776 | 17.612 | 765.378 | 0.268 | 5.558 | 133.420 | 31.373 | 44.357 | 30.969 | 17.741 | 17.179 | 770.015 | 0.271 | 5.620 | 62.775 | 54.276 | 46.698 | 50.294 | 29.861 | 28.848 | 628.935 | 0.204 | 3.334 |
| 20:00 | 78.063 | 37.096 | 98.667 | 47.316 | 5.337 | 5.414 | 664.665 | 0.239 | 3.445 | 58.237 | 52.469 | 39.586 | 64.204 | 28.792 | 28.604 | 614.837 | 0.206 | 3.450 | 46.777 | 55.489 | 43.895 | 67.978 | 29.086 | 28.406 | 604.486 | 0.205 | 3.183 |
| 21:00 | 82.609 | 35.182 | 97.440 | 48.724 | 5.489 | 5.555 | 676.082 | 0.241 | 3.654 | 58.039 | 50.735 | 24.024 | 61.564 | 38.979 | 42.164 | 623.279 | 0.205 | 4.160 | 54.427 | 54.362 | 39.432 | 69.220 | 29.152 | 28.321 | 617.061 | 0.207 | 3.569 |
| 22:00 | 69.251 | 35.452 | 97.569 | 49.444 | 5.196 | 5.182 | 630.033 | 0.235 | 3.079 | 74.243 | 52.341 | 25.345 | 51.110 | 30.573 | 29.486 | 621.726 | 0.212 | 4.084 | 43.699 | 50.648 | 24.541 | 62.200 | 39.120 | 42.471 | 582.891 | 0.203 | 3.664 |
| 23:00 | 98.090 | 29.410 | 28.038 | 38.078 | 16.832 | 16.713 | 586.559 | 0.236 | 4.371 | 57.875 | 51.029 | 34.257 | 65.144 | 28.663 | 28.426 | 599.609 | 0.207 | 3.382 | 45.723 | 53.327 | 39.114 | 69.062 | 29.283 | 28.593 | 587.909 | 0.206 | 3.090 |

**5.5. Computational Performance of the Economic and Environmental Load Dispatching Framework**

Here the effectiveness of the particle filtering algorithm in tracking the states and producing acceptable solutions for the previously presented cases, is discussed. Tables 32 and 33 show the mean squared error for each of the measurements compared to the states for both synthetic function sets.

Table 32: Measurement of mean squared error for the first synthetic $x - z$ pair

| Particle Set Size | 30 Replications | 60 Replications | 90 Replications | 120 Replications |
|---|---|---|---|---|
| 50 | 4.2522 | 4.1573 | 4.1545 | 4.1376 |
| 100 | 4.2196 | 4.1535 | 4.1918 | 4.1478 |
| 150 | 4.2056 | 4.159 | 4.1331 | 4.1388 |
| 200 | 4.2062 | 4.1442 | 4.1419 | 4.1333 |
| 250 | 4.3585 | 4.1594 | 4.1371 | 4.1419 |
| 300 | 4.3487 | 4.1856 | 4.1376 | 4.1794 |

For the first pair of functions $x$ and $z$, as the number of replications increases the mean squared deviation decreases with the average dropping from 4.2657 for 30 replications to 4.1646 with 120 replications, while the differences in particle set sizes does not have a significant impact on the results. The effectiveness of the function $z$ to track the function $x$ depends on the number of replications more than the number of particles in the filter. Table 13 reveals that for the second pair of functions $x$ and $z$, the mean squared deviation increases along with the number of replications with an average increasing from 0.7881 for 30 replications to 0.7993 with 120 replications. Similar to the results obtained from the first set of functions, the differences in particle set sizes do not have a significant impact on the results. Overall, the effectiveness of the function $z$ to track the function $x$ depends on the number of replications more than the number of particles in the filter. The first observation function converges to the state as the

replications increase while the second observation function diverges from the state as the number of replications increases. The ability of the first measurement function to track the state in the first synthetic case is not as good as in the second case, however as the number of replications increases the parameters selected for the measurement functions make the function converge to the state in the first case, and diverge from the state in the second case, as the number of replications increases.

Table 33: Measurement of mean squared error for the second synthetic $x - z$ pair

| Particle Set Size | 30 Replications | 60 Replications | 90 Replications | 120 Replications |
|---|---|---|---|---|
| 50 | 0.7846 | 0.7929 | 0.7954 | 0.7965 |
| 100 | 0.779 | 0.7951 | 0.7993 | 0.7976 |
| 150 | 0.7801 | 0.7919 | 0.7956 | 0.7954 |
| 200 | 0.7008 | 0.7928 | 0.7957 | 0.7959 |
| 250 | 0.7821 | 0.796 | 0.7979 | 0.7962 |
| 300 | 0.7784 | 0.792 | 0.7941 | 0.7968 |

The results regarding computational performance of the proposed framework are presented in Figure 45. The figure shows that as the number of particles increases the time that the algorithm takes also increases, this same effect can also be evidenced for the number of particles. However, there is a linear relationship between the increase in computational time and the increase in replications, while the increase in computational time is exponential with respect to the increase in the particle set size. It is important to highlight that all of the scenarios run quite fast, with computational times that range from 6.1932 seconds to 124.0879 seconds. The proposed research has been conducted leveraging the Virtual Computing Facilities (Cloud) at the Industrial Energy Assessment Center of University of Miami. This virtual center has a configuration composed of 375 Intel 2.66 GHz CPUs cores for a total computational power of 1THz, 1.5 TB RAM, 100 TB online storage, 720 Gbps of wire-speed Ethernet switching, 1.2 Gbps firewall

throughput, and 60 TB backup tap library. This facility also enables reduced compatibility testing and application troubleshooting.
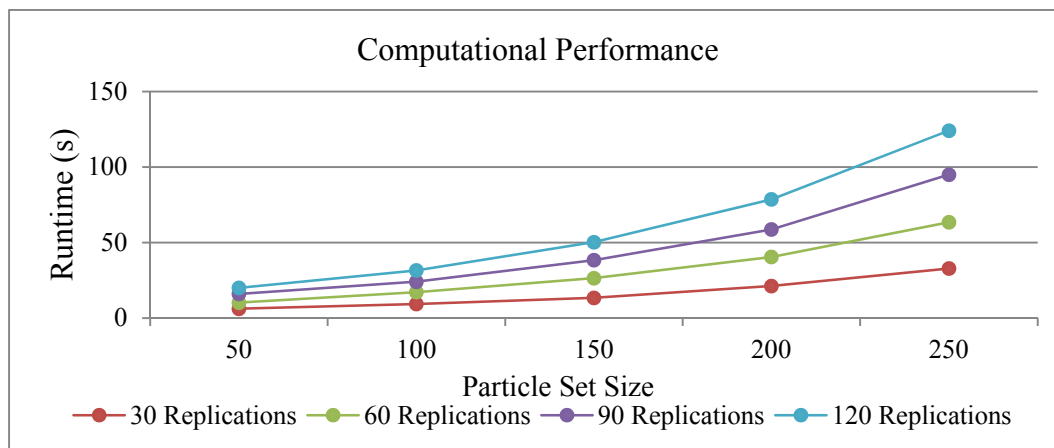


Figure 45: Computational time (in seconds) of the proposed framework

We have developed a decision making framework involving particle filtering for load dispatching to solve the EELD problem. The proposed method has been first validated using synthetic functions, and then benchmarked against the earlier works presented in literature via the use of IEEE-30 bus test system with constant and dynamic load points.

# Chapter 6: Optimal Placement of Distributed Generation

The power dispatch problem considered in this study involves two distinctive objectives for the implementation of distributed generation. The first objective involves the economic load dispatch for the network so that the resources are used in the most cost effective manner. The second objective involves the optimal placement of distributed generation for minimal power loss in the network. These two objectives have been faced using the multi-objective optimization algorithm described in Chapter 3, which has been adapted to this specific setting.

## 6.1. Formulation of the Economic Load Dispatch Problem

The economic load dispatch involves the determination of the output of electric resources to reliably meet the short-term system demand, while minimizing cost and power loss; ensuring that constraints of power balance and capacity limits in the system are met. The total cost of the generated electricity is provided by $\sum \alpha_i + \beta_i G_i + \gamma_i G_i^2$, where $\alpha_i$, $\beta_i$, and $\gamma_i$, are the cost coefficients of the $i^{th}$ generator, and $G_i$ represents the amount of the real power output obtained from the $i^{th}$ generator. Here, the generator set includes $\mu$ number of central generation facilities and $\nu$ number of distributed generation units, presented as $G_i \in \{CG_1, CG_2, \cdots, CG_\mu, DG_1, DG_2, \cdots, DG_\nu\}$. The total power loss can be defined as

$$P_{loss} = \sum_{i=1}^{N}(G_i - L_i), \qquad\qquad \text{Eq. (54)}$$

where $P_{loss}$ represents the total power loss, $N$ is the total number of buses and $L_i$ is the real load at bus $i$.

The constraints that must be satisfied in the economic dispatch problem are

$$G_i^{min} \leq G_i \leq G_i^{max} \qquad\qquad \forall i, \ \text{Eq. (55)}$$

$$G_i - L_i - V_i \sum_{j=1}^{N} V_j[C_{ij}cos(\delta_i - \delta_j) + T_{ij}sin(\delta_i - \delta_j)] = 0 \quad \forall i, \ \text{Eq. (56)}$$

$$Q_i - R_i - V_i \sum_{j=1}^{N} V_j[C_{ij}sin(\delta_i - \delta_j) + T_{ij}cos(\delta_i - \delta_j)] = 0 \quad \forall i. \ \text{Eq. (57)}$$

The generation capacity constraints are shown in Eq. (55), where the real power output of each generator is restricted with minimum ($G_i^{min}$) and maximum ($G_i^{max}$) capacities. The power balance constraints shown in Eq. (56) and Eq. (57) ensure that the load provided to the system covers the total demand while considering the energy loss during transmission. Eq. (56) addresses the real power balance, where $V_i$ is the voltage magnitude at bus $i$, $\delta_i$ is the voltage angle at bus $i$, $C_{ij}$ is the transfer conductance between buses $i$ and $j$, and $T_{ij}$ denotes the transfer susceptance between buses $i$ and $j$. In Eq. (57), which addresses the reactive (imaginary) power balance, $Q_i$ is the reactive power generated at the $i^{th}$ bus, and $R_i$ is the reactive load at bus $i$.

The transfer conductance and transfer susceptance are the real and imaginary elements of the bus admittance matrix $Y$. The bus admittance matrix represents the nodal admittance between the different buses of a power system and is a measure of how easily a current may flow between the buses. The admittance is defined as the inverse of the

impedance, which is a measure of the opposition that a circuit presents to the flow of current when a voltage is applied, and extends the concept of electrical resistance to alternating current circuits.

### 6.2. Optimal Placement of Distributed Generation Problem

The location of different sources of distributed generation may be considered optimal if it is such that the amount of power loss in the system is minimized. To this end, we specify the idea how the admittance matrix of the system and the equivalent resistance between slack bus and other buses is changed if the distributed power generation unit is added at one of the buses in the system in this section. According to Wang and Nehrir's (2004) proposed framework, in a networked system of $N$ buses, the admittance matrix $Y^0$ is defined in Eq. (58) where bus number one is assumed to be the slack bus. Adding distributed generation at bus $j$ causes the admittance to change to $Y$. $Y$ is defined in Eq. (59) where $Y_{11} = Y_{11}^0 + Y_{jj}^0 + 2Y_{1j}^0$, $Y_{1k} = Y_{1k}^0 + Y_{jk}^0$ $(k = 2, \dots, j-1)$, $Y_{1k} = Y_{1(k+1)}^0 + Y_{j(k+1)}^0$ $(k = j, \dots, N-1)$, $Y_{k1} = Y_{1k}$ $(k = 2, \dots, N-1)$

$$Y^0 = \begin{bmatrix} Y_{11}^0 & \cdots & Y_{1k}^0 & \cdots & Y_{1N}^0 \\ \vdots & & \vdots & & \vdots \\ Y_{N1}^0 & \cdots & Y_{Nk}^0 & \cdots & Y_{NN}^0 \end{bmatrix} \qquad \text{Eq. (58)}$$

$$Y = \begin{bmatrix} Y_{11} & \cdots & Y_{1k} & \cdots & Y_{1(N-1)} \\ \vdots & & \vdots & & \vdots \\ Y_{(N-1)1} & \cdots & Y_{(N-1)k} & \cdots & Y_{(N-1)(N-1)} \end{bmatrix} \qquad \text{Eq. (59)}$$

assuming that the original load on the system is given by $S_L^0 = [S_{L1}^0, S_{L2}^0, \cdots, S_{LN}^0]$, and the original generated power is given by $S_G^0 = [S_{G1}^0, S_{G2}^0, \cdots, S_{GN}^0]$. Once the distributed

generator is added at bus $j$, the new load vector can be presented as $S_L = [S_{L1}, S_{L2}, \cdots, S_{LN}]$, where $S_{Li} = L_i + jR_i$, $S_{L1} = 0$, $S_{Li} = S_{Li}^0$ for load buses and $S_{Li} = \max\{L_i^0 - G_i, 0\}$ for P-V buses. In this formulation, we assume that at bus 1 real and reactive power consumed by the load are supplied directly by the generation at that bus, whereas the reactive power load at P-V buses may be provided by the external power source at the bus. The power loss in the system after adding distributed generation at bus $j$ is achieved by minimizing $F_j = \sum_{i=1}^{N} ER_{1i}(j)|S_{Li}|^2$, where $ER_{1i}(j)$ is the equivalent resistance between bus $i$ and bus 1, and is defined as

$$ER_{1i}(j) = \begin{cases} \text{Real}(Z_{11} + Z_{ii} - 2Z_{1i}), & i < j \\ \text{Real}(Z_{11} + Z_{(i-1)(i-1)} - 2Z_{1(i-1)}), & i > j \end{cases}. \qquad \text{Eq. (60)}$$

Where $Z$ is the impedance matrix ($Z = Y^{-1}$), and it is important to note that $ER_{11}(j) = ER_{1j}(j) = 0$.

In order to add more than one source of distributed generation into the system, the admittance matrix may be updated sequentially so that all of the sources of distributed generation are accounted for. In a similar fashion, the equivalent resistance is to be updated sequentially to account for all of the sources of distributed generation. With this framework, there are two ways to ensure that the voltage at each of the buses is held within the acceptable range if the suggested optimal locations lead to the violation of this constraint. The first alternative is to relocate the source of distributed generation from the optimal suggested bus to other buses that are close to the optimal, until the voltage constraints are met. The second alternative to ensure that voltage constraints are not

violated is to decrease the amount of power generated by distributed generation and to optimize the system again.

Figure 46 illustrates the adaptation of the particle filtering based optimization framework proposed to solve the multi-objective optimization problem. The framework begins by initializing the number of samples for the initial random sampling stage and for the resampling stages, defining the non-dominated set as an empty set, and defining the number of iterations to perform. Once initialization is completed; the data for buses, lines, and cost is read for the performance of the random sampling stage. The admittance matrix is then updated to reflect the distributed generation levels from the random dispatch, and used to calculate the resulting loads and the equivalent resistance. Once the admittance has been updated and the equivalent reactance has been calculated, the resultant power generation as well as the loss is evaluated at the swing bus to ensure the power balance constraints are met.

Once power balance is ensured for all of the samples, the non-dominated solution set is calculated and sampling densities are generated. Three sampling densities are generated where the first one is generated within the samples of the non-dominated solution set and the other two are generated from the extreme points of the non-dominated solution set and their closest extreme points of the sampling space. The next step is to perform sampling from each distribution. The new samples are then used to update the admittance matrix as the process iterates. Once the desired number of iterations is reached, the final non-dominated solution set is calculated.
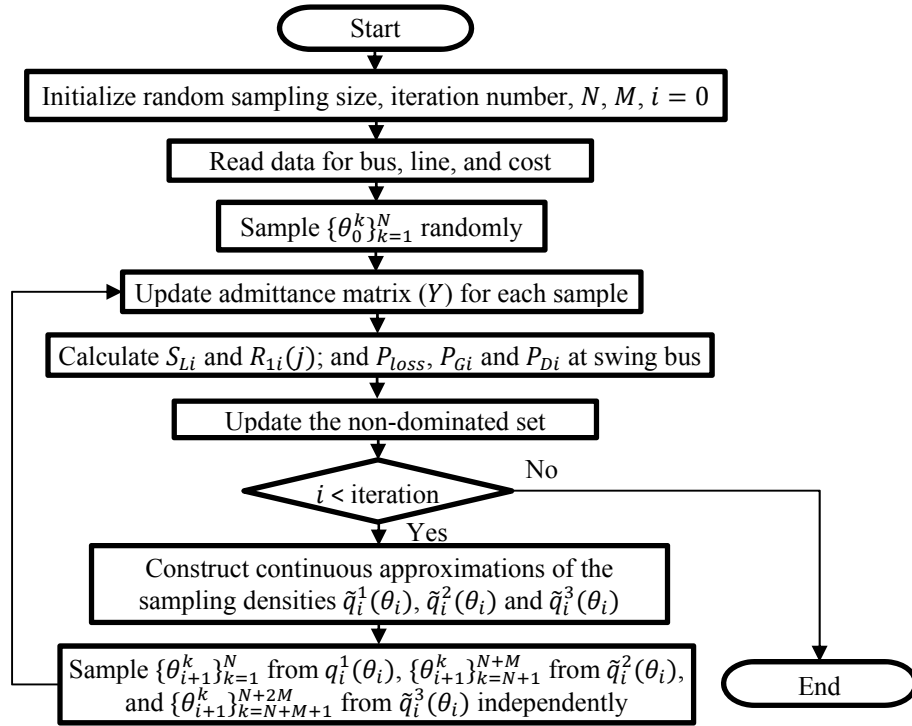
Figure 46: Flowchart of operations performed at proposed particle filtering based optimization algorithm

## 6.3. Evaluation of the Proposed Framework for Optimal Placement of Distributed Generation

In order to establish the validity of the distributed generation penetration optimization framework proposed in this study, we use the IEEE-30 bus test system as an assessment case where the cost data for the generation capacities and parameters of both the central generation and distributed generation units are obtained from (Phonrattanasak, 2010). Synchronous generators (rotating energy conversion machines) from microturbine technology are considered as the sources of distributed generation, as they provide a reliable and easily controllable source of distributed generation and do not depend on environmental factors such as solar irradiation, cloud cover, or wind speed as the case in renewable sources of distributed generation. The modeling of different renewable sources

of the energy generation within the proposed framework will be addressed as part of the future venues of this work.

### 6.3.1. Modified IEEE-30 Bus Test System for Distributed Generation Penetration

IEEE-30 bus test system has been used in the literature and in practice as one of the standard test cases for power systems. The data with the characteristics of the IEEE-30 bus test system has been obtained from the Power Systems Test Case Archive of the Department of Electrical Engineering at the University of Washington (2012). The IEEE-30 bus system represents a part of the American Electric Power System in Midwestern U.S. The system consists of a total of 30 buses and 41 lines, where there are 6 generation buses, 19 load buses, and 5 buses that neither generate nor request electricity, as shown in Figure 47.
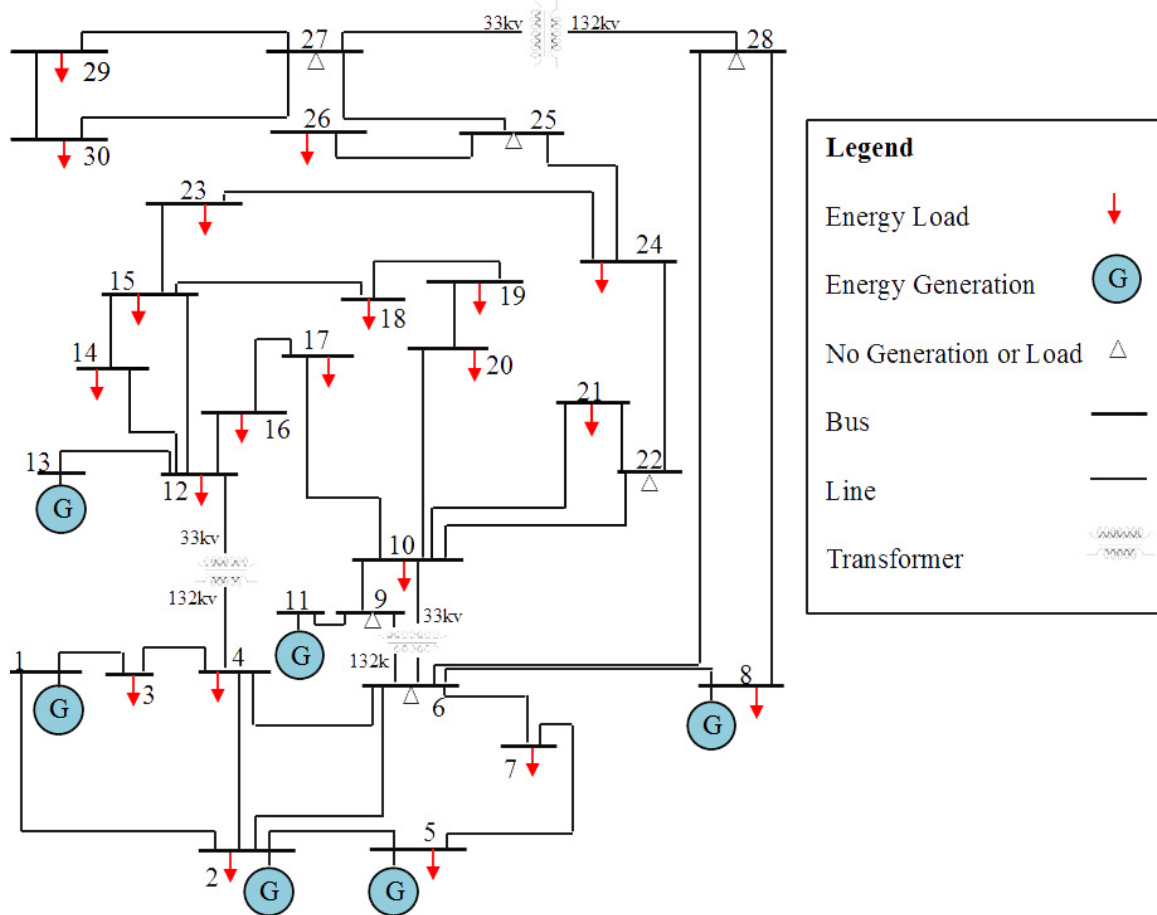
Figure 47: Modified IEEE-30 Bus Test System for Distributed Generation Penetration

The cost parameters related to the power generation for the different central generation units, as well as for the distributed generation are shown in Table 34, where the capacity for central generation units ranges from 10 MW at buses 8 and 13 to 200 MW at bus 1, while the distributed generation units have a capacity ranging between 0 and 10 MW.

Table 34: IEEE-30 Cost Data

| Generation Unit | Bus | Capacity | | Cost | | |
|---|---|---|---|---|---|---|
| | | Min | Max | $\alpha$ | $\beta$ | $\gamma$ |
| 1 | 1 | 50 | 200 | 2 | 2 | 0.00375 |
| 2 | 2 | 20 | 80 | 1 | 1.75 | 0.00175 |
| 3 | 5 | 15 | 50 | 3 | 1 | 0.00625 |
| 4 | 8 | 10 | 35 | 1 | 1.25 | 0.00834 |
| 5 | 11 | 12 | 40 | 1.5 | 3 | 0.025 |
| 6 | 13 | 10 | 30 | 1 | 3 | 0.025 |
| DG | - | 0 | 10 | 5 | 1 | 0 |

(Phonrattanasak, 2010)

### 6.3.2. Optimization of Distributed Generation Penetration

The particle filtering-based multi-objective optimization framework has been implemented using Matlab R2010b on an Intel Core2 Duo E8600 Computer having 4GB of RAM. In order to provide validation for the proposed framework, we have used the case presented by Wang (2004) where a source of 15MW of distributed generation is added to the IEEE-30 system. The results of these simulations are shown in Figure 48, where the minimal power loss is achieved when distributed generation is added at bus 5 with a power loss of 15.482 MW, just as in the results presented by Wang (2004) providing validation to the framework's ability to find the best locations to introduce distributed generation to a networked system and minimize the resulting power loss of the electric dispatch.
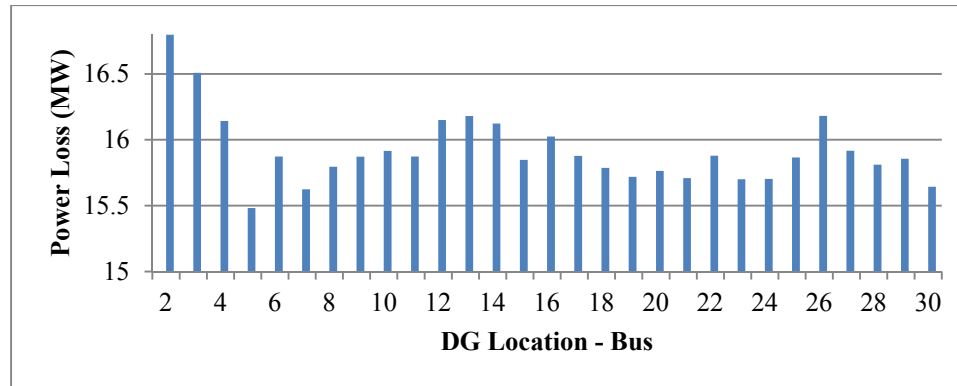
Figure 48: Power loss from placing a 15MW source of distributed generation at different buses within the IEEE-30 system with central generation at buses 1 and 2.

There are two factors that may affect the performance of the framework: the number of iterations performed and the size of the particle set used for sampling within each iteration. In order to evaluate these two factors, two separate sets of experiments have been performed. The results from these experiments let us to determine appropriate parameters, in terms of number of iterations and particle set sizes, to run the framework in the different proposed scenarios.

To test the effect of the number of iterations on the obtained results, the framework has been evaluated using a fixed initial particle set and a total of 64 particles in the sampling stages. Independent runs with different number of iterations were performed under this setting as shown in Figure 49. The figure shows that as the number of iterations increases, the solutions with lower cost improve within each non-dominated solution set. Furthermore, there are no significant benefits in increasing the total number of iterations beyond 30, as the different non-dominated solution sets converge to the same solutions.
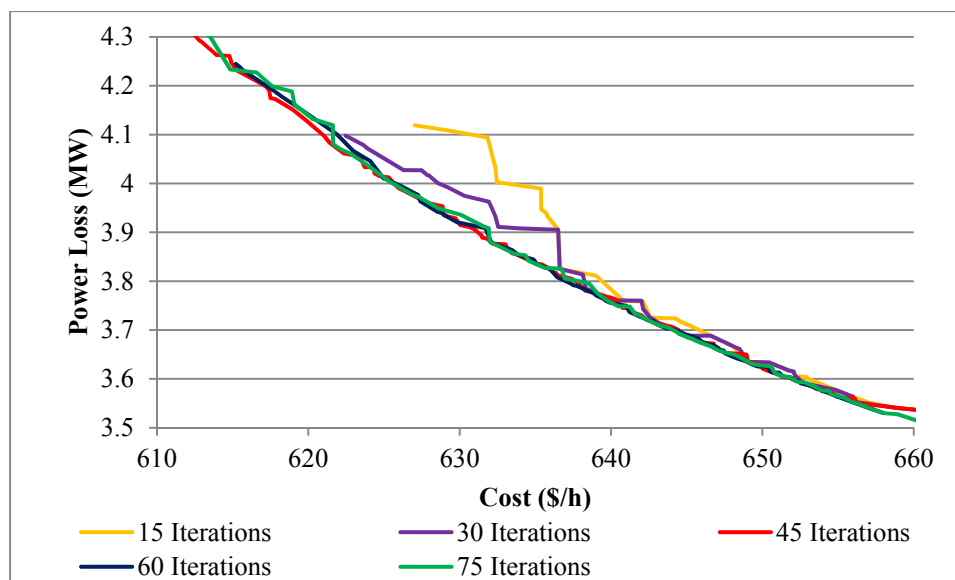
Figure 49: Comparison of different number of iterations.

In order to evaluate the effect of the particle set sizes in the sampling stages, the framework has been evaluated using a fixed initial particle set and 15 iterations. Independent runs with different particle set sizes have been performed under these conditions as shown in Figure 31. In order to evidence the effect of the different particle set sizes clearly, a small number of iterations have been selected. Figure 50 depicts how an increase in the number of particle set sizes impacts (increases) the size of the non-dominated solution set and generates a longer Pareto front with more alternatives. Having a particle set of 32 particles leads to only one non dominated solution with a cost of $664.76 per hour and a power loss of 3.467MW, while having a particle set of 192 particles leads to solutions that range from $665.96 per hour with a power loss of 3.486 MW to $604.53 per hour with a power loss of 4.681 MW.
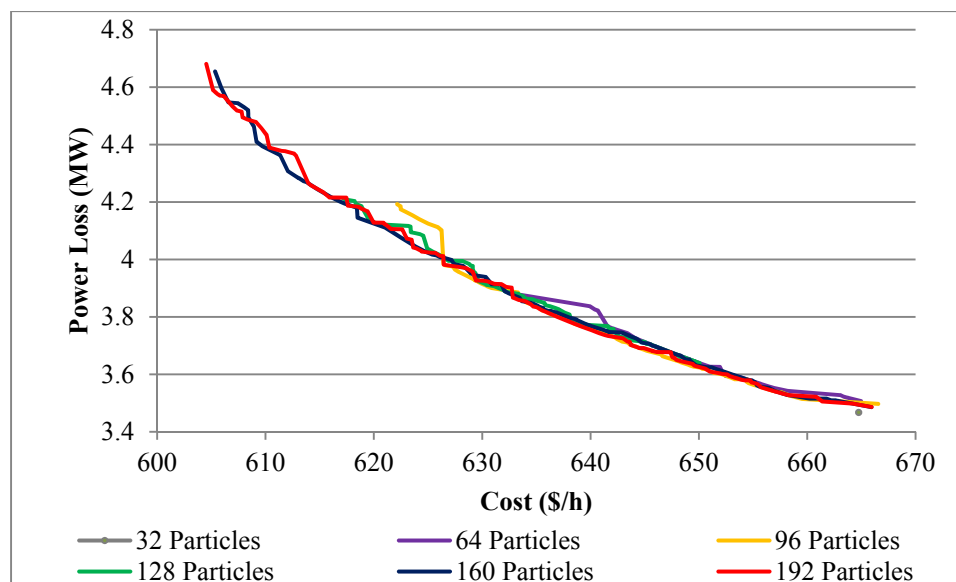
Figure 50: Comparison of different particle set sizes.

Based on these results we have conducted experiments using 25 iterations, 100 particles in the initial random sampling stage, 100 particles for the first sampling stage, and 60 particles for the resampling stage. The experiments have been conducted over five different scenarios where the system is allowed to have "*no distributed generation (DG)*", "*at most one distinct source of DG*", "*at most two distinct sources of DG*", "*at most three distinct sources of DG*", and "*non-predetermined number of sources of DG*", respectively. The results associated with each one of these scenarios are summarized below.

### 6.3.3. Scenario 1: Predetermined Number of Sources of Distributed Generation

In this scenario, we enable the framework to use a predetermined number of sources of distributed generation, ranging from zero sources of distributed generation, up to three

sources of distributed generation. Table 35 shows the minimum cost dispatch from the
non-dominated solution sets generated with zero, one, two and three sources of
distributed generation.

Table 35: Minimum cost dispatch using predetermined number of sources of distributed
generation.

| | | Sources of Distributed Generation | | | |
|---|---|---|---|---|---|
| | | 0 | 1 | 2 | 3 |
| Generation (MW) | Bus 1 | 100.504 | 92.078 | 80.381 | 85.255 |
| | Bus 2 | 80 | 80 | 80 | 80 |
| | Bus 5 | 50 | 50 | 50 | 50 |
| | Bus 7 | 0 | 0 | 7.25 | 6.11 |
| | Bus 8 | 35 | 35 | 35 | 7.35 |
| | Bus 9 | 0 | 9.3 | 10 | 8.72 |
| | Bus 11 | 13.305 | 12 | 12 | 12 |
| | Bus 13 | 10 | 10 | 13.169 | 10.923 |
| Power Loss (MW) | | 5.409 | 4.978 | 4.4 | 4.608 |
| Cost ($/h) | | 596.0181 | 582.642 | 575.976 | 553.411 |

When the system is not allowed to employ any distributed generation source and
rather forced to utilize centralized generation units at all times, the non-dominated
solution set achieves the best cost with a resulting power loss is of 5.409 MW at a cost of
596.0181$/h. The non-dominated solution set for this number of sources of distributed
generation is shown in Figure 51. In this figure, the results presented by Phonrattanasak
(2010) for the economic and environmental dispatch problem are shown in red. In this set
of results, the generation at buses 1, 2, 5, 8, 11, 13 is 113.919 MW, 67.425 MW, 26.671
MW, 33.843 MW, 29.471 MW and 18.836 MW, respectively. The power loss for these
generation parameters was calculated to be 5.971 MW at a cost of 667.186$/h. It can be
seen in the figure that the solution from Phonrattanasak is clearly dominated by the non-
dominated set from the proposed framework.
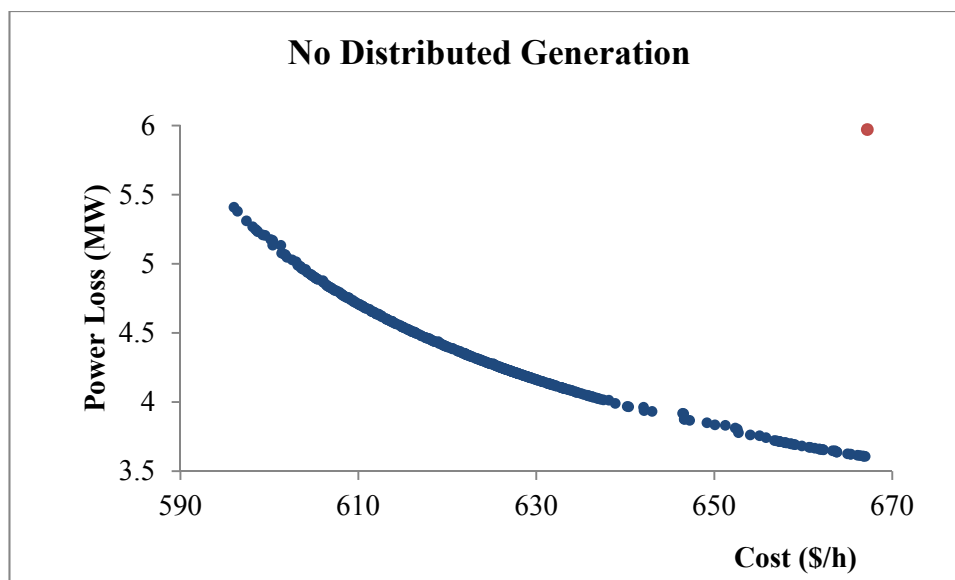
Figure 51: Non-dominated solution set with no sources of distributed generation.

It has been found that the best location for the deployment of one distributed generation unit is at bus 9, when the system is allowed to employ one source of distributed generation unit, since generation at this bus is part of all of the solutions of the non-dominated set. In this case, the non-dominated solution set achieves the best cost with a resulting power loss of 4.978 MW at a cost of 582.642$/h. The non-dominated solution set for one source of distributed generation is depicted in Figure 52.

When the system is allowed to employ two sources of distributed generation units, the best locations for their deployment have been found to be buses 7 and 9, as generation at both of these buses is part of all of the solutions of the non-dominated set. Here, the best cost of 575.976$/h is achieved with a resulting power loss of 4.400 MW. Figure 53 shows the non-dominated solution set with two sources of distributed generation.

The results from the proposed framework show that if there is an opportunity to locate three different sources of distributed generation, the optimal results are achieved

when locating distributed generation at buses 7 and 9, while not deploying a third source of distributed generation in the network. Here, the best cost of 553.411 $/h is reached with a resulting power loss of 4.608 MW.
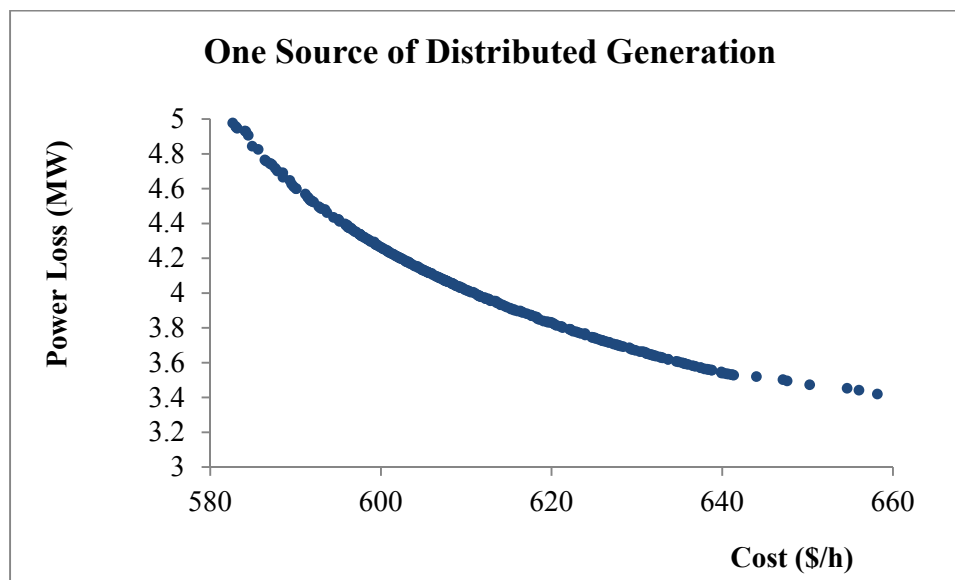


Figure 52: Non-dominated solution set with one source of distributed generation.
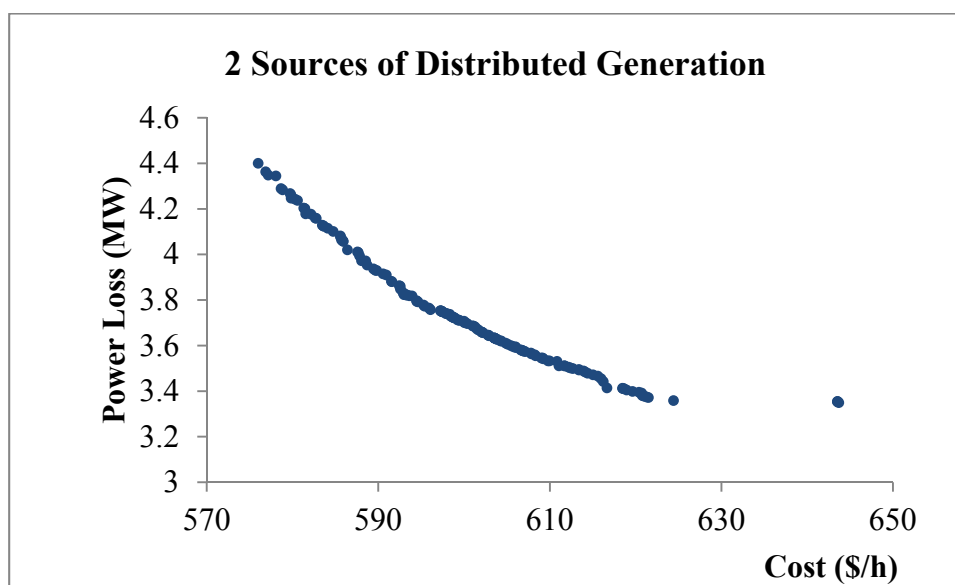


Figure 53: Non-dominated solution set for Scenario 3 (two sources of distributed generation).

It may be seen that when the goal is to minimize the cost of the energy dispatch, the inclusion of one source, two sources, and three sources of 10 MW of distributed generation may lead to a cost reduction of 2.24%, 3.36% and 7.15% in the dispatch cost per hour, respectively.

The minimum power loss dispatch, for the different number of sources of distributed generation is shown in Table 36. In this case, when the system is limited to central generation only, the minimum power loss of 3.607 MW is reached at a cost of 666.949 $/h. When one source of distributed generation is used in the system, the minimum power loss dispatch achieves a power loss of 3.42 MW at a cost of 658.182 $/h. In the case that the system is allowed to use two sources of distributed generation, a minimum power loss of 3.35 MW is reached with an associated cost of 643.657 $/h. Finally, in the case that three sources of distributed generation are used, the minimum power loss that can be achieved is of 3.318 MW with a cost of 628.045 $/h. It may be seen that when the goal is to minimize the power loss of the energy dispatch, the inclusion of one source, two sources, and three sources of 10 MW of distributed generation may lead to a cost reduction of 5.18%, 7.13% and 8.01% in the dispatch cost per hour, respectively.

Table 36: Minimum power loss dispatch using a predetermined number of sources of distributed generation.

| | | Sources of Distributed Generation | | | |
|---|---|---|---|---|---|
| | | 0 | 1 | 2 | 3 |
| Generation (MW) | Bus 1 | 52.007 | 50.615 | 49.741 | 44.871 |
| | Bus 2 | 80 | 73.312 | 75.642 | 79.465 |
| | Bus 5 | 50 | 50 | 50 | 50 |
| | Bus 7 | 0 | 0 | 4.4 | 71 |
| | Bus 8 | 35 | 35 | 35 | 35 |
| | Bus 9 | 0 | 9.29 | 9.53 | 4.57 |
| | Bus 11 | 40 | 40 | 40 | 35.796 |
| | Bus 13 | 30 | 28.603 | 22.204 | 29.917 |
| Power Loss (MW) | | 3.607 | 3.42 | 3.35 | 3.318 |
| Cost ($/Hr) | | 666.949 | 658.182 | 643.657 | 628.045 |

## 6.3.4. Scenario 2: Non-predetermined Number of Sources of Distributed Generation Units

In the case that the system has no limit to the number of sources of distributed generation, the non-dominated solution set achieves the best cost with total central generation of 163.81 MW and total distributed generation of 121.99 MW. Here, the resulting power loss is 2.400 MW at a cost of 547.514 $/h. Furthermore, the non-dominated solution set achieves the best power loss with total central generation of 165.665 MW and total distributed generation of 119.81 MW, where the resulting power loss is 2.075 MW at a cost of 578.170 $/h. This scenario's non-dominated solution set is shown in Figure 54.
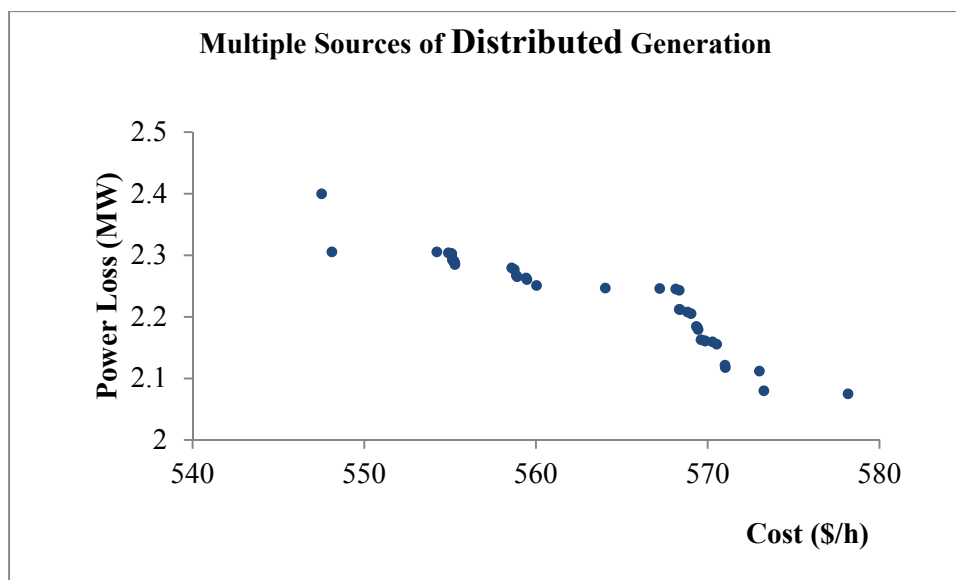
Figure 54: Non-dominated solution set for Scenario 2 (multiple sources of distributed generation).

The comparison of the different levels of distributed generation penetration is provided in Figure 55, where it can be seen that the addition of distributed generation is beneficial in terms of both operational cost and power loss reductions. It is also noted that the non-dominated sets generated with more sources of distributed generation dominate those generated with less distributed generation.

We have developed a comprehensive framework to optimize the penetration level of distributed generation in an energy distribution network based on particle filtering. The developed framework is able to identify the best locations for any specified number of distributed generation sources in terms of their benefits for power loss reduction and operational costs. The proposed framework has been demonstrated on the IEEE-30 bus system, where it has been found that the best location for the deployment of one source of distributed generation is bus 9, while the best locations for the deployment of two sources of distributed generation are buses 7 and 9. Furthermore, it has been found that given the possibility of using three sources of distributed generation the algorithm's non-dominated

solution set is generated using distributed generation only at buses 7 and 9 and the third source of distributed generation is not deployed. The results yield to power losses as low as 2.075 MW and operational costs as low as 547.51$/h when letting the framework use any number of sources of distributed generation. The developed framework has been implemented generically so that it may be implemented on any networked bus system and it may be used to optimize the deployment of any specific number of sources of distributed generation within a network.



Figure 55: Comparison of non-dominated solution sets with different distributed generation sources.

# Chapter 7: Conclusions

We have evaluated the integrated electric utility network in terms of three different aspects, long-term electric utility resource planning, the short-term environmental economic load dispatch, and the optimal deployment of distributed generation sources within the electric network. In order to conduct these analyses the development of two different frameworks have been developed a continuous-discrete modular simulation and optimization framework and a particle filtering based multi-objective optimization framework.

The presented continuous-discrete modular simulation includes the integration of discrete decisions and events with continuous processes into the same simulation environment, harmonizing the different spatiotemporal granularities from the discrete and continuous parts of the simulation. The framework also includes the modular integration of different resources into the simulation, such that different resources may be included or excluded from the simulation environment to accurately represent the available alternatives considered for a specific simulation.

The developed particle filtering based multi-objective optimization framework includes the development of a sequential importance sampling stage and a resampling stage. The sequential importance sampling leverages the information contained within the non-dominated set of solutions generated by the framework to increase the thoroughness of the generated solution set, while the resampling mechanism uses the non-dominated

set's extreme points and the closest extreme points in the search space to ensure that the algorithm does not converge to local optimums. This framework promises suitability for both numerical and combinatorial multi-objective optimization problems.

The performance of the proposed approach has been evaluated against that of well-established algorithms in the literature. Experimental results have shown that the developed particle filtering based multi-objective optimization framework is able to perform better than its competitors in problem instances of convexity, non-convexity, multimodality and non-uniformity; especially in terms of distance from the non-dominated solution set and the Pareto front. However, in problems involving discrete Pareto fronts, the developed framework does not perform as well as its competitors and has room for improvement.

### 7.1.1. Electric Utility Resource Planning

In terms of the long-term electric utility resource planning, using the two developed frameworks has enabled us to establish the best combination of resource investments for electric power generation and storage capacities and to evaluate the effectiveness of including an expansion to the nuclear energy generation capacity, as part of the comprehensive energy resource plan. The developed tool involves a modular modeling approach for the processes of different nature that exist within this complex system, and will help the utility companies conduct resource planning using the developed particle filtering based optimization for multi-objective optimization in a realistic simulation environment.

The proposed approach has been successfully demonstrated for the electric utility resource planning at a scale of the state of Florida. In this case, for a planning horizon of 30 years, by including only the installed nuclear capacity of 3.924 GW, the energy demand may be met to a fulfillment of 95% at an minimum annual cost of $4.628 billion, with annual emissions of 31.226 million of tons of greenhouse gases, when including 2,301 MW of energy storage capacity, and 22.752 GW of fossil fuel energy generation; alternatively the energy demand may be met to a fulfillment of 95% with minimum annual emissions of 9.112 million tons of greenhouse gases, with annual costs of $11.936 billion, when including 3,507 MW of energy storage capacity, 8.842 GW of fossil fuel energy generation, and 99.601 GW of renewable generation. The inclusion of an expansion in the nuclear energy generation capacity of by including four new 1,100 MW AP1000 Nuclear plants leads to an installed capacity of 8.324 GW, with this installed capacity the energy demand may be met to a fulfillment of 95% with minimum annual emissions of 0.070 million tons of greenhouse gases, with annual costs of $15.539 billion, including 4,588 MW of energy storage capacity, 88 MW of fossil fuel energy generation, and 135.758 GW renewable energy generation; with minimum annual cost, the demand may be met to a fulfillment of 95% at an annual cost of $5.111 billion, with emissions of 25.122 million tons of greenhouse gases per year, with an energy storage capacity of 2,301 MW and fossil fuel energy generation capacity of 18.352 GW.

The inclusion of the extra nuclear generation capacity leads to an increase in the minimum cost solution of $483 million per year, however there is a reduction of 6.1 million tons of greenhouse gases per year. This suggests that under a cost minimization scenario, an effective greenhouse gas emissions tax should account at least for this

difference and would only lead to a shift in the capacity plan if it is at least at this level of $79.14 per ton of greenhouse gas emissions. If the goal of the capacity plan is to minimize emissions, the expanded nuclear capacity should be deployed since it offers solutions with lower emissions, at a lower cost, starting at an emissions level of 25.12 million tons per year.

### 7.1.2. Economic and Environmental Load Dispatching

In terms of the short-term environmental economic load dispatch, our developed frameworks have been validated using synthetic functions, and benchmarked against earlier works from the literature, using the IEEE-30 bus test system with constant and dynamic load points. Results obtained from the synthetic experiments have revealed that the proposed algorithm is able to track the system state quite closely with a mean squared error of up to 0.7993. The proposed approach has been found to deliver good set of Pareto optimal solutions comparable to those found in the literature, and better in terms of costs.

### 7.1.3. Optimal Placement of Distributed Generation

In terms of the optimal placement of distributed generation, our developed frameworks have been used to identify the best locations for any specified number of distributed generation sources in terms of their benefits for power loss reduction and operational costs within an energy network.

The proposed method has been demonstrated on a modified version of the IEEE-30 bus system, for which it has been found that the best location for the deployment of one source of distributed generation is bus 9, while the best locations for the deployment of two sources of distributed generation are buses 7 and 9. Furthermore, it has been found that given the possibility of using three sources of distributed generation the algorithm's non-dominated solution set is generated using distributed generation only at buses 7 and 9 and the third source of distributed generation is not deployed. The results yield to power losses as low as 2.075 MW and operational costs as low as 547.51$/h when letting the framework use any number of sources of distributed generation. The developed framework has been implemented generically so that it may be implemented on any networked bus system and it may be used to optimize the deployment of any specific number of sources of distributed generation within a network.

## 7.2. Future Work

There are various avenues for further research spawning from this work. Theoretical improvements to the particle filtering based multi-objective optimization framework include the use of clustering the solutions in the non-dominated solution set, so that resampling is performed using the samples on the extremes of each cluster. This may lead to better results in terms of convergence and enable the algorithm to handle problems with discontinuous Pareto fronts better.  In addition, further research may also be conducted in order to determine 1) the optimum number of particles that should be sampled in both the sequential sampling and resampling stages of the framework, and 2)

the optimum number of extreme points that should be used to construct the resampling distributions. Finally, functional constraints that involve the interaction of the different decision variables could also be implemented into the particle filtering based multi-objective optimization framework in order to increase the number of problems that can be solved using this approach.

For the evaluation of the long-term electric utility resource planning, the used framework has been modeled as an independent network, therefore, its connection with the rest of the energy grid, including energy pricing policies and energy markets should be considered as part of the future work. Additionally, the proposed framework has only focused on energy generation using nuclear energy, fossil fuels, and solar and wind energy generation; further venues of the framework may incorporate energy generation using other sources such as biofuels, or hydroelectric generation. Moreover, issues regarding security and cyber-security in nuclear energy generation, as well as nuclear waste management, when addressing long-term resource planning should be studied in further research. Furthermore, this framework provides an aggregate capacity plan of electric resources, but the location and operation of the different energy generation resources, at a dispatch level should also be considered in further venues.

In terms of the short-term environmental economic load dispatch problem, the proposed framework may be extended to problems with more objectives than just the minimization of the environmental impacts and operational cost of the dispatch, such that aspects like power losses, security and the resilience of the network may also be included.

Regarding the optimal deployment of distributed generation sources within the electric network, future work includes the incorporation of the environmental

implications of deploying different sources of distributed generation into the distributed energy network. Furthermore, the framework may be extended to consider the characteristics of different types of distributed generation, location specifics (i.e., natural resource availabilities such as solar irradiation or wind speed for renewables), and operational policies and restrictions.

# References

Abido, M. A. 2003. Environmental/Economic Power Dispatch Using Multiobjective Evolutionary Algorithms, *IEEE Transactions on Power Systems*, 18(4):1529–37.

Abido, M. A. 2006. Multiobjective Evolutionary Algorithms for Electric Power Dispatch Problem, *IEEE Transactions on Evolutionary Computation*, 10(3): 315-29.

Abido, M. A. 2003. A Novel Multiobjective Evolutionary Algorithm for Environmental/Economic Power Dispatch, *Elect Power Syst Res*, 65(1): 71–81.

Abido, M. A. 2003. A Niched Pareto Genetic Algorithm for Environmental/economic Power Dispatch. *Elect Power Syst Res*, 25(2):97–105.

Ackermann, T., Knyazkin. V. 2002 Interaction between Distributed Generation and the Distribution Network: Operation Aspects, in *Transmission and Distribution Conference and Exhibition 2002: Asia Pacific*. **2**, 1357–1362.

Akpinar, A., Komurcu, M.I., Kankal, M., Ozolcer, I.H., Kaygusuz, K. (2007) Energy Situation and Renewables in Turkey and Environmental effects of Energy Use. *Renewable and Sustainable Energy Review,* **12**, 2013–39.

Azimi-Sadjadi, B., Krishnaprasad, P., 2005. Approximate Nonlinear Filtering and its Application in Navigation. *Automatica*, **41** (6), 945–956.

Beaudin, M., Zareipour, H., Scellenbergable, A., and Resehart W. (2010) Energy Storage for Mitigating the Variability of Renewable Energy Sources: An Updated Review. *Energy for Sustainable Development,* **14** (4), 302-314.

Benitez-Rios, F., G., Garcia-Lagos, F., Joya, G., Atencia, M., Sandoval, F. 2011. Optimization of Distributed Generation Penetration in Distributed power Electric Systems, *International Conference on Power Engineering, Energy and Electrical Drives,* 1-6.

Bhagwan, D., Patvardhan C. 1999. Solution of Economic Load Dispatch using Real Coded Hybrid Stochastic Search, *International Journal of Electrical Power & Energy Systems*, 21(3): 165-70.

Black & Veatch. 2009. Fossil Fuel Generation. Available online: <http://www.bv.com/ Downloads/Resources/Reports/20090212_FossilFuelGeneration.pdf> (Accessed: December 2010).

Bois, B., Wald, L., Pieri, P., Van Leeuwen, C., Commagnac, L., Chery, P.H., Christen, M., Gaudillère, J.-P., and Saur, E (2008) Estimating Spatial and Temporal Variations in Solar Radiation within Bordeaux Winegrowing Region using Remotely Sensed Data. *Journal International des Sciences de la Vigne et du Vin*, **42**, 15-25.

Borg, I. 1982. Coal as an Option for Power Generation in U.S. Territories of the Pacific. *Energy* **7(**11), 875-895.

BP Solar. 220W Photovoltaic module BP 3220T. Available online at: <http://www.bp.com/liveassets/bp_internet/solar/bp_solar_usa/STAGING/local_assets/downloads_pdfs/pq/BP3220T_1-10.pdf> (Accessed: December 2010).

Cadogan J., B., Eisenberg L. 1975. Environmental Control of Electric Power Systems. *ISA Transactions*. **14,** 217-224.

CBC. 2003. Blackout by the Numbers, Available online at: <http://www.cbc.ca/news/background/poweroutage/numbers.html> (Accessed: April 2011).

Chakrabarti, A., Halder, S. 2010. Power System Analysis: Operation and Control. *New Delhi: PHI Learning Private Limited*, Print.

Celik, N., Son, Y. 2012, Sequential Monte Carlo-based Fidelity Selection in Dynamic-data-driven Adaptive Multi-scale Simulations, *International Journal of Production Research*. **50** (3), 843-865.

Chen, H., Cong, Y., Yang, W., Tan, C., Li, Y., Ding, Y. 2009. Progress in Electrical Energy Storage System: A Critical Review. *Progress in Natural Science*, **19** (3), 291–312.

Chen, H., Li, M., Chen, X. 2009. Using Diversity as an Additional-objective in Dynamic Multi-objective Optimization Algorithms, *Second International Symposium on Electronic Commerce and Security*, 484-487.

Chen, W. S., Bakshi, B. R., Goel, P. K., Ungarala, S. 2004. Bayesian Estimation of Unconstrained Nonlinear Dynamic Systems via Sequential Monte Carlo Sampling. *Industrial and Engineering Chemistry Research*, **43** (14), 4012–4025.

Chowdhury, A. A., Agarwal, S.K., and Koval, D. O. 2003. Reliability Modeling of Distributed Generation in Conventional Distribution Systems Planning and Analysis. *IEEE Transactions on Industry Applications*, **39** (5), 1493-1498.

Dagdougui, H., Minciardia, R.,  Ouammi, A., Robbaa, M., and Sacilea, R. 2010. Modelling and Control of a Hybrid Renewable Energy System to Supply Demand of a Green-Building. *International Congress on Environmental Modelling and Software Modelling for Environment's Sake*.

Dapkus, W. D., Bowe, T.R. 1984. Planning for New Electric Generation Technologies: A Stochastic Dynamic Programming Approach, *IEEE Transactions on Power Apparatus and Systems*, PAS-103(6), 1447-1453.

Das, I., Dennis, J. E. 1998. Normal-Boundary Intersection: A New Method for Generating the Pareto Surface in Nonlinear Multicriteria Optimization Problems. *SIAM Journal on Optimization* **8, (**3), 631-657.

De Freitas, J. F. G., Noranjan, M., Gee, A. H.,  Doucet, A. 2000. Sequential Monte Carlo Methods to Train Neural Network Models. *Neural Computation*, **12**, 955–993.

Deb, K. 1989. Genetic Algorithms in Multimodal Function Optimization. *Master thesis, University of Alabama*.

Deb, K., Pratap, A., Agarwal, S., Meyarivan, T. 2002. A Fast and Elitist Multiobjective Genetic Algorithm: NSGA-II, *IEEE Transactions on Evolutionary Computation*, **6** (2), 182-197.

Del Moral, P., Doucet, A., Jasra, A. 2006. Sequential Monte Carlo Samplers. *Royal Statistical Society*, **68**, 411–436.

Delson J., K. 1974. Controlled Emission Dispatch, *IEEE Transactions on Power Apparatus and Systems*,  Pk **9d** (5), 1359-66.

Department of Energy (DOE), Energy Storage. Available online: <http://www.oe. energy.gov/storage.htm> (Accessed: January 2011).

Dinçer, F. 2011. The Analysis on Photovoltaic Electricity Generation Status Potential and Policies of the Leading Countries in Solar Energy. *Renewable and Sustainable Energy Reviews,* **15** (1), 713-720.

Doucet, A., Godsill, S., Andrieu, C.  2000. On Sequential Monte Carlo Sampling Methods for Bayesian Filtering, *Statistics and Computing*, **10**, 197–208.

Energy Information Administration (EIA), Annual Energy Review 2011. Available online: http://www.eia.gov/totalenergy/data/annual/#summary (Accessed: January 2012).

Energy Information Administration (EIA), Annual Energy Review 2010. Available online: <http:// www.eia.doe.gov/emeu/aer/pdf/aer.pdf> (Accessed: January 2011).

Energy Information Administration (EIA), Annual Energy Outlook 2011 Early Release Overview. Available online: <http://www.eia.gov/forecasts/aeo/pdf/0383er% 282011%29.pdf> (Accessed: January 2011).

Energy Information Administration (EIA), Annual Energy Review 2009. Available online: <http:// www.eia.doe.gov/emeu/aer/pdf/aer.pdf> (Accessed: January 2011).

Energy Information Administration (EIA), Average Quality of Coal by State of Origin: Total (All Sectors). Available online: <http://www.eia.doe.gov/cneaf/electricity/cq/ cqaxlfilees3.html> (Accessed: January 2011).

Energy Information Administration (EIA), Assumptions to the Annual Energy Outlook 2010 – Electricity Market Module. Available online: <http://www.eia.doe.gov/oiaf/ aeo/assumption/electricity.html> (Accessed: January 2011).

Energy Information Administration (EIA), Energy Glossary. Available online: <http:// www.eia.gov /glossary/index.cfm> (Accessed: January 2011).

Energy Information Administration (EIA), Natural Gas Annual 2009. Available online: <http://www.eia.gov/pub/oil_gas/natural_gas/data_publications/natural_gas_annual/c urrent/pdf/nga09.pdf> (Accessed: January 2011).

Erdogu, E. 2009. On the Wind Energy in Turkey. *Renewable and Sustainable Energy Review*, **13**, 1361–1371.

Eyer, J., Iannucci, J., Corey, G. 2004. Energy Storage Benefits and Market Analysis Handbook. Technical Report, Sandia Laboratories, Sandia National Laboratories Albuquerque, New Mexico and Livermore, California.

Federal Energy Regulatory Commission (FERC), Economic Dispatch: Concepts, Practices and Issues, November 13, 2005, Available online: <http://www.ferc.gov/ eventcalendar/Files/ 20051110172953-FERC20Staff 20Presentation.pdf> (Accessed: April 2011).

Finnigan O. E., Fouad A. A. 1974. Economic Dispatch with Pollution Constraints, *IEEE Winter Power Meeting*, 155-8

Fonseca, C. M., Flemming, P. J. 1995. An Overview of Evolutionary Algorithms in Multiobjective Optimization. *Evolutionary Computation*, **3** (1) 1-16.

Foote, C. E. T., Burt, G. M., Elders, I. M., Ault, G. W. 2005. Developing Distributed Generation Penetration Scenarios. *International Conference on Future Power Systems,* 6-18.

Florida Power and Light (FPL), Solar Projects. Available online: <http://www.fpl.com/solar> (Accessed: December 2010).

Florida Power and Light (FPL), St. Lucie Fact Sheet. Available online: <http://www.stluciewind. com/project/stlucie_fact_sheet.pdf> (Accessed: December 2010).

Gardner, J., Haynes, T. 2007. Overview of Compressed Air Energy Storage. Office of Energy Research, Policy and Campus Sustainability, Boise State University. Available online: <http://coen.boisestate.edu/WindEnergy/resources/ER-07-001.pdf> (Accessed: January 2011).

Garrity, T. F., Wilkins, D. R. 1993. The Nuclear Option for U. S. Electrical Generating Capacity Additions utilizing Boiling Water Reactor Technology, *IEEE Transactions on Energy Conversion*, **8** (2) 327-331.

George, G. R. 2007. Financing New Nuclear Capacity: Will the 'Nuclear Renaissance' Be a Self-Sustaining Reaction? *The Electricity Journal*, **20** (3) 12-20.

Gent M. R., Lament J. W. 1971. Minimum-Emission Dispatch, IEEE Transactions on Power Apparatus and Systems, *Power Apparatus and Systems-90*, 2650 – 2660.

Goddard Institute for Space Studies, GISS Surface Temperature Analysis (GISTEMP), online at http://data.giss.nasa.gov/gistemp/ (Accessed: December 2010)

GoGreenSolar. Mitsubishi Electric UD5 series. Available online: <http://www. gogreensolar. info/specs/PV-UDxMF5.pdf> (Accessed: December 2010).

Golabi, K., Kirkwood, C. W., Sicherman, A. 1981. Selecting a Portfolio of Solar Energy Projects using Multiattribute Preference Theory, *Management Science,* **22** (2), 174–189.

Goldberg, D. E., Richardson, J. 1987. Genetic Algorithms with Sharing for Multimodal Function Optimization. *Proceedings of the Second International Conference on Genetic Algorithms*, 41–49.

Goldberg, D. E. 1989. Genetic Algorithms in Search, Optimization and Machine Learning 1st Ed. Addison-Wesley Longman Publishing Co., Inc., Boston, MA, USA.

Gong, D., Zhang, Y., Qi, C. 2010. Environmental/Economic Power Dispatch using a Hybrid Multi-objective Optimization Algorithm, *Electrical Power and Energy Systems*. **32**, 607-14.

Gordon, N., Salmond, D., Smith, A. 1993. Novel Approach to Nonlinear/Non-Gaussian Bayesian State Estimation. *IEE Proceedings F-Radar and Signal Processing*, **140** (2), 107–113.

Grainger, J. J., Stevenson, W. D. 1994. Power System Analysis, New York, NY: McGraw Hill, Inc.

Gudowski, W. 2005. Nuclear Waste Management: Status, Prospects and Hopes, Nuclear Physics A. *Proceedings of the 22nd International Nuclear Physics Conference* (Part 2) **752**, 623-632.

Gurgur, C. Z., Jones, M. 2010. Capacity Factor Prediction and Planning in the Wind Power Generation Industry, *Renewable Energy*, **35**, 2761-2766.

Hajela, P., Lin, C. Y. 1992. Genetic Search Strategies in Multicriterion Optimal Design. *Structural and Multidisciplinary Optimization*, **4**, 99–107.

Hadjipaschalis. I., Poullikkas, A., Efthimiou, V. 2009. Overview of Current and Future Energy Storage Technologies for Electric Power Spplications, *Renewable Sustainable Energy,* **13** (6–7), 1513–1522.

Ho, D. T., Frunt, J., Myrzik, J. M. A. 2009. Photovoltaic Energy in Power Market. *6th International Conference on the European Energy Market*, 1–5.

Hobbs, B. F. 1995. Optimization methods for electric utility resource planning. *European Journal of Operational Research*, **83**, 1-20.

Hobbs, B. F., Nelson, S. K. 1992. A Nonlinear Bilevel Model for Analysis of Electric Utility Demand-side Planning Issues. *Annals of Operations Research*, **34** (1), 255-274.

Horn, J., Nafpliotis, N., Goldberg, D. 1994. A Niched Pareto Genetic Algorithm for Multiobjective Optimization. *Proceedings of the First IEEE Conference on Evolutionary Computation,* **1**, 82 –87.

Hota, P. K., Barisal, A. K., Chakrabarti, R. 2010. Economic Emission Load Dispatch through Fuzzy Based Bacterial Foraging Algorithm, *International Journal of Electrical Power & Energy Systems,* **32** (7), 794-803.

Hu, J., Fu, M., Marcus, S. I. 2007. A Model Reference Adaptive Search Method for Global Optimization, *Operations Research*, **55** (3) 549-568.

Ishibuchi, H., Murata, T. 1996. Multi-objective Genetic Local Search Algorithm, *Proceedings of IEEE International Conference on Evolutionary Computation*, 119-124.

Ichihara, Y. 2001. A Perspective on Nuclear Power Generation in the Future Electric Power Industry – for Nonspecialists in the Electric Power Related Industries, *Proceedings of the IEEE*, **89** (12) 1793-1807.

Intergovernmental Panel on Climate Change (IPCC), Summary for Policymakers: The Science of Climate Change, IPCC Working Group I. Available online: <www.ipcc.ch> (Accessed: December 2010)

Jaszkiewicz, A. 2002. Genetic Local Search for Multiple Objective Combinatorial optimization, *European Journal of Operations Research*, **137** (1), 50–71.

Ji, C., Zhang, Y., Tong, M., Yang, S. 2008. Particle Filter with Swarm Move for Optimization. *Proceedings of the 10th international conference on Parallel Problem Solving from Nature: PPSN X*, 909-918.

Jones, M., Hope, C., and Hughes, R. 1990. A Multiattribute Value Model for the Study of UK Energy Policy. *Journal of Operations Research Society,* **41** (10), 919–929.

Kessides, I. N. 2010. Nuclear Power: Understanding the Economic Risks and Uncertainties, *Energy Policy*, **38** (8), 3849-3864.

Khare, V. R., Yao, X., Deb, K. 2003. Performance Scaling of Multi-objective Evolutionary Algorithms. *Evolutionary Multi-Criterion Optimization,* 376–390.

Knowles, J., Corne, D. 1999. The Pareto Archived Evolution Strategy: A New Baseline Algorithm for Multi-objective Optimization. *Proceedings of the 1999 Congress on Evolutionary Computation*, 98–105.

Kobayashi, T. 2003. Vision of the Future of the Photovoltaic Industry in Japan. *Proceedings of the 3rd world conference on photovoltaic energy conversion*, 2538–2543.

Koutroumpezis, G. N., Safigianni, A. S. 2009. Optimum Distributed Generation Penetration in a Distribution Network, *IEEE Bucharest PowerTech,*, 1-8.

Krishnaprasad, P., Azimi-Sadjadi, B. 2004. A Particle Filtering Approach to Change Detection for Nonlinear Systems. *EURASIP Journal on Advances in Signal Processing,* **15**, 2295–2305.

Kuo, C. C. 2005. Generation Dispatch under Large Penetration of Wind Energy Considering Emission and Economy, *Energy Conversion and Management*. **51** (1): 89-97.

Kursawe, F. 1992. Evolution Strategies for Vector Optimization. *Proceeding of the 10th International Conference on Multiple Criteria Decision Making*, 187–193.

Lamont, J. W., Gent, R. 1973. Environmentally-Oriented Dispatching Techniques, *Pm. PICA 8th,* 421-7.

Lei, G. 2002. Adaptive Random Search in Quasi-Monte Carlo Methods for Global Optimization. *Computers & Mathematics with Applications,* **43**, 747 – 754.

Li, H., Zhang, Q. 2009. Multiobjective Optimization Problems with Complicated Pareto Sets, Moea/d and Nsga-ii. *IEEE Transactions on Evolutionary Computation,* **13** (2) 284 –302.

Li, X. D. 2003. A Non-dominated Sorting Particle Swarm Optimizer for Multiobjective Optimization, *Genetic and Evolutionary Computation, Lecture Notes in Computer Science* **2723**, 37–48.

Liao, G. C. 2011. A Novel Evolutionary Algorithm for Dynamic Economic Dispatch with Energy Saving and Emission Reduction in Power System Integrated Wind Power, *Energy*, **36** (2): 1018-29.

Liu, D., Tan, K. C., Goh, C. K., Ho, W. K. 2007. A Multiobjective Memetic Algorithm Based on Particle Swarm Optimization, *IEEE Transactions on Systems, Man, and Cybernetics, Part B: Cybernetics*, **37** (1), 42-50.

Likens, G. E., Driscoll, C. T., Buso, D.C. 1996. Long-Term Effects of Acid Rain: Response and Recovery of a Forest Ecosystem. *Science*, **272**, 244-246.

Lopez-Ibanez, M., Stuetzle, T. 2012. The Automatic Design of Multi-Objective Ant Colony Optimization Algorithms, *IEEE Transactions on Evolutionary Computation*, article in press.

Malik, A. S. 2001. Modeling and Economic Analysis of DSM Programs in Generation Planning. *International Journal of Electrical Power and Energy Systems*, **23** (5), 413-419.

Marcus, G. H. 2000. Considering the Next Generation of Nuclear Power Plants, *Progress in Nuclear Energy*, **37** (1-4) 5-10.

Maricar, N. M. 2004. Efficient Resource Development in Electric Utilities Planning Under Uncertainty, *Dissertation submitted to the Faculty of the Virginia Polytechnic Institute and State University*.

Markvart, T. (ed.). 2000. Solar Electricity, John Wiley & Sons, Chichester, UK.

Mazhari, E., Zhao, J., Celik, N., Lee, S., Son, Y-J, Head, L. 2011. Hybrid Simulation and Optimization-based Design and Operation of Integrated Photovoltaic Generation, Storage Units, and Grid. *Simulation Modelling Practice and Theory*, **19**, 463–481.

McDaniels, T. L. 1996. A Multiattribute Index for Evaluating Environmental Impact of Electric Utilities. *Journal of Environmental Management,* **46**, 57–66.

Míguez, J. 2007. Analysis of Selection Methods for Cost-reference Particle Filtering with Applications to Maneuvering Target Tracking and Dynamic Optimization. *Digital Signal Processing,* **17** (4), 787 – 807.

Míguez, J. 2010. Analysis of a Sequential Monte Carlo Method for Optimization in Dynamical Systems. *Signal Processing,* **90** (5), 1609 – 1622.

Mitsubishi Heavy Industries. Products. Available Online <http://www.mhi.co.jp/en/ products/ detail/products.html> (Accessed: January 2011)

Mostaghim, S., Teich, J. 2003. Strategies for Finding Good Local Guides in Multi-objective Particle Swarm Optimization (MOPSO), *Proceedings of the 2003 IEEE Swarm Intelligence Symposium*, 26- 33.

Nanda, J., Kothari, D. P., Lingamurthy, K. S. 1988. Economic-emission load dispatch through goal programming techniques, *IEEE Transactions on Energy Conversion*, **3** (1), 26-32

National Renewable Energy Lab (NREL), Wind Research – Wind Integration Datasets. Available online: <http://www.nrel.gov/wind/integrationdatasets/> (Accessed: December 2010).

Neco. SunPower E19 / 318 Solar Panel <http://www.neco.com.au/media/upload/file/ Sunpower%20 Panels.pdf> (Accessed: December 2010).

Next Era Energy Resources, Brochures and Factsheets. Available online: <http://www. nexteraenergyresources.com/content/who/brochures.shtml> (Accessed: December 2010).

Panigrahi, B. K., Pandi, V. R., Sharma, R., Das, S., Das, S. 2011. Multiobjective Bacteria Foraging Algorithm for Electrical Load Dispatch Problem, *Energy Conversion and Management*. **52** (2), 1334-42.

Papandreou, V., Shang, Z. 2008. A Multicriteria Optimization Approach for the Design of Sustainable Utility Systems. *Computers & Chemical Engineering*, **32** (7), 1589-1602.

Patel, M. R. 2006. Wind and solar power systems: Design, analysis, and operation, Taylor & Francis, Boca Raton, FL.

Phonrattanasak, P. 2010. Optimal Placement of DG using Multiobjective Particle Swarm Optimization, *Proceedings of the 2nd International Conference on Mechanical and Electrical Technology,* 342-346.

Qing, Y., Wei-Qing, X., Bao-chuan, J. 2010. Multi-population Binary Ant Colony Algorithm with Concrete Behaviors for Multi-objective Optimization Problem, *IEEE International Conference on Information Management and Engineering*, 274-281.

Rashad, S. M. 2006. Nuclear Power and the Environment Prospects and Challenges, *National Radio Science Conference,* Inv3, 1-32.

Rudolph, G. 1999. Evolutionary Search Under Partially Ordered Sets, *Department of Computer Science/LS11, University of Dortmund*, Tech. Rep. CI-67/99.

Sheu, J. B. 2008. Green Supply Chain Management, Reverse Logistics and Nuclear Power Generation, *Transportation Research Part E: Logistics and Transportation Review*, **44** (1) 19-46.

Skoplaki, E., and Palyvos, J. 2010. Operating Temperature of Photovoltaic Modules: A Survey of Pertinent Correlations. *Renewable Energy,* **34** (1), 23-29.

Smrekar, J., Assadi, M., Fast, M., Kuštrin, I., De, S. 2009. Development of Artificial Neural Network Model for a Coal-fired Boiler using Real Plant Data. *Energy,* **34** (2), 144-52.

Solanki, S. K., Krivova, N. A. Wenzler, T. 2005. Irradiance models. *Advances in Space Research*, **35**, 376-383.

Solar Home, Evergreen 210W Module B-Grade ES-A-21. Available online: <http://www.solarhome.org/evergreen210wmoduleb-gradees-a-21.aspx> (Accessed: December 2010).

Solar Home, Kyocera 205W Module KD205GX-LPU. Available online: <http://www.solarhome.org/kyocera205wmodulekd205gx-lpu.aspx> (Accessed: December 2010).

Srinivas, N. Deb, K. 1994. Multiobjective Optimization using Nondominated Sorting in Genetic Algorithms. *Evolutionary Computation*, **2**, 221–248.

Stoll, H. G. 1989. Least-Cost Electric Utility Planning, John Wiley and Sons, New York, NY.

Succar, S., Williams, R.H. 2008. Compressed Air Energy Storage: Theory, Resources, and Applications for Wind Power. *Princeton Environmental Institute.* Available online: <http://www.princeton.edu/pei/energy/publications/texts/SuccarWilliams_PEI_CAES_2008April8.pdf> (Accessed: January 2011).

Sullivan, R. L. 1972. Minimum Pollution Dispatching, *IEEE Summer Power Meeting*, 672-687.

Sullivan, R. L., Hackett, D. F. 1973. Air Quality Control Using a Minimum Pollution-Dispatching Algorithm, *Environmental Science & Technology*. **7** (11): 1019-1022.

Sun, T. S., Wu, W. C., Tsai, S. J., Liu, C. C., Chiu, S. Y., Hsieh, S. T. 2008. Particle Swarm Optimizer for Multi-objective Problems based on Proportional Distribution and Cross-over Operation, *IEEE International Conference on Systems, Man and Cybernetics*, 12-15.

Suna, D., Polo, A. L., Haas, R., Schiener, C., Resch, G. 2008. Global Context, Environmental Costs and Energy Portfolio Analysis for Urban PV. Technical report. Energy Economics Group, Vienna University of Technology, 1–39.

SunPower, SunPower T0 Tracker. Available online at: <http://us.sunpowercorp.com/cs/Satellite?blobcol=urldata&blobheader=application%2Fpdf&blobheadername3=Content-Disposition&blobheadervalue3=attachment%3B+filename%3D637%252F52%252FT0%2BTracker%2BSpec%2BSheet%2Bfor%2BDownload%252C0.pdf&blobkey=id&blobtable=MungoBlobs&blobwhere=1300258501616&ssbinary=true> (Accessed: December 2010).

Suntech. STP275 – 24/ Vd <http://www.suntech-power.com/goodyear/pdf/STP280_24Vd_UL%28H4%20Connector%29_AZ.pdf> (Accessed: December 2010).

Suzlon, S88-2.1 MW Generator. Available Online <http://www.suzlon.com/pdf/Suzlon-S88-2.1MW-product-brochure.pdf> (Accessed: January 2011).

Talaq, J. H., EI-Hawary, M. E. 1994. A Summary of Environmental/Economic Dispatch Algorithms. *IEEE Transactions on power systems,* **9** (3):1508-16.

Tang, L., Wang, X. 2012. A Hybrid Multi-objective Evolutionary Algorithm for Multi-objective Optimization Problems, *IEEE Transactions on Evolutionary Computation*, article in press.

Tekiner, H., Coit, D. W., Felder, F.A. 2010. Multi-period Multi-objective Electricity Generation Expansion Planning Problem with Monte-Carlo Simulation, *Electric Power Systems Research*, **80** (12), 1394-1405.

Ter-Gazarian, A. 1994. Energy Storage for Power Systems. Stevenage, Harts., U.K.: P. Peregrinus on Behalf of the Institution of Electrical Engineers.

Trehan, N. K., Saran, R. 2003. Nuclear Power Revival, *Nuclear Science Symposium Conference Record*, **5**, 3630- 3633.

Tseng, L. Y., Chen, C. 2009. Multiple Trajectory Search for Unconstrained/Constrained Multi-objective Optimization, *IEEE Congress on Evolutionary Computation*, 1951-1958.

University of Washington, Power Systems Test Case Archive – UWEE, Available online at: <http://www.ee.washington.edu/research/pstca> (Accessed: December 2011)

Ünveren, A., Acan, A. 2007. Multi-objective Optimization with Cross-Entropy Method: Stochastic Learning with Clustered Pareto Front, *IEEE Congress on Evolutionary Computation*, 25-28.

U.S.-Canada Power System Outage Task Force. 2004. Final Report on the August 14, 2003 Blackout in the United States and Canada: Causes and Recommendations.

U.S. Senate. Energy Policy Act of 2005 (EPAct)

Vahidinasab, V., Jadid, S. 2010. Joint Economic and Emission Dispatch in Energy Markets: A Multiobjective Mathematical Programming Approach, *Energy*, **35** (3), 1497-1504.

Van Veldhuizen, D. A. 1999. Multiobjective evolutionary algorithms: Classifications, analyses, and new innovations. *Ph.D. thesis, Air Force Institute of Technology, Wright-Patterson AFB.*

Voropai, N. L., and Ivanova, E. Y. 2002. Multicriteria Decision Analysis Technique in Electric Power System Expansion Planning. *Electrical Power and Energy Systems,* **24**, 71–78.

Wang, C., Nehrir, M. H. 2004. Analytical Approaches for Optimal Placement of Distributed Generation Sources in Power Systems, *IEEE Transactions on Power Systems*, **19**, 2068-2076.

Wang, S., Wang, Y., Liu, B., Gui, W. 2011. A Hybrid Sequence Sampling Technique and its Application to Multi-objective Optimization of Blending Process, *30th Chinese Control Conference*, 2135-2140.

Wang, X. and McDonald, J. R. 1994. Modern Power System Planning, McGraw-Hill (Europe), Maidenhead, UK.

Weber, J. D. 1997. Implementation of a Newton-based Optimal Power Flow Into a Power System Simulation Environment, *Master thesis, University of Illinois at Urbana-Champaign.*

Williams, B., Mcmullan, J. and Campbell, P. 1994. Clean Power Generation from Coal. *Fuel,* **73** (7), 1069-1073.

World Wind Energy Association, World Wind Energy Report 2010. Available online at: <http://www.wwindea.org/home/images/stories/pdfs/worldwindenergyreport2010> (Accessed: December 2011)

Wu, K., Nagurney, A., Liu, Z., and Stranlund, J. 2006. Modeling Generator Power Plant Portfolios and Pollution Taxes in Electric Power Supply Chain Networks: A Transportation Network Equilibrium Transformation. *Transportation Research Part D: Transport and Environment,* **11** (3), 171-90.

Wu, L. H., Wang, Y. N., Yuan, X. F., Zhou, S. W. 2010. Environmental/Economic Power Dispatch Problem using Multi-objective Differential Evolution Algorithm, *Electric Power Systems Research*, **80**, 1171-81.

Yang, Y., Guo, X., and Wang, N. 2010. Power Generation from Pulverized Coal in China. *Energy*, **35** (11), 4336-4348.

Zahavi, J., Eisenberg, L. 1975. Economic-Environmental Power Dispatch, *IEEE Transactions on Systems, Man, and Cybernetics*, **SMC-5** (5), 485-489.

Zahedi, A. 2011. Maximizing Solar PV Energy Penetration using Energy Storage Technology. *Renewable and Sustainable Energy Reviews,* **15** (1), 866-70.

Zhang, Q., Li, H. 2007. MOEA/D: A Multi-objective Evolutionary Algorithm Based on Decomposition, *IEEE Transactions on Evolutionary Computation*, **11** (6), 712-731.

Zhou, E., Fu, M., Marcus, S. I. 2008. A Particle Filtering for Randomized Optimization Algorithms, *Proceedings of the 40th Conference on Winter Simulation*, 647-654.

Zitzler, E., Deb, K., Thiele, L. 2000. Comparison of Multiobjective Evolutionary Algorithms: Empirical Results. *Evolutionary Computation* **8** (2), 173–195.

Zitzler, E., Thiele, L. 1999. Multiobjective Evolutionary Algorithms: A Comparative Case Study and the Strength Pareto Evolutionary Algorithm. *IEEE Transactions on Evolutionary Computation* **3** (4), 257–271.

# Appendix 1: IEEE-30 Dynamic Load

Table A1: Real power load June 21

| June 21 | Bus 2 | Bus 3 | Bus 4 | Bus 5 | Bus 7 | Bus 8 | Bus 10 | Bus 12 | Bus 14 | Bus 15 | Bus 16 | Bus 17 | Bus 18 | Bus 19 | Bus 20 | Bus 21 | Bus 23 | Bus 24 | Bus 26 | Bus 29 | Bus 30 |
|---|---|---|---|---|---|---|---|---|---|---|---|---|---|---|---|---|---|---|---|---|---|
| 0:00 | 21.514 | 2.359 | 7.932 | 90.132 | 20.522 | 27.235 | 4.158 | 10.099 | 4.717 | 6.411 | 3.573 | 10.064 | 3.098 | 8.910 | 2.137 | 17.287 | 2.765 | 6.746 | 3.098 | 2.564 | 10.744 |
| 1:00 | 20.518 | 3.199 | 6.496 | 86.927 | 22.521 | 27.088 | 4.073 | 11.071 | 4.856 | 7.193 | 4.168 | 9.987 | 2.930 | 8.943 | 1.639 | 14.957 | 3.143 | 9.240 | 4.156 | 1.552 | 9.418 |
| 2:00 | 22.138 | 3.447 | 7.474 | 87.378 | 21.371 | 28.756 | 6.701 | 9.768 | 6.967 | 8.111 | 3.038 | 8.063 | 2.349 | 8.575 | 1.730 | 15.523 | 2.751 | 7.747 | 3.092 | 1.720 | 11.110 |
| 3:00 | 18.590 | 3.636 | 6.005 | 88.503 | 21.365 | 29.816 | 6.729 | 9.006 | 4.408 | 6.257 | 4.340 | 8.209 | 2.626 | 8.678 | 1.341 | 14.666 | 4.180 | 9.329 | 2.213 | 2.782 | 8.570 |
| 4:00 | 20.387 | 3.409 | 5.692 | 87.480 | 21.961 | 28.959 | 5.674 | 8.727 | 4.737 | 7.561 | 2.584 | 6.946 | 2.762 | 8.614 | 2.350 | 14.776 | 2.429 | 6.931 | 2.306 | 3.095 | 9.519 |
| 5:00 | 19.591 | 3.085 | 6.032 | 83.252 | 19.274 | 26.968 | 5.707 | 10.691 | 4.969 | 7.060 | 4.292 | 7.587 | 3.495 | 9.649 | 2.521 | 17.077 | 2.784 | 6.845 | 4.178 | 1.436 | 9.176 |
| 6:00 | 20.639 | 1.404 | 6.625 | 84.571 | 19.604 | 26.271 | 4.616 | 11.619 | 6.165 | 6.155 | 3.965 | 9.588 | 3.896 | 9.621 | 2.183 | 15.563 | 3.450 | 9.242 | 2.294 | 3.083 | 8.360 |
| 7:00 | 19.668 | 1.950 | 7.139 | 85.062 | 21.208 | 25.793 | 6.143 | 11.477 | 6.658 | 7.396 | 3.081 | 8.432 | 3.261 | 7.262 | 2.994 | 16.277 | 4.089 | 7.258 | 3.412 | 1.709 | 8.427 |
| 8:00 | 21.575 | 2.555 | 6.052 | 85.214 | 19.318 | 26.923 | 6.089 | 10.494 | 5.333 | 6.177 | 2.470 | 7.524 | 3.901 | 7.675 | 1.353 | 17.061 | 4.145 | 7.455 | 4.593 | 2.891 | 10.281 |
| 9:00 | 21.189 | 1.521 | 8.317 | 88.479 | 22.028 | 27.100 | 6.413 | 10.397 | 5.633 | 6.308 | 2.135 | 9.276 | 3.356 | 7.569 | 1.598 | 16.816 | 3.062 | 7.730 | 4.331 | 1.656 | 9.704 |
| 10:00 | 20.524 | 2.459 | 8.131 | 92.956 | 22.770 | 28.082 | 6.300 | 10.780 | 6.986 | 9.119 | 2.218 | 10.193 | 4.037 | 8.293 | 1.456 | 16.857 | 3.926 | 8.493 | 2.941 | 3.383 | 10.557 |
| 11:00 | 23.855 | 3.757 | 7.132 | 96.968 | 24.447 | 30.796 | 4.447 | 12.407 | 6.855 | 7.403 | 2.532 | 10.114 | 2.755 | 10.401 | 1.213 | 16.320 | 3.600 | 7.982 | 2.612 | 1.901 | 9.374 |
| 12:00 | 24.537 | 2.771 | 8.642 | 98.883 | 25.476 | 30.819 | 6.361 | 13.075 | 7.113 | 9.204 | 3.266 | 9.656 | 3.937 | 8.262 | 1.487 | 18.201 | 2.991 | 9.346 | 4.272 | 2.098 | 12.346 |
| 13:00 | 24.888 | 1.753 | 7.876 | 101.826 | 26.254 | 31.688 | 4.870 | 13.284 | 7.546 | 8.655 | 4.167 | 9.238 | 2.771 | 10.883 | 1.660 | 19.721 | 3.896 | 8.249 | 3.056 | 1.630 | 11.907 |
| 14:00 | 22.055 | 2.586 | 8.982 | 100.547 | 24.526 | 34.559 | 5.823 | 11.949 | 6.323 | 7.136 | 4.004 | 10.495 | 4.280 | 10.327 | 3.220 | 19.782 | 3.080 | 9.313 | 3.499 | 3.350 | 11.708 |
| 15:00 | 25.128 | 3.210 | 9.687 | 103.190 | 23.445 | 33.067 | 5.367 | 11.004 | 7.589 | 8.789 | 2.853 | 9.849 | 2.810 | 10.999 | 2.931 | 17.602 | 3.760 | 8.424 | 4.823 | 3.006 | 11.530 |
| 16:00 | 20.983 | 3.555 | 6.075 | 90.796 | 21.295 | 29.893 | 4.231 | 11.312 | 4.425 | 8.447 | 3.941 | 10.250 | 3.894 | 10.640 | 1.521 | 16.993 | 1.988 | 8.685 | 3.351 | 1.962 | 10.180 |
| 17:00 | 20.412 | 3.474 | 7.386 | 91.900 | 21.137 | 28.970 | 6.160 | 11.977 | 5.203 | 8.771 | 2.355 | 8.493 | 3.356 | 9.744 | 2.680 | 18.302 | 3.730 | 9.311 | 2.841 | 2.961 | 11.855 |
| 18:00 | 21.629 | 2.957 | 6.233 | 87.450 | 20.894 | 27.103 | 5.624 | 11.764 | 6.086 | 6.711 | 3.276 | 7.160 | 3.295 | 10.265 | 2.812 | 17.624 | 3.580 | 9.239 | 2.902 | 2.317 | 11.253 |
| 19:00 | 21.580 | 2.613 | 8.080 | 86.715 | 22.583 | 28.078 | 6.473 | 10.316 | 5.064 | 6.929 | 3.914 | 8.668 | 3.590 | 9.812 | 1.242 | 17.111 | 2.162 | 8.077 | 3.438 | 1.480 | 11.494 |
| 20:00 | 19.983 | 2.254 | 8.586 | 87.093 | 22.838 | 29.781 | 6.276 | 9.470 | 4.503 | 8.661 | 3.017 | 9.257 | 2.358 | 8.399 | 2.315 | 18.083 | 2.307 | 8.021 | 2.476 | 1.836 | 10.935 |
| 21:00 | 20.840 | 1.618 | 7.715 | 87.241 | 22.327 | 28.224 | 6.282 | 11.032 | 4.590 | 6.010 | 2.365 | 9.685 | 3.506 | 9.882 | 1.698 | 17.067 | 3.381 | 9.226 | 4.245 | 3.030 | 11.381 |
| 22:00 | 20.797 | 2.239 | 5.874 | 86.134 | 19.917 | 28.015 | 3.989 | 10.249 | 5.758 | 6.760 | 2.374 | 8.178 | 3.344 | 9.499 | 1.244 | 17.850 | 2.713 | 8.844 | 2.681 | 1.526 | 11.028 |
| 23:00 | 19.301 | 2.735 | 7.508 | 84.628 | 19.964 | 28.769 | 5.815 | 11.337 | 5.908 | 8.731 | 3.883 | 9.129 | 2.086 | 8.108 | 1.293 | 17.818 | 2.613 | 6.691 | 2.664 | 3.245 | 9.788 |

Table A2: Reactive power load June 21

| June 21 | Bus 2 | Bus 3 | Bus 4 | Bus 5 | Bus 7 | Bus 8 | Bus 10 | Bus 12 | Bus 14 | Bus 15 | Bus 16 | Bus 17 | Bus 18 | Bus 19 | Bus 20 | Bus 21 | Bus 23 | Bus 24 | Bus 26 | Bus 29 | Bus 30 |
|---|---|---|---|---|---|---|---|---|---|---|---|---|---|---|---|---|---|---|---|---|---|
| 0:00 | 13.105 | 2.208 | 1.932 | 18.851 | 10.103 | 28.137 | 1.618 | 6.385 | 1.432 | 1.978 | 2.269 | 6.575 | 1.544 | 3.307 | 0.556 | 11.665 | 1.325 | 6.959 | 3.856 | 1.417 | 2.762 |
| 1:00 | 14.104 | 0.882 | 2.550 | 18.608 | 11.123 | 28.808 | 3.687 | 8.752 | 2.442 | 1.953 | 3.080 | 6.039 | 1.605 | 3.494 | 1.715 | 10.785 | 2.247 | 5.877 | 2.250 | 2.572 | 3.400 |
| 2:00 | 11.108 | 1.217 | 1.987 | 20.435 | 9.507 | 28.542 | 2.782 | 7.293 | 3.657 | 2.507 | 2.411 | 6.491 | 1.265 | 3.868 | 0.763 | 11.258 | 2.775 | 6.423 | 2.775 | 1.913 | 4.130 |
| 3:00 | 11.682 | 1.241 | 1.401 | 19.056 | 9.978 | 27.898 | 3.974 | 6.052 | 1.345 | 4.590 | 1.158 | 6.955 | 1.890 | 4.959 | 2.334 | 9.577 | 1.242 | 7.556 | 2.238 | 2.480 | 4.170 |
| 4:00 | 13.556 | 2.779 | 2.582 | 17.767 | 11.727 | 26.200 | 1.744 | 6.928 | 3.775 | 3.834 | 3.138 | 6.271 | 2.031 | 5.109 | 0.691 | 12.261 | 0.941 | 6.236 | 3.261 | 2.307 | 2.566 |
| 5:00 | 13.477 | 2.210 | 2.179 | 17.481 | 11.062 | 25.756 | 2.109 | 8.056 | 1.536 | 3.100 | 2.688 | 4.481 | 0.800 | 4.956 | 0.537 | 11.515 | 2.827 | 6.804 | 2.762 | 2.177 | 1.890 |
| 6:00 | 11.118 | 1.874 | 1.655 | 16.771 | 10.272 | 26.980 | 3.728 | 8.012 | 2.679 | 3.733 | 1.129 | 7.000 | 2.340 | 2.713 | 0.737 | 10.195 | 1.487 | 5.242 | 3.687 | 1.800 | 4.216 |
| 7:00 | 13.025 | 1.022 | 2.734 | 18.537 | 10.342 | 27.224 | 2.551 | 6.598 | 2.267 | 2.794 | 1.215 | 6.427 | 2.097 | 3.168 | 0.503 | 11.307 | 2.128 | 6.362 | 1.722 | 1.662 | 2.354 |
| 8:00 | 12.913 | 1.770 | 1.955 | 19.742 | 12.227 | 28.729 | 3.537 | 6.129 | 1.578 | 2.534 | 1.317 | 6.108 | 2.205 | 3.837 | 1.747 | 11.474 | 2.147 | 5.324 | 3.186 | 2.529 | 2.204 |
| 9:00 | 12.443 | 1.208 | 4.083 | 21.007 | 11.231 | 27.256 | 2.675 | 7.383 | 1.255 | 3.754 | 2.168 | 5.258 | 0.837 | 4.300 | 1.931 | 9.643 | 2.662 | 7.604 | 3.507 | 1.718 | 4.573 |
| 10:00 | 14.467 | 1.127 | 2.703 | 20.598 | 12.089 | 31.558 | 3.259 | 7.616 | 3.116 | 4.003 | 3.003 | 5.967 | 2.336 | 5.251 | 0.412 | 12.939 | 3.047 | 6.534 | 1.631 | 0.528 | 1.684 |
| 11:00 | 12.577 | 1.135 | 2.309 | 21.106 | 13.596 | 30.239 | 1.585 | 9.685 | 3.012 | 2.196 | 3.326 | 5.296 | 2.778 | 2.950 | 2.262 | 10.673 | 1.694 | 7.477 | 3.349 | 0.526 | 2.926 |
| 12:00 | 15.376 | 1.590 | 1.620 | 21.585 | 10.875 | 30.058 | 2.537 | 9.514 | 3.087 | 4.466 | 3.193 | 7.385 | 1.616 | 3.993 | 1.988 | 10.795 | 1.872 | 7.270 | 2.565 | 1.584 | 3.958 |
| 13:00 | 13.180 | 2.323 | 4.388 | 23.912 | 11.667 | 32.638 | 2.460 | 8.212 | 3.395 | 2.337 | 3.214 | 7.641 | 2.270 | 3.559 | 2.074 | 13.817 | 1.658 | 6.762 | 2.159 | 0.583 | 3.032 |
| 14:00 | 14.974 | 2.298 | 1.464 | 23.919 | 11.066 | 32.367 | 4.345 | 10.032 | 2.353 | 4.939 | 2.472 | 7.822 | 2.882 | 3.343 | 0.935 | 13.378 | 3.005 | 7.014 | 2.607 | 1.276 | 3.184 |
| 15:00 | 15.691 | 3.069 | 1.819 | 22.043 | 11.696 | 33.256 | 4.440 | 8.956 | 3.134 | 3.960 | 1.332 | 7.453 | 1.048 | 3.480 | 2.136 | 12.515 | 2.674 | 7.794 | 3.026 | 2.329 | 3.214 |
| 16:00 | 11.982 | 0.752 | 3.208 | 20.055 | 10.328 | 30.358 | 1.965 | 7.536 | 3.738 | 4.797 | 3.388 | 5.928 | 2.561 | 3.703 | 1.152 | 11.686 | 2.003 | 5.918 | 1.887 | 1.939 | 4.371 |
| 17:00 | 13.593 | 2.685 | 2.824 | 18.645 | 10.700 | 30.142 | 3.890 | 8.441 | 3.109 | 2.171 | 1.409 | 5.881 | 2.093 | 3.064 | 1.369 | 10.522 | 1.619 | 6.438 | 3.846 | 0.683 | 4.747 |
| 18:00 | 11.694 | 2.191 | 3.573 | 17.783 | 10.207 | 29.068 | 3.935 | 7.768 | 3.237 | 4.434 | 2.592 | 5.277 | 0.778 | 4.979 | 0.668 | 11.310 | 2.678 | 5.640 | 3.400 | 1.444 | 3.430 |
| 19:00 | 12.415 | 1.364 | 4.023 | 17.640 | 10.793 | 28.364 | 3.392 | 8.604 | 1.223 | 4.832 | 3.299 | 4.534 | 1.437 | 2.840 | 2.237 | 9.656 | 1.465 | 5.634 | 3.220 | 2.264 | 3.219 |
| 20:00 | 12.228 | 1.551 | 1.341 | 20.564 | 9.866 | 28.813 | 3.797 | 7.527 | 2.194 | 2.906 | 2.767 | 6.398 | 1.193 | 4.813 | 2.286 | 12.468 | 1.337 | 6.737 | 2.605 | 2.166 | 3.357 |
| 21:00 | 13.141 | 2.343 | 2.895 | 19.357 | 11.326 | 28.931 | 2.442 | 7.852 | 1.912 | 2.170 | 3.245 | 6.980 | 1.319 | 4.654 | 1.528 | 9.587 | 1.337 | 5.226 | 1.752 | 1.967 | 4.188 |
| 22:00 | 14.276 | 0.703 | 1.434 | 20.287 | 11.782 | 26.584 | 2.393 | 6.198 | 3.531 | 4.201 | 3.203 | 6.931 | 2.295 | 3.314 | 2.075 | 10.150 | 2.967 | 6.036 | 1.535 | 0.900 | 4.249 |
| 23:00 | 12.980 | 2.756 | 2.662 | 17.926 | 11.960 | 28.141 | 3.801 | 7.974 | 2.144 | 4.692 | 1.424 | 6.188 | 1.180 | 3.374 | 0.512 | 11.352 | 2.798 | 5.300 | 2.341 | 1.609 | 4.503 |